STUDIES ON COLD BONDING AND SOME ASPECTS OF REDUCTION OF IRON ORE - COAL/CHAR COMPOSITE PELLET SYSTEM

by

SUJAY KUMAR DUTTA

DEPARTMENT OF METALLURGICAL ENGINEERING

INDIAN INSTITUTE OF TECHNOLOGY, KANPUR

JULY, 1991

STUDIES ON COLD BONDING AND SOME ASPECTS OF REDUCTION OF IRON ORE - COAL/CHAR COMPOSITE PELLET SYSTEM

A Thesis Submitted
in Partial Fulfilment of the Requirements
for the Degree of

DOCTOR OF PHILOSOPHY

by

SUJAY KUMAR DUTTA

to the

DEPARTMENT OF METALLURGICAL ENGINEERING

INDIAN INSTITUTE OF TECHNOLOGY, KANPUR

JULY, 1991

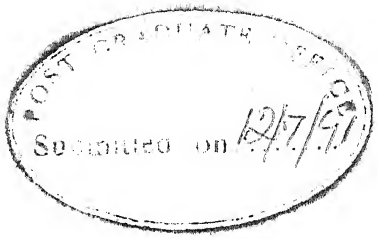

CERTIFICATE

It is certified that the work contained in the thesis entitled **Studies on Cold Bonding and Some Aspects of Reduction of Iron Ore - Coal / Char Composite,** by Sujay Kumar Dutta has been carried out under my supervision and that this work has not been submitted elsewhere for a degree.

JULY, 1991

(**A. Ghosh**)
Professor
Department of Metallurgical Engineering
Indian Institute of Technology
Kanpur

MME-1991-D-DUT-STU

SYNOPSIS

Name of Student : **SUJAY KUMAR DUTTA** Roll No : **8710665**

Degree for which submitted : **Ph.D.** Department : **Met.Engg.**

Thesis Title : **Studies on Cold Bonding and Some Aspects of Reduction of Iron Ore - Coal / Char Composite Pellet System**

Name of thesis supervisor : **Dr.A. GHOSH, Professor**

Metallurgical Engineering

Month and year of thesis submission : **July, 1991**

The term **Composite Pellet** is being employed here to mean pellet containing mixture of fines of iron bearing oxide and carbonaceous material (coal, coke, char), which has been imparted sufficient green strength for subsequent handling by cold bonding technique. The pellet should have sufficient strength to withstand high temperature and stresses in reduction furnaces.

Blast furnace process is now facing problems like shortage of good quality coke, and higher investment cost for furnace and auxiliary equipments. In India, there is shortage of pig iron, which is a basic raw material for cupola. Again the rapid growth of electric arc furnaces has resulted in short supply of scrap in India. Now a days sponge iron is a substitute for scrap.

Indian iron ore deposits are partly soft and friable in nature. So they contain a good amount of superfines (-200 mesh)

rich in iron content (65 pct and above). These are known as **Blue Dust**. Estimated reserves of blue dust in India is around 550 million tonnes. India has a large reserve of non-coking coal as well. Fines of coal and coke are generated during mining and coking respectively. Therefore if composite pellets made from blue dust and coal/char/coke fines are subjected to reduction or reduction smelting in furnaces for extraction of iron, they would offer the following advantages :

(1) resource utilization and lower environmental pollution,

(2) increase in productivity in furnaces such as rotary kiln for sponge ironmaking due to faster reduction in intimate mixture of oxide and reductant,

(3) providing a substitute for pig iron in cupola.

Objective of present investigation is two-fold :

(1) to prepare composite pellets by various methods of cold bonding technique in the laboratory and evaluate their properties; this would be a contribution towards development of cold-bonding technology,

fundamental investigations on reduction of composite pellets, including auxiliary studies as back-up investigations with emphasis on kinetics.

The thesis consists of eight chapters. Chapter 1 covers literature review. Some conclusions drawn from literature were :

(1) there have been very few fundamental studies on reduction of composite pellets,

(2) most of the investigators employed char, coke as reductant and not coal,

(3) after introducing composite pellet into a furnace, it takes about 10 to 15 minutes to bring it to furnace temperature; by that time significant extent of reduction and other reactions take place.

Therefore, from a fundamental point of view, it is desirable to carry out reduction studies in non-isothermal mode. hence it was decided to heat composite pellets at suitable heating rates and investigate features of non-isothermal reduction. It was also decided to carry out the following auxiliary sets of measurements for better understanding of reduction behaviour of composites.

(1) Measurement of degree of reduction etc. as well as examination by X-ray and scanning electron microscopy of reduced pellets.

(2) Rate of reduction of blue dust (isothermal) by H_2 and CO

(3) Devolatilization of coal (non-isothermal).

Chapter 2 deals with raw materials characterization, pellet preparation and testing. For preparation of composite pellets various cold bonding techniques were tried. For inorganic binders, cold bonding was tried using autoclave and also without using autoclave. Total number of trials was approximately 200. Dry compressive strengths have been reported in this chapter. It was possible to obtain dry strength of more than 300 N/pellet in some systems and more than 150 N/pellet in many trials. Ore-char composites exhibited few times higher strength as compared to ore-coal composite pellets. Finer particle sizes also improved strength.

Chapter 3 is concerned with apparatus and procedures. There were two experimental set-ups for this study.

(1) set-up for non-isothermal reduction studies

(2) thermogravimetry set-up for isothermal kinetic studies.

The non-isothermal set-up was specially fabricated in the laboratory for this investigation. Reaction chamber containing the pellet was moved at controlled speed into the vertical furnace chamber by a stepper motor assembly. Temperature measurement as well as gas analysis by gas chromatograph were carried out at intervals of time. Pure Ar was continuously passed through the reaction chamber at known flow rate. After the sample reached the maximum temperature (i.e. 1273 K), the reaction chamber was withdrawn from the furnace quickly and cooled.

Isothermal set-up consisted of Cahn 1000 automatic recording electrobalance. Blue dust powder was subjected to flowing H_2 or CO gas for measurement of weight loss as function of time.

Chapter 4 reports technique of measurement of degree of reduction for composite pellets. For reduction of iron oxides by coal, the weight loss of the sample arises not only from oxygen loss, but also loss of carbon, volatile matter etc present in pellet. Review of literature showed that research workers employed various techniques. Except for the laborious method of analysis of metallic Fe, ferrous and ferric oxides, the others are not suited for composite pellet. Therefore, a new procedure was adopted for determining degree of reduction for composite pellet after trials.

Chapter 5 deals with evaluation of composite pellets prepared by various techniques. Measurements consisted of

compressive strength before and after reduction, degree of reduction, volume change after reduction. Strength after reduction was upto 95 N per pellet and it was correlated with volume change. There is no relationship with dry compressive strength.

Chapter 6 presents results and discussions on kinetics of reduction of blue dust by H_2 and CO. Small particles of blue dust in the form of thin (0.4 to 1.5 mm) unconsolidated beds were subjected to reduction in flowing H_2 or CO gas. Temperatures were from 898 to 1123 K for H_2, and 1073 to 1373 K for CO reduction. Reduction by CO was carried out in two-stages : for stage I : (Fe_2O_3 ——> Fe_xO) 50:50::CO:CO_2, and for stage II : (Fe_xO ——> Fe) 50:50::CO:Ar were employed. It was found that rates were not increasing with increasing temperature uniformly but exhibiting maxima/minima type behaviour. It was found that such anomalous behaviours had been observed by other workers for unsintered beds. These have been attributed to structural changes in bed, especially sintering upon reduction.

The line of approach for treatment of data was worked out on the basis of detailed considerations and trials in various ways. Finally, it was decided to take the least square fitted slope of initial approximate straight line in f vs t curves as a measure of initial rate (k). By plotting k vs l (bed depth) for H_2 reduction, it was found that rate (k) decreased with increase of bed depth of sample at different temperatures presumably due to diffusion limitations in bed. By extrapolating the k vs l lines to l = 0, values of $(k)_{l \to 0}$ were obtained. $(k)_{l \to 0}$ was taken as a measure of chemical rate constant (k_c). For CO reduction,

trends were not that systematic. Therefore k at l = 0.4 was taken as a measure of chemical rate constant (k_c). Reliable activation energies could not be determined due to anomalous variation of rate with temperature.

Chapter 7 reports results and discussions of non-isothermal reduction of composite pellets, as well as investigations on devolatilization of coal. It has been demonstrated that good reproducibility was obtained amongst duplicate sets of experiment.

Temperature difference amongst thermocouples located at pellet centre and few mm above pellet was mostly less than 20 K and sometime upto 30 K during non-isothermal reduction. The behaviour pattern has been explained and a procedure evolved to find out average pellet temperature from temperature measured outside pellet.

In non-isothermal experiments, principal gases evolved were CO, CO_2, H_2 along with minor quantity of CH_4. Volumetric evolution rate of gases could be found out from GC data. This allowed calculation of total oxygen loss associated with CO and CO_2 evolution, as well as quantity of hydrogen liberated from the samples.

The principal observation in experiments on devolatilization of coals was that oxygen loss from sample as CO and CO_2 was significantly larger than that expected from removable oxygen content of coal. The excess oxygen has been attributed to combined as well as strongly adsorbed H_2O and CO_2 due to presence of binder as well as the pellet making procedure inspite of oven drying of pellets. Weigth loss of pellets after non-isothermal

runs confirmed significant extra weight loss due to extraneous sources.

This finding has been quantitatively utilized for estimation of fractional reductions due to carbon (f_c) and hydrogen (f_{H_2}) in ore-coal/char composite pellets. f_{H_2} was also calculated from hydrogen balance. Uncertainties in these calculations have been discussed. Most samples showed significant reduction by hydrogen.

An ore-coal composite showed comparable degree of reduction with corresponding ore-char composite. But the former had superior strength after reduction as compared to the latter. Degree of reduction ranged between 46 to 99 pct, strength and volume change upon reduction ranged between 12 to 73 N/pellet and -16 to 108 pct respectively.

X-ray diffraction studies showed that the oxide consisted of Fe_xO and Fe. This allowed quantitative comparison of rates of reduction of iron ore by CO at 1173 K between non-isothermal and isothermal investigation. The agreement is considered to be satisfactory. Scanning electron micrographs of pellets after reduction showed typical features such as growth of whiskers, ridges in wustites, sintering of reduced iron.

Chapter 8 contains summary, conclusions and suggestions for further work.

ACKNOWLEDGEMENT

The author take this opportunity to express deepest sense of appreciation and gratitude to Dr.A. Ghosh, Professor, Metallurgical Engineering Department, Indian Institute of Technology, Kanpur for suggesting the problem, inspiring guidance, and valuable discussions he had with him from time to time.

He gratefully acknowledges Prof.R.N. Biswas, Electrical Engineering Department for providing the stepper motor, and Prof.R.K. Ray, Metallurgical Engineering Department for encouragement during this study.

The author wishes to thank Mr.P. Tiwari for his contribution in the thermogravimetry set-up with Cahn Electrobalance, and Mr.V.C. Srivastova for designing the stepper motor controller.

He sincerely acknowledges the help and active cooperation received from the staff members of Metallurgical Engineering Department specially Mr.A. Sharma, Mr.S.R. Chaurasia, Mr.V.P. Vora, Mr.R.C. Sharma, Mr.B. Jain, Mr.Uma Shankar, Mr.P.K. Pal, Mr.R.K. Prasad, Mr.S.B.Shukla, Mr.D.P. Tripathi and Mr.Ram Avatar at various stages of this study. Thanks are due to Mr.B.D. Biswas for nice typing of the manuscript and Mr.V.P. Gupta for tracing the figures.

Thanks are also due to all his laboratory mates and friends specially Mr.S.K. Choudhary, Mr.T.K. Roy, Mr.R.K. Goyal and Mr.I. Basak for their cooperation.

The author sincerely thank to the M.S.University of Baroda in general and in particular to Prof.M.N. Desai (former Vice-chancellor) for sponsoring him under Quality Improvement Programme; Prof.S.B. Pandya (former Dean, Faculty of Tech.& Engg.), Prof.V.L. Gadgeel (Vice Dean and former Head, Metallurgical Engg.Dept.) and Prof.N.S.S. Murti, Head, Metallurgical Engg. Dept., Faculty of Tech.& Engg., for relieving him from his duty for this study.

The author sincerely acknowledges Dept.of Education, Ministry of Human Resource Development, Government of India for awarding the fellowship under Q.I.P.scheme.

Thanks are also due to all his colleagues specially Mr.A.B. Lele, Prof.S.K. Agarwal and Mr.M.N. Patel Faculty members of Metallurgical Engg. Dept., M.S.University of Baroda, for their cooperation and encouragement during this work.

This study would not have been possible without the patience and cooperation of author's wife Gopa, and other members of his family, Sukriti and Shouvik. The author is thankful to his elder brother, and teacher Mr.Sushil Dutta and Dr.Bisnupada Mukhopadhyay, respectively for their continuous support and encouragement for this study.

The author wishes to thank to the Direct Reduction Process Development Division (DRPDD), R&D Centre for Iron and Steel, SAIL, Ranchi, for providing raw materials for this study.

The goodwill, inspiration and help of many friends and relatives whose names are not included here were a great asset in completing the work.

I.I.T., Kanpur

12th. July, 1991

(S.K. Dutta)

dedicated

to

my parents

Late Sachindra Mohan Dutta & Late Sarmila Dutta

LIST OF CONTENTS

		Page
	SYNOPSIS	iii
	LIST OF FIGURES	xix
	LIST OF TABLES	xxiv
	LIST OF SYMBOLS	xxvii
CHAPTER		
1	LITERATURE REVIEW	1
1.1	Introduction	1
1.2	Literature Review on Composite Pellet	7
1.2.1	Preparation of composite pellets	9
1.2.2	Reduction of composite pellets	11
1.2.3	Use of composite pellets in furnaces	13
1.2.4	Concluding remarks	21
1.3	Brief Review of Mechanism and Kinetics of Reduction of Composite Pellets	22
1.3.1	Kinetics of pyrolysis of coal	23
1.3.2	Kinetics of carbothermic reduction and gasification reaction	29
1.4	Kinetics of Non-isothermal Reduction	37
1.5	Plan of Work	41
2	RAW MATERIALS CHARACTERIZATION, PELLET PREPARATION AND TESTING	43
2.1	Characterization of Raw Materials	43
2.1.1	Size analysis	43

CHAPTER			Page
	2.1.2	Chemical analyses of raw materials	45
	2.1.3	Preparation of coal char	47
	2.1.4	Preparation of lime	47
2.2	Pellet Preparation		47
	2.2.1	Procedure for pellet making	48
	2.2.2	Selection of binders	51
2.3	Testing of Composite Pellets		53
	2.3.1	Concluding remarks on dry strength of pellets	56
2.4	Pellet Making Procedure for Fundamental Studies		58
3	APPARATUS AND PROCEDURE		66
3.1	Apparatus		66
	3.1.1	Set-up for non-isothermal studies	66
	3.1.2	Apparatus for isothermal measurements	72
3.2	Experimental Procedure		76
	3.2.1	Non-isothermal kinetic studies	76
	3.2.2	Auxiliary studies and measurements	82
4	MEASUREMENT OF DEGREE OF REDUCTION		88
4.1	Literature Review		89
4.2	Measurement Technique Adopted in the Present Investigation		94
4.3	Trials		96
	4.3.1	Assessment of carbon loss due to reaction of oxygen in ore	96
	4.3.2	Trial on char gasification with hydrogen	97

CHAPTER		Page
4.4	Concluding Remarks	102
5	A COMPARATIVE STUDY OF PROPERTIES OF VARIOUS TYPES OF COMPOSITE PELLETS	103
5.1	Evaluation of Pellet Properties	103
5.1.1	Compressive strength	104
5.1.2	Non-isothermal reduction	104
5.2	Results and Discussions	105
5.2.1	Dry strength	105
5.2.2	Degree of reduction	106
5.2.3	Volume change	107
5.2.4	Strength after reduction	107
6	RESULTS AND DISCUSSIONS ON REDUCTION OF BLUE DUST BY HYDROGEN AND CARBON MONOXIDE	120
6.1	Literature Review on Gaseous Reduction of Iron Ores or Oxies	120
6.2	Method of Data Analysis Adopted in the Present Investigation	124
6.2.1	Introduction	124
6.2.2	Empirical treatment of data	125
6.3	Results	127
6.4	Discussions of Results	132
6.4.1	Processing of f vs t data	132
6.4.2	Determination of rate constant (k_c)	145
6.4.3	Interpretation of k_c	149

CHAPTER			Page
7	RESULTS AND DISCUSSIONS ON NON-ISOTHERMAL REDUCTION OF COMPOSITE PELLETS		154
7.1	Simultaneous Measurement of Ambient and Sample Core Temperature		156
7.2	Gas Chromatography-Calibration and Data Processing Procedure		163
7.3	Non-Isothermal Devolatilization of Coal		168
7.4	Non-Isothermal Reduction of Composite Pellets		173
	7.4.1	Results and their reproducibility	173
	7.4.2	Discussions on exit gas composition	180
	7.4.3	Estimation of extent of reduction of ore by carbon and hydrogen	185
	7.4.4	Comparison of reduction behaviour of ore-coal and ore-char composities	191
	7.4.5	X-ray diffraction studies	192
	7.4.6	Comparison of rate of reduction by CO in non-isothermal and isothermal reduction experiments	195
	7.4.7	Scanning electron microscopic studies	198
8	SUMMARY AND CONCLUSIONS		204
8.1	Summary of Studies		204
8.2	Salient Findings and Conclusions		208
	8.2.1	Evaluation of binder and pellet making procedure	208

CHAPTER			Page
	8.2.2	Fundamental studies of non-isothermal reduction and coal devolatilization	209
	8.2.3	Kinetics of reduction of blue dust by H_2 and CO	211
8.3	Suggestions for Further Work		212
REFERENCES			213
APPENDIX			
A	Data on Reduction of Blue Dust by Hydrogen		221
B	Data on Reduction of Blue Dust by Carbon Monoxide		233
C	Data on Gas Chromatographic Analyses of Exit Gas for Non - Isothermal Reduction of Composite Pellets		243
D	Program for Data Processing of H_2 Reduction of Blue Dust		251

LIST OF FIGURES

Figure	Title	Page
1.1	Variation of wind drum pressure and stack gas composition with metallics from pellets in a cupola	16
1.2	Variation of stack gas and hot blast temperatures with metallic from pellets in a cupola	17
1.3	Variation of C, Si, Mn and S of hot metal with metallics from pellets in a cupola	19
1.4	Thermogravimetric curves, TGA and DTG of carbonization of coal and coal/iron oxide mixtures	27
1.5	Kinetic data for non-isothermal reaction in an ore-char mixture under an argon atmosphere	39
2.1	Schematic representation of the pellet making unit	50
3.1	Set-up for non-isothermal kinetic studies of composite pellet reduction (schematic)	67
3.2	Temperature profile of furnace for non-isothermal studies	69
3.3	Schematic diagram of the thermogravimetry set-up with cahn electrobalance	74
3.4	Schematic diagram of the gas train used with thermogravimetry set-up	75

Figure	Title	Page
3.5	Hanging assembly for thermogravimetry	84
4.1	Rate of gasification of Hutar coal char in hydrogen	100
4.2	Rate of gasification of Bachra coal char in hydrogen	101
5.1	Volume change vs strength after reduction for different pellets	108
6.1	Fractional reduction vs time plots for hydrogen reduction of blue dust at 973 K	129
6.2	Fractional reduction vs time plots for hydrogen reduction of blue dust at constant bed depth	131
6.3	Overall fractional reduction vs time plots for reduction of blue dust by CO	133
6.4	Fractional reduction vs time plots for second stage reduction of blue dust in CO-Ar mixture at constant bed depth	134
6.5	Curves showing fit with experimental f vs t data	136
6.6	(df/dt) vs bed depth at f = 0.3 and f = 0.5 for hydrogen reduction of blue dust	137
6.7	(df/dt) vs bed depth at f = 0.3 and f = 0.5 for carbon monoxide reduction of blue dust	138

Figure	Title	Page
6.8	-ln(1 - f) vs t plots for H_2 reduction of blue dust	140
6.9	-ln(1 - f) vs t plots for CO reduction of blue dust	141
6.10	log(df/dt) vs log(1 - f) curves for H_2 reduction of blue dust	143
6.11	Comparison of reduction data with parabolic rate law	144
6.12	f vs t curves approximately as two intersecting straight lines	146
6.13	k vs 1 for hydrogen reduction of blue dust	147
6.14	k vs 1 for carbon monoxide reduction of blue dust	148
6.15	ln k_c vs 1/T plots for gaseous reduction of blue dust	152
7.1	Variation of ΔT with temperature in non-isothermal studies of composite pellets (Hutar coal/char)	157
7.2	Variation of ΔT with temperature in non-isothermal studies of composite pellets (Bachra coal/char)	158
7.3	Variation of ΔT with temperature in non-isothermal studies of composite pellets at low speed	159

Figure	Title	Page
7.4	Calibration of gas chromatograph in hydrogen carrier gas	164
7.5	Variation of exit gas composition and $\dot{W}_o$ with temperature in non-isothermal devolatilization studies	169
7.6	Reproducibility of exit gas compositions amongst duplicate sets of experiments	177
7.7	Reproducibility of (a) degree of reduction and (b) strength after reduction amongst duplicate sets of experiments	178
7.8	Variation of exit gas composition and $\dot{W}_o$ with temperature in non-isothermal studies at high heating rate for low pct Hutar coal	181
7.9	Variation of exit gas composition and $\dot{W}_o$ with temperature in non-isothermal studies at low heating rate for low pct Bachra coal	182
7.10	Variation of exit gas composition and $\dot{W}_o$ with temperature in non-isothermal studies at low heating rate for high pct char	183

Figure	Title	Page
7.11	Comparison of degree of reduction of ore-coal and corresponding ore-char composite pellet	193
7.12	Comparison of (a) strength and (b) volume change upon reduction for ore-coal and ore-char pellets	194
7.13	Scanning electron micrographs for reduced composite pellets	201 & 202

LIST OF TABLES

Table	Title	Page
1.1	Estimated reserves of blue dust in major Indian iron ore mines	5
1.2	Scrap and composite pellets charged in cupola	15
1.3	Distribution of volatiles for a raw bituminous coal	25
2.1	Size analyses of raw materials	44
2.2	Analysis of blue dust	45
2.3	Proximate analyses of coal and char	46
2.4	Ultimate analyses of coals	46
2.5	Analyses of coal ash	46
2.6	Compressive strengths of dry composite pellets using organic binders	60
2.7	Compressive strengths of dry composite pellets using inorganic binders (without autoclave)	61
2.8	Compressive strengths of dry composite pellets using inorganic binders (with autoclave)	62
2.9	Compressive strengths of dry composite pellets using combination of organic and inorganic binders	65
3.1	Calibration equations for flowmeters at STP	76
3.2	Solubility of gases in water	77
3.3	Dimensions of inconel crucibles	85
4.1	Thermodynamic data for methane formation	98

Table	Title	Page
5.1	Specifications of composite pellets prepared in laboratory for evaluation	110
5.2	Specifications of SAIL composite pellets	112
5.3	Test results for composite pellets with Hutar coal and char	114
5.4	Test results for composite pellets with Bachra coal and char	118
5.5	Test results for SAIL composite pellets	119
6.1	Variables for H_2 and CO reduction of blue dust	128
6.2	Specific rate constants (k) and chemical rate constants (k_c) for reduction by H_2 and CO	150
7.1(a)	Oxygen balance calculation for devolatilization experiments	171
7.1(b)	Hydrogen balance calculation for devolatilization experiments	171
7.2	Variables for non-isothermal reduction of composite pellets	174
7.3	Experimental conditions for non-isothermal reduction of composite pellets	175
7.4	Results for non-isothermal reduction of composite pellets	179
7.5	Removable oxygen and fractional reductions in non-isothermal studies of composite pellets	188
7.6	Calculation of f_{H_2} from hydrogen balance in non-isothermal studies	191

Table	Title	Page
7.7	Results of X-ray diffraction studies	195
7.8	Comparison of experimental and calculated rate of reduction of iron oxide by CO for non-isothermal studies	197
7.9	Details of SEM samples	200
7.10	Summary of SEM observations	203

LIST OF SYMBOLS

A	=	Pre-exponential constant
a	=	Dimensionless kinetic parameter
a_o, a_1, a_2, a_3	=	Empirical constants
B	=	Heating rate
E	=	Activation energy, $KJ.mol^{-1}$
F	=	Fractional weight loss
f	=	Fractional reduction
f_b	=	Fraction of blue dust present in composite pellet
f_c	=	Fractional reduction of iron ore by C
f_{H_2}	=	Fractional reduction of iron ore by H_2
f_o	=	Fraction of oxygen present in Fe_2O_3
$f_{o(coal)}$	=	Fraction of organic oxygen in coal
f_{coal}	=	Fraction of coal in pellet
$FC_{(char)}$	=	Fixed carbon contain of char sample, g
ΔG^o	=	Standard free energy change
h	=	Height difference in flowmeter, cm
I_1, I_2, I_3	=	Constants
K_e	=	Equilibrium constant
k	=	Rate constant, s^{-1}
k_c	=	Chemical rate constant, s^{-1}
k_n	=	n th order rate constant, s^{-1}

L	=	Distance from top of the furnace, mm
l	=	Bed depth of the sample (blue dust), mm
p	=	Fractonal concentration of Fe_2O_3 in blue dust
P_i	=	Partial pressure of gas species i, bar
Q_i	=	Volumetric flow rate of gas species i, $cm^3.s^{-1}$
R	=	Gas constant
T	=	Temperature, K
T_1	=	Ambient temperature, K
T_2	=	Core temperature of the pellet, K
T_p	=	Average pellet temperature, K
T_s	=	Surface temperature, K
t	=	time, s
V_1, V_2	=	Volumes of pellet before and after reduction, mm^3
ΔV	=	Change in volatile matter of coal
ΔV_o	=	Volatile matter of raw coal
ΔW	=	Weight loss of pellet, g
$(\Delta W)_{I,T}$	=	Total oxygen consumed during 1st stage of CO reduction, g
$(\Delta W)_{II}$	=	Weight loss in 2nd stage of CO reduction, g
ΔW_o	=	Weight of oxygen removed from iron oxide, g
ΔW_{ch}	=	Total weight loss of char, g
$\Delta W_o'$	=	Total oxygen loss due to evolution of CO and CO_2, g
ΔW_o^C	=	Oxygen loss associated with reduction of iron oxides by carbon, g
ΔW_o^H	=	Equivalent oxygen removed from iron oxide in sample by H_2 reduction, g

$(\Delta W^i)_{II}$ = Total removable oxygen present at the start of second stage reduction of CO, g

W_o^l = Total weight of removable oxygen present in iron oxide, g

W_p^i = Initial weight of composite pellet, g

W_o^r = Total weight loss during H_2 reduction, g

$\dot{W}_c$ = Rate of weight loss of carbon, $g.s^{-1}$

$\dot{W}_o$ = Rate of weight loss of oxygen, $g.s^{-1}$

$\dot{W}_o^c$ = Rate of oxygen loss due to carbon, $g.s^{-1}$

X_i = Volume fraction of species i

x = Dimensionless kinetic parameter

α = Degree of reduction

CHAPTER 1

LITERATURE REVIEW

1.1 Introduction

The term **Composite Pellet** is being employed here to mean pellet containing mixture of fines of iron bearing oxide and carbonaceous material (coal, coke, char), which has been imparted sufficient green strength for subsequent handling by cold bonding technique. The pellet should have sufficient strength to withstand high temperature and stresses in reduction furnaces.

Reduction of iron oxide/ore by carbon is a key metallurgical reaction in ironmaking. Several investigations[1-14] have been carried out on the reduction of iron oxide/ore by carbon. Most of them[1,3,7-11] employed mixtures of iron oxide or iron ore powder with carbon powder. Sometimes the oxide was agglomerated into micropellets before use[6,8,9,13,14].Several investigators[3-5,7,12,14] also prepared pellets by compaction at high pressure. All the above were concerned with kinetic studies in laboratory. In a way these are also investigations on composite pellets. However in the context of the present study these will not be considered as composite pellets since investigators were not concerned with strength as well as subsequent use of pellets. So cold bonding had not been resorted

to by them. However these studies are of considerable help in understanding of reduction behaviour of composite pellets.

Blast furnace process is the best for ironmaking as of now. However this fully established process is now facing problems like shortage of good quality coke, and higher investment cost for furnace and auxiliary equipments. Energy experts also have forecast that in the coming decade the cost of high grade coking coal would rise at a much faster rate than electricity and non-coking coal[15].

Pig iron is the basic raw material for cupolas in iron foundries. Traditionally, major integrated steel plants have been the producers and suppliers of pig iron to foundries. Pig iron is also produced in small quantities in electric smelting furnaces. In India, foundries are showing a steady growth, and iron castings of superior quality are also in demand. However, during the last two decades or so there is shortage of pig iron in India[16]. The demand far outstrips the supply, leading to serious problems of non-availability. Hence foundries have been demanding import of pig iron. The total installed capacity of foundries in India is around 2.3 million tonnes. A projection[17] is available regarding the demand and indigenous availability of pig iron in the next decade as follows :

Unit : X 1000 tonnes

Year	Demand	Availability	Shortfall
1990 - 1991	1830	1702	128
1994 - 1995	2200	1864	336
1999 - 2000	2800	2548	252

However estimates vary and it seems the current shortage is at least 300,000 to 400,000 tonnes per year.

Again the rapid growth of electric arc furnace steelmaking process in the last decade has created a growing demand for steel scrap, as a result of which the scrap is in short supply in India. In recent years, significant improvement in steel plant yield (from 81-83pct to 94-95pct) has decreased the amount of in-plant generated scrap, and resulted in a shortage of scrap supply throughout the World[18]. That is why sponge iron has been fast gaining in popularity throughout the World because it is a substitute for steel scrap. Advantages of sponge iron as a feed material are well known[19]. Keeping in view of short fall between demand and generation of scrap, the Government of India has granted licence to 10 plants for producing sponge iron of about 3.5 million tonnes per year.The total installed capacity for production of sponge iron in India is 1.4 million tonnes per year[20].

India has a large deposit of non-coking coal with reserves about 63 billion tonnes, which constitutes 77pct of the total coal reserves[21]. On the other hand natural gas reserves are restricted only to western and north-eastern India as of now. Price of natural gas is also high (presently around Rs.2000 per 1000 Nm^3 gas)[20]. It is also reported[22] that the production cost of sponge iron with natural gas as a reductant is expected to be higher than that produced with non-coking coal. Therefore, 8 out of 10 sponge iron plants in India are based on rotary kiln process which would use non-coking coal.

However, rotary kiln processes suffer from drawbacks such as[23] :

(i) low productivity due to long residence time in the kiln,

(ii) low carbon content in the sponge iron produced (around 0.2pct),

(iii) inability to use fines by conventional pelletization due to high cost of heat hardening of pellets.

Recent studies by various researchers have demonstrated that cold-bonded composite pellets can be successfully charged as burden material in cupola[24-28] or rotary kiln[28-30]. Reduction is much faster with composite pellets than with ordinary iron ore pellets or lumps. This lowers residence time in rotary kiln by a factor of 6 to 8, thus improving productivity. Reduction of oxide has been achieved satisfactorily in cupola as well.

Indian iron ore deposits are soft and friable in nature. So they contain quite a good amount of superfines (-200 mesh) rich in iron content (65pct and above) and low gangue content. These are known as **Blue Dust**. Estimated reserves of blue dust in India is around 550 million tonnes[31]. The data for Indian iron ore mines are presented in Table 1.1[32]. Apart from this, around 4 million tonnes of fine slimes containing 55 to 60pct Fe are generated every year by ore washing plants in India[31]. Again a lot of coal fines and coke breeze are also produced during coal mining and coking of coal respectively. Utilization of these fines for extracting metal is of vital concern for resource

conservation and pollution control.

Interest in iron oxide/ore-carbon composite pellet technology has been there for many years without any significant successful application in ironmaking. The principal technological problem was to produce such composite pellets at low cost. Advances in cold bonding technology has brightened the prospects. It has been well known for a long time that reduction of iron oxide is about an order of magnitude faster, if the pellet contains mixture of oxide fines and carbon fines. Use of such composite pellets will also lead to utilization of blue dust and coal fines or coke breeze.

Table 1.1

Estimated Reserves of Blue Dust in Major Indian Iron Ore Mines[32]

Unit : X 10^6 tonnes

Sl.No.	Mines	Estimated Reserves	Sl.No.	Mines	Estimated Reserves
1	Bailadila	183.0	7	Daitari	8.8
2	Chiria	134.0	8	Kiriburu	7.0
3	Noamundi	67.7	9	Barsua	6.0
4	Gua	23.0	10	Kalta	4.0
5	Bolani	11.0	11	Meghataburu	3.0
6	Donimalai	9.0	12	Joda	1.9

Therefore technological relevance of iron ore-coal/coke composite pellets has been recognized. As mentioned earlier that composite pellets have been used partially or fully as burden material in cupola[24-28], rotary kiln[28-30] and even blast furnace[28,33,34]. Some studies[35-42] have been conducted on preparation and reduction characteristics of composite pellets as well.

In cupola, as the feed material goes down it is gradually heated up and hence reduction of oxide in composite pellet would occur non-isothermally. The same is true for rotary kiln or blast furnace also. In the laboratory too it has been found that it takes 15 minutes or so to bring the pellet to the temperature in the so-called isothermal kinetic investigations and significant reduction takes place by then.

Therefore, from a fundamental point of view, it is desirable to carry out non-isothermal reduction studies. However, not a single non-isothermal investigation could be located in literature on composite pellets. During reduction of ore-coal composite pellets, evolution of hydrocarbons also takes place due to pyrolysis of coal. Decomposition of hydrocarbons also occurs at high temperature (above 900 K). Simultaneously gasification of carbon by CO_2 takes place. Hence the overall process will be a coupled reaction of evolution of hydrocarbons, decomposition of hydrocarbons, reduction of iron oxide,and gasification reaction. Again, very little information is available on interaction of these simultaneous phenomena on reduction behaviour.

The present thesis has been divided into eight chapters. Chapter 1 reviews the literature on composite pellets and reduction kinetics. It also contains plan of work. Chapter 2 reports on raw material characterization, composite pellet preparation,testing of pellet strength, and discussion of the test results. Chapter 3 contains the design and fabrication features of the apparatus used for non-isothermal studies, apparatus used for isothermal studies, and the experimental procedures. Chapter 4 reports on measurement of the degree of reduction. Chapter 5 presents the results on reduction and strength measurements on composite pellets from different sources including those prepared by author. Chapter 6 discusses the reduction kinetics of blue dust by H_2 and CO gas. Chapter 7 presents results and discussions of fundamental non-isothermal kinetic studies of composite pellets. Chapter 8 contains the conclusions reached from the present investigation, and suggests the scope for future study.

1.2 Literature Review on Composite Pellet

The iron and steel industries produce large quantities of waste materials as by-product. These materials include blast furnace dust, basic oxygen furnace dust, mill scale, fine metallic scrap, iron ore fines, coke breeze,and coal dust. Pelletizing has proved satisfactory for agglomeration of fine materials. However, conventional pelletization process requires hardening of the pellets by firing at near fusion temperature

(1500 to 1600 K) using mostly oil-fired furnaces. Therefore, production costs of these indurated pellets are increasing day by day due to the increasing oil price. Alternative energy saving process is the **cold-bonding technology** for pellet making which is becoming more and more popular now-a-days all over the World.

The pellets are hardened in cold-bonding processes due to physico-chemical changes of the binder at low temperatures, the free ore grains remaining intact. This benefits the reducibility of pellets as well[43]. Details of cold-bonding processes for ordinary pellets are available in standard texts[43,44].

The ore-reductant composite pellets can be prepared only by cold-bonding technology. A composite pellet contains iron oxide and carbon fines. When the composite pellet is introduced into a furnace for heat hardening,carbon will burn off before the oxide particles get chance to develop strength through sintering due to oxidizing atmosphere around. Moreover hydrocarbons etc. will be liberated. All these would, first of all, mean loss of reductants. Secondly evolution of gases would cause disintegration of pellets. Thermal stresses due to heating would be aggravating this tendency.

Therefore, for increasing green strength of composite pellets,binders are to be added to bind the particles at room temperature or at somewhat elevated temperature (maximum 500 K or so). General requirement for good quality agglomerates includes sufficient strength for handling, transportation and outside storage, as well as complete reduction in iron and steel furnaces

without degradation or excessive swelling[34].

1.2.1 Preparation of composite pellets

Research workers tried to prepare iron oxide/ore + coal/coke/char composite pellets. Various organic as well as inorganic binders have been tried. Starch-based binders, dextrin, molasses and oil slush are some organic binders[23,30,38]. Bentonite[45], cement[26,35,41,46], sponge iron powder[29,42],quick lime[47],lime and silica[25,27,28,37] have been employed as inorganic binders.

Hatarasen and Dian[45] prepared composite pellets with 2pct Bentonite as a binder. Three types of oxides were used, viz.mill scale, Indian iron ore, and Telive concentrate. Pellets were made with 15pct coke dust.

Composite pellets were prepared from 88.9pct waste material (basic oxygen furnace dust,mill scale, blast furnace dust and blast furnace sludge in 2.2:1.3:1:1 ratio) and 11.1pct coke breeze along with 10pct cementious binder[35]. After 28 days of ageing, compressive strength of pellets was found as 1080 N. Duran et al[26], and Takahashi et al[41,46] also employed cement binder for making iron oxide + coal/coal char composite pellets.

The Michigan Technological University, USA carried out work since 1960 on the strengthening of pellets by hydrothermal bonding. Lime and silica flour were added to the mixture of iron bearing material and coal or coke dust. The pellets were strengthened in an autoclave by steam curing for 1 to 2 hours at 5.1 to 20.4 bar pressure. This process is known as MTU-cold bond

process[25,27,34]. Compressive strengths of MTU composite pellets were reported[27] to vary from 952 to 2037 N per pellet (13 to 25.4 mm diameter pellets). Lotosh et al[33] also used autoclave for preparing ore-coal pellets. Industrial production of autoclaved pellets (which contain 5pct coal) were made with quick lime as binder[47].

Xi-lun[29] used sponge iron powder as binder for ore-coke pellets. He found that the compressive strength of 100 to 200 N per pellet (8 to 10 mm diameter) was suitable for direct charging into rotary kiln. Ganguly and Patalah[42] also employed sponge iron fines as a binder for ore-coal composite pellets.

Research and Development Centre for Iron and Steel (RDCIS) at Ranchi, studied[30] the possibilities of different organic binders for making ore-coal composite pellets. Concentrates of Kudremukh iron ore and blue dust from Gua mines, and Hutar coal have been used as iron ore and coal respectively. Some trials were also given with activated char, petroleum coke and Assam coal. -100 mesh size raw materials were taken and 5,10,15pct coal were added. The investigators used molasses, oil slush and starch based binder as organic binders and Bentonite, sodium silicate, lime as inorganic binders. Except starch based binder, all other binders did not yield sufficient strength. Concentration of starch based binder was 0.5 to 5.0pct, and it showed that with increase of binder concentration, the strength of composite pellet also increased. Maximum strength was reported as 250 N per pellet (6 to 10 mm diameter) with 5pct binder. It was also reported[23] that green strength of the composite pellets

increased upto 300 N per pellet by using dextrin as binder. Small amounts of phenol formaldehyde were employed with success to improve the decrepitation characteristics of the pellets.

1.2.2 Reduction of composite pellets

It has been reported by many investigators that reduction of composite pellets is an order of magnitude faster as compared to that of ordinary pellets by solid carbonaceous reductants[25,27,28,30,34,37].

MTU cold-bonded pellets[25,27,28] were prepared from iron oxide fines with 15 to 20pct carbonaceous fines. It was observed that the largest portion of the carbon present in the composite pellets was consumed in 15 minutes at a temperature of 1366 K, and the pellets got completely metallized in 5 to 15 minutes at higher temperatures.

It has been reported[30] that with a reduction time of 15 minutes at 1323 K, the degree of metallization was more than 84pct. The investigators also observed that increasing coal content in composite pellets increased the degree of metallization as well as carbon percentage in reduced pellets.

Kiselev et al[36] studied the reduction kinetics of ore-carbon composite pellets prepared from magnetic concentrates with 8,12 and 17pct of solid reductant. Mathematical analyses of results were also carried out.

Seaton et al[37] investigated the reduction kinetics of hematite/magnetite + coal char composite pellets in temperature range of 1073 to 1473 K. They observed that at lower temperature

(1273 K) hematite pellets reduced faster than the magnetite ones. The rate of reaction increased with increasing temperature, and the reduction of hematite appeared to be enhanced by increasing the lime content. They found that the steps $Fe_2O_3 \longrightarrow Fe_3O_4 \longrightarrow$ FeO and $Fe_3O_4 \longrightarrow$ FeO took place rapidly during early stages of reduction. They also measured the surface and center temperatures of the composite pellets. It was found that 15,27 and 10 minutes were needed for the pellets to reach thermal equilibrium at 1273, 1373 and 1473 K respectively.

The potentiality of petroleum coke known as flexicoke as a solid reducing agent for iron oxides in the manufacturing of cold bonded composite pellets has been reported[39]. The investigators observed that the flexicoke could be employed as a solid reductant to yield level of reduction in excess of 90pct, and degree of metallization of approx.85pct.

Hatarasen and Dian[45] carried out pre-reduction of iron ore + coke/coal pellets in a revolving furnace. The degree of reduction achieved was not less than 74pct and the compressive strength of the pellets was not less than 1200 N per pellet.

Takahashi et al[46] carried out reduction experiments for cold bonded pellets containing char by using a pressurized moving bed reactor in laboratory. They found that the crushing strength of the pellet decreased remarkably in the moving bed during the reduction upto the degree of reduction of 20pct. However, the reduction of the pellets proceeded without much change of shape and volume.

Sidorskii et al[48] investigated the influence of slag-forming additions to the mix for iron ore-carbon pellets on metallized product quality. Petroleum coke acted as carbon source and additives were Na_2CO_3 and $CaCO_3$. They found that addition of these mixed carbonates to the pellets contributed to lower strength but better properties so as not to cause excessive swelling during metallization.

1.2.3 Use of composite pellets in furnaces

1.2.3.1 Cupola

Composite pellets have been tested in cupola as burden material and results are reported[24-28] to be encouraging. They could be reduced completely and melted within normal retention time in the cupola. Trials[24] were given in a laboratory size cupola (457 mm i.d. and 4572 mm height) with low grade iron ore (32pct total Fe and 24.5pct SiO_2) + char (70pct fixed C,10pct ash) composite briquettes. The ratio (by weight) of briquettes to coke into charge was kept from 3:1 to 5:1. Composite briquettes contained 73pct ore, 11pct char, 6pct lime, and rest binder. Heat for the process was supplied by the burning coke bed, not by the carbon contained in the composite which was only sufficient to satisfy the reduction reactions. The iron oxide was reduced to iron by the carbon of the char within the briquette. The investigators found that cupola operated smoothly during the smelting trials. The percentage of iron recovered in the cast iron from ore entering the process was about 75pct for all three trials.

Keiser et al[25] have reported test results of production size cupolas (5 to 40 tonnes per hour) with a charge of 5 to 100pct iron units from MTU composite pellets. Most of the tests were carried out with a charge consisting of 70pct of the iron units in the oxide form (i.e., as composite pellet) and 30pct from scrap. 100pct burden of composite pellets in cupola was also successful. The melting rate by using 100pct pellet charge was approximately 50pct of that for an all scrap charge.

Experiments[26] were conducted in an industrial cupola (1200 mm i.d.) with 5 and 10pct composite pellets in the charge. Black heart malleable cast iron of the ferritic and pearlitic grades was produced without significant changes in the melting rate, metal temperature in the cupola spout, coke rate, slag volume and blast rate of the cupola.

Goksel et al[27,28] claimed much success by using MTU Pelle Tech composite pellets as a burden material in a cupola. Initial tests were conducted in a 305 mm diameter highly instrumented research cupola. The success of the tests led to subsequent tests in 1372,1422,1981 and 2438 mm diameter hot blast production cupolas. The results demonstrated that composite pellets were an excellent charge material and produced various grades of iron including ductile iron, gray iron and conventional pig iron. Another programme in a commercial 1981 mm diameter hot blast cupola started with conventional scrap charge without any composite pellets. The scrap was gradually replaced by equivalent iron units as composite pellets. 20,50 and 100pct of the metallic iron units were supplied by composite pellets (as shown in Table

1.2). The pellets were produced from waste iron oxide and coke fines. It has been reported that reduction of composite pellets was completely satisfactory in all tests and practically all iron units were recovered.

Blast air pressure had to be increased with increasing pellet percentages (Figure 1.1), but were still acceptable for good cupola operation according to investigators[27,28]. The stack gas temperature generally remained between 475 to 589 K (Figure 1.2). Slag volume and separation, as well as slag viscosity were normal during the tests. However, basicity adjustments were made

Table 1.2

Scrap and Composite Pellets Charged in Cupola[27]

Materials	Normal Scrap Charge		Composite Pellet Charge Metallics from Pellet					
			20(pct)		50(pct)		100(pct)	
	Weight		Weight		Weight		Weight	
	Kg	(pct)	Kg	(pct)	Kg	(pct)	Kg	(pct)
Metallics :								
Comp.Pellets	-	-	363	18.88	907	47.17	959	98.56
Steel # 2	567	23.86	-	-	-	-	-	-
Steel Fragments	1418	59.68	1451	75.46	907	47.17	-	-
Steel Pl.& St.	282	11.87	-	-	-	-	-	-
Siliconcarbide	109	4.59	109	5.66	109	5.66	14	1.44
	2376	100.00	1923	100.00	1923	100.00	973	100.00
Coke	272	11.45	302	15.70	454	23.61	295	30.32
Limestone	90	3.79	23	1.20	-	-	-	-
Gravel	-	-	-	-	9	0.47	32	3.29
Total	2738		2248		2386		1300	

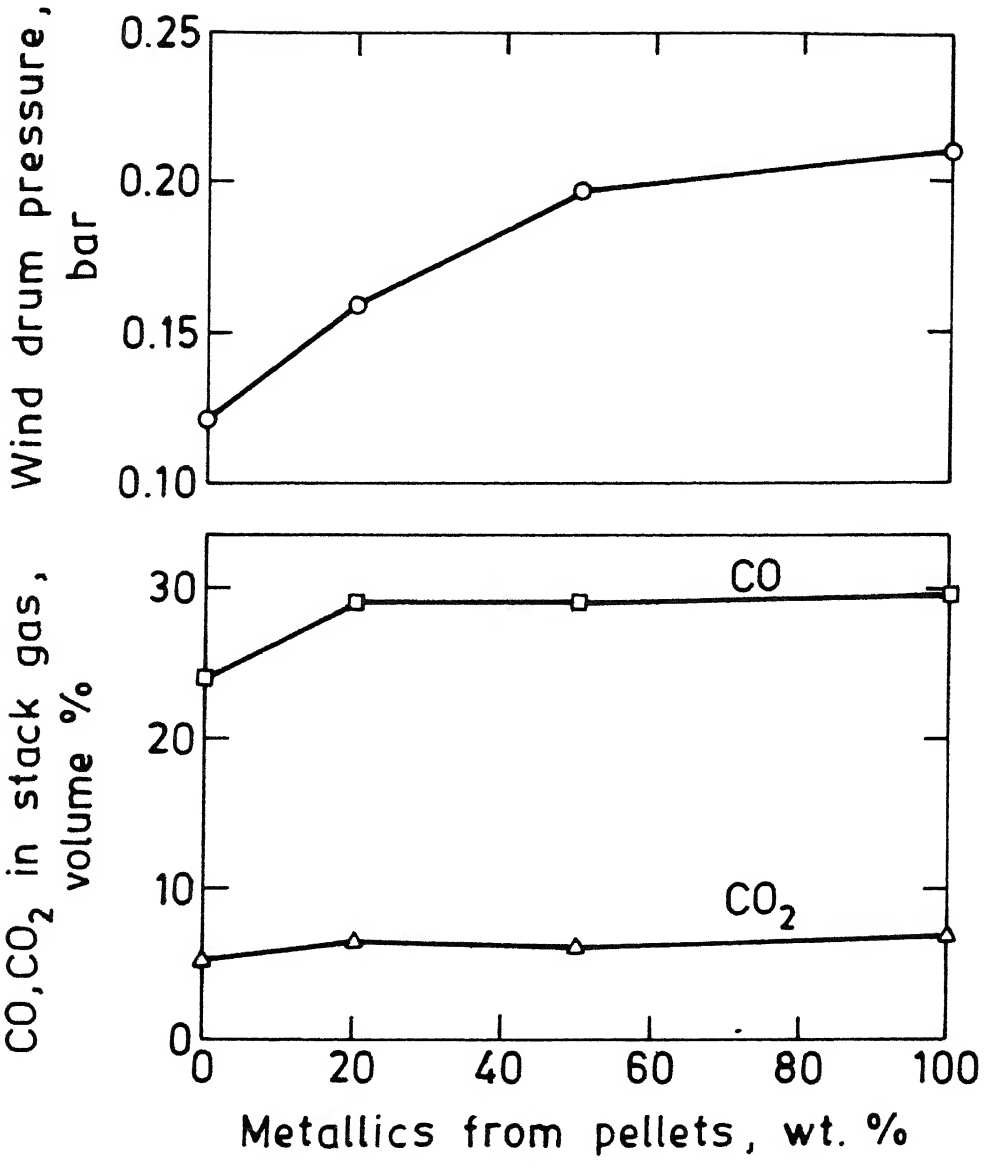

Fig. 1.1. Variation of wind drum pressure and stack gas composition with metallics from pellets in a cupola[27].

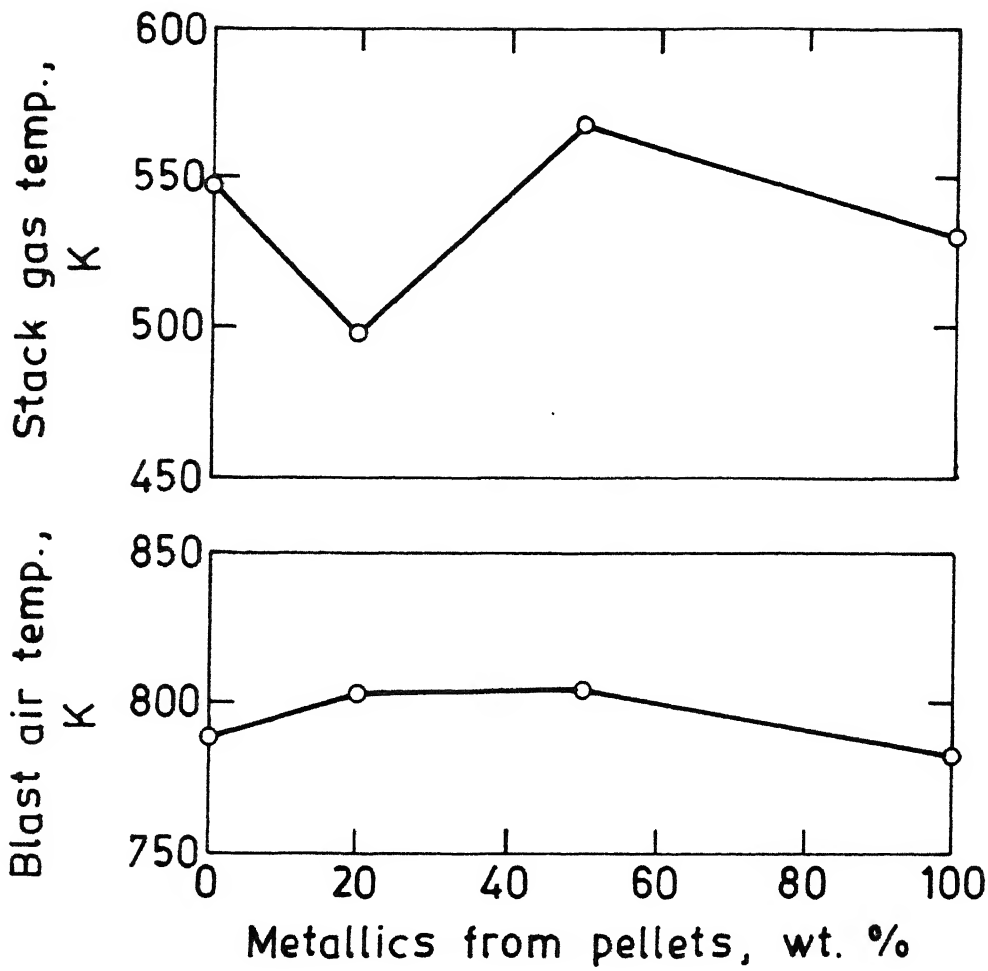

Fig. 1.2. Variation of stack gas and hot blast temperature with metallics from pellets in a cupola[27,28].

by adding lime, gravel, or fluorspar to the charge as shown in Table 1.2. The slag volume increased in proportion to the quantity of the pellets in the charge, but this never exceeded the volume for blast furnace operation. Metal/carbon ratio and metal melting rate decreased as percent pellets in the charge was increased. These were due to the higher heat requirement for reduction of pellets and also to increase in slag volume. However, the metal temperature remained between 1755 to 1811 K. Figure 1.3 shows variation of metal composition with change of pellet percent in charge.

The advantages of composite pellets as a feed material in cupola can be summarised as follows.

(i) Shortage of pig iron/scrap can be avoided by replacement of pig iron/scrap with composite pellets.

(ii) Price of the composite is expected to be more stable than price of pig iron or scrap, which depends on demand and supply of the market.

(iii) Instead of large size cupola coke (100x150 mm), the cheaper small size blast furnace coke (50x75 mm) can be used.

(iv) Sulphur content in metal can be controlled by adjusting the carbon and basicity of the pellets.

(v) Composite pellets are uniform in size.

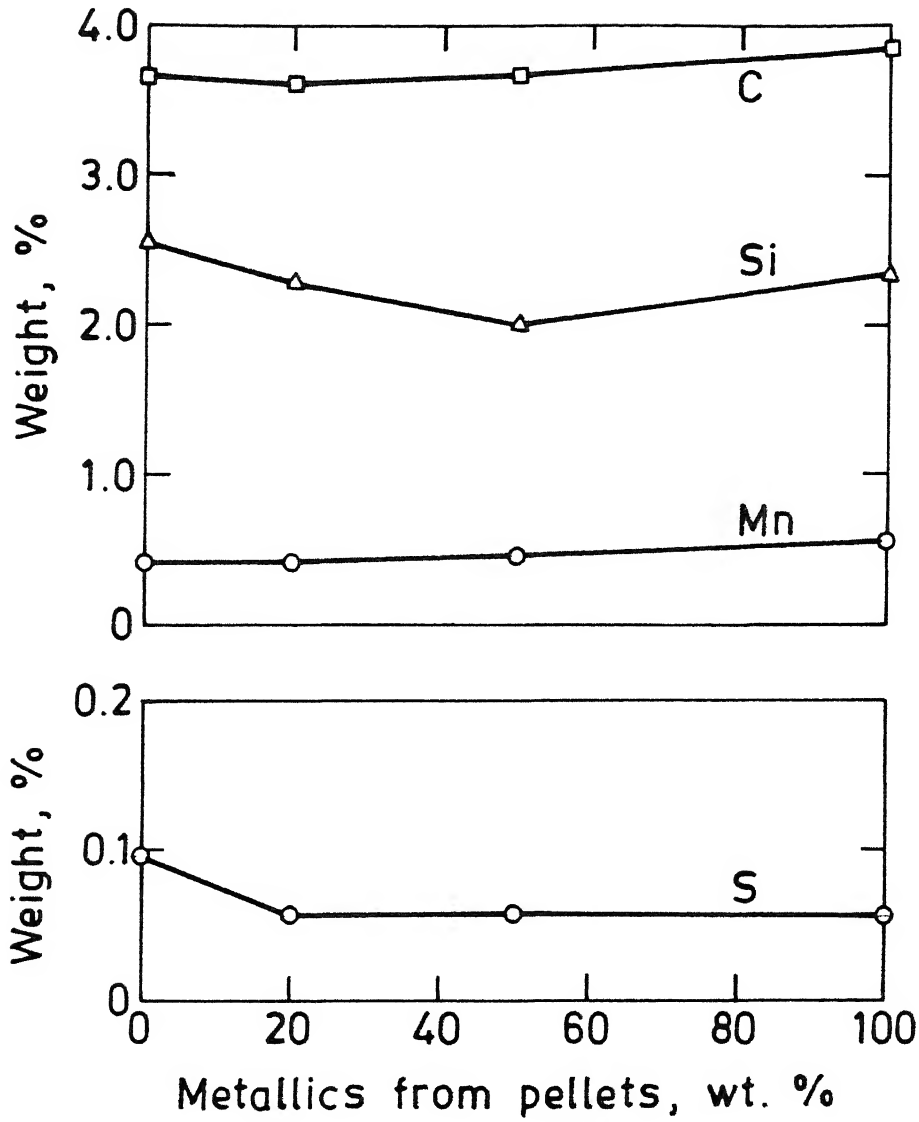

Fig. 1.3. Variation of C,Si,Mn and S of hot metal with metallics from pellets in a cupola[27,28].

1.2.3.2 Rotary kiln

Composite pellets were also charged to the rotary kiln for production of sponge iron[28-30]. They were metallized in approximately 7 minutes when the flame temperature of the kiln was about 1589 K. Total residence time in the kiln was reduced to 40 minutes from 8 to 10 hours. It was observed that the production of a given kiln (with composite pellet charge) would be more than double the production obtained by using feed coal and either iron oxide pellets or lump ore[28]. This was due to rapid reduction rate of composite pellets. It was also found[29] that the compressive strength of 100 to 200 N per pellet (8 to 10 mm diameter) was suitable for direct charging into rotary kiln. Metallization rate was about 95pct with less than 6pct powder formation.

Trials[30] were also given in a pilot scale rotary kiln (645 mm i.d. x 1750 mm length) at Research and Development Centre for Iron and Steel, SAIL,Ranchi. The investigators observed about 85 to 94pct metallization and 1.2 to 2.0pct carbon content in sponge iron which was achieved after about 35 to 45 minutes of residence at a reduction temperature of 1313 to 1353 K. Ore/coal ratio was 9.0 in pellets.

Therefore, advantages of composite pellets used as a feed material in a rotary kiln are as follows[23].

(i) Increased productivity : a highly efficient reduction behaviour which leads to a drastic reduction in the retention time thereby improving productivity many folds.

(ii) Improved product quality: an improved metallurgical quality of the product due to increased carbon content (0.5 to 1.0pct) in the sponge iron with good metallization.

1.2.3.3 Blast furnace

Composite pellets were also used as feed material to blast furnace. Weiss et al[28] conducted blast furnace test of approx. 5000 tonnes of MTU cold bonded pellets with success. The pellets were produced from waste iron oxides that included mill scale (56.7pct), BOF dust (18.9pct), blast furnace flue dust (14.4pct), and binders (7pct burnt lime and 3pct silica flour). Pellets contained approx. 5pct carbon. Compressive strength was 1814 N per pellet (19 mm diameter). The test consisted of a 15 days period when the burden contained 10pct MTU pellets, 56.7pct conventional pellets and 33.3pct sinter. Test results showed that the waste iron oxide pellets could be handled satisfactorily without any significant degradation. The furnace was operated at low wind rates with no adverse effects observed.

It has been also reported[33] that 32.6pct ore-coal composite pellets in the burden charged to a large blast furnace reduced coke rate. It was recommended that the coal ash content should not exceed 11pct.

1.2.4 Concluding remarks

From the literature review it is clear that composite pellets have been successfully produced. Test results have also

established that they can be used as feed material in cupola, rotary kiln and even blast furnace. However, it has not yet picked up commercially in a significant way. This is due to the cost of production of pellets. Weiss et al[28] carried out cost calculations on use of their PTC pellets in cupola and tried to demonstrate that it was economically viable. However informations on economics are by and large not available in other literatures. Local conditions, future trends and developments are going to dictate economics. No definite comment is possible at this stage. However, it is clear that composite pellets have bright prospects in alternative ironmaking processes and as replacement of pig iron in cupola. It seems that this holds true for India as well.

1.3 Brief Review of Mechanism and Kinetics of Reduction of Composite Pellets

During reduction of iron ore-coal composite pellets, evolution of volatile matter takes place due to pyrolysis of coal. Decomposition of hydrocarbons at high temperature and gasification of carbon by CO_2 and H_2O are other reactions.

Pyrolysis of coal generates reducing gases such as hydrogen and carbon monoxide. So the reduction of iron oxides is due partly to reaction with these reducing gases as follows.

$$3Fe_2O_3(s) + H_2/CO(g) = 2Fe_3O_4(s) + H_2O/CO_2(g) \quad ...(1.1)$$

$$Fe_3O_4(s) + H_2/CO(g) = 3FeO(s) + H_2O/CO_2(g) \quad ...(1.2)$$

$$FeO(s) + H_2/CO(g) = Fe(s) + H_2O/CO_2(g) \quad ...(1.3)$$

Decomposition of hydrocarbons also occurs at high temperature :

Higher hydrocarbons(g) $\xrightarrow{\text{By cracking}}$ lower hydrocarbons(g) + C(s) ...(1.4)

Gasification of carbon by carbon dioxide and steam takes place as follows.

$$C(s) + CO_2(g) = 2CO(g) \quad ...(1.5)$$

$$C(s) + H_2O(g) = CO(g) + H_2(g) \quad ...(1.6)$$

CO and H_2 thus generated again act as reductants for iron oxides in ore. It is to be noted further that if only carbon is employed as reductant then gasification of C by CO_2 (Eq.1.5) and reduction of oxides by CO are the only reactions of concern. Therefore, carbothermic reduction and gasification of C by CO_2 are often discussed together in fundamental kinetic studies in the loboratory.

Hence in this section the following topics will be very briefly reviewed.

1) Kinetics of pyrolysis of coal
2) Kinetics of carbothermic reduction and gasification reaction.

1.3.1 Kinetics of pyrolysis of coal

There are several books[49,50] which have given comprehensive coverage to the subject of coal. A recent review[51] on the chemistry of coal is also worth noting.

During the pyrolysis of coal, a substantial weight loss occurs because of the evolution of volatile matters. The amount

and the composition depend on type of coal, size of coal, and the conditions prevailing in reaction chamber. A series of consecutive and parallel reactions occur during pyrolysis of coal. Although most of the uncombined water is driven off below 375 K, this water is not completely removed until the temperature reaches around 575 K[49]. Significant devolatilization does not start until a temperature of 625 to 675 K[50] is attained.

There are two stages of devolatilization of coal[51,52]:

a) primary devolatilization at 625 to 875 K

and b) secondary devolatilization above 875 K.

Tar and gases evolve during the primary devolatilization, while only gases (mainly H_2, CO) are evolved during the secondary devolatilization. All the three processes, drying, primary and secondary devolatilization are endothermic in nature.

Coal undergoes a series of complex physical and chemical changes upon heating[49]. The heating of coal causes thermal rupture of bonds, and volatile fragments escape from the coal. The extent to which the coal devolatilizes varies greatly (less than 5pct to over 60pct) as a function of final temperature. The proportions of various products change with changes in pyrolysis temperature. A variety of products are produced during devolatilization of coal, including tar and hydrocarbon liquids, hydrocarbon gases, CO_2, CO, H_2, H_2O etc[50]. Volatiles are released from coal in approximately the following order[49] with progressive rise of temperature :

H_2O, CO_2, CO, C_2H_6, CH_4, tar + liquid, H_2.

Table 1.3 reports the distribution of volatile products of a raw bituminous coal (35pct volatile matter, 52.7pct fixed carbon and 12.3pct ash)[53] as example.

Table 1.3

Distribution of Volatiles for a Raw Bituminous Coal[53]

Coal Component Devolatized	Fraction per g. (C + H + O)	Volatile Species	Fraction per g.(C + H + O)
Carbon	0.67	CO	0.15
Hydrogen	0.14	H_2O	0.12
Oxygen	0.19	CH_4	0.17
		C_2H_6	0.13
		C_6H_6	0.30
		H_2	0.04
		C(tar)	0.10
Total	1.00		1.01

Cypres and Soudan-Moinet[52,54] studied the influence of the presence of iron oxide on coal pyrolysis, and the relation between the release of volatile matter from coal and the reduction of iron oxides. They pyrolysed samples by blending 70pct bituminous coal with 30pct of either hematite or magnetite, and heated them from room temperature to 1273 K at the rate of

3.2 $K.min^{-1}$. They found that in the primary devolatilization zone, the weight loss of the coal-magnetite mixture showed only the coal devolatilization. Magnetite was not reduced below 873 K. On the contrary, between 673 to 823 K, Fe_2O_3 was reduced to Fe_3O_4 with losses of water and a little CO_2. They also observed that the yields of saturated hydrocarbons slightly decreased in the presence of iron oxides, mainly Fe_2O_3. In the secondary devolatilization zone, the reduction of iron oxides decreased H_2 yield and increased of CO, H_2O and CH_4 yields.

Between 873 to 1273 K, Cypres et al[54] found that the rate of weight loss of the blends passed through two maxima : the first, a minor one, at around 1000 K, and the second, much more pronounced at around 1173 K (Figure 1.4). For the coal-hematite blend, the reduction was completed at 1223 K. The two most effective reducing gases evolved at suitable temperatures were hydrogen and carbon monoxide. They also observed that the evolution of hydrogen was significant above 873 K, with a maximum at around 1073 K. The quantity of hydrogen evolved from the blends was reduced compared to coal alone, especially in the region of the maxima.

Hydrogen, therefore, played an important part in the reduction of iron oxides in that zone. Consequently, there was a significant generation of CO and CO_2 from the blends in the reduction zone. From X-ray diffractions, they[54] concluded that between 673 and 773 K the hematite reduced to magnetite. In the two blends the reduction of magnetite started at around 873 K. From the onset of that reduction, in addition to wustite, a

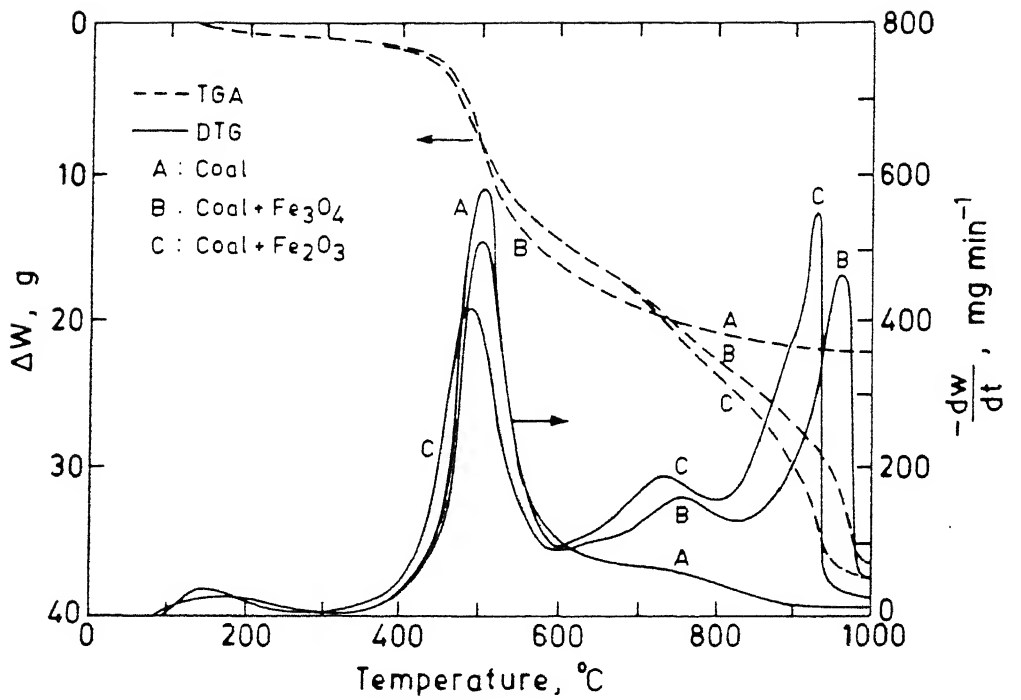

Fig. 1.4. Thermogravimetric curves, TGA and DTG, of carbonization of coal and coal/iron oxide mixtures[54].

little iron was detected. At around 1073 K the wustite reached its maximum percentage. Afterwards it rapidly got reduced to iron.

The general rate equation for the devolatilization of coal may be written as[51] :

$$\frac{dx}{dt} = k_n (a - x)^n \qquad \ldots(1.7)$$

where x is a dimensionless kinetic parameter, $\Delta V/\Delta V_o$

t is time

k_n is n th order rate constant

a is a dimensionless kinetic parameter

ΔV is change in volatile matter of coal

ΔV_o is volatile matter of raw coal.

Solving for the second order, Eq.(1.7) gives the following :

$$\frac{1}{a - x} = \frac{1}{a - x_i} + k_2 t \qquad \ldots(1.8)$$

where $x = x_i$ at $t = 0$.

Similarly, the following equation is obtained for the first order reaction :

$$\ln \left(\frac{a - x_i}{a - x}\right) = k_1 t \qquad \ldots(1.9)$$

For zeroeth order, the equation reduces to :

$$x = x_i + k_o t \qquad \ldots(1.10)$$

The k values were obtained from plots of $1/(a-x)$ vs. t for the second order, $\ln[(a-x_i)/(a-x)]$ vs. t for the first order and x vs. t for the zeroeth order reactions, respectively. The k values so obtained at different temperatures may be used for the determination of activation energies from the Arrhenius type plots.

It has been reported[51] that the devolatilization process could not be described by a single reaction rate. At 673 to 800 K, the overall reaction rate was initially of second order, followed by a first order. The low values of activation energy of about 6 to 7 K Cal/mol (25.1 to 29.3 KJ/mol) was found[49,51]. Therefore the overall pyrolysis process above 673 K might be described by an initial second order decomposition reaction followed by a first order diffusion process in which the escape of the products of decomposition through the pore system is rate determining.

1.3.2 Kinetics of carbothermic reduction and gasification reaction

1.3.2.1 General features

Kinetically reduction of oxide in composite pellet is significantly by carbon (i.e. carbothermic reduction) in a mixture of iron oxide and carbon. If the composite pellet uses char or coke as reductant then this is wholly carbothermic reduction. If, on the other hand, coal is used then reduction will be partly by gases evolved due to pyrolysis of coal,

especially H_2 and CO[52,54]. Kinetics of reduction by H_2 and CO would not be separately reviewed since its salient features are well published. Relevant points would be brought in chapter 6, which would report on reduction of blue dust by these gases as a part of the present investigation. Therefore only carbothermic reduction would be reviewed here.

There have been a book by Bogdandy and Engell[55], and several reviews[56-58] from time to time on this topic. Therefore this section will be very brief and highlight only important features. The carbothermic reduction takes place vide the following two component reactions.

i) Reduction of iron oxides :

$$m\ Fe_xO_y(s) + CO(g) = n\ Fe_zO_w(s) + CO_2(g) \qquad ...(1.11)$$

where Fe_xO_y denotes Fe_2O_3 or Fe_3O_4 or Fe_xO, and Fe_zO_w denotes Fe_3O_4 or Fe_xO or Fe.

ii) Gasification of carbon :

$$C(s) + CO_2(g) = 2CO(g) \qquad ...(1.12)$$

Now it has been universally accepted that carbothermic reduction takes place via the above two reactions i.e. through gaseous intermediates.

Kinetic study of carbothermic reduction of iron oxides suffers from two major difficulties[14].

a) As the solid reductant i.e. carbon is present alongwith the oxide, the sample can not be gradually heated to reaction temperature. This is because reduction reaction can start at around 1000 K.

b) The weight loss suffered by a carbon-oxide mixture is the sum total of weight losses due to removal of oxygen from oxide and weight loss due to gasification of carbon.

To calculate the rate of reduction, it becomes essential to separate the weight loss of oxygen from that of carbon. Rao[3] attempted to separate these two with the help of some theoretical considerations. But this approach suffered from some untenable assumptions. On the other hand Otsuka and Kunii[1], Ghosh and co-workers[8,9] measured the amount of gas generated as well as analysed the product gas composition as a function of time with the help of either gas chromatograph or oxygen sensor.

If the volumetric flow rate (Q) of gas generation and composition of the product gases are known, one can find out the rate of weight loss of carbon ($\dot{W}_c$) and oxygen ($\dot{W}_o$) in the following manner :

$$Q_{CO} = Q.X_{CO} \qquad \ldots(1.13)$$

$$Q_{CO_2} = Q.X_{CO_2} \qquad \ldots(1.14)$$

where Q_{CO} , Q_{CO_2} are volumetric flow rates and X_{CO} , X_{CO_2} are volume fractions of carbon monoxide and carbon dioxide respectively in product gas.

$$\dot{W}_o = \frac{16}{22400} (Q_{CO} + 2\, Q_{CO_2}) \ g.s^{-1} \qquad \ldots(1.15)$$

$$\dot{W}_c = \frac{12}{22400} (Q_{CO} + Q_{CO_2}) \ g.s^{-1} \qquad \ldots(1.16)$$

Both interfacial chemical reaction as well as mass transfer have been found to control the rates of both reduction reaction as well as gasification. The overall rate is sometimes affected by rate of heat transfer as well since it is endothermic[58].

Kinetics of carbothermic reduction has been studied mostly by taking powder mixture of graphite, coke or charcoal with iron oxides or ores. This situation is very complex for heat and mass transfer analysis.

Carbothermic reduction of iron oxide has generally been found to be controlled by gasification reaction. Such a conclusion has been arrived at from the following observations.

i) Activation energy is high going upto about 400 KJ/mol[1,3,6,8]. This is the nature of gasification reaction also.

ii) Catalysts, including freshly reduced metallic iron, which enhance gasification of carbon by CO_2, have also been found to enhance rate of carbothermic reduction[1,8,9].

Therefore the characteristics of gasification reaction shall be briefly dealt with. So far as the reduction of oxide is concerned it would suffice here to state that the reduction has been found to be stagewise, i.e.

$$Fe_2O_3 \longrightarrow Fe_3O_4 \longrightarrow Fe_xO \longrightarrow Fe$$

This is true in general, and especially if the oxide particles are small in size.

1.3.2.2 Kinetic features of gasification reaction

Coming to kinetics of gasification reaction, there have been numerous investigations over the past several decades, and investigators arrived at many divergent conclusions.

Cokes, carbon and synthetic graphites are highly porous with pores ranging from about 10 Å to several microns in diameter. The kinetic steps involved are gas film diffusion, diffusion through pores and chemical reaction at gas-solid interface. It has been established that the chemical reaction is exclusively rate controlling below 1373 K, if the size of the graphite particle is not large (diameter less than 3 mm or so). Such a conclusion has been arrived at from evidences, such as high activation energy (335 to 377 $KJ.mol^{-1}$) and strong influence of solid and gaseous impurities even in trace quantities. For chemical reaction control, the entire internal pore surface area should be active and the rate of loss of carbon should be proportional to the volume of the particle.

By the every method of manufacture, carbon comes out with infinite spectrum of structural imperfections and surface defects. Again some solid inorganic materials, moisture, H_2 etc. catalyse or inhibit the reaction even if they are present in ppm level. Regarding rate and mechanism of this reaction most authors[8,12,14] have proposed that the rate of the surface chemical reaction can be represented by following form :

$$\text{rate} = \frac{I_1 P_{CO_2}}{1 + I_2 P_{CO} + I_3 P_{CO_2}} \qquad \ldots(1.17)$$

where I_1, I_2 and I_3 are constants.

The first step in the reaction is the formation of a surface oxide C(O), on an active free site (C_f) at the surface :

$$CO_2(g) + C(s) \longrightarrow C(O) + CO(g) \qquad \ldots(1.18)$$

The second step is the break down of the surface oxide to form gaseous CO leaving a new active site behind :

$$C(O) \longrightarrow CO(g) + C_f \qquad \ldots(1.19)$$

It may be pointed out that the rate decreases enormously with increase of percentage of CO in the gas. The rate of gasification with pure CO_2 at 1 bar has been found to be 10^2 times larger compared to a gas of 90pct CO-10pct CO_2 at 1173 K[56]. The rate of gasification is also enhanced by catalytic effect of metallic iron even at very low concentrations. This has been reported by a number of investigators[1,8,9,14].

To summarize, kinetics of gasification reaction is characterized by :

a) a large variation in rate by orders of magnitude depending on nature of sample and experimental conditions,

b) a high activation energy in the range of 210 to 375 $KJ.mol^{-1}$,

c) significant inhibition of rate by CO, which is the product of the reaction,

and d) significant catalysis and inhibition by a number of elements and compounds, including metallic iron.

The above features have confirmed that the rate of the reaction is primarily controlled by slow surface chemical reaction step. However, it has also been found that mass transfer partially controls the rate under some circumstances such as large particle size and higher temperature. Heat transfer limitation may also affect the rate to some extent.

In order to determine the rate of surface reaction, several investigators have tried to eliminate mass transfer resistance by experimental design. Some have attempted to calculate effectiveness factor mathematically and thus to eliminate mass transfer resistance to find out true (i.e. intrinsic) surface chemical reaction rate.

Carbon samples are highly porous. The rate has been found to be proportional to specific surface area by and large. Therefore, specific surface area is one of the most important parameters contributing to kinetics of the reaction.

1.3.2.3 Factors affecting carbothermic reduction

Coming back to the reduction of iron oxide by carbon, the variables which are found to affect the reduction kinetics are (1) temperature, (2) particle size of iron oxide as well as carbon, (3) fixed carbon / total iron ratio, and (4) catalyst.

Temperature has a pronounced effect on the carbothermic reduction rate. It may be noted that activation energy varies

over a wide range starting from 56 KJ.mol^{-1} to 418 KJ.mol^{-1}. It is worth mentioning here that activation energy measured at various degrees of reduction differ quite a bit from stage to stage. On an average, early stage of reduction is characterized by high activation energy (240 to 300 KJ.mol^{-1}) indicating that it is controlled by gasification reaction since activation energy for reduction reaction varies approximately between 40 to 100 KJ.mol^{-1}. The second stage is associated with much lower activation energy. It has been concluded that this is due to catalytic effect of freshly produced iron.

Particle size is another important factor which contributes quite significantly on the reduction rate. Investigators[1,3,7] have found that lowering of carbon particle size enhances the rate.

Many workers[2,3,6,7,12] studied the effect of amount of carbon on reduction rate. Rao[3] employed amorphous carbon for reduction of hematite at the temperature range of 1123 to 1280 K. He varied the molar Fe_2O_3/C ratio from 1:1.5 to 1:9 and found that higher proportion of carbon enhanced the reduction rate markedly. He also found that at 1280 K, the time for 50pct. reduction decreased from 35 to 10 minutes when Fe_2O_3/C ratio increased from 1:1.5 to 1:9. Fruehan[7] observed that when the percentage of coconut char was increased from 10 to 30, the rate of reduction of wustite increased from around 12 mg.min^{-1} to 38 mg.min^{-1} at 1273 K. Srinivasan and Lahiri[6], Ajersch[12] also confirmed that increase in amount of carbon in the mixture of oxide and carbon enhanced the reduction rate.

The literature review shows that some workers[1,8,9] observed considerable catalytic effect whereas some others[3] did not notice it or it was not considerable. Catalytic effect is significant only in samples where fine particles of iron oxide/ore and carbon are mixed, and made into briquette by pressing. This way the surface area of contact between the solids is enhanced thus increasing the catalytic effect[8]. Bandyopadhyay[14] has discussed about the factors affecting such catalysis in details.

1.4 Kinetics of Non-Isothermal Reduction

In gas-solid reaction studies, e.g. reduction of iron ores by hydrogen or carbon monoxide, isothermal kinetic studies are possible in the laboratory. The method is to introduce the solid sample into the hot zone of the furnace under an inert atmosphere. The reactive gas is introduced only when the sample has attained temperature. However a composite pellet would behave in a different way. Here reactions would start during rise of temperature of the sample even in inert atmosphere due to presence of carbon as well as progressive devolatilization of coal, which generates reducing gases. Some published literatures[10,37] on the so-called isothermal reduction studies of composites confirm that a significant fraction of reduction actually took place initially while the sample temperature was rising (approx. first 15 minutes or so). In this context non-isothermal kinetic study of composite pellet has certain

advantages, since here temperature rise can be controlled as desired.

Moreover in actual industrial reactors such as blast furnace, rotary kiln or cupola, reduction is non-isothermal. Hence non-isothermal studies simulate it better and provide more reliable information on the behaviour of the system. Some other advantages of non-isothermal kinetic studies have been summarized by Ray and Sewell[59].

Mookherjee et al[60] studied the kinetics of reduction of iron ore fines by Hutar coal char fines. They plotted non-isothermal kinetic data as ln [- ln (1 - f)] vs. 1/T (Figure 1.5) where f is fractional reaction and T is absolute temperature. They found three linear segments in the temperature ranges 539 to 1359 and 483 to 1313 K for heating rates of 20 and 10 $K.min^{-1}$, respectively. The three linear segments were more prominent for the higher heating rate as compared to the lower heating rate. The apparent activation energy value for the final stage was 114 $KJ.mol^{-1}$.

On another set of data, they[60] analyzed non-isothermal data by using the method of Ingraham, i.e. by plotting ln $[\frac{Bf}{T^2}]$ vs. $\frac{1}{T}$, where B is the heating rate. The activation energy was found to be 119 $KJ.mol^{-1}$. The third set of non-isothermal data, for reduction in large crucibles, was analyzed by using Ginstling - Brounshtein equation, which yielded an activation energy of 111.7 $KJ.mol^{-1}$. The activation energy for non-isothermal reduction was much lower than the value determined for isothermal reduction.

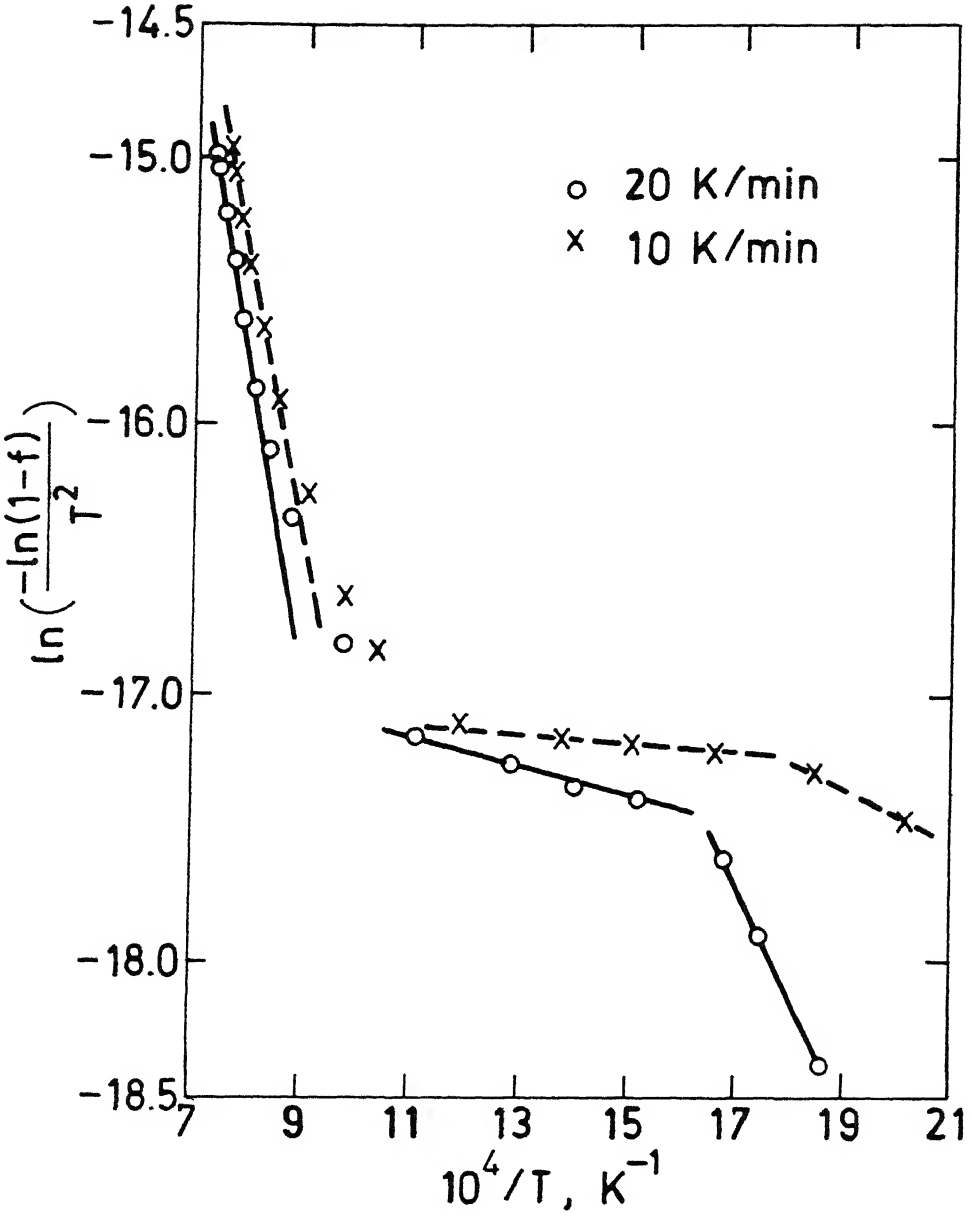

Fig. 1.5. Kinetic data for non-isothermal reaction in an ore-char mixture under an argon atmosphere[60].

There are various experimental techniques for non-isothermal kinetic studies. These have been reviewed by Ray and Sewell[59]. The basic equation of non-isothermal kinetic equation is derived by the following three equations[61,62].

1) The kinetic law in the differential form :

$$\frac{d\alpha}{dt} = k\,\phi\,(\alpha) \qquad \ldots(1.20)$$

where α denotes the degree of reduction, t, the time and, k the rate constant.

2) The Arrhenius type relationship i.e. temperature coefficient of the rate constant :

$$k = A \exp(-E/RT) \qquad \ldots(1.21)$$

where E is activation energy, A is a pre-exponential constant, R is the gas constant, and T is the temperature.

3) The variation of temperature with time :

$$T = \phi\,(t) \qquad \ldots(1.22)$$

where ϕ (t) is an appropriate function.

In the case of a constant heating rate (B), Eq.(1.22) has the differential form :

$$\frac{dT}{dt} = B \qquad \ldots(1.23)$$

Combining Eqs.(1.20) and (1.21) :

$$\frac{d\alpha}{dt} = A \exp(-E/RT).\phi\,(\alpha) \qquad \ldots(1.24)$$

From Eq.(1.23) :

$$dT = B\,dt \quad or \quad dt = dT/B \qquad ...(1.25)$$

Now,again combining Eqs.(1.24) and (1.25) :

$$\frac{d\alpha}{\phi(\alpha)} = \frac{A}{B} .\exp(-E/RT).\, dT \qquad ...(1.26)$$

$$Let \int \frac{d\alpha}{\phi(\alpha)} = \int g'(\alpha).\, d\alpha = g(\alpha) \qquad ...(1.27)$$

Hence, by integrating Eq.(1.26) :

$$g(\alpha) = \frac{A}{B}\int_0^T \exp(-E/RT).\, dT \qquad ...(1.28)$$

This basic equation (1.28) in non-isothermal kinetics can be analyzed by graphical and analytical techniques to obtain the values of the kinetic parameters E and A provided reliable value of α as function of time is available[59].

1.5 Plan of Work

I: Raw material characterization,

II: Preparation of composite pellets by various methods,

III: Studies of composite pellets prepared by various methods as well as collected from outside source for evaluation of properties,

IV: Intensive study of kinetics of reduction of some selected ore-coal and ore-char combinations; this part is to be taken up as a fundamental study and is to consist of reduction of composite pellets carried out non-isothermally; this is because the nature of the system is such that reaction takes place non-isothermally even in supposedly isothermal measurement programme.

V: Auxiliary studies :

i) hydrogen reduction of iron ore (isothermal)

ii) carbon monoxide reduction of iron ore (isothermal)

iii) devolatilization of coal (non-isothermal)

iv) X-ray diffraction studies of reduced pellets

v) scanning electron microscopy of reduced pellets

VI: Interpretation of results.

CHAPTER 2

RAW MATERIALS CHARACTERIZATION, PELLET PREPARATION AND TESTING

The content of this chapter is divided into three main parts :

(i) characterization and preparations of raw materials

(ii) preparation of composite pellets with different binders

(iii) testing of pellets.

2.1 Characterization and Preparations of Raw Materials

The starting raw materials were obtained from the Direct Reduction Process Development Division (DRPDD), Research and Development Centre for Iron and Steel, SAIL, Ranchi. The sources of raw materials were :

Blue dust	:	Bailadila mine, M.P. (Dark gray colour)
Non-coking coal	:	i) Hutar mine, Bihar ii) Bachra mine, Bihar

2.1.1 Size analysis

Thorough mixing of each raw material was done before and after size analysis. A porcelain jar was used for mixing. About 1 Kg raw material along with six ceramic balls (19.2 mm

diameter) was kept in the jar, which was then allowed to rotate at 85 rpm for 5 hours for mixing.

Size analysis of raw material was carried out in sieve shaker for 15 minutes. Results are presented in Table 2.1. Jerks were avoided subsequently to prevent segregation during transportation and handling the raw materials.

Table 2.1

Size Analyses of Raw Materials

Material	Mesh Size (ASTM)	Pct Retained	Cumulative Pct Retained
Blue dust	- 100 + 200	38.3	38.3
	- 200 + 270	38.6	76.9
	- 270 + 325	4.4	81.3
	- 325	18.5	99.8
Hutar coal	- 100 + 200	33.6	33.6
	- 200 + 270	34.7	68.3
	- 270 + 325	0.2	68.5
	- 325	31.5	100.0
Bachra coal	- 100 + 200	34.7	34.7
	- 200 + 270	36.5	71.2
	- 270 + 325	0.9	72.1
	- 325	27.8	99.9

2.1.2 Chemical analyses of raw materials

Chemical analysis of blue dust was done according to the standard methods available in the book[63]. Total removable oxygen was determined by hydrogen reduction using the thermogravimetric set-up of Bandyopadhyay[14] at 1173 K. Analysis of blue dust is presented in Table 2.2.

Table 2.2

Analysis of Blue Dust

Total Fe (pct)	Av**	Total Removable Oxygen (pct)	Av	Fe_2O_3 (pct) (By Chem Analysis)	(By H_2 Red)*	Av	Moisture (pct)	Av	LOI** (pct)	Av
66.7		28.6		95.1	95.7		0.07		0.70	
	66.5		28.8			95.4		0.07		0.72
66.3		29.0					0.07		0.73	

* Fe^{2+} = negligible, SiO_2 = 1.6 pct, Al_2O_3 = 1.8 pct.

** Av = Average, LOI = Loss on ignition.

Proximate analyses of coals were done according to the standard method. The results have been reported in Table 2.3. The ultimate analyses (Table 2.4) were performed by the Coal Survey Laboratory, Central Fuel Research Institute (CFRI), Ranchi, while ash analysis (Table 2.5) was done at Analytical Laboratory, IIT, Kanpur.

Table 2.3

Proximate Analyses of Coal and Char

Type of Coal/ Char	Moisture (pct)	Volatile Matter (pct)	Ash (pct)	Fixed Carbon (pct)
Hutar coal	6.2	32.5	11.6	49.7
Hutar char	-	0.6	18.7	80.3
Bachra coal	6.0	24.0	28.0	42.0
Bachra char	-	-	40.0	60.0

Table 2.4

Ultimate Analyses of Coals

(As Received)

Type of Coal	Carbon (pct)	Hydrogen (pct)	Nitrogen (pct)	Sulphur (pct)	Oxygen (pct)
Hutar	59.9	3.4	1.3	0.3	23.5
Bachra	50.5	4.0	0.6	1.0	15.9

Table 2.5

Analyses of Coal Ash

Type of Coal	SiO_2 (pct)	Fe_2O_3 (pct)	Al_2O_3 (pct)	CaO (pct)	MgO (pct)	Na_2O (pct)	K_2O (pct)	TiO_2 (pct)
Hutar	60.5	4.7	27.2	2.9	1.6	2.6		0.2
Bachra	59.0	9.6	15.0	2.3	3.4	6.7	1.9	-

2.1.3 Preparation of coal char

The starting material for preparation of coal char was Hutar and Bachra coals both of which are non-coking. Sized coal (Table 2.1) was taken on two silica boats (24x100 mm and 23x80 mm). The charmaking furnace (detail given elsewhere[14]) was maintained at around 1223 K. Before introducing the sample in the furnace, nitrogen was passed through the reaction chamber at a flow rate of 16.67 $Cm^3.s^{-1}$ for at least 10 minutes to ensure neutral atmosphere. The coal was allowed to devolatilize for one hour under continuous flow of nitrogen gas. The char sample was allowed to cool down under nitrogen gas for around 10 minutes. Then the boats were taken out and the last stage cooling was done under cover and finally in desiccator. The char was kept in glass bottle and stored in oven (at 373 K).

2.1.4 Preparation of lime

Calcite crystal was used as starting material for preparation of burnt lime. After crushing the calcite crystal, sized particles were taken in an one end closed mullite tube (25 mm i.d.). The mullite tube was kept in a silicon carbide heated furnace at 1373 K for one hour. From the weight loss, it was calculated that 97 pct calcite was calcined. Next particles were ground further to get required sizes.

2.2 Pellet Preparation

There are different types of binders available for pelletmaking. Binder is that material which serves as a bridge

between the particles and thus increases the green or dry strength of the bonded particles.

Binder must satisfy the following requirements :

(i) spread out uniformly over the surface of particles,

(ii) give sufficient green and dry strength of bonds,

(iii) be harmless to the operating personnel,

and (iv) be cheap and easily available in the market.

2.2.1 Procedure for pellet making

Procedure in nut shell consisted of :

(i) grinding and sizing of raw materials and binders as decided,

(ii) weighing and dry mixing,

(iii) mixing with water (standardized at 15 pct of weight of blue dust),

(iv) making of cylindrical pellets using pellet making unit in the laboratory,

(v) air drying for 15 minutes to 24 hours depending on binder etc.,

(vi) hardening of pellets using different procedures to be described later,

(vii) oven drying or air drying,

and (viii) storing in desiccator.

Some details are noted below for record.

It was observed in the literatures that fine (-325 mesh) raw materials as well as fine binders improved strength of

the pellets. But blue dust can not be taken at -325 mesh as such, since it is available at source as -100 mesh size. Further grinding or sizing will not be economic. Hence raw materials i.e. blue dust and coals were used as -100 mesh size particles in this study.

Several procedures were tried for dry mixing of fines, as noted below.

M1 : mixing by magnetic stirrer for 10 minutes

M2 : mixing by Fritsch pulverisette (Germany) for 30 minutes and futher mixing by magnetic stirrer for 5 to 10 minutes

M3 : mixing by hand with the help of a small steel plate (10x20 mm) in a beaker for 10 minutes

M4 : mixing by pulverisette for 10 minutes.

Subsequent mixing with water was done by hand and the mix transferred immediately to pellet making unit.

Figure 2.1 presents sketch of the pellet making unit. The procedure was to fill up the cylindrical die cavity with the wet mix, place the mandrel on to the mix, and then give one impact to the mix by releasing the weight and making it fall freely on the mandrel. One impact to the powder mixture was given to simulate the impact (due to rotation and fall of the materials) occuring during commercial pelletizing process. Diameter of dry pellet varied from 10.3 to 10.5 mm and height varied from 10.3 to 12.0 mm.

After pellets were made, their dry compressive strength and also strength after reduction were measured by INSTRON 1195

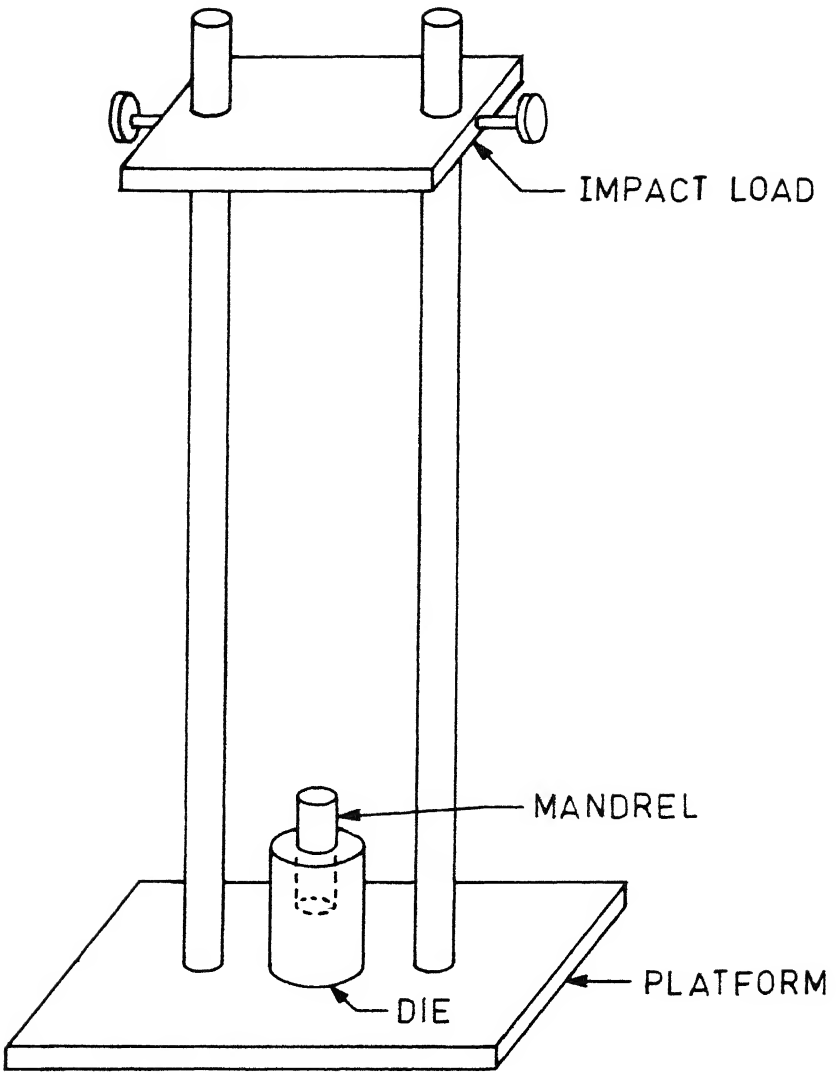

Fig. 2.1. Schematic representation of the pellet making unit.

Model (Germany) at a scanning speed of 1 mm.min^{-1}.

Many trials were given for selecting a suitable cold-bonding process, as it was realized that the success of the process depended heavily on attaining sufficient strength of the composite pellets. Total number of trials was approximately 200.

2.2.2 Selection of binders

The binders selected for this investigation, may be broadly classified into three types.

(i) Organic binder

(ii) Inorganic binder

(iii) Organic-inorganic combined binders

2.2.2.1 Organic binders

Dextrin, thermo-setting resin (TSR), polyvinyl alcohol (PVA), methanol, and their combinations were employed as organic binder.

2.2.2.2 Inorganic binders

Most common inorganic binders viz. Bentonite, cement, lime, silica, calcium hydroxide, sodium silicate, calcium carbonate, etc. were used in this study.

From processing point of view, the procedure can be classified as :

(i) cold bonding without use of autoclave

(ii) cold bonding using autoclave.

In cupola, the main source of gangue materials (SiO_2, Al_2O_3, etc.) are from ash of coke. Slag of cupola is typically acidic in nature (55 pct SiO_2, 30 to 37 pct CaO, rest Al_2O_3 and FeO) in India. Hence it was decided that the maximum amount of CaO and minimum possible amount of SiO_2 would be added so as to obtain desirable slag basicity in cupola without additional flux charging. Although the results of cement and lime combination are encouraging, but their use as binder is restricted due to increase of the gangue content in composite pellets. Accordingly different types of mixtures were used as binder as listed below.

Mix I : 66.7pct CaO(-325 mesh) + 33.3pct SiO_2(as received)

Mix II : 71.4pct CaO(-325 mesh) + 28.6pct SiO_2(as received)

Mix III : 75.0pct CaO(-325 mesh) + 25.0pct SiO_2(as received)

Mix IV : 77.8pct CaO(-325 mesh) + 22.2pct SiO_2(as received)

Mix V : 72.7pct CaO(-325 mesh) + 27.3pct SiO_2 (-325 mesh)

Mix VI : 78.6pct Slaked lime + 21.4pct SiO_2 (-325 mesh)

Mix VII : 78.6pct $Ca(OH)_2$(as received) + 21.4pct SiO_2 (-325 mesh)

S Mix V : 72.7pct CaO(-200 mesh) + 27.3pct SiO_2 (-325 mesh)

S MixVII: 78.6pct high purity $Ca(OH)_2$ (as received) + 21.4pct SiO_2 (-325 mesh).

All the above mixtures were prepared by mixing in pulverisette for 30 minutes. Slaked lime was prepared by adding -325 mesh powder of lime to water. They were mixed and kept overnight, filtered, dried at 373 K for 3.5 hours, and then ground to powder.

Autoclave (series 4500, Parr Instrument Co., USA) was employed for hardening of pellets by steam pressure (13 to 27 bar). Total time and maximum temperature were varied from 2.5 to 9.5 hours,and 460 to 500 K respectively. Bonding is based on the thermal hydration of silicates by water vapour in the autoclave. The strengthening of pellets is a result of the formation of hydrated calcium silicates.

2.2.2.3 Organic-inorganic combined binders

Different combinations of organic and inorganic binders were tried : dextrin, TSR, sugar, Bentonite, lime and $Ca(OH)_2$. Composite pellets were dried in oven only or treated with CO_2 gas and subsequently oven dried to develop the strength of pellets.

2.3 Testing of Composite Pellets

Some blue dust-Hutar coal (12pct) composite pellets were produced by using organic binder, the results of compressive strength is presented in Table 2.6. It may be noted from the Table 2.6 that 4 pellets were tested in each mix (i.e. sample). Compressive strengths were measured for dry pellets (oven or air dried). Only the values of compressive strength mostly above 150 N per pellet and some cases below that value have been reported. The values varied mostly by $\pm$ 10 to 20pct from the average value in a sample. It may be noted from the Table 2.6 that the maximum strength achieved by organic binders was above 300 N per pellet by using either 4pct TSR or 3pct TSR and 1pct

dextrin. The organic binder tends to form polymer bridges at the points of contact between the particles to ensure good dry strength of pellet.

As the amount of TSR is decreased below 3pct the strength of the pellet also decreased. But dextrin did not show any trend. Maximum strength of 181 N per pellet was obtained by using 3pct dextrin. PVA, PVA and methanol, dextrin, PVA and methanol were also tried but not with success. However TSR at 3pct or above gave a strength of about 300 N.

The results of compressive strength of composite pellets using inorganic binders are reported in Tables 2.7 and 2.8. The compressive strength of composite pellets (B1) was 202 N per pellet by using 8pct cement and 2pct lime (both -100 mesh). When -325 mesh size cement and lime at the same composition were used, then strength increased to 357 N per pellet (B9).Although cement and lime combination gave good strength of pellets by natural ageing, but ultimately slag volume during smelting of pellets in furnace would be increased by using these binder combinations to the pellets. Hence it was decided to search an alternative binder combination.

Table 2.8 presents the results of compressive strength of pellets hardened by using autoclave. 8pct cement and 2pct lime combination did not show much difference (218 N per pellet) by using autoclave (B16). With Mix V (CaO and SiO_2) the strength of pellets was 83 N per pellet (B87). But using -325 mesh sizes of blue dust and coal at the same condition (B88), the strength increased by about 2.5 times (204 N per pellet). This trend

(about 1.2 times increased strength of pellets) was also observed by using Mix VI (slaked lime and silica) (B89 and B90). It shows that fineness of particles has significant effect on strength.

Since the compressive strengths of pellets prepared by Mix VI (slaked lime and silica) as binders (B89) were similar (195 N) to those of pellets (B91) prepared by Mix VII [$Ca(OH)_2$ and SiO_2 combination], $Ca(OH)_2$ was used subsequently instead of slaked lime. With 11pct Mix V (CaO and SiO_2) the strength of pellets was obtained as 83 N per pellet and the strength of pellets by using 14pct Mix VII ($Ca(OH_2$ and SiO_2) was 196 N per pellet. For second case (Mix VII) $Ca(OH)_2$ pct was too high, since $Ca(OH)_2$ was costly than CaO. To lower down the binder cost, combination of Mix V and Mix VII was tried without sacrificing strength of pellets. It was found that 4pct Mix V and 9pct Mix VII gave good strength (225 N per pellet) and good reproducibility (B95, B98, B103 and B108) as well.

Preparing -325 mesh size particles of CaO was very difficult so standard mixtures (designated as S Mix) were prepared in bulk by using -200 mesh size particles of CaO (S Mix V). It was found that the strength of pellets (224 N per pellet) by using 4pct S Mix V and 9pct S Mix VII (B 108) was similar to pellets by using 4pct Mix V and 9pct Mix VII (B 95). As mentioned earlier S Mix VII employed pure $Ca(OH)_2$ (imported) in contrast to Mix VII, which used ordinary grade.

Lime plays an important role in the autoclaved pellet production. The chemical dispersion of the lime during transformation from CaO to $Ca(OH)_2$ leads to an increase in its

specific surface area from 5-6,000 cm^2/g after grinding to 50-80,000 cm^2/g after hydration[47]. Chemical interaction between $Ca(OH)_2$, silica and constituents of ore in the mix (oxides of iron and aluminium) takes place during autoclave treatment of the pellets i.e. under hydrothermal condition. A poly-mineral cementing binder forms as a result, which contains calcium hydroxide, hydro-silicates and hydro-ferrites of calcium, ferritic and alumino-ferritic garnet in gel-like and fine crystal form[47,64]. Therefore, addition of $Ca(OH)_2$ in binder may help the reactions favourably.

Composite pellets with Hutar coal char have higher strength (more than 4 times) than ore-Hutar coal pellets (B102 and B103). For higher pct (24pct), it was about 7.5 times (B105 and B106). Composites with Bachra coal had more strength (about double) than those with Hutar coal (B108 and B114). But it was not true for higher pct.

Table 2.9 reports compressive strengths of pellets with combined organic-inorganic binders. No autoclaving was done. Samples B51 to B69 employed dextrin, TSR and Bentonite in various proportions as binder. Maximum strength obtained was 317 N per pellet (B63). Samples B74 and B75 were given a short treatment with CO_2 gas. With sugar and $Ca(OH)_2$, a strength of upto 369 N per pellet was obtained.

2.3.1 Concluding remarks on dry strength of pellets

(i) Compressive strength of more than 300 N per pellet and in many cases more than 150 N per pellet could

be obtained with many sets of binder combinations as mentioned earlier.

(ii) Maximum strength of pellets achieved by organic binders was above 300 N per pellet by using either 4pct TSR or 3pct TSR and 1pct dextrin.

(iii) For inorganic binders (without using autoclave),maximum strength of pellets obtained was about 200 N per pellet by using 8pct cement and 2pct lime (both -100 mesh). Hardening was done by natural ageing for 5 days. By using -325 mesh size of binders,the strength increased about 1.7 times.

(iv) 4pct Mix V (CaO and SiO_2) and 9pct Mix VII ($Ca(OH)_2$ and SiO_2) combination used as binder gave good strength (225 N per pellet) and good reproducibility as well.

(v) -325 mesh size of ore and coal gave much higher strength as compared to -100 mesh particles.

(vi) Use of -325 mesh size binders gave much higher strength as compared to -100 mesh size binders.

(vii) It has been established that ore-char composites develop few times higher strength in comparison to ore-coal composites.

(viii) Composites with Bachra coal had more strength (about double) than those with Hutar coal.

2.4 Pellet Making Procedure for Fundamental Studies

As mentioned in introduction, one part of the present investigation was to make composite pellets in various ways, also collect pellets from outside sources, and test them for dry strength, reduction etc. for comparison. Another part was fundamental kinetic study under non-isothermal condition of some pellets prepared according to a standard procedure to be adopted on the basis of data presented in Tables 2.6 to 2.9.

Since organic binders are costly, it was decided to use inorganic binders, such as CaO, SiO_2 and $Ca(OH)_2$. Although -325 mesh blue dust and coal fines yielded pellets of much higher strength as compared to -100 mesh size, the latter size was selected for fundamental studies since grinding to -325 mesh would involve significant cost from commercial point of view.

Use of autoclave for steam curing and hardening, therefore, would be desirable to obtain appropriate level of dry strength and for better reproducibility, as demonstrated through trial.

The procedure was standardized as follows.

Binder mixtures were prepared by first mixing with spatula in a beaker, then mixing for 30 minutes in pulverisette. The mixtures were kept in oven at 373 K. Compositions of mixtures were :

(a) S Mix V : 72.7pct CaO(-200 mesh) and 27.3pct SiO_2 (-325 mesh)

(b) S Mix VII: 78.6pct high purity $Ca(OH)_2$ (made in Poland) and 21.4pct SiO_2 (-325 mesh)

Weighed amounts of blue dust, coal or char were taken along with 4pct S Mix V and 9pct S Mix VII (pct wt. w.r.t. wt. of blue dust) as binders. As Table 2.8 shows that this binder combination yielded high strength. It also has a high CaO/SiO_2 ratio. Amount of slag per tonne of metal should be kept as low as possible. Since the gangue of ore and ash of coal are high in silica,a high CaO/SiO_2 ratio in binder would give advantage in this connection.

All powders were mixed properly by hand with a spatula, then by pulverisette for 10 minutes. Water (15pct) was added to the mixed powders and again mixed properly. Then pellets were produced by one impact as described earlier. After 1 hour air drying, pellets were kept for predrying at 373 K for 14 to 16 hours. Then they were placed in autoclave for hardening. Total time was 6 hours for autoclaving. Cooling time was 75 minutes. Then the pellets were allowed to dry at 373 K for 16 hours, and subsequently stored in desiccator.

Table 2.6

Compressive Strengths of Dry Composite Pellets Using Organic Binders

* All pct. wt. w.r.t. wt. of blue dust
* Coal : Hutar coal (12pct)
* Mixing code : M1
* Treatment : T1 = First air drying; then dried in oven (423 K, 24 hrs)
* Binder code : D = Dextrin, T = TSR

Sample No	Binder (Code)	(pct)	Air Drying (Mins)	Compressive Strength (N per Pellet)	Average Compressive Strength (N per Pellet)
B 37	D	4	90	184 139 157 168	162
B 38	D	3	15	196 157 162 208	181
B 47	D + T	2 + 2	15	224 138 161 256	195
B 46	T	4	15	300 358 327 330	329
B 56	T	3	15	305 295 290 250	285
B 57	T + D	3 + 0.5	15	218 345 285 319	292
B 62	T + D	3 + 1	15	338 388 296 335	339
B 66	T	2	30	126 140 97 154	129

Table 2.7

Compressive Strengths of Dry Composite Pellets Using Inorganic Binders (Without Autoclave)

* All pct. wt. w.r.t. wt. of blue dust
* Coal : Hutar coal (12pct)
* Mixing code : M2, M3
* Air drying : 24 hours
* Treatment : T2 = water sprayed for 5 days once every 24 hrs
* Code :C = Cement, B = Bentonite, L = Lime, LS = $CaCO_3$, HL = $Ca(OH)_2$

Sample No	Binder (Code)	(pct)	Size (Mesh)	Mode of Mixing	Treatment	Comp. Strength (N/Pellet)	Av Comp. Strength (N/Pellet)
B 8	C	8	-	M2	T2	153	122
	+	+				103	
	B	0.5				114	
						117	
B 1	C	8	-	M2	T2	196	202
	+	+				205	
	L	2	-100			215	
						193	
B 9	C	8	-325	M2	T2	344	357
	+	+				424	
	L	2	-325			275	
						385	
B 2	C	6	-	M2	T2	153	182
	+	+				204	
	L	4	-100			190	
						180	
B 5	C	10		M2	T2	111	124
	+	+				130	
	LS	3				158	
						95	
B 3	C	6		M2	T2	161	181
	+	+				208	
	L	2				158	
	+	+				198	
	HL	2					
B 6	C	8	-	M3	T2	122	148
	+	+				167	
	L	2	-100			160	
						141	
B 13	B	4		M3	T1	68	70
						98	
						54	
						58	

Table 2.8

Compressive Strengths of Dry Composite Pellets Using Inorganic Binders (With Autoclave)

* All pct. wt. w.r.t. wt. of blue dust
* Mixing code : M1, M2, M4
* Treatment : T3 = Steam - curing by autoclave (Max Temp 463 - 496 K)
* Code : BD = Blue dust, HC = Hutar coal, HCC = Hutar coal char
  BC = Bachra coal, BCC = Bachra coal char
  (Size -100 mesh, unless mentioned)
  C = Cement, L = Lime, MX1= Mix I, MX3 = Mix III, MX5= Mix V,
  MX6 = Mix VI, MX7 = Mix VII, SM5 = S.Mix V, SM7 = S.Mix VII

Sample No	Coal/Char (Code)	(pct)	Binder (Code)	(pct)	Mode of Mixing	Autoclave Total Time (hrs)	Max Pr (bars)	Comp. Strength (N/Pellet)	Av Comp. Strength (N/Pellet)
1	2	3	4	5	6	7	8	9	10
B 16	HC	12	C + L	8 + 2	M2	5.5	13.6	332 165 158	218
B 30	HC	12	MX3	8	M1	9.5	24.5	123 95 63	94
B 33	HC	12	MX1	9	M1	9.0	21.0	137 130 95 121	121
B 87	HC	12	MX5	11	M1	6.0	21.8	75 92 95 68	83
B 88 (-325 mesh) (BD -325 mesh)	HC	12	MX5	11	M1	6.0	21.8	202 180 231	204
B 89	HC	12	MX6	14	M1	6.0	20.8	198 223 173 185	195
B 90 (-325 mesh) (BD -325 mesh)	HC	12	MX6	14	M1	6.0	20.8	245 275 242 255	254

Table 2.8 (Contd.)

1	2	3	4	5	6	7	8	9	10
B 91	HC	12	MX7	14	M1	6.0	23.1	196 215 203 170	196
B 95	HC	12	MX5 + MX7	3.7 + 9.0	M4	6.0	25.2	220 235 225 220	225
B 98	HC	12	MX5 + MX7	4 + 9	M4	6.0	23.5	208 163 197 208	194
B 99	HC	12	MX7	14	M4	6.0	23.5	308 292 298 275	293
B 103	HC	12	MX5 + MX7	4 + 9	M4	6.0	25.9	246 253 306 155	240
B 102	HCC	12	MX5 + MX7	4 + 9	M4	6.0	25.9	1110 1225 935 850	1030
B 105	HC	24	SM5 + SM7	4.8 + 9.3	M4	6.0	25.9	100 95 94 100	97
B 106	HCC	26.5	SM5 + SM7	4 + 9	M4	6.0	25.9	750 700 788 700	735
B 108	HC	12	SM5 + SM7	4 + 9	M4	6.0	26.5	230 226 220 220	224
B 110	HC	24	SM5 + SM7	6 + 10	M4	6.0	25.9	117 111 123 129	120
B 114	BC	12	SM5 + SM7	4 + 9	M4	6.0	24.8	476 590 550 460	519

Table 2.8 (Contd.)

1	2	3	4	5	6	7	8	9	10
B 117	BC	14.3	SM5 + SM7	4 + 9	M4	6.0	25.9	396 408 433 378	404
B 118	BC	28.6	SM5 + SM7	4 + 9	M4	6.0	25.9	93 109 92 93	97
B 126	BCC	17.9	SM5 + SM7	4 + 9	M4	6.5	23.8	515 854 724 888	745
B 127	BCC	35.8	SM5 + SM7	4 + 9	M4	6.0	22.1	508 521 375	468
B 31	BCC	12	MX3	8	M1	9.0	24.5	464 435 231	377

Table 2.9

Compressive Strengths of Dry Composite Pellets Using Combination of Organic and Inorganic Binders

* All pct. wt. w.r.t wt. of blue dust
* Coal : Hutar coal (12pct)
* Mixing code : M1
* Treatment : T1
* Binder code : D =Dextrin, B =Bentonite, T =TSR, HL =$Ca(OH)_2$, Su = Sugar, L = Lime

Sample No	Binder (Code)	(pct)	Air Drying (Minutes)	Compressive Strength (N per Pellet)	Av Compressive Strength (N per Pellet)
B 51	D	2.0	15	156	124
	+	+		97	
	B	0.5		130	
				112	
B 63	T	3.0	15	363	317
	+	+		238	
	D	0.5		347	
	+	+		320	
	B	0.5			
B 68	T	2.0	30	172	155
	+	+		127	
	B	1.0		153	
				167	
B 69	T	2.0	30	184	170
	+	+		160	
	D	0.5		179	
	+	+		158	
	B	0.5			
B 74	HL	8.0	20	433	369
	+	+		423	
	Su	11.5		350	
				268	
B 75	L	6.0	20	236	235
	+	+		281	
	Su	10.0		218	
				205	

CHAPTER 3

APPARATUS AND PROCEDURE

The entire experimental programme has been listed in Plan of Work (Sec 1.5). Out of these, the apparatus and procedure for raw material characterization, pellet making and testing of pellet strength have already been presented in chapter 2. This chapter deals with apparatus and procedure for high temperature experiments.

Two experimental set-ups were used for the present investigation :

(i) set-up for non-isothermal kinetic studies

and (ii) thermogravimetry set-up for isothermal kinetic studies.

3.1 Apparatus

3.1.1 Set-up for non-isothermal studies

Schematic representation of the set-up is shown in Figure 3.1. It had five main components :

(i) furnace with temperature controller

(ii) reaction chamber with pellet assembly

(iii) stepper motor with controller

(iv) gas chromatograph

and (v) capillary flowmeter.

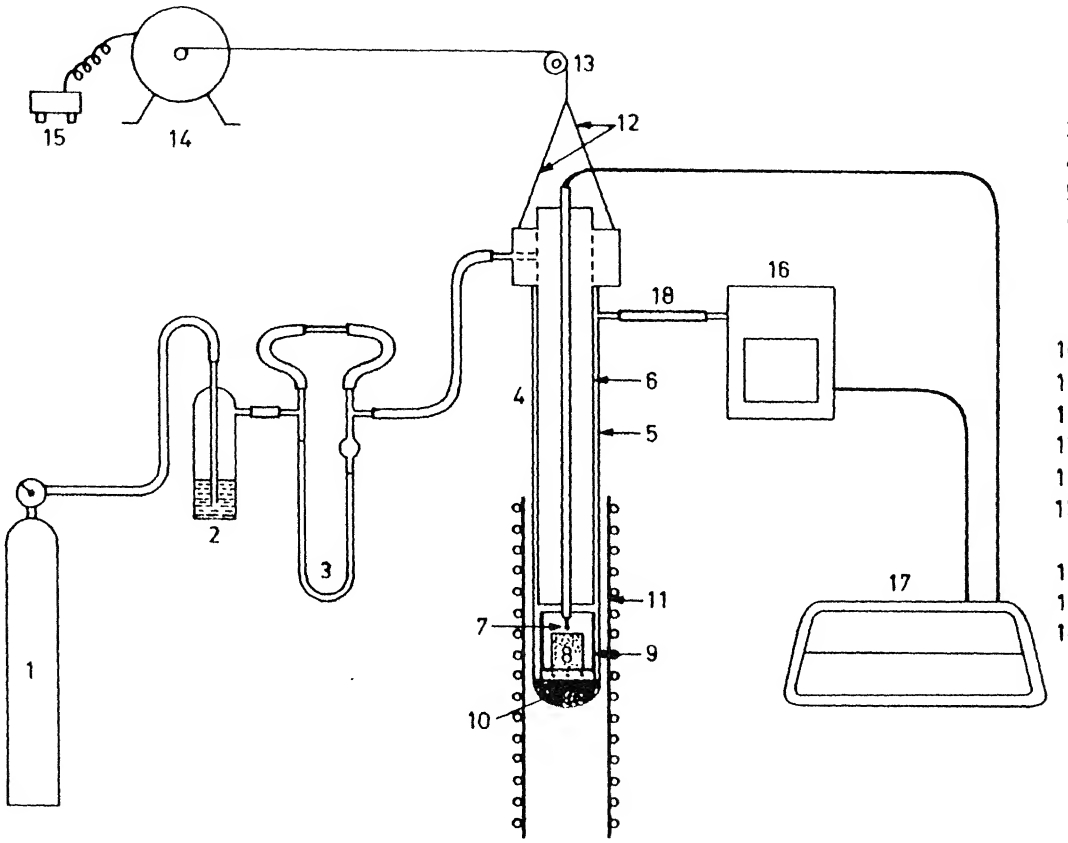

1. ARGON GAS CYLINDER
2. BUBBLER
3. CAPILLARY FLOW METER
4. REACTOR CHAMBER
5. SILICA TUBE
6. MULLITE TUBE
7. THERMOCOUPLE
8. SAMPLE
9. INCONEL CRUCIBLE
10. ALUMINA BULK FIBER
11. FURNACE
12. NICHROME WIRE
13. PULLEY
14. STEPPER MOTOR
15. STEPPER MOTOR CONTROLLER
16. GAS CHROMATOGRAPH
17. RECORDER
18. ANHYDROUS $CaCl_2$ TUBE

Fig. 3.1. Setup for non-isothermal kinetic studies of composite pellet reduction (schematic).

These are described below. This unit was specially fabricated for this investigation.

3.1.1.1 Furnace with temperature controller

A kanthal-wound vertical furnace of 500 mm length was employed for heating the reaction chamber. The temperature of the furnace was controlled (±5 K) by Electromax controller (Leeds and Northrup Co., USA) actuated by a chromel-alumel thermocouple. Figure 3.2 shows temperature profile of the furnace. A constant temperature zone of about 50 mm length could be obtained at the centre of the furnace.

3.1.1.2 Reaction chamber with pellet assembly

Figure 3.1 shows the reaction chamber used for non-isothermal study. It was a 15 mm i.d.and 420 mm length transparent fused silica tube with one end closed. To cut down the dead volume of reaction chamber, a mullite tube (13 mm o.d. and 395 mm length) was inserted into the silica tube. A Pt/Pt-10 pct Rh thermocouple was inserted into the silica tube through the mullite tube, so that the tip of the thermocouple was just 4 to 5 mm above the sample. Arrangement was also made so that the tip of the thermocouple could be inserted into the sample to monitor the core temperature if required. Special sample holder was designed and fabricated from inconel rod. It was a crucible with perforated bottom. Arrangement was also made to flush the reaction chamber with an inert gas,which was passed through the mullite tube. This was necessary to initially flush out entrapped air,and subsequently the product gas mixture out into the gas

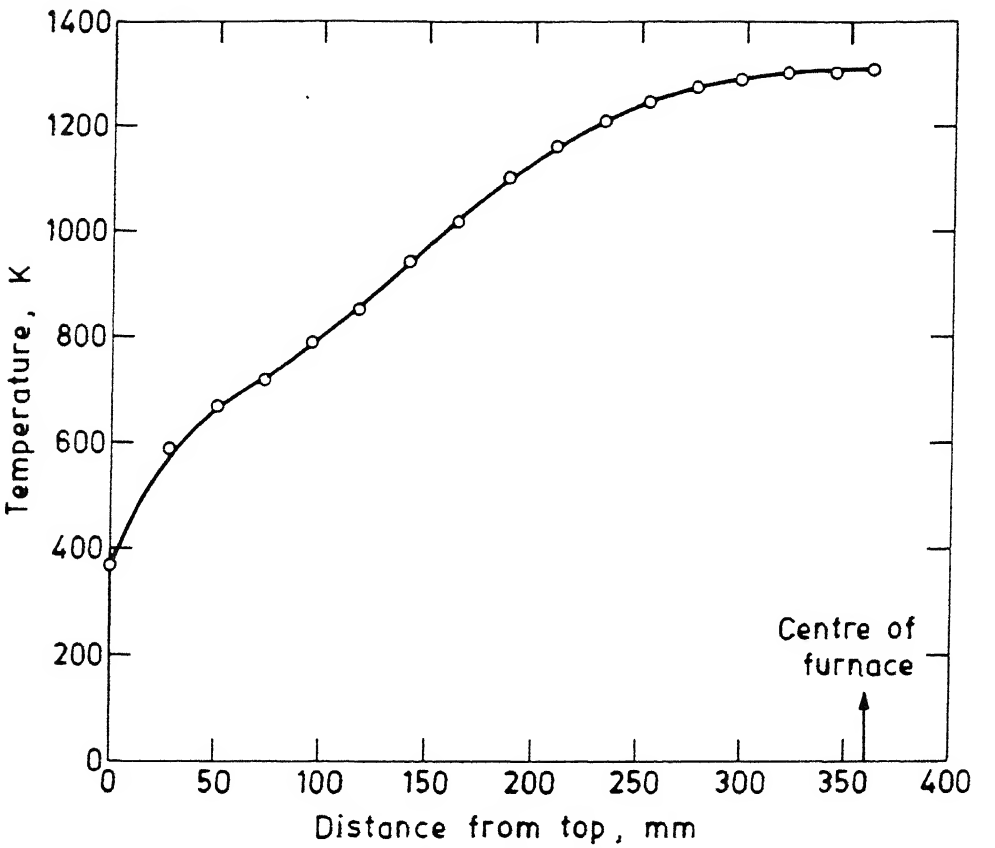

Fig. 3.2. Temperature profile of furnace for non-isothermal studies.

chromatograph. Another reason for passing inert gas through reaction chamber was to avoid any back diffusion of air into the reaction zone from outside by maintaining a positive pressure inside the reaction chamber. All precautions were taken to avoid any leakage into the reaction chamber.

3.1.1.3 Stepper motor assembly

The basic purpose of the reversible stepper motor (Automatic Electric Pvt Ltd,Bombay; type : SS-312, input voltage : 12V DC, 200 steps/rev) was to introduce the reaction chamber slowly into the furnace for non-isothermal studies. Stepper motor controller was designed and fabricated at IIT,Kanpur for maximum 9999 steps and with three speeds (15, 30 and 95 steps.min^{-1}). To cover the required distance, 1450 steps were necessary.

In non-isothermal kinetic studies,it was decided to simulate residence time of charge in foundry cupola,which is approximately 1 hour. 30 steps per min allowed a total travel time of 48 mins of pellet from room temperature to hot zone temperature of furnace (1273 K),and 15 steps per min gave residence time of 96 mins.

3.1.1.4 Gas chromatograph

Gas chromatograph (to be abbreviated as GC) employs the principle of selective adsorption of various gases in a mixture on a solid adsorbent. It has two columns packed with adsorbents. A carrier gas,usually hydrogen, is continuously passed through the two columns. When a mixture of gases is

injected into the carrier gas stream of one of the columns, it is carried along the column. However the adsorbent slows down the rates of travel of the strongly adsorbed gaseous components with respect to weakly adsorbed ones. If the length of the column is long enough, the components get separated from one another, and emerge from the column one after the other. The quantity of each component is evaluated with the help of a thermal conductivity detector (TCD). This is recorded as a peak on a voltage-time recorder.The area under the peak is directly proportional to the quantity of the species in gas mixture responsible for peak. The species can be identified by its retention time in the column. The specification of the Gas chromatograph is as follows.

Manufacturer : Chromatography and Instruments Co, Baroda

Model : 1984

Columns : Carbosieve S-II , Silica gel.

3.1.1.5 Capillary flowmeter

Capillary flowmeter consisted of a fine capillary. It had been designed and fabricated in this laboratory earlier for measuring very low flowrate (maximum 1 $cm^3.s^{-1}$). The calibration equation of the capillary flowmeter can be represented as :

$$Q = 0.0288\ h - 1.98 \times 10^{-4} \qquad \ldots(3.1)$$

where Q is flowrate of argon, $cm^3.s^{-1}$ at STP and h is height difference in flowmeter, cm.

3.1.2 Apparatus for isothermal measurements

It consisted of a furnace, Cahn electrobalance, and gas train. These are described below.

3.1.2.1 Furnace

A platinum-rhodium wound vertical furnace of 210 mm length was used in the study. The temperature of the furnace was controlled (± 2 K) by Electromax controller (Leeds and Northrup Co, USA) actuated by a chromel-alumel thermocouple. An alumina tube (17.5 mm i.d., 400 mm height) acted as reaction chamber. The alumina tube was fitted with two brass heads (one at the top and the other one at the bottom) to provide air tight fitting covers. Thermocouple and gas inlet tube were inserted through the bottom of the furnace. The thermocouple emf was measured by a digital millivolt meter (Vaiseshika Electron Devices,Ambala Cantt; type 7709). Silicone rubber 'O' rings and high temperature silicone sealant were used to make the set-up leak-proof.

3.1.2.2 Cahn electrobalance

The Cahn 1000 (Cahn Instruments, USA) is an automatic recording and sensitive weight measurement instrument. It can weigh up to 100 gms and is sensitive to changes as small as 1 microgram. The balance is divided into two sections. One is the control unit for all controls and outputs of the balance. The other part is the weighing unit which detects the actual weight. The control unit was connected to a strip chart recorder (Digital Electronies Ltd, Bombay; type: Omniscribe B 5000) to

record changes of weight during the reaction with time. Figure 3.3 shows the schematic diagram of the Cahn electrobalance and furnace system.

3.1.2.3 Gas train

The basic purpose of the gas train was to monitor the flow rate of the gases and to purify them from probable impurities present. Figure 3.4 presents the line diagram of the gas train.

Purified argon gas free from oxygen, moisture and carbon dioxide was employed for flushing and to maintain an inert atmosphere in the reaction chamber.Carbon dioxide was employed as a mixing gas with carbon monoxide for carrying out reduction of blue dust at isothermal condition. Hydrogen was used for reduction of blue dust, as well as for regenerating BTS catalyst (BASF, Germany) after every 10 to 15 runs.

Gases were passed through bubbler and capillary flowmeter. They were then passed through the BTS catalyst furnace at 460 K. BTS catalyst (5x5 mm cylinder) contains 30 pct of copper in a very finely dispersed form stabilized on a ceramic substrate. Due to very high surface area, the fine copper particles have high efficiency to remove oxygen from gases at relatively low temperature. BTS catalyst was also used to remove oxygen from inert gases.

Next, gases were passed through anhydrous calcium chloride and drierite ($CaSO_4$) columns before introduction into reaction chamber. Drierite has a low equilibrium residual water

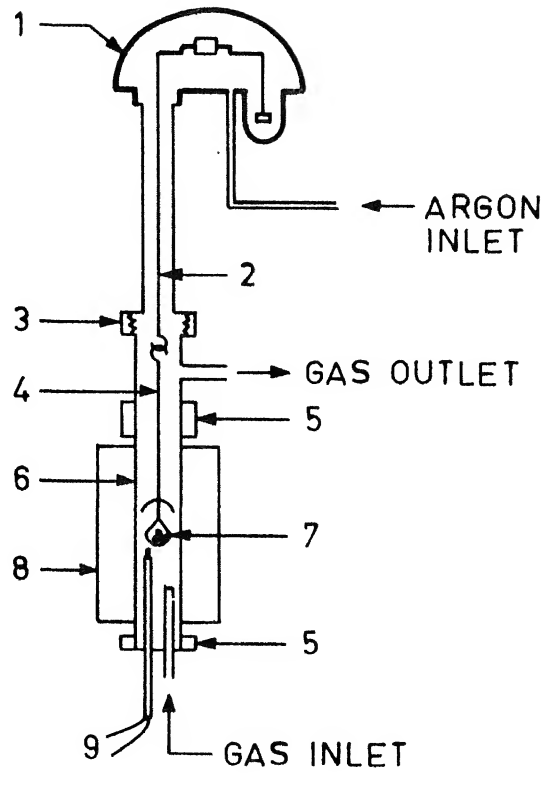

1 CAHN BALANCE
2 INCONEL ROD
3 SCREW CAP
4 HANGING ARRANGEMENT
5 COOLING ARRANGEMENT
6 ALUMINA TUBE
7 SAMPLE
8 PLATINUM-RHODIUM WOUND FURNACE
9 CHROMEL-ALUMEL THERMOCOUPLE

Fig. 3.3. Schematic diagram of the thermogravimetry setup with Cahn electrobalance.

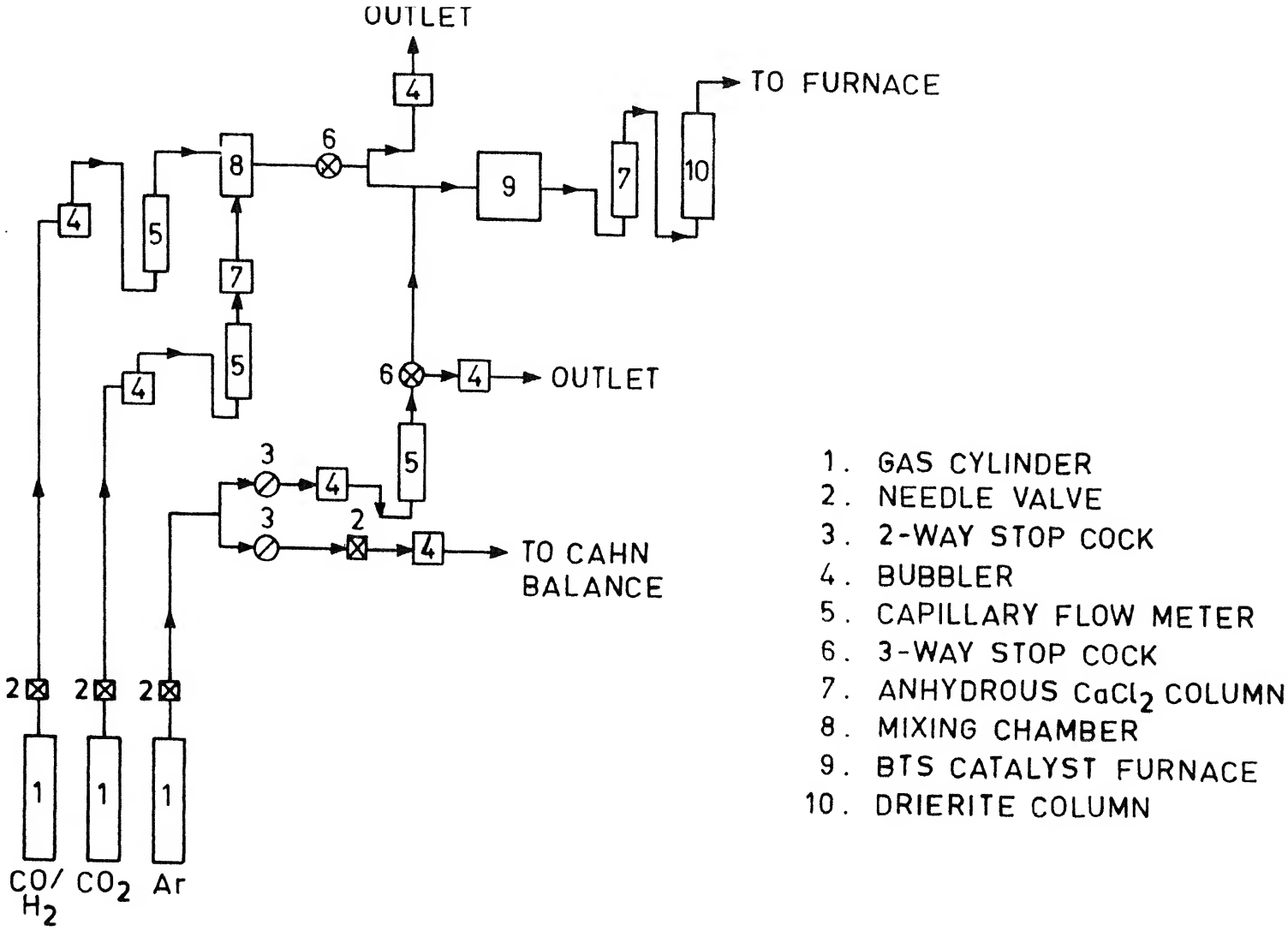

Fig. 3.4. Schematic diagram of the gas train used with thermogravimetry setup.

vapour content and therefore, it was used after the anhydrous calcium chloride column in the gas train for efficient removal of moisture.

The calibration of individual flowmeter was done. Results are presented in Table 3.1 in equation form after data fitting by linear regression.

Table 3.1

Calibration Equations For Flowmeters at STP

Gas	Flowmeter (No)	Equation
Ar	3	Q = 0.8531 h + 1.136
H_2	2	Q = 0.2178 h + 0.090
CO	2	Q = 0.0981 h + 0.073
CO_2	1	Q = 0.2960 h + 0.249

3.2 Experimental Procedure

3.2.1 Non-isothermal kinetic studies

3.2.1.1 Trials

Before arriving at the actual procedure, many set of trials were given.

(i) It was initially tried to measure the rate of evolution of product gases with the help of soap-bubble meter, but without success. Wet test meter could not be used to measure the

rate of product gases due to presence of water in wet test meter,which would absorb lot of CO_2 gas (solubility of CO_2 gas in water is 0.759 cm^3/cm^3 of water at 298 K and 1 bar pressure[65]). So it was decided that capillary flowmeter (30 to 50 $cm^3.s^{-1}$ capacity) would be employed for this purpose.

(ii) Next set of trials was carried out with the help of a capillary flowmeter. The reaction chamber was moved into the furnace by manually operating the stepper motor. Very little height difference at the capillary flowmeter was observed. Hence it was concluded from this set of trials that very small amount of gases was coming out from the reaction chamber due to :

either a) leakage in the system,

or b) insensitivity of the flowmeter.

(iii) Then trials were given to collect the product gases in measuring cylinder by water displacement. Some gas was collected, but that was far below the estimated volume.

H_2, CO, CO_2, CH_4, NH_3, H_2S, H_2O and higher hydrocarbon gases were expected to evolve during pyrolysis of coal at the time of heating of composite pellet. Table 3.2 reports the solubility of gases in water at 298 K and 1 bar pressure[65,66].

Table 3.2

Solubility of Gases in Water

(cm^3/cm^3 of water)

H_2	CO	CO_2	H_2S	CH_4	NH_3
0.0175	0.0214	0.759	2.282	0.03	639.0

So one possible reason was dissolution of gases in water especially with respect to CO_2 etc. Hence it was decided that gas would be collected by pushing of water from the top. A thin plastic disk would be kept to float on water to prevent direct contact of gases with water. However it was abandoned due to problems like leakage etc.

(iv) Finally trials were carried out with pure argon gas (Iolar 2) flow in the reaction chamber at low flow rate (0.15 to 0.25 $cm^3.s^{-1}$). The product gas was analysed by gas chromatograph. Since argon flow rate was fairly precisely known and controlled during experiment, the volumetric rates of evolution of individual gaseous species (Q_i) could be calculated from these measurements at intervals of time as follows :

$$Q_i = Q_{Ar} \times \text{volume fraction of i in gas as determined by GC} \quad \ldots(3.2)$$

It was concluded that the procedure was satisfactory.

(v) Further trials were also given to the GC for adjusting its operating parameters such as oven temperature, filament current etc in order to obtain retention times of gases within certain limit for both hydrogen and argon carrier gas. This was necessary in order to determine composition of product gas as function of time.

3.2.1.2 Procedure

Since it was not possible to monitor weight loss as function of time during the course of reduction of composite pellet under non-isothermal condition, it was decided to monitor

Recorder settings (dual pen) :

(i) Voltage scale : pen Y_1: 5mV full scale
(for gas analyses)
pen Y_2: 10mV full scale
(for sample temperature)

(ii) Chart speed : 10 $mm.min^{-1}$.

The apparatus described in section 3.1.1 (Figure 3.1) was employed for fundamental non-isothermal kinetic study of composite pellets. The GC was switched on as per standard procedure at least 4 hours before beginning of a run in order to stabilize its operation.

Composite pellet of measured dimensions was taken in a inconel sample holder and weighed by a semimicro balance (W.M.Ainsworth and sons.Inc,USA). Sample holder with pellet was placed inside the reaction chamber. Then top of the reaction chamber was sealed properly with gas inlet and thermocouple arrangement. The gas outlet tube of the reaction chamber was connected to the gas chromatograph by a fine nylon tube (2.5 mm i.d.). Reaction chamber was flushed with pure argon (Iolar 2) at a low flow rate (0.25 $cm^3.s^{-1}$ at STP). The furnace temperature was controlled at 1273 K. The reaction chamber was hanged from a pully by nichrome wire at the top of the furnace.

At zero time,the stepper motor controller and recorder were simultaneously started. This allowed introduction of the reaction chamber into the furnace at a pre-determined speed. The temperature of the sample was continuously recorded with time by the recorder. Time to time product gas mixture was injected into

the gas chromatograph through the auto injector and peaks obtained in the recorder. After the reaction chamber reached the desired distance (i.e. pellet at centre of the furnace),the stepper motor was stopped. Then immediately reaction chamber was taken out from the hot zone of the furnace and allowed to cool at low temperature zone. Sufficient time was allowed to the sample to cool upto 300 K in inert atmosphere. Then the sample was taken out from the reaction chamber and preserved in a desiccator for further studies. This procedure was again repeated for next run.

3.2.1.3 Simultaneous measurement of ambient and sample core temperatures

In non-isothermal studies the thermocouple tip was located 4 to 5 mm above the pellet surface. It is expected that the centre temperature of the pellet would be somewhat lower than this due to slow heat transfer during heating as well as endothermic reaction taking place. For interpretation of results it would be desirable to know the average temperature of pellet as function of time. This requires simultaneous measurement of centre temperature of pellet as well.

Since it was not possible to introduce two thermocouples when gas analysis was also undertaken,separate experiments were carried out to simultaneously measure centre temperature and usual ambient temperature 4 to 5 mm above surface by two thermocouples. For this purpose special pellets were prepared to insert the thermocouple tip at the core of the pellet. Procedure was the same as discussed earlier in Section

3.2.1.2, except that product gas analysis was not done in these experiments.

3.2.2 Auxiliary studies and measurements

Several sets of auxiliary experiments were carried out as listed below :

(i) hydrogen reduction of blue dust

(ii) carbon monoxide reduction of blue dust

(iii) devolatilization of coals

(iv) X-rays of non-isothermally reduced composite pellets

(v) SEM observation of non-isothermally reduced pellets

(vi) testing of composite pellets for strength,both before and after reduction (procedure already discussed in chapter 2 and again to be discussed in chapter 5, swelling of pellets to be discussed in chapter 5)

(vii) measurement of degree of reduction of pellet after non-isothermal study. This will be taken up in chapter 4.

3.2.2.1 Reduction of blue dust by hydrogen / carbon monoxide

Instrument settings :

(a) Cahn electrobalance :

Pct sample wt	: off
Filter	: on/off

Auto range expander : on

Meter and recorder range (MRR) : 10 mg

Weight suppression range : 10 g

Output : 10 mV

(b) Recorder :

Voltage scale : 10 mV full scale

Chart speed : 10 $mm.min^{-1}$

Reduction was carried out isothermally. Set-ups are shown in Figures 3.3 and 3.4. After the furnace attained the operating temperature, sufficient time was given for the stabilization of temperature. The furnace was flushed with purified argon gas (4.17 $cm^3.s^{-1}$ at STP) to remove all entrapped air and to maintain a neutral atmosphere. Blue dust (oven dried) was taken in an inconel crucible (Table 3.3) and weighed by semimicro balance. Initially the furnace was in lowered position. The hanging assembly is shown in Figure 3.5.

The crucible with blue dust sample was hanged from the Cahn electrobalance. Then the furnace was raised by jacks to proper position,and hooked up with the balance to make it gas tight. Argon gas was flowing from the top of the Cahn balance as well as bottom of the furnace. Now the sample was initially weighed in balance and recorder was set at zero position by adjusting the weight suppression at the Cahn balance controller. The sample temperature and furnace temperature were equalized by allowing some more time and the recorder was rezeroed. In the mean time flow of hydrogen/carbon monoxide/carbon dioxide was adjusted in

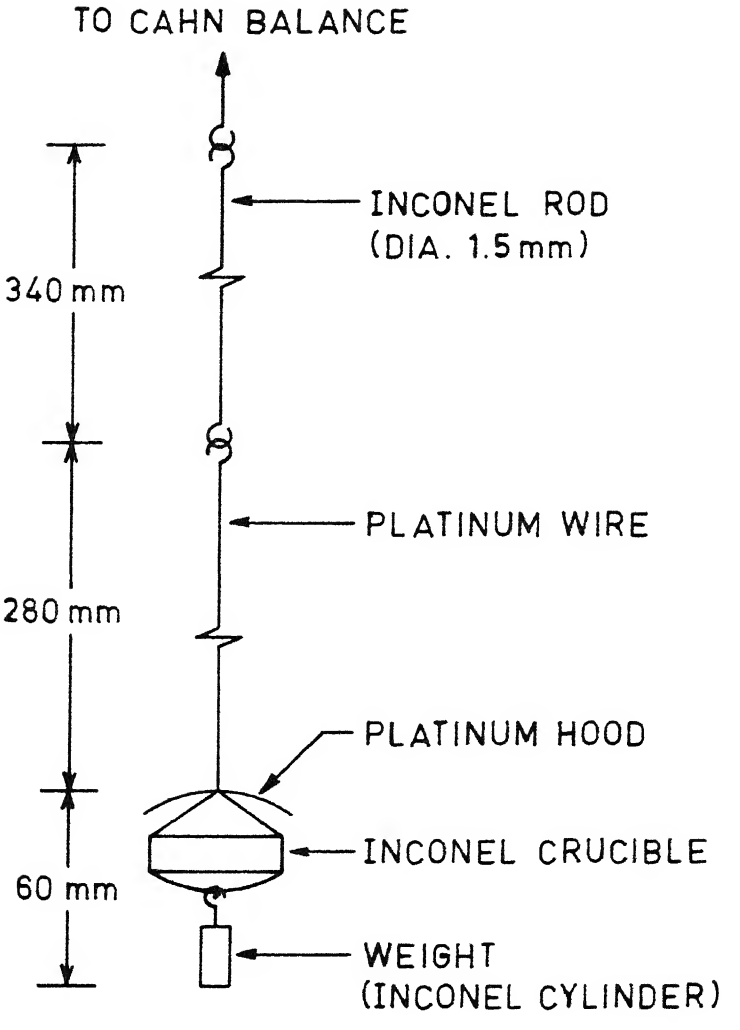

Fig. 3.5. Hanging assembly for thermogravimetry.

the flowmeter and allowed to flow through bypass. Then with the help of a 3-way stopcock flow of gas at the bottom inlet of the furnace tube was switched over from argon to H_2 or $CO-CO_2$ or CO-Ar gas as the case may be. At the top of the balance argon flow was on at very low rate in order to protect the balance chamber from reactive furnace gases. Any small weight change occurring during gaseous reduction was recorded as a function of time by the voltage-time recorder. After the reduction was over, flow of reactive gas was again substituted by argon flow. Allowing 2 to 3 minutes of argon flow, the furnace was disconnected from the balance and lowered down by jacks. The sample was taken out. Now the furnace was ready for the next run.

Table 3.3

Dimensions of Inconel Crucibles

Crucible No.	i.d. (mm)	Lip Height (mm)	Amount of Blue Dust (mg)	Bed Depth (mm)
I	10.50	2.0	100.0	0.44
II	10.25	3.9	200.0	1.05
III	10.50	4.7	300.0	1.50

3.2.2.2 Devolatilization of coals

Non-isothermal set-up was used for devolatilization study. Procedure followed was similar to non-isothermal kinetic study of composite pellets (as discussed in Section 3.2.1.2).

Settings for gas chromatograph operation were the same as noted in Sec.3.2.1.2 for H_2 and Ar carrier gas.

Standard pellets were prepared from mixture of alumina powder (98 pct pure,-100 mesh size) and coal (-100 mesh) with the help of binder (4 pct S.Mix V and 9 pct S.Mix VII). The pellets were steam curing by autoclave. Alumina powder behaves as an inert material. It was used to simulate composite pellet geometry etc. so that the devolatilization rates are more representative of composite pellets.

3.2.2.3 X - ray studies

A few samples were selected for X-ray diffraction study. Samples were collected after non-isothermal reduction of composite pellets. By hand grinding,reduced pellets were powdered and spread on a glass slide. Then few drops of acetone were added. With the help of another slide,the powder was spread uniformly on the slide. It was allowed to dry and placed in the X-ray machine (Rich-Seifert and Co, Germany; type : Debyeflex 2002,MZ III) holder for X-ray diffraction.

Settings of X-ray diffractometer:

i) Cu K_α with monochromatic X-rays

ii) Scanning speed : 3 degree.min^{-1} (for 2θ)

iii) Counts per min : 2K

iv) Time constant : 10 sec

v) Current : 20 mA

vi) Voltage : 30 KV

vii) Chart speed : 30 mm.min^{-1}.

3.2.2.4 Scanning electron microscopy (SEM)

Samples were taken after non-isothermal reduction of composite pellets. Since the conductivity of samples was very poor, it required gold plating. Initially after putting the samples inside the deposition chamber, argon gas was passed into the chamber. Then the pump was switched on for evacuation of the chamber. When the pressure in chamber reached 1.2 to 1.5 torr, the plating current was switched on at 10 mA (1.3 KV) for required time (4 mins, auto off). Time was adjusted accordingly (2 mins, 4 mins etc.).

SEM (JEOL, JSM 840A) observations were done for the following samples :

i) non-isothermally reduced samples

ii) fractured surfaces of the reduced samples

Few photographs were taken.

CHAPTER 4

MEASUREMENT OF DEGREE OF REDUCTION

For reduction of iron oxides by carbon, a major difficulty with experiments is that the extent of the reduction can not be found out directly from the weight loss of the sample since this is made up of both oxygen and carbon losses. For ore-coal composite pellets, the weight loss of the sample arises not only from oxygen and carbon loss, but also the loss of volatile matter and residual moisture present in pellet. Since only weight loss of the sample is not sufficient, some additional measurements are required for estimating the degree of reduction(α), which is defined as follows.

$$\alpha = \frac{\text{weight of oxygen removed from iron oxide X 100}}{\text{total weight of removable oxygen present in iron oxide}}$$

$$= \frac{\Delta W_o}{W_o^i} \times 100 \qquad \ldots(4.1)$$

Attempts have been made to solve this problem in various ways, and a satisfactory procedure has been evolved. This chapter is concerned with this issue exclusively.

4.1 Literature Review

For determining the degree of reduction for carbothermic reduction, research workers have employed various techniques. Most of the investigations reported here employed carbon,such as graphite, coconut char, coal char as reductant. In these cases the product gas consists of CO and CO_2 only and its analysis is straight forward. However that would not be the case if coal is used, because then other gases such as H_2, CH_4 etc. also would be present.

Otsuka and Kunii[1] investigated reduction of iron oxide by graphite in flowing argon. They collected product gas samples into sampling devices at suitable time intervals and analysed the same by gas chromatograph to obtain the composition of the gaseous products. Overall reaction rate as well as rates of weight loss of oxygen ($\dot{W}_o$) and carbon ($\dot{W}_c$) were calculated from the flow rate and composition (X_{CO} , X_{CO_2}) of exit gas from the reaction chamber.

$$\dot{W}_o = \frac{16Q}{22400} .(X_{CO} + 2X_{CO_2}) \qquad ...(4.2)$$

where $\dot{W}_o$ is rate of oxygen loss in gms per sec, Q is volumetric flow rate in cm^3 per sec (at STP), X is volume fraction of gas, 16 is atomic mass of oxygen.

$$\Delta W_o = \int_0^t \dot{W}_o \, dt \qquad ...(4.3)$$

where t is time in secs. Therefore ΔW_o and hence degree of

reduction (α) were calculated with the help of Eqs.(4.1) to (4.3). Experimental data of weight loss measured by balance were employed as cross check for the experimental errors involved in gas analysis and flow measurement.

Rao[3] carried out reduction of hematite powder by amorphous carbon powder. He measured weight of the specimen before and after reduction and pct weight loss was determined. The fractional reaction f, at time t, was calculated using the relation,

$$f = (100\ \Delta W_t\ /\ MW_o) \qquad \ldots(4.4)$$

where $(100\ \Delta W_t\ /\ W_o)$ = weight loss pct at time t,

and M = weight loss pct corresponding to complete reduction.

So Rao took f as a measure of degree of reduction. This would be correct only if the composition of product gas remains constant throughout the experiment. However it has been found[1,8] that gas composition changes during the course of reaction in a major way.

Ghosh et al[4] also collected the evolved gas during the reduction of hematite ore-coal char briquette. Weight of the sample was measured before and after reduction. The gas and reduced material were analysed. Pct reduction was calculated from the analysis, as the pct of total oxygen removed in accordance with Eq.(4.1). It is not clear how the gas analysis was utilized.

Reeve et al[5] determined the rates of reduction of the composite pellet with iron oxide and char or coke. The progress

of reaction was monitored by the increase in pressure within the constant volume system as measured by a 0 to 760 mm absolute pressure transducer connected to a side arm in the cold part of the system. A starting pressure of 400 mm Hg by introducing argon was chosen so that the final pressure within the system after the reduction did not exceed one atmosphere. No information is available about the method of calculation of degree of reduction.

Srinivasan and Lahiri[6] mixed powders of natural hematite and graphite,and prepared pellets by hand for reduction studies. They measured the progress of reduction with time by noting the weight changes in the pellet and product gas analysis. The amount of CO_2 absorbed in a given time interval was determined from the increase in weights of the absorption tubes. The amount of CO present in the outcoming gas stream was determined from the weight change and CO_2 absorption data. At any instant, the degree of reduction was evaluated from above data.

Abraham and Ghosh[8] studied reduction of iron oxide-graphite powder mixture as well as oxide pellet-graphite powder system. They basically followed the approach of Otsuka and Kunii[1], but with entirely different measurement technique. In their investigation, a sensitive capillary flowmeter was employed to measure the rate of evolution of product gases (i.e. CO and CO_2). Gas composition was determined by an oxygen sensor employing a calcia-stabilized zirconia (CSZ) solid electrolyte tube. This allowed determination of X_{CO} and X_{CO_2} in the gas phase from measured oxygen potential of gas since the reductant was pure carbon and the product gas was CO and CO_2. From flow rate and

composition of gas as function of time, $\dot{W}_c$ and $\dot{W}_o$, ΔW_o and α were determined as function of time,and total oxygen using Eqs.(4.1) to (4.3).

Gokhale, Sengupta and Ghosh[9] investigated reduction of iron ore-graphite powder mixture as well as ore pellet-graphite powder system. They determined the rates of loss of oxygen ($\dot{W}_o$) and carbon ($\dot{W}_c$) by measuring instantaneous flow rates of product gases by precision capillary flowmeter. Gas composition was estimated by assuming stagewise reduction ($Fe_2O_3 \longrightarrow Fe_3O_4 \longrightarrow Fe_xO \longrightarrow Fe$) and equilibrium of gas with iron oxides all through.

Bryk and Lu[10] studied reduction of commercial magnetic iron ore concentrates and carbon mixtures. High volatile coals were used. Samples were taken out after various times in the hot zone and chemically analysed. Total iron, metallic iron, FeO and Fe_3O_4 percentages were determined. Degree of reduction was calculated on the basis of these data.

Mookherjee, Ray and Mukherjee[11] carried out reduction of iron ore fines surrounded by coal or char fines. They measured the overall degree of reduction (α) by using equation of Chernyshev and co-workers from the total iron analysis in ore and reduced mass.

$$\alpha = K_1 \left(\frac{\%Fe_T^r - \%Fe_T^i}{\%Fe_T^r \,.\, \%Fe_T^i} \right) .100 \qquad \ldots(4.5)$$

where K_1 = ratio of weight of iron to that of oxygen in initial ore

$\%Fe_T^i$ = pct of total iron in initial ore

$\%Fe_T^r$ = pct of total iron in reduced mass.

Ajersch[12] investigated reduction of iron oxide pellets with graphite. He calculated conversion rates from the weight loss data on the assumption that the oxide produced only CO gas. Such an assumption is not valid.

Srivastava and Sharma[13] prepared a core pellet from the mixture of iron ore and coal,and further coated it with the iron ore only. They determined the degree of reduction by using Eq.(4.1). Loss in weight due to carbon loss was calculated by estimating remaining carbon content in reduced pellet after each reduction. It is not clear how it was done. Oxygen loss was calculated by subtraction of other losses.

Bandyopadhyay[14] studied reduction of iron oxide by graphite or coconut char. He determined weight loss and also analysed the product gas by gas chromatograph at suitable time intervals. Overall reaction rate as well as $\dot{W}_c$, $\dot{W}_o$ were calculated from the weight loss and product gas composition (X_{CO}, X_{CO_2}).

Gonzales and Jeffes[67] have proposed a method of calculation to assess the chemical composition of partially reduced iron oxides. The method is based on the observed relationship between the degree of reduction and the corresponding degree of metallization of samples. The correlation can be used to determine the proportions of Fe^0,Fe^{2+},and Fe^{3+} from total iron analysis of pellets after reduction. The method

of determining the composition of reduced samples requires an accurate initial chemical analysis of the material, including gangue and loss on ignition.

4.2 Measurement Technique Adopted in the Present Investigation

As stated earlier, the technique of determination of degree of reduction (α) is simpler if the reductant is carbon since the product gas would consist of CO and CO_2 only. Here from measurements of flow rate and gas composition or weight loss and gas composition as function of time, it is possible to calculate α . As already reported a number of investigators adopted these methods[1,6,8,9,14]. However it would pose difficulties if coal is used as reductant due to evolution of other gases. Therefore this method would lead to errors in the present investigation.

Several investigators have calculated degree of reduction from chemical analysis of partially reduced pellets[4,10,11], as already presented in literature review. However this would be correct only if residual char or carbon in the reduced composite can be separately determined. For example Eq. (4.5) would yield correct value of α , if pct Fe means that in the ore part only, and not in the composite. However no investigator has mentioned whether carbon / char was separately determined or separated from reduced mass before undertaking analysis of total iron etc.

Therefore it was decided to try a simple method to determine degree of reduction (α), viz., by hydrogen reduction of partially reduced composites. The decision was prompted by

availability of the precision thermogravimetry apparatus in the laboratory (Sec. 3.1.2.2). The assumption behind the present method is that only the remaining oxygen present in the partially reduced pellet will react with hydrogen, and thus the weight loss would correspond to residual oxygen in pellet only.

Hydrogen reduction of pellets, reduced in non-isothermal studies, was carried out in the Cahn electrobalance set-up. Details of the set-up and procedure have already been presented in Sections 3.1.2 and 3.2.2.1 respectively. Hydrogen flow rate was maintained at 5 $cm^3.s^{-1}$ (at STP). The temperature selected after trials was 1023 K. The degree of reduction (α) was calculated by the following equation.

$$\alpha = \frac{\Delta W_o}{W_o^i} \times 100 = \frac{W_o^i - W_o^r}{W_o^i} \times 100 \qquad \ldots(4.6)$$

where W_o^r is total weight loss during hydrogen reduction, gms; and W_o^i is total removable oxygen present in composite pellet, gms.

$$\text{Again,} \quad W_o^i = W_p^i . f_b . p . f_o \qquad \ldots(4.7)$$

where W_p^i = initial weight of composite pellet, gms

f_b = fraction of blue dust present in composite pellet

p = fractional concentration of Fe_2O_3 in blue dust

f_o = fraction of oxygen present in Fe_2O_3.

Hence from total weight loss data (W_o^r) of hydrogen reduction of reduced pellet and initial weight of composite

pellet before non-isothermal study,the degree of reduction can be calculated using Eq. (4.6).

However it is to be noted that there are two possible sources of error :

(i) loss of carbon due to reaction of char with residual oxygen in ore during hydrogen reduction

(ii) loss of carbon due to the reaction :

$$C(s) + 2H_2(g) = CH_4(g) \qquad ...(4.8)$$

Hence it was necessary to consider and give trials to determine how serious these sources of errors would be before adopting this method.

4.3 Trials

4.3.1 Assessment of carbon loss due to reaction of oxygen in ore

Firstly,carbothermic reduction rate is orders of magnitude slower than hydrogen reduction rate at 1023 K. Secondly,there is not much contact between carbon and oxide since most of the oxides are reduced to iron. Therefore error from this source is expected to be insignificant. Anyway to confirm this point few samples of partially reduced composite pellets were kept in flowing argon gas at 1023 K. Changes of weight were insignificant in one hour,thus confirming the above expectation.

4.3.2 Trial on char gasification with hydrogen

4.3.2.1 Thermodynamic considerations

As already stated one source of measurement error may be loss of carbon by reaction with hydrogen. Gasification with hydrogen occurs according to reaction (4.8) for which

$$\Delta G^{o} = -16520 + 12.25\ T \log T - 15.62\ T \quad cal/mol^{68} \quad ...(4.9)$$

The equilibrium constant (K_e) for this reaction is given as :

$$K_e = \frac{P_{CH_4}}{a_C\ (P_{H_2})^2} \quad ...(4.10)$$

where P_{CH_4}, P_{H_2} are the partial pressures of methane and hydrogen respectively, in bar; and a_C is the activity of carbon in char, which may be assumed equal to 1.

$$\text{Again} \quad P_{H_2} + P_{CH_4} = 1 \quad ...(4.11)$$

From the above considerations, P_{CH_4} in equilibrium with carbon and H_2 were calculated. These are presented in Table 4.1. It may be noted that although P_{CH_4} values are not high, they are significant enough to conduct trials on kinetics of gasification of char by hydrogen.

Table 4.1

Thermodynamic Data for Methane Formation

Temperature (K)	ΔG^{o} (Cal/mol)	K_e	P_{CH_4} (bar) (Equilibrium)
1073	6554.7	0.046.	0.042
1023	5219.8	0.077	0.066
973	3897.8	0.133	0.105
923	2589.5	0.245	0.164

4.3.2.2 Measurements of char gasification rates

About 100 mg sample (Hutar char or Bachra char) was taken in a cylindrical stainless steel net basket. Hydrogen reaction studies were carried out at 923 to 1073 K in thermogravimetry set-up with Cahn electrobalance. Hydrogen flow rate was 5 $cm^3.s^{-1}$ (at STP). About 20 trials were given for this set of experiment. Fractional weight loss of carbon (f_{ch}) was calculated by following equation :

$$f_{ch} = \frac{\Delta W_{ch}}{FC_{(char)}} \qquad \ldots(4.12)$$

where ΔW_{ch} is total weight loss of char, gms

and $FC_{(char)}$ is fixed carbon contain of char sample, gms

4.3.2.3 Results and discussions

Figures 4.1 and 4.2 show the results of reaction of coal char with hydrogen. It may be noted that as the temperature was increased, the fractional weight loss of carbon also increased. Both the coal chars showed the same trend for all temperatures. The reaction rates are very slow particularly at 923 and 973 K.

From the trials of reduction of reduced composite pellet (broken pieces) by hydrogen, it was observed that initially rate of reaction was very fast, at the end the rate was slow. Therefore,the total time taken to complete the reduction was about 2 to 3 hours.This was too long. After few more trials,it was found that the time could be decreased to about 1 hour by carrying out thermogravimetry at 1023 K,as well as loading the pellet after breaking it into smaller pieces.

As may be noted from Figs 4.1 and 4.2 that losses of carbon in 1 hour at 1023 K were 0.0165gm and 0.0285gm per gm of carbon for Hutar and Bachra char respectively. In original composite pellets Fe_2O_3 / C weight ratios varied from 3 to 11. The lowest ratio was 3. This gives oxygen / carbon ratio as 0.9. Assuming a degree of reduction of 80 pct,oxygen left in composite pellet per gm of Fe_2O_3 would be 0.3(1-0.8) i.e. 0.06gm. Oxygen removed would be (0.3-0.06),i.e. 0.24gm. Assuming the gas to have 75 pct CO and 25 pct CO_2 on average,carbon loss would be 0.144gm. So,residual carbon in partially reduced pellet per gm of Fe_2O_3 would be approximately (1/3-0.144),i.e.0.189gm.

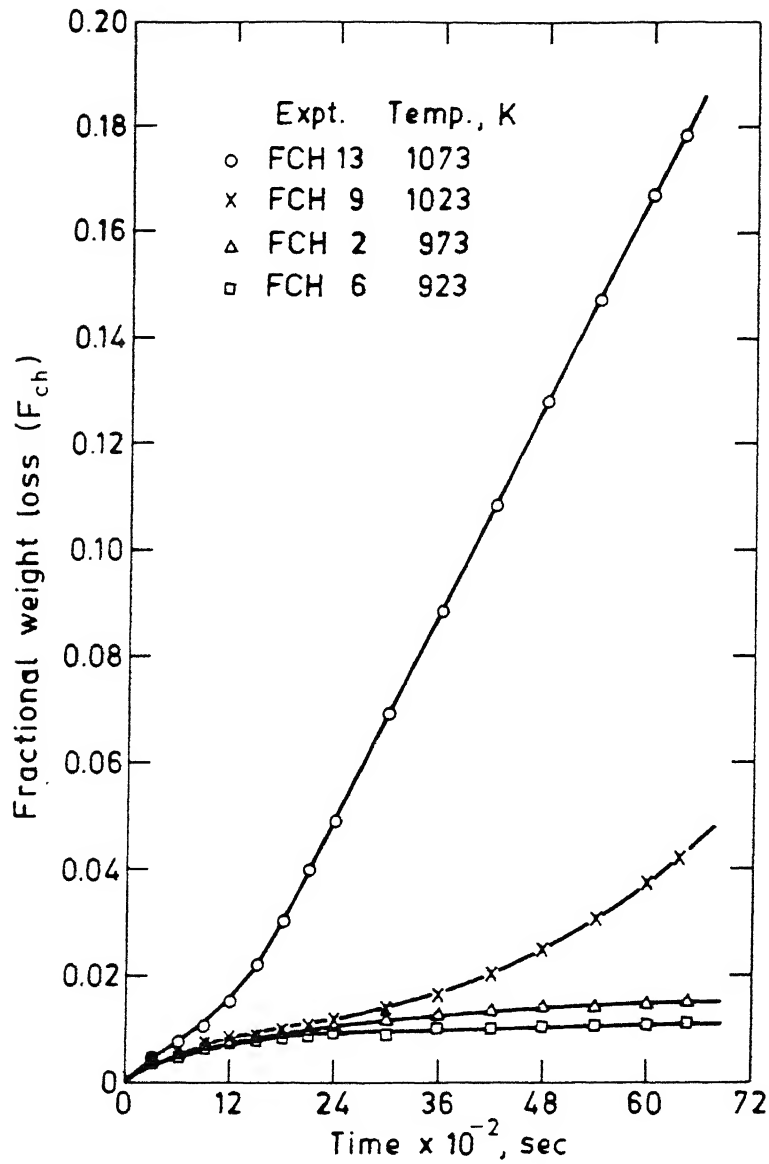

Fig. 4.1. Rate of gasification of Hutar coal char in hydrogen.

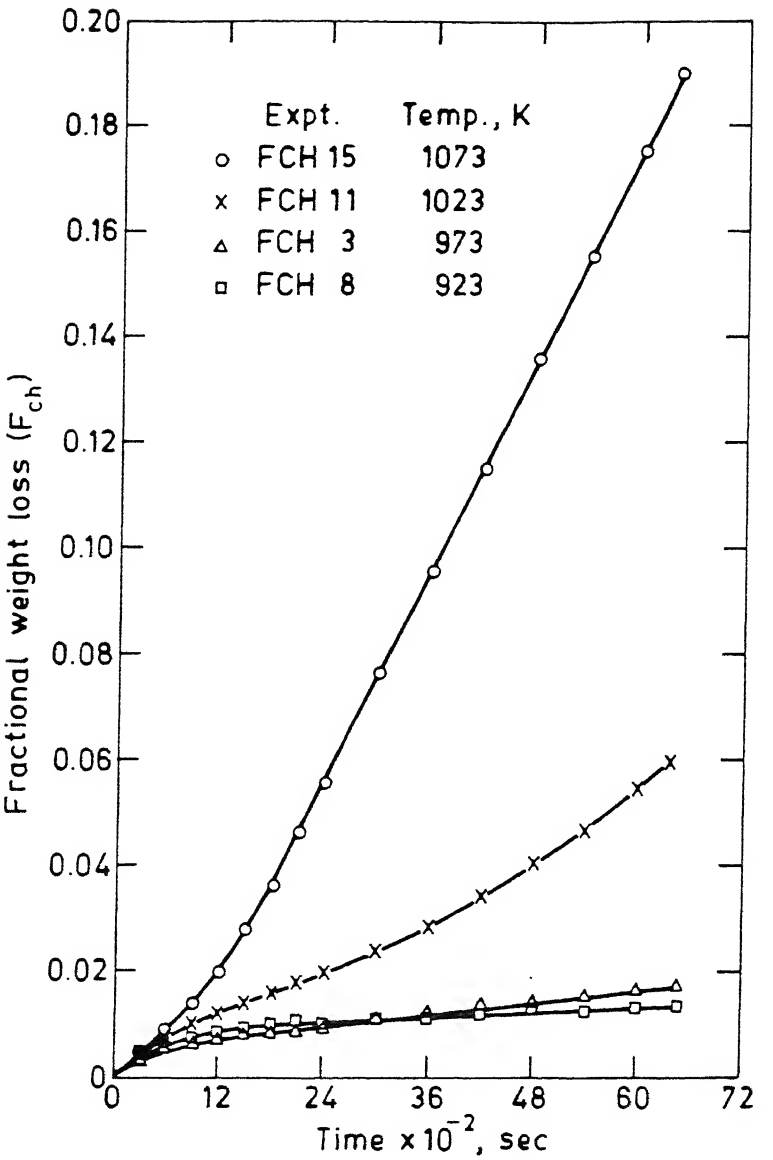

Fig. 4.2. Rate of gasification of Bachra coal char in hydrogen.

Hence maximum loss of carbon at 1023 K and 1 hour due to reaction with hydrogen, therefore, would be (0.189x0.0285)gm i.e.0.0054gm/gm Fe_2O_3. This represents (100 x 0.0054/0.06) i.e. approx 9 pct of residual oxygen. It would be lower for Hutar char.

4.4 Concluding Remarks

The above assessment indicates that pct error (expressed as pct of degree of reduction) may be as high as 10 pct at 1023 K. However it is to be recognised that the rate of carbon gasification by hydrogen in partially reduced composites is expected to be much lower as compared to that in the present trial due to diffusional resistances inside the composite. Hence actual error should be much lower. It has also been shown that error arising from reaction of oxygen with carbon in pellet at 1023 K is insignificant. Hence determination of degree of reduction of a partially reduced composite pellet by treatment with hydrogen at 1023 K in a thermogravimetry set-up appears to be quite satisfactory. Hence it was adopted in the present investigation.

CHAPTER 5

A COMPARATIVE STUDY OF PROPERTIES OF VARIOUS TYPES OF COMPOSITE PELLETS

Several composite pellets prepared during this investigation by various binders and techniques were selected for evaluation of properties. In addition, efforts were made to collect composite pellets from various outside sources for comparative study. But this could be achieved only from one source viz. Direct Reduction Process Development Division, R & D Centre for Iron and Steel, SAIL, Ranchi. 8 types of their composite pellets were also taken for evaluation.

As stated earlier, the purpose of this part of investigation was to collect data and note behaviour pattern of pellets prepared in various ways as a contribution towards development of cold bonding technology. Table 5.1 presents the compositions of prepared pellets used in this investigation.

5.1 Evaluation of Pellet Properties

Two types of measurements were carried out.

(i) Compressive strength before and after reduction

(ii) Reduction characteristics, such as degree of reduction and volume change upon reduction; reduction was carried out in non-isothermal set-up.

5.1.1 Compressive strength

To measure the compressive strength of a pellet, it is subjected to uniform loading between two parallel plates until the pellet is ruptured[44]. It was carried out in INSTRON 1195 Model at a scanning speed 1 mm. min^{-1}. Average compressive strength of dry pellets before reduction was obtained from four readings for each set of pellets. Strengths of composite pellets were measured after carrying out non-isothermal reduction as well. Compressive strengths of unreduced pellets which were prepared in this laboratory, have been reported already in Tables 2.6 to 2.9. From these some were selected for further evaluations here. These are summarized in Table 5.1. Dry strengths of unreduced pellets which were collected from SAIL,are presented in Table 5.2.

5.1.2 Non-isothermal reduction

Non-isothermal reduction tests of composite pellets were performed using the set-up for non-isothermal kinetic study as discussed in Section 3.1.1 . Furnace temperature was controlled at 1273 $\pm$ 5 K. Speed of reactor was 0.124 mm. sec^{-1}. Time taken by the pellet to reach hot zone was 48 minutes. Initial and final weights of each pellet were taken before and after reduction respectively. Initial and final dimensions of pellet were also noted before and after reduction. Fractional weight loss of pellets (F) was calculated as follows.

$$F = \frac{\Delta W}{W_p^i} \qquad \ldots (5.1)$$

where ΔW is loss of weight of pellet during non-isothermal reduction, gms and W_p^i is initial weight of composite pellet, gms.

The change of volume of the pellets due to reduction, was calculated as follows.

$$\text{Volume change (in pct)} = \frac{V_2 - V_1}{V_1} \times 100 \qquad \ldots (5.2)$$

where V_1, V_2 are the volumes of pellet before and after reduction, mm^3.

The degree of reduction of the reduced pellets was determined by hydrogen reduction of non-isothermally reduced pellets (details in chapter 4). The degree of reduction was calculated by Eq.(4.6).

5.2 Results and Discussions

Results of pellet testing are summarised in Tables 5.3 to 5.5. Property wise discussions are noted below.

5.2.1 Dry strength

From Table 5.2, it may be noted that by using 3.3pct dextrin (D4) in SAIL pellet, strength was 234 N per pellet.

However the strength of prepared pellets in this laboratory was 181 N per pellet by using 3 pct dextrin as binder (B38, Table 2.6). This difference may be ascribed to different method for preparing pellets. However it is to be confirmed. In the case of 2 pct dextrin the strength were more or less same (B52, Table 2.6 and D10, Table 5.2).

5.2.2 Degree of reduction

The degree of reduction varied from 35 to 50 pct for ore-Hutar coal (12 pct) composite pellets. But by using $Ca(OH)_2$ and sugar as binder (B74), the degree of reduction increased to above 62 pct with the same amount of coal in the pellets. The degree of reduction for ore-Hutar coal char pellets (B102) was higher as compared to ore-Hutar coal pellets (B95). Maximum degree of reduction was achieved for the pellets with 24 pct Hutar coal (B105) and for the pellets with 26.5 pct Hutar coal char (B106). The values were 85.0 and 85.5 pct respectively. The degree of reduction for SAIL pellets varied from 35 to 63 pct.

The degree of reduction achieved are dependent on various factors, such as, reactivity of coal, amount of volatile matter present in coal, nature of binder etc. It was not the purpose of this part of investigation reported in this chapter to carry out studies on this aspect. The objective of this part of study was kept limited to a preliminary evaluation of composite pellets prepared in a variety of ways. It is hoped that this would provide the basis for further research and development work in this area.

5.2.3 Volume change

In most of the cases volume changes were positive i.e. swelling took place. Swelling varied from 1.0 to 79.5 pct. Shrinkage took place only for pellets of B9 and B107. With organic binder (dextrin), maximum swelling occured (B38). This was also noticed for SAIL pellets (D2). Dextrin and china clay combined binder used in SAIL pellets exhibited shrinkage. By using Mix V and Mix VII as binder in pellet preparation, the swelling was restricted to 10-15 pct only.

5.2.4 Strength after reduction

The strength after reduction of pellets varied from a few N to 95 N per pellet. This is directly related to the volume change. Maximum post-reduction strengths were achieved for pellets B9 and B114,where volume changes were only about 1 pct and 9.5 pct respectively. With large swelling,pellets were disintegrated after reduction, particularly for organic binders (B38, B47). Similar trend was also observed for SAIL pellets (D2). Number D12 had good post-reduction strength with little shrinkage.

Volume change of pellets during reduction is a complex phenomenon. It depends on many variables. In connection with Blast furnace ironmaking,it has been observed that swelling causes degradation,i.e.,crumbling of iron-bearing materials upon reduction[69]. Figure 5.1 shows volume change vs strength after reduction for ore + Hutar coal and ore + Bachra coal pellets as well as pellets collected from SAIL. The numbers in parentheses

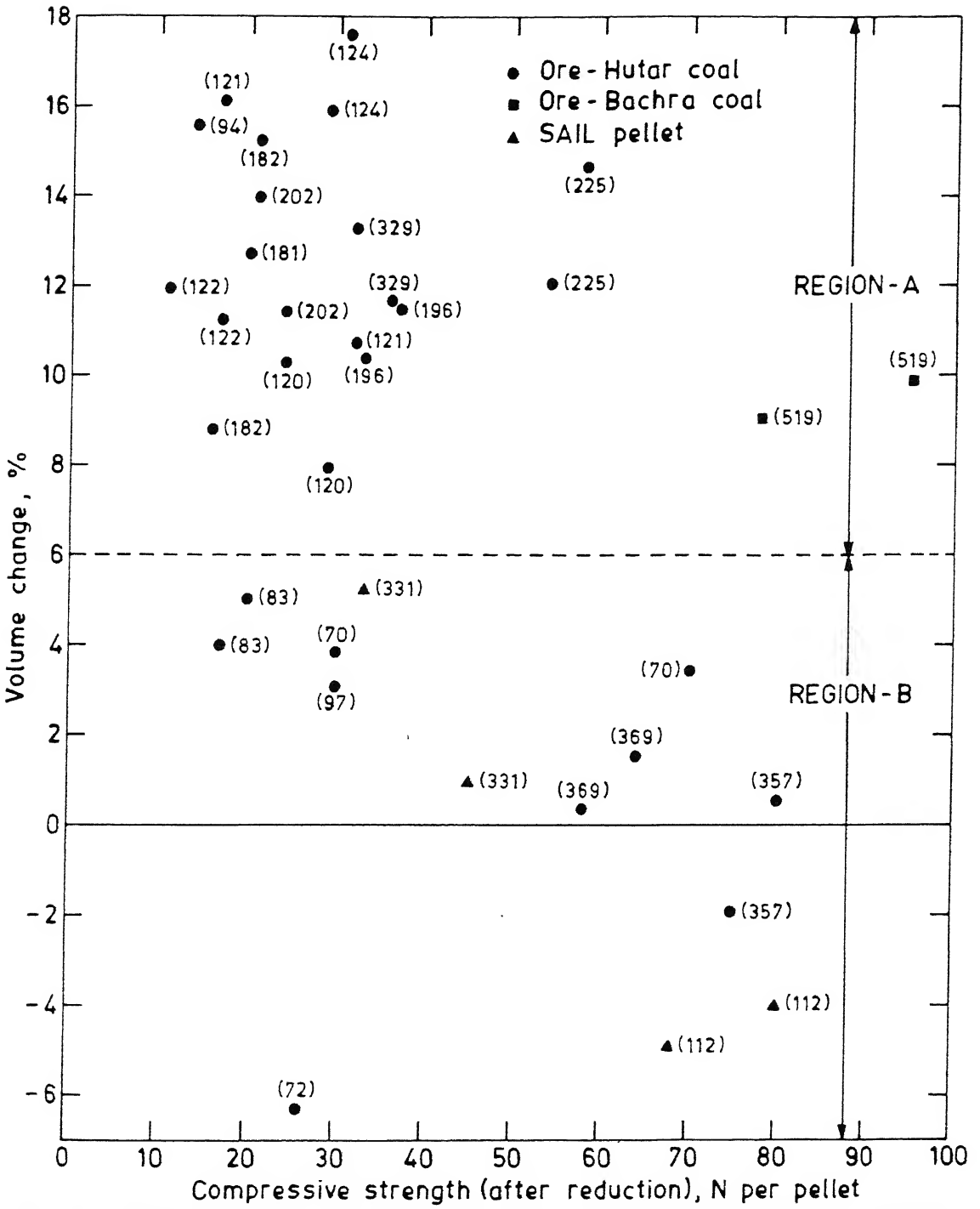

Fig. 5.1. Volume change vs. strength after reduction for different pellets (numbers in parentheses are dry strengths).

denote dry strength before reduction. Broadly the Fig. 5.1 can be divided into two regions (A and B). Approximately above 6pct swelling is region A,and below that is region B. In region A data are very scattered due to use of different binder combination,so there is no clear trend. But in region B,there is a clear trend,i.e.,less the swelling higher is strength after reduction. Moreover it may be noted that swelling or strength after reduction did not show any trend with dry compressive strength of pellets before reduction.

Table 5.1

Specifications of Composite Pellets Prepared in Laboratory for Evaluation

* All pct wt w.r.t. wt of blue dust
* Code : C = Cement, L = Lime, B = Bentonite, LS = $CaCO_3$,
HL = $Ca(OH)_2$, D = Dextrin, T = TSR, Su = Sugar,
MX1 = Mix I, MX3 = Mix III, MX5 = Mix V, MX7 = Mix VII,
SM5 = S Mix V, SM7 = S Mix VII
HC = Hutar coal, HCC = Hutar coal char
BC = Bachra coal, BCC = Bachra coal char
* Treatment : WA = Water ageing, DO = Dried in oven at 423 K,
TC =Treated with CO_2, SC =Steam curing in autoclave

Sample No (Ref.Ch.2)	Coal/Char (Code)	(pct)	Binder (Code)	(pct)	+ (Code)	(pct)	Treatment
1	2	3	4	5	6	7	8
B 1	HC	12	C	8	L	2	WA
B 9	HC	12	C	8	L	2	WA
B 8	HC	12	C	8	B	0.5	WA
B 5	HC	12	C	10	LS	3	WA
B 2	HC	12	C	6	L	4	WA
B 3	HC	12	C	6	L	2	WA
					+ HL	2	
B 13	HC	12	B	4			DO
B 38	HC	12	D	3			DO
B 47	HC	12	D	2	T	2	DO
B 46	HC	12	T	4			DO
B 63	HC	12	T	3	D	0.5	DO
					+ B	0.5	
B 74	HC	12	HL	8	Su	11.5	TC
B 30	HC	12	MX3	8			SC
B 33	HC	12	MX1	9			SC
B 91	HC	12	MX7	14			SC
B 87	HC	12	MX5	11			SC
B 95	HC	12	MX5	3.7	MX7	9	SC
B107	HC	24	SM5	4	SM7	9	SC

Table 5.1 (Contd.)

1	2	3	4	5	6	7	8
B 105	HC	24	SM5	4.8	SM7	9.3	SC
B 110	HC	24	SM5	6	SM7	10	SC
B 102	HCC	12	MX5	4	MX7	9	SC
B 106	HCC	26.5	SM5	4	SM7	9	SC
B 114	BC	12	SM5	4	SM7	9	SC
B 31	BCC	12	MX3	8			SC

Table 5.2

Specifications of SAIL Composite Pellets

* All pct wt w.r.t. wt of blue dust / ore
* Code : BD = Blue dust, GIO = Gua iron ore, GBD = Gua blue dust,
PC = Parascole coal, SOC = Sonepur coal,
HOC = Haripur coal
D = Dextrin, PF = Phenol formaldehyde, CC = China clay

Sample No	Iron Ore	Coal (Code)	Coal (pct)	Binder (Code)	Binder (pct)	Av Dia (mm)	Compressive Strength (N/Pellet)	Av Comp Strength (N/Pellet)
1	2	3	4	5	6	7	8	9
D 1	BD	PC	11.1	D	4.4	10.6	365	331
				+	+	10.4	280	
				PF	1.1	10.7	310	
						11.1	368	
D 2	BD	PC	11.1	D	4.4	10.1	170	170
						9.6	117	
						9.7	231	
						10.5	160	
D 3	BD	SOC	11.1	D	4.4	12.4	318	366
						12.6	402	
						12.8	315	
						11.4	430	
D 4	BD	HOC	11.1	D	3.3	12.8	228	234
						11.6	151	
						12.5	308	
						11.0	250	
D 5	BD	HOC	11.1	D	2.8	11.9	183	197
						12.0	194	
						12.3	244	
						10.6	165	
D 9	GIO	HOC	11.1	D	2.8	11.8	108	117
						11.4	113	
						10.9	143	
						10.4	105	

Table 5.2 (Contd.)

1	2	3	4	5	6	7	8	9
D10	GBD	HOC	11.1	D	2.2	11.3	82	99
				+	+	10.9	105	
				CC	0.6	11.6	108	
						10.2	100	
D12	GBD	HOC	11.1	D	2.2	11.7	118	112
				+	+	10.6	109	
				CC	1.1	10.5	100	
						9.6	120	

Table 5.3

Test Results For Composite Pellets With Hutar Coal And Char

****

Expt Set No = 1

Hutar Coal

****

Sample No = B 1

Samp Wt (g)	Wt Loss (g)	Fr Wt Loss	Degree of Red (pct)	Av Comp St (N/pellet)	(After Red) Comp St (N/pellet)	Vol Change (pct)
1.8056	0.3386	0.1875	40.88	202	21	14.05
1.8001	0.3513	0.1951	40.96	202	24	11.46

Sample No = B 9

Samp Wt (g)	Wt Loss (g)	Fr Wt Loss	Degree of Red (pct)	Av Comp St (N/pellet)	(After Red) Comp St (N/pellet)	Vol Change (pct)
1.9761	0.3704	0.1875	39.59	357	75	-1.91
1.7842	0.3233	0.1812	39.17	357	80	0.55

Sample No = B 8

Samp Wt (g)	Wt Loss (g)	Fr Wt Loss	Degree of Red (pct)	Av Comp St (N/pellet)	(After Red) Comp St (N/pellet)	Vol Change (pct)
1.8661	0.3419	0.1832	50.26	122	11	11.97
1.9781	0.3558	0.1799	46.68	122	17	11.27

Sample No = B 5

Samp Wt (g)	Wt Loss (g)	Fr Wt Loss	Degree of Red (pct)	Av Comp St (N/pellet)	(After Red) Comp St (N/pellet)	Vol Change (pct)
1.8327	0.3335	0.1820	38.19	124	29	15.94
1.8099	0.3334	0.1842	39.39	124	31	17.59

Sample No = B 2

Samp Wt (g)	Wt Loss (g)	Fr Wt Loss	Degree of Red (pct)	Av Comp St (N/pellet)	(After Red) Comp St (N/pellet)	Vol Change (pct)
1.8344	0.3305	0.1802	36.79	182	16	15.30
1.9281	0.3324	0.1724	35.93	182	16	8.80

Sample No = B 3

Samp Wt (g)	Wt Loss (g)	Fr Wt Loss	Degree of Red (pct)	Av Comp St (N/pellet)	(After Red) Comp St (N/pellet)	Vol Change (pct)
1.9162	0.3514	0.1834	37.25	181	15	20.21
1.9639	0.3540	0.1802	35.71	181	20	12.70

Sample No = B 13

Samp Wt (g)	Wt Loss (g)	Fr Wt Loss	Degree of Red (pct)	Av Comp St (N/pellet)	(After Red) Comp St (N/pellet)	Vol Change (pct)
1.8715	0.2970	0.1587	40.84	70	70	3.44
1.7149	0.2767	0.1613	42.68	70	30	3.86

Sample No = B 38

Samp Wt (g)	Wt Loss (g)	Fr Wt Loss	Degree of Red (pct)	Av Comp St (N/pellet)	(After Red) Comp St (N/pellet)	Vol Change (pct)
1.8523	0.3731	0.2014	36.83	181	**	**
1.8367	0.4190	0.2281	40.06	181	**	79.45

Sample No = B 47

Samp Wt (g)	Wt Loss (g)	Fr Wt Loss	Degree of Red (pct)	Av Comp St (N/pellet)	(After Red) Comp St (N/pellet)	Vol Change (pct)
1.8343	0.4876	0.2658	44.31	195	3	37.15
1.8577	0.4150	0.2234	41.15	195	**	35.20

Sample No = B 46

Samp Wt (g)	Wt Loss (g)	Fr Wt Loss	Degree of Red (pct)	Av Comp St (N/pellet)	(After Red) Comp St (N/pellet)	Vol Change (pct)
1.8000	0.3464	0.1924	45.05	329	36	11.70
1.7307	0.3369	0.1946	44.91	329	32	13.29

** Sample was broken after non-isothermal reduction.

Sample No = B 63

Samp Wt (g)	Wt Loss (g)	Fr Wt Loss	Degree of Red (pct)	Av Comp St (N/pellet)	(After Red) Comp St (N/pellet)	Vol Change (pct)
1.8428	0.3504	0.1901	45.00	317	16	22.97
1.8317	0.3541	0.1933	45.98	317	18	19.77

Sample No = B 74

Samp Wt (g)	Wt Loss (g)	Fr Wt Loss	Degree of Red (pct)	Av Comp St (N/pellet)	(After Red) Comp St (N/pellet)	Vol Change (pct)
1.8755	0.5477	0.2920	67.57	369	58	0.34
1.9753	0.5757	0.2915	61.95	369	64	1.57

Sample No = B 30

Samp Wt (g)	Wt Loss (g)	Fr Wt Loss	Degree of Red (pct)	Av Comp St (N/pellet)	(After Red) Comp St (N/pellet)	Vol Change (pct)
1.8215	0.3189	0.1751	35.94	94	16	20.68
1.8280	0.3225	0.1764	35.71	94	14	15.60

Sample No = B 33

Samp Wt (g)	Wt Loss (g)	Fr Wt Loss	Degree of Red (pct)	Av Comp St (N/pellet)	(After Red) Comp St (N/pellet)	Vol Change (pct)
1.8963	0.3262	0.1720	36.88	121	17	16.18
1.7816	0.3039	0.1706	37.74	121	32	10.74

Sample No = B 91

Samp Wt (g)	Wt Loss (g)	Fr Wt Loss	Degree of Red (pct)	Av Comp St (N/pellet)	(After Red) Comp St (N/pellet)	Vol Change (pct)
1.7648	0.3597	0.2038	43.23	196	37	11.49
1.8171	0.3720	0.2047	43.42	196	33	10.41

Sample No = B 87

Samp Wt (g)	Wt Loss (g)	Fr Wt Loss	Degree of Red (pct)	Av Comp St (N/pellet)	(After Red) Comp St (N/pellet)	Vol Change (pct)
1.9122	0.4011	0.2098	45.27	83	20	5.01
1.8400	0.3862	0.2099	45.67	83	17	4.00

Sample No = B 95

Samp Wt (g)	Wt Loss (g)	Fr Wt Loss	Degree of Red (pct)	Av Comp St (N/pellet)	(After Red) Comp St (N/pellet)	Vol Change (pct)
1.8743	0.3954	0.2110	42.29	225	54	12.07
1.9201	0.3953	0.2059	41.77	225	58	14.66

Sample No = B107

Samp Wt (g)	Wt Loss (g)	Fr Wt Loss	Degree of Red (pct)	Av Comp St (N/pellet)	(After Red) Comp St (N/pellet)	Vol Change (pct)
1.6374	0.5525	0.3375	83.86	72	26	-6.30

Sample No = B105

Samp Wt (g)	Wt Loss (g)	Fr Wt Loss	Degree of Red (pct)	Av Comp St (N/pellet)	(After Red) Comp St (N/pellet)	Vol Change (pct)
1.5951	0.5343	0.3350	85.09	97	30	3.09

Sample No = B110

Samp Wt (g)	Wt Loss (g)	Fr Wt Loss	Degree of Red (pct)	Av Comp St (N/pellet)	(After Red) Comp St (N/pellet)	Vol Change (pct)
1.5786	0.5292	0.3352	83.39	120	29	7.96
1.6382	0.5518	0.3368	81.11	120	24	10.32

****

Expt Set No = 2

Hutar Coal Char

****

Sample No = B102

Samp Wt (g)	Wt Loss (g)	Fr Wt Loss	Degree of Red (pct)	Av Comp St (N/pellet)	(After Red) Comp St (N/pellet)	Vol Change (pct)
1.9313	0.3757	0.1945	57.85	1030	56	35.26
2.0888	0.3941	0.1887	59.21	1030	55	40.92

Sample No = B106

Samp Wt (g)	Wt Loss (g)	Fr Wt Loss	Degree of Red (pct)	Av Comp St (N/pellet)	(After Red) Comp St (N/pellet)	Vol Change (pct)
1.6520	0.4673	0.2828	86.91	735	15	67.71
1.6746	0.4577	0.2733	83.94	735	25	67.52

Table 5.4

Test Results For Composite Pellets With Bachra Coal And Char

****

Expt Set No = 3

Bachra Coal

****

Sample No = B114

Samp Wt (g)	Wt Loss (g)	Fr Wt Loss	Degree of Red (pct)	Av Comp St (N/pellet)	(After Red) Comp St (N/pellet)	Vol Change (pct)
2.0480	0.3608	0.1762	36.80	519	95	9.91
1.8821	0.3198	0.1699	33.59	519	78	9.04

****

Expt Set No = 4

Bachra Coal Char

****

Sample No = B 31

Samp Wt (g)	Wt Loss (g)	Fr Wt Loss	Degree of Red (pct)	Av Comp St (N/pellet)	(After Red) Comp St (N/pellet)	Vol Change (pct)
1.8154	0.2628	0.1448	40.50	377	20	9.42
1.8118	0.2614	0.1443	38.86	377	28	9.98

Table 5.5

Test Results For SAIL Composite Pellets

****

Expt Set No = 5

SAIL PELLET

****

Sample No = D 1

Samp Wt (g)	Wt Loss (g)	Fr Wt Loss	Degree of Red (pct)	Av Comp St (N/pellet)	(After Red) Comp St (N/pellet)	Vol Change (pct)
1.8138	0.4096	0.2258	53.80	331	33	5.23
1.6540	0.3700	0.2237	54.60	331	45	0.97

Sample No = D 2

Samp Wt (g)	Wt Loss (g)	Fr Wt Loss	Degree of Red (pct)	Av Comp St (N/pellet)	(After Red) Comp St (N/pellet)	Vol Change (pct)
1.5125	0.3836	0.2536	62.68	170	3	83.04
1.5376	0.3772	0.2453	55.83	170	**	94.30

Sample No = D 3

Samp Wt (g)	Wt Loss (g)	Fr Wt Loss	Degree of Red (pct)	Av Comp St (N/pellet)	(After Red) Comp St (N/pellet)	Vol Change (pct)
2.1323	0.4840	0.2270	48.21	366	20	25.29
1.4302	0.3204	0.2240	36.96	366	20	18.71

Sample No = D12

Samp Wt (g)	Wt Loss (g)	Fr Wt Loss	Degree of Red (pct)	Av Comp St (N/pellet)	(After Red) Comp St (N/pellet)	Vol Change (pct)
1.8998	0.2862	0.1506	36.34	112	80	-4.00
1.6422	0.2428	0.1479	34.78	112	68	-4.93

CHAPTER 6

RESULTS AND DISCUSSIONS ON REDUCTION OF BLUE DUST BY HYDROGEN AND CARBON MONOXIDE

As mentioned earlier, due to use of coal as reductant in composite pellet, gases such as H_2, CH_4, CO are produced. So reducing gases (H_2, CO) take part in reduction of pellet. Hence, for fundamental investigation, it is also desirable to study reduction of blue dust by H_2 as well as CO in an attempt to know more about how reduction of blue dust-coal composite pellet occurs.

6.1 Literature Review on Gaseous Reduction of Iron Ores or Oxides

From the time of Edstrom[70] in 1950S, innumerable fundamental and laboratory investigations have been reported in literature on reduction of iron ores and oxides by H_2 or CO. It is neither possible nor necessary to review all these. One may refer to some reviews[55,57,71-73] already available. Therefore the literature review in this chapter would be brief and restricted to issues concerned.

In the present investigation small particles of blue dust in the form of thin (0.4 to 1.5 mm) unconsolidated and unsintered beds were subjected to reduction in flowing H_2 or CO

gas. It may be noted here that Tiwari[74] made measurements of reduction rates of two other iron ore samples in $CO-CO_2$ gas. He employed sintered porous pellets of small size (less than 5 mm). He found that rates were not increasing with increasing temperature uniformly but exhibiting maxima/minima type behaviour as function of temperature.

This behaviour pattern is in contrast with measurements of reduction rates of iron oxides/ores carried out on larger samples (cubes and spheres of 5 to 15 mm size, mostly 10 mm) by Ghosh and co-workers[75-77] in this laboratory. The cubes were cut from natural ores. Spheres were sintered (porous and dense). Reducing gas was hydrogen. In these investigations, no anomalous behaviour or maxima/minima were found either with respect to temperature or size. Moreover data fitted reasonably well with McKewan type equation.

Therefore the present literature review is concerned only with the anomalous behaviours observed in unsintered bed of iron ore or oxide fines as well as in small particles, either sintered or natural.

Literature reports may be summarised as follows.

i) The maxima/minima type variation of rate with respect to temperature has been observed for reduction of magnetite as well as for small particles of hematite (less than 4 mm or so) by several workers[70,72,78-82].

ii) These anomalies have been ascribed to sintering and densification of reduced iron layer[81,82], swelling of particle during reduction especially in CO[72],

crystallographic changes during the course of reduction[78,79,82]. These are complex phenomena and sometimes are quite sensitive to initial composition and structure of oxide[57,72,79], gas composition and the manner in which the reduction is carried out[57,72].

iii) In the last two decades there have been extensive investigation of structures of partially reduced samples by microscopy, SEM, EPMA and X-ray[78-80,82-91] as well as measurements of pore surface area, pore size distribution by BET and mercury porosimetry[55,81,92-95]. Attempts have been made to classify morphologies[84,85,89,93].

iv) It has been established now that mode of reduction may be topochemical, internal reduction type or mixed[57,72,80,95,96] depending on conditions. Less is control by diffusion (i.e. lower temperature, smaller and more porous particles), the mode tends towards uniform internal reduction. In particles larger than 5 mm, it is mostly mixed mode[72,96]. For small sizes, it is either uniform reduction or mixed type depending on circumstances[72,97].

v) The **grain model** of porous solids consisting of grains with micropores and intergranular macropores, provides a good basis for generalization[57,98].

vi) Reduction of iron oxide goes through stages, viz. Fe_2O_3 ——> Fe_3O_4 ——> Fe_xO ——> Fe, the last one being the most important. Rate measurements have been carried out

both for overall reaction or for various stages separately[56-58,93]. From a fundamental point of view, the latter provides more insight into kinetics.

vii) The kinetic steps may be broadly classified into interfacial chemical reaction (at pore surfaces), diffusion of gases through porous product layer(s), mass transfer through external gas boundary layer. For fundamental understanding the last step is to be eliminated from limiting rate either experimentally (adequate gas flow rate) and/or theoretical corrections. So the relative contribution of chemical reaction to rate control is more dominant at smaller particle sizes and lower temperatures. Hence it is mostly the practice to use very small particles (less than 2 mm or so) to obtained chemical rate constants. So far as lower temperature is concerned, the variation of the gas diffusivity ratio D_e/D_{12} also drastically decreases[72] (where D_e is the effective diffusivity, and D_{12} is the molecular interdiffusivity for a binary mixture 1-2). Thus it cannot be stated with certainty that reduction would always tend towards more chemical control.

viii) Chemical rate constants determined by various workers differ both in units as well as in magnitudes. Some workers[58,93] have attempted rationalization.

ix) The activation energy does not have much fundamental significance. It is simply an empirically determined

temperature coefficient. No wonder it shows a wide scatter (10-15 KJ/mol to 80-100 KJ/mol)[56,57,93].

6.2 Method of Data Analysis Adopted in the Present Investigation

6.2.1 Introduction

In view of complexities and anomalous behaviour of blue dust reduction by H_2 or CO (especially in smaller sizes), it is concluded that :

i) no mathematical model is capable of satisfactorily describing the entire course of reduction; as a matter of fact, they can not even be extrapolated from one set of investigation to another; this is also the view of some others[80],

ii) even simple empirical laws, like 1st order rate expression, can not be taken as applicable as there is no basis for the same.the same.

Therefore the following procedure is suggested as the rational approach to investigations of reduction kinetics of iron ores by gases in unsintered beds or small particles.

a) Rate measurements are carried out.

b) Some physical examination of partially reduced samples etc. is done in order to understand the situation better.

c) Quantitative analysis of rate data should be as general and empirical as possible.

6.2.2 Empirical treatment of data

Fractional reduction (f) can be calculated from the weight loss measurements by using the relation :

$$f = \frac{\Delta W_o}{W_o^i} \qquad \ldots(6.1)$$

where W_o^i is initial weight of removable oxygen in ore and ΔW_o is loss of weight upon reduction.

Most general approach is polynomial fitting of f vs t data (where t is time of reduction) and taking (df/dt) as measure of rate.

Again, $$\frac{df}{dt} = \phi\ (X, Y, T, l) \qquad \ldots(6.2)$$

where X is characteristics of solid, Y is gas composition, T is temperature, l is particle size or depth of the unsintered bed of fines whichever is appropriate.

At fixed Y, T and l

$$\frac{df}{dt} = \phi\ (X) = \phi\ (X_i, f) \qquad \ldots(6.3)$$

where X_i is initial characteristics of solid before starting reduction.

For a specific sample, X_i is fixed.

Hence,

$$\frac{df}{dt} = \phi\ (f) \qquad \ldots(6.4)$$

This is the basis for the generalized approach where df/dt at some fixed value of f is taken as a measure of characteristic rate for an experiment.

If one assumes functional form for ϕ (f) and it gives satisfactory fit with data, then one may evaluate rate constant in a somewhat different way. The parabolic rate law for rate control by diffusion of gases through porous product layer, which is a flat plate, is an example. The relationship is :

$$1 - (1 - f)^2 = k't \qquad \ldots(6.5)$$

where k' is a constant.

The most general empirical approach is to assume

$$\frac{df}{dt} = k\,(1 - f)^n \qquad \ldots(6.6)$$

where n is the empirical reaction order (it may be fractional as well). k is rate constant. Eq.(6.6) is similar to general rate equation for the devolatilization of coal (Eq.1.7). This kind of approach is quite common in solid state reactions, phase transformation, grain growth[99], and oxidation of metals[100].

An alternative approach is to take the initial rate, i.e. $(\frac{df}{dt})_{t \to 0}$, as a measure of rate of reduction. In view of morphological changes during reduction such as growth of iron layer, only the initial rate is really the true index of rate unhindered by structural changes.

However the determination of initial rate suffers from errors, viz :

i) incubation, unsteady state experimental conditions at the beginning,

and ii) some uncertainties in polynomial fitting of f vs.t data as t ——> 0.

Therefore, it is in a way better to take the least square fitted slope of initial approximate straight line in f vs. t curves as a measure of initial rate.

6.3 Results

Table 6.1 sumarizes the experimental conditions for H_2 and CO reduction of blue dust. Experimental data including values of fractional reduction (f) at different times are presented in Appendix A for reduction by H_2 and Appendix B for 2nd stage (Fe_xO —> Fe) of reduction by CO. Temperature was controlled at ± 2 K approximately. Care exercised to control gas composition for gas mixtures has been presented in chapter 3. Readability of weight loss was ± 0.02 mg, which is quite precise for the purpose of present investigation.

Figure 6.1 shows fractional reduction (f) vs. time (t) plot for reduction by H_2 at different bed depths (l) at 973 K. Initially for lower bed depth (l), the rate of reduction was larger. The trend was reversed at f > 0.5, i.e. higher the value of l higher was the rate. Similar trends were also observed at other temperatures.

Table 6.1

Variables for H_2 and CO Reduction of Blue Dust

Sl.No.	Variable	Number	Remarks
1	Iron Ore	1	Blue dust
2	Temperature	4	a) 898 to 1123 K for H_2 b) 1073 to 1373 K for CO
3	Bed depth	3	0.44, 1.05 and 1.50 mm
4	Flow rate	1	8.33 $cm^3.s^{-1}$ (STP)
5	Gas composition		
	a) For H_2	1	100pct
	b) For CO	2	i) 50:50::CO:CO_2 for stage I : Fe_2O_3 ⟶ Fe_xO ii) 50:50::CO:Ar for stage II : Fe_xO ⟶ Fe

Total numbers of experiments = 24 + 24 = 48 (including reproducibility)

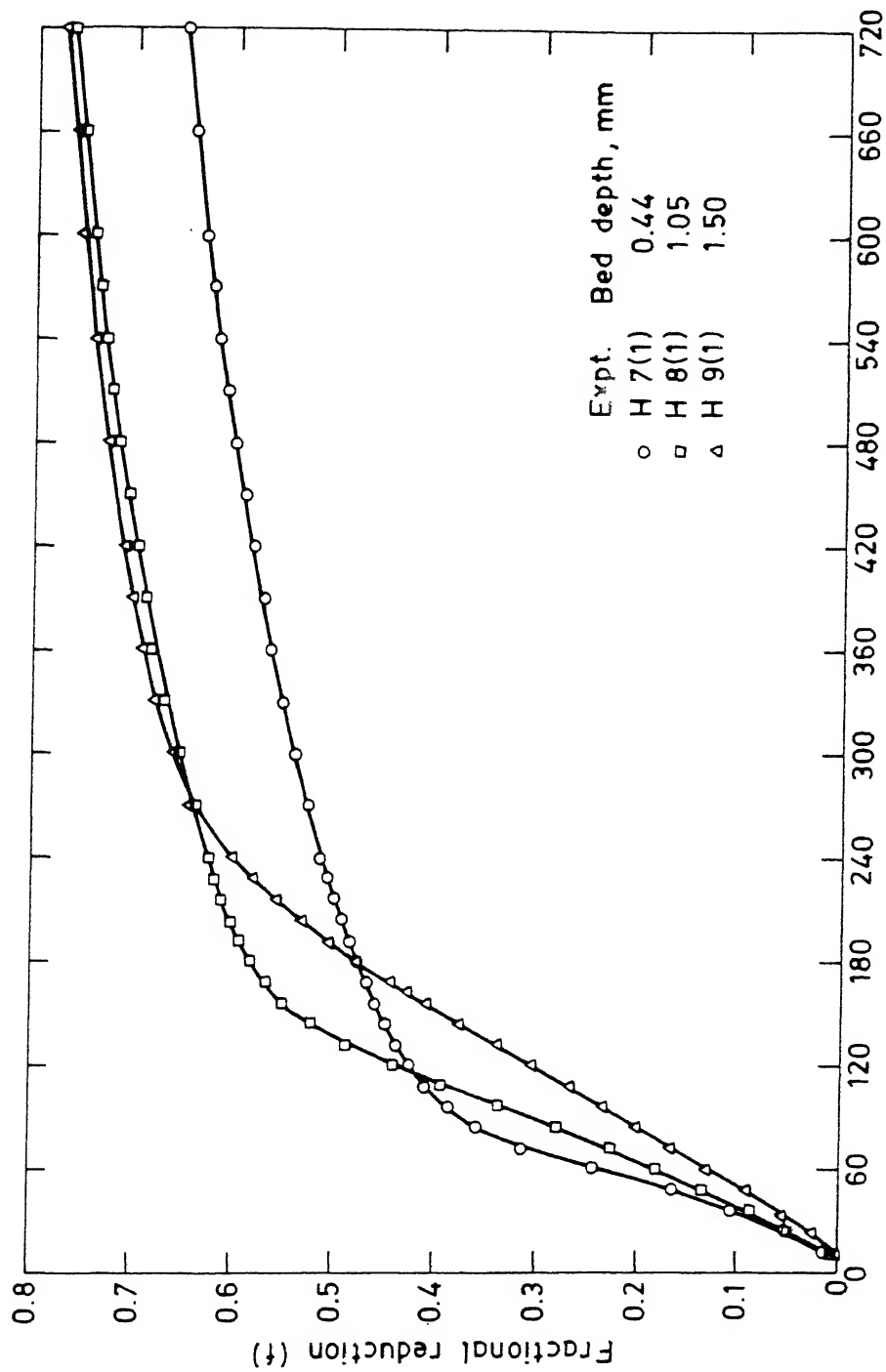

Fig. 6.1. Fractional reduction vs. time plots for hydrogen reduction of blue dust at 973K.

Figure 6.2 presents f vs. t plot for H_2 reduction of blue dust at different temperatures for samples with medium bed depth (i.e. l = 1.05 mm). It was observed that as temperature increased the initial rate also increased. But above f = 0.5, the rate was minimum at 973 K. As stated in Sec.6.1, this type of anomalous behaviour has been observed by a large number of investigators[70,72,74,78-82], and were ascribed to sintering and densification of reduced iron layer[81,82].

Reduction of blue dust in CO bearing gas mixture was carried out in two stages (Table 6.1). Procedure for CO reduction has already been discussed in chapter 3 (Section 3.2.2.1). After the sample attained temperature, flow of gas at the reaction tube was switched over from argon to $CO-CO_2$ mixture (50:50) for first stage reduction. When the weight loss was nearly constant, the first stage (i.e. $Fe_2O_3 \longrightarrow Fe_xO$) reduction was assumed to be over. Then flow of $CO-CO_2$ gas was again substituted by argon flow. Sufficient time was allowed to establish a neutral atmosphere. Then further second stage reduction (i.e. $Fe_xO \longrightarrow Fe$) was carried out by CO-Ar mixture (50:50). Pure CO was not employed to avoid deposition of carbon by reverse of gasification reaction.

The overall fractional reduction (f_{ov}) for CO reduction was calculated on the basis of Eq.(6.1) :

$$\text{i.e. } f_{ov} = \frac{\Delta W_o}{W_o^i}$$

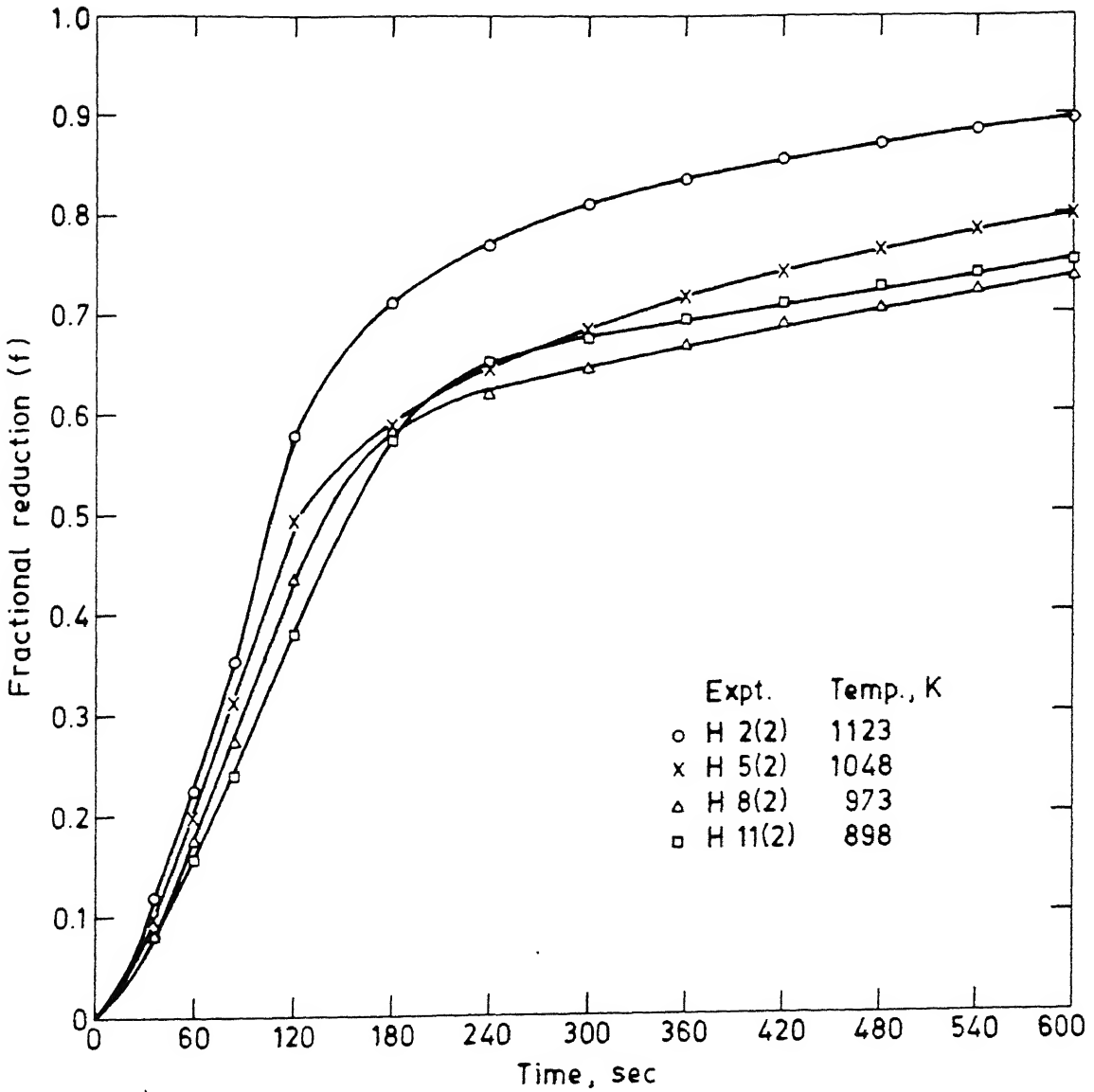

Fig. 6.2. Fractional reduction vs. time plots for hydrogen reduction of blue dust at constant bed depth.

Figure 6.3 shows f_{ov} vs. t curve for overall blue dust reduction by CO. It illustrates the 2-stage reduction programme.

Second stage reduction (i.e. Fe_xO —> Fe) was given importance in this investigation. Hence fractional reduction of blue dust for second stage (f_{II}) was calculated as follows.

$$f_{II} = \frac{(\Delta W)_{II}}{(W_o^{\,i})_{II}} \qquad \ldots(6.7)$$

where $(\Delta W)_{II}$ is weight loss in 2nd stage at any time and $(W_o^{\,i})_{II}$ is the total removable oxygen present at the start of second stage reduction,

$$\text{i.e. } (W_o^i)_{II} = W_o^i - (\Delta W)_{I,T} \qquad \ldots(6.8)$$

where $(\Delta W)_{I,T}$ is the total oxygen consumed during first stage of CO reduction. Figure 6.4 presents f_{II} vs. t plot for second stage reduction by CO at different temperatures. Time in this case, of course, is counted from the beginning of 2nd stage.

6.4 Discussions of Results

6.4.1 Processing of f vs t data

From this point onwards, for carbon monoxide reduction discussion will be restricted to f_{II} only. In order to discuss it along with hydrogen reduction, f_{II} would be designated as f.

Fractional reduction may be expressed as a 3rd order polynomial function of time as :

$$f = a_o + a_1 t + a_2 t^2 + a_3 t^3 \qquad \ldots(6.9)$$

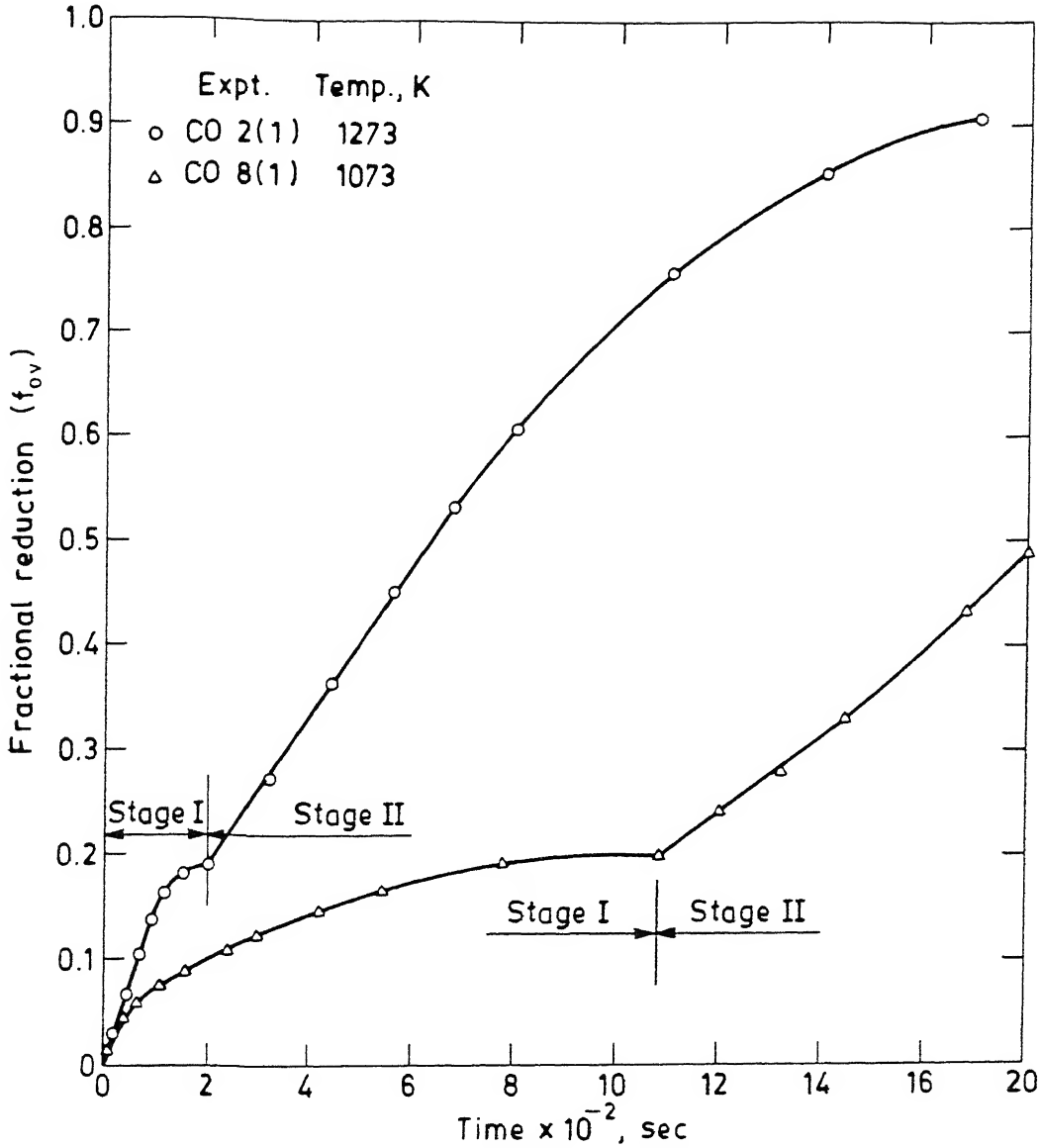

Fig. 6.3. Overall fractional reduction vs. time plots for reduction of blue dust by CO.

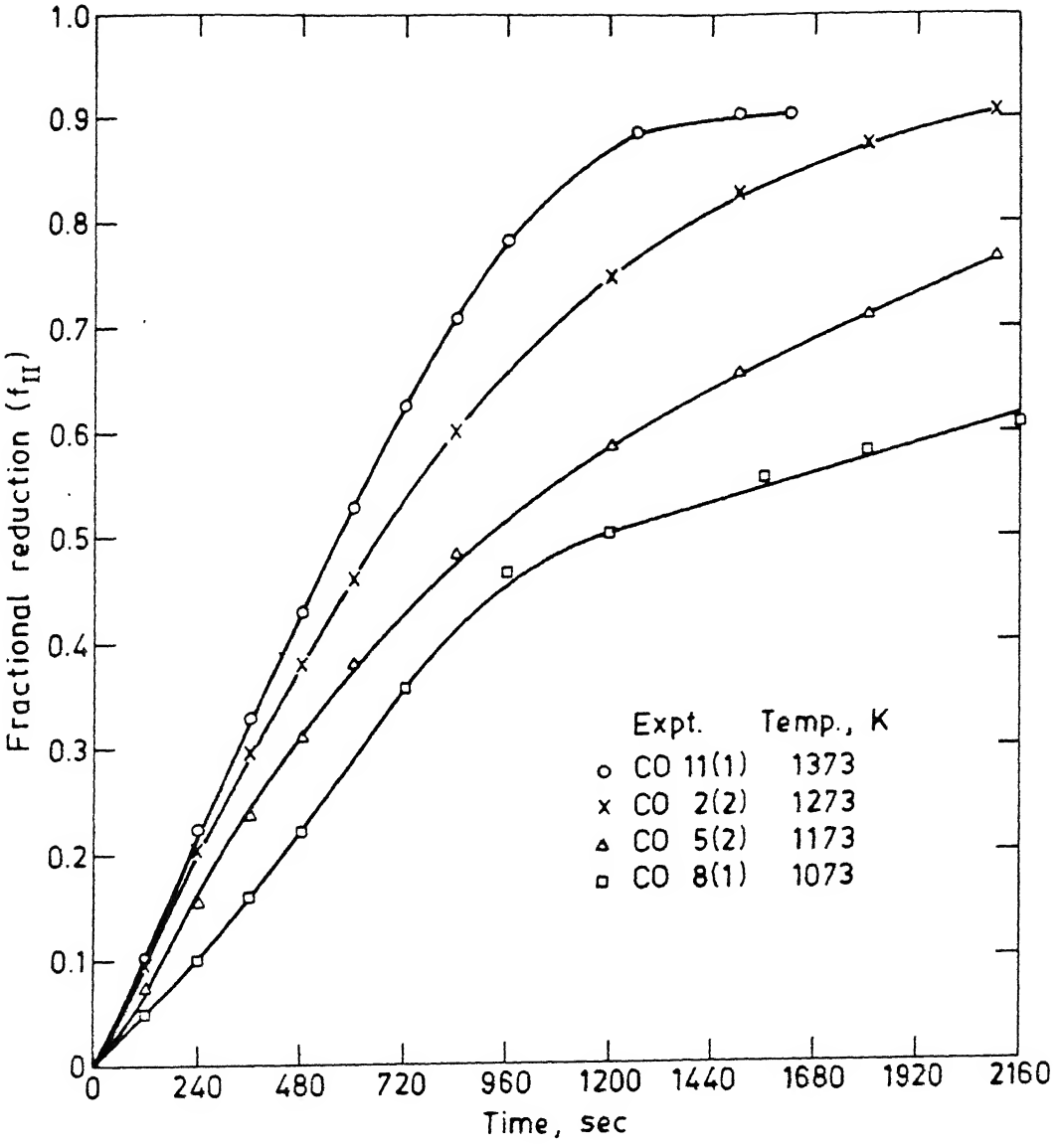

Fig. 6.4. Fractional reduction vs. time plots for second stage reduction of blue dust in CO–Ar mixture at constant bed depth.

where a_0, a_1, a_2 and a_3 are empirical constants. The constants were determined by statistical fitting of f vs. t data with the above Eq. (6.9). The computar programs have been presented in Appendix A and B.

Figure 6.5 shows some polynomial fitted curves for reduction by H_2 as well as CO. Values of constants are available in Appendix A and B. It was found to be in close agreement with experimental values of f.

Kinetic steps in reduction process here are :

i) mass transfer in gas boundary layer above the bed of particles; H_2 or CO is transferred from bulk gas to bed surface and H_2O or CO_2 in the reverse direction,

ii) diffusion through voids in bed. It is a case of counter diffusion of either H_2 and H_2O or CO and CO_2,

iii) chemical reaction at particle surfaces.

If the reduction rate is controlled only by the chemical reaction step, then rate should be independent of bed depth. For mass transfer control, rate of reduction should decrease as bed depth (l) increases. In Figures 6.6 and 6.7, df/dt at f = 0.3 and f = 0.5 have been taken as measure of rate and these have been plotted as function of l. As stated in Sec.6.2.2 this is one of the general empirical methods of expressing rate. As may be noted that for 2nd stage of CO-reduction, there is no systematic trend. For H_2 reduction, the curves mostly exhibit a maxima-type behaviour. With temperature variation, no trend was observed for both cases.

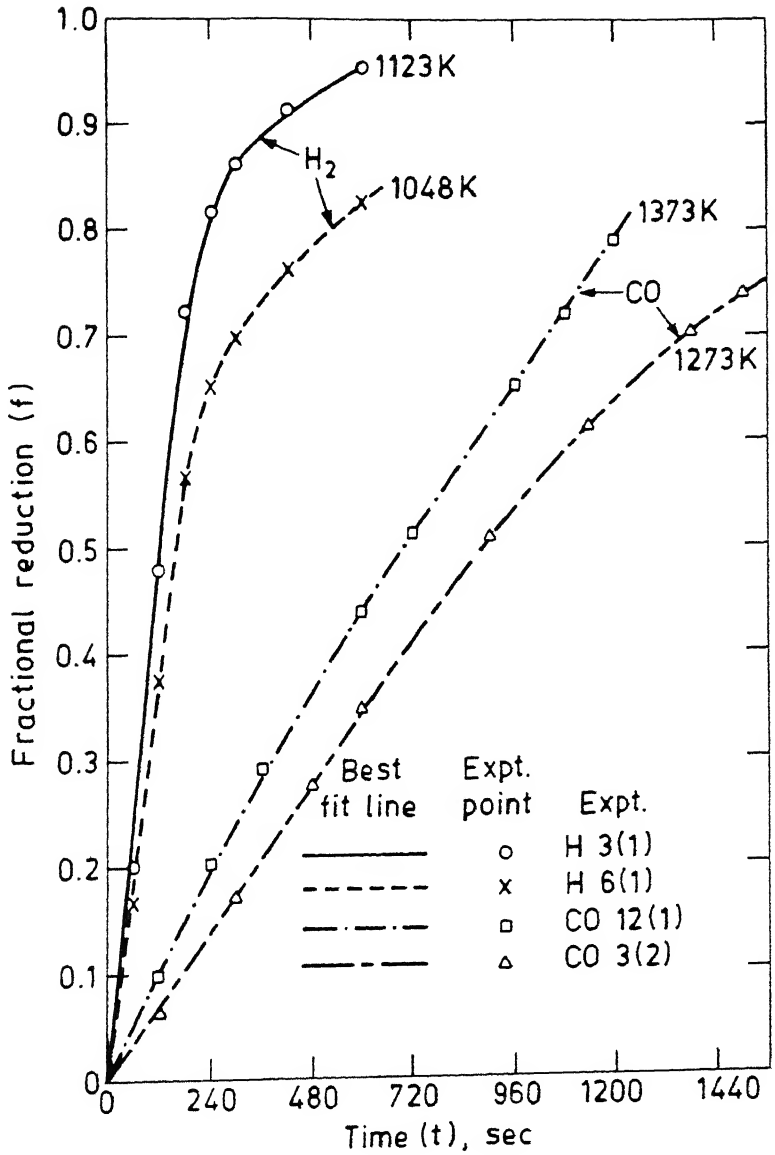

Fig. 6.5. Curves showing fit with experimental f vs. t data.

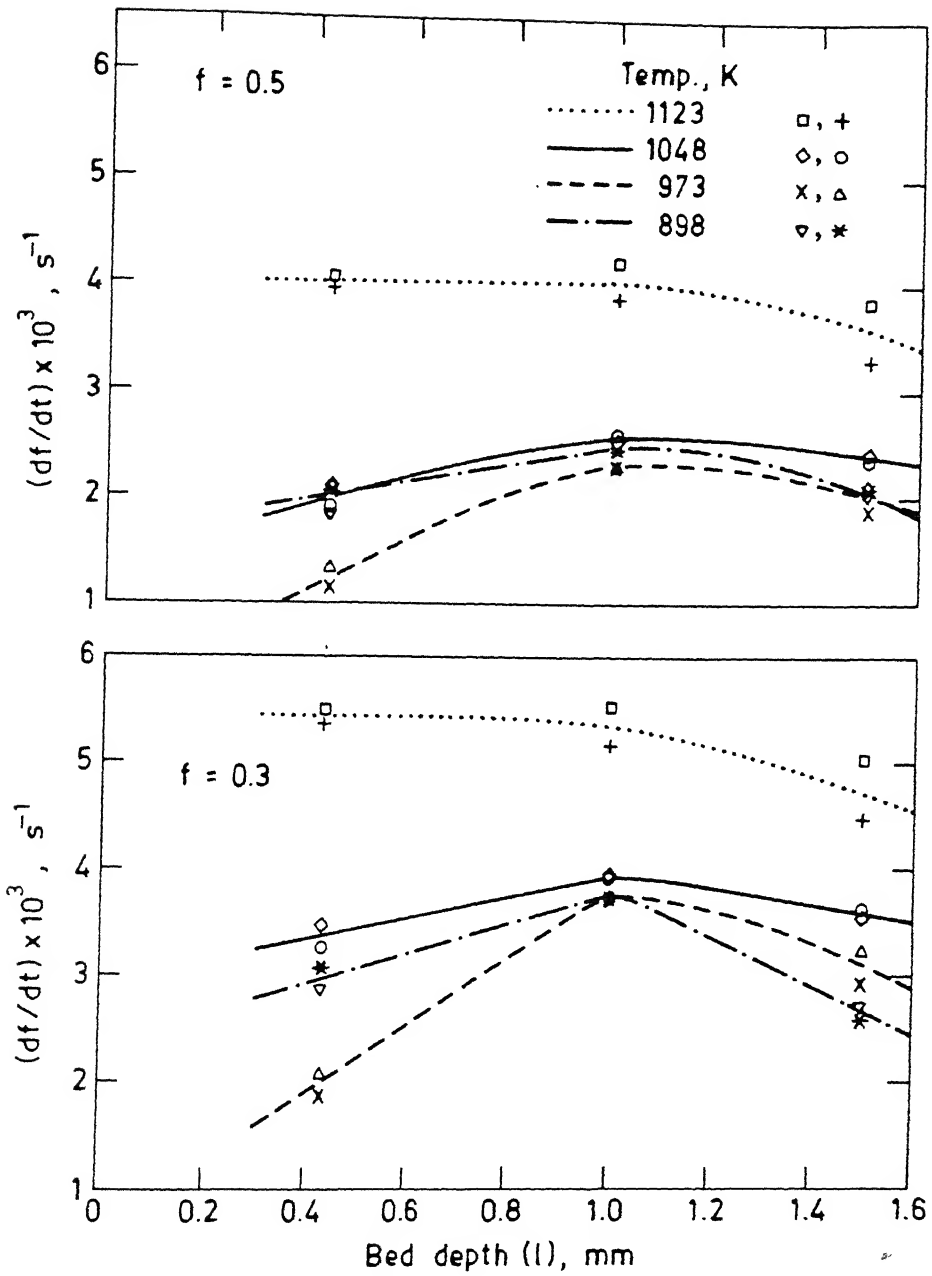

Fig. 6.6. df/dt vs. bed depth at f = 0.3 and f = 0.5 for hydrogen reduction of blue dust.

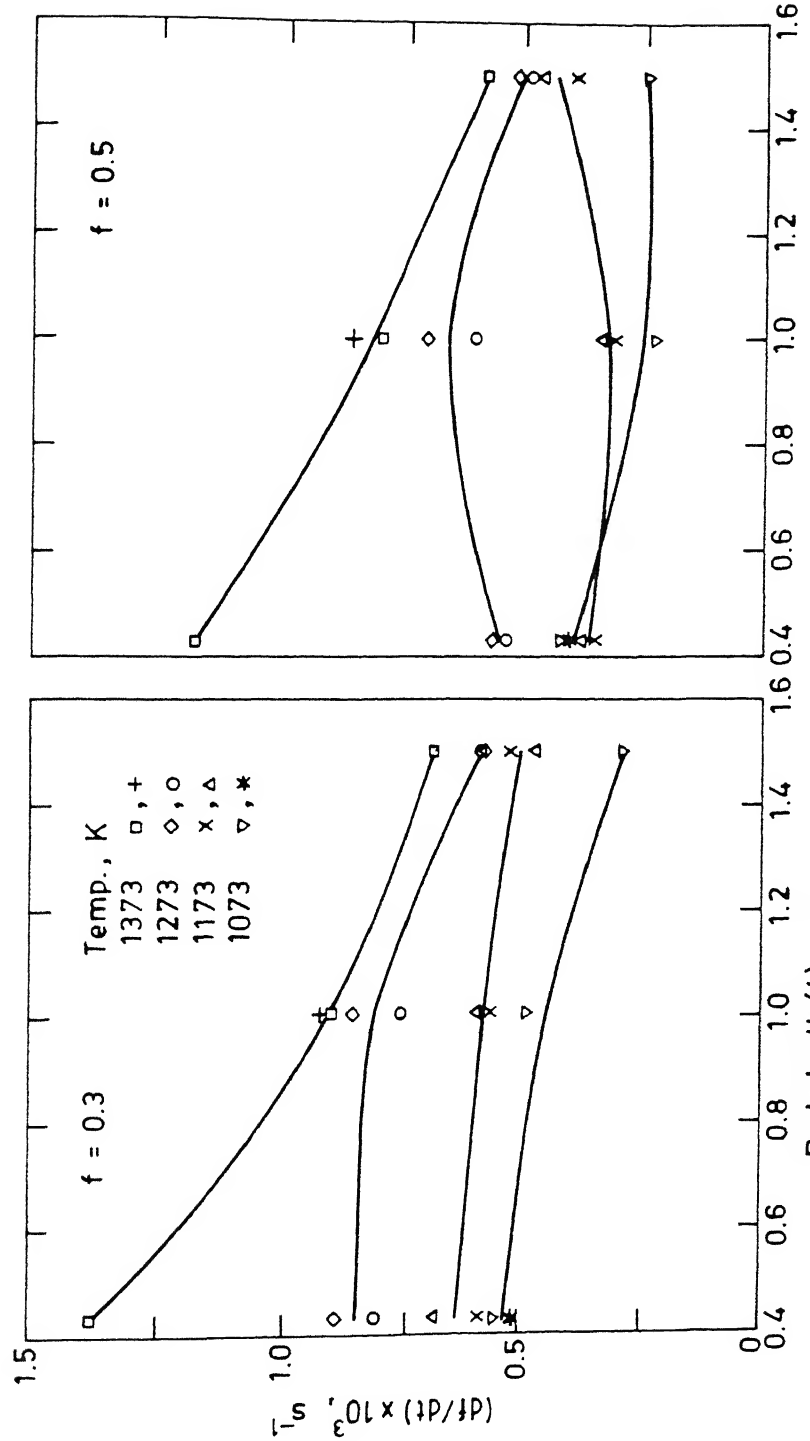

Fig. 6.7. df/dt vs. bed depth at f = 0.3 and f = 0.5 for carbon monoxide reduction of blue dust.

Basic purpose of these measurements is to determine the intrinsic rate constants for reduction of blue dust by H_2 and CO. Theoretically, one can obtain it at a hypothetical zero bed depth (i.e. $l \longrightarrow 0$), since there would not be any mass transfer resistance of bed then. However $(k)_{l \to 0}$ may still suffer from mass transfer resistance in gas boundary is not significant. The purpose of figures 6.7 and 6.8 were to get rate constants at $l \longrightarrow 0$, by extrapolating the curves upto $l = 0$. But that was not possible due to irregular trends. Hence it was decided that other approaches should be tried.

For first order reaction, Eq.(6.6) becomes :

$$\frac{df}{dt} = k\,(1 - f) \qquad \ldots(6.10)$$

where k is the specific rate constant.

By integrating between limits t=0, f=0 to t=t, f=f,

$$-\ln\,(1 - f) = kt \qquad \ldots(6.11)$$

This approach was employed by Turkdogan[72].

Figures 6.8 and 6.9 show attempts to fit data with Eq.(6.11) for reduction by H_2 and CO respectively. Here also data could not be fitted as straight lines, thus demonstrating that it is also not a valid approach.

An nth order reaction yields a rate equation as given in Eq.(6.6).

Taking logarithm of Eq.(6.6),

$$\log\left(\frac{df}{dt}\right) = \log k - n \log\,(1 - f) \qquad \ldots(6.12)$$

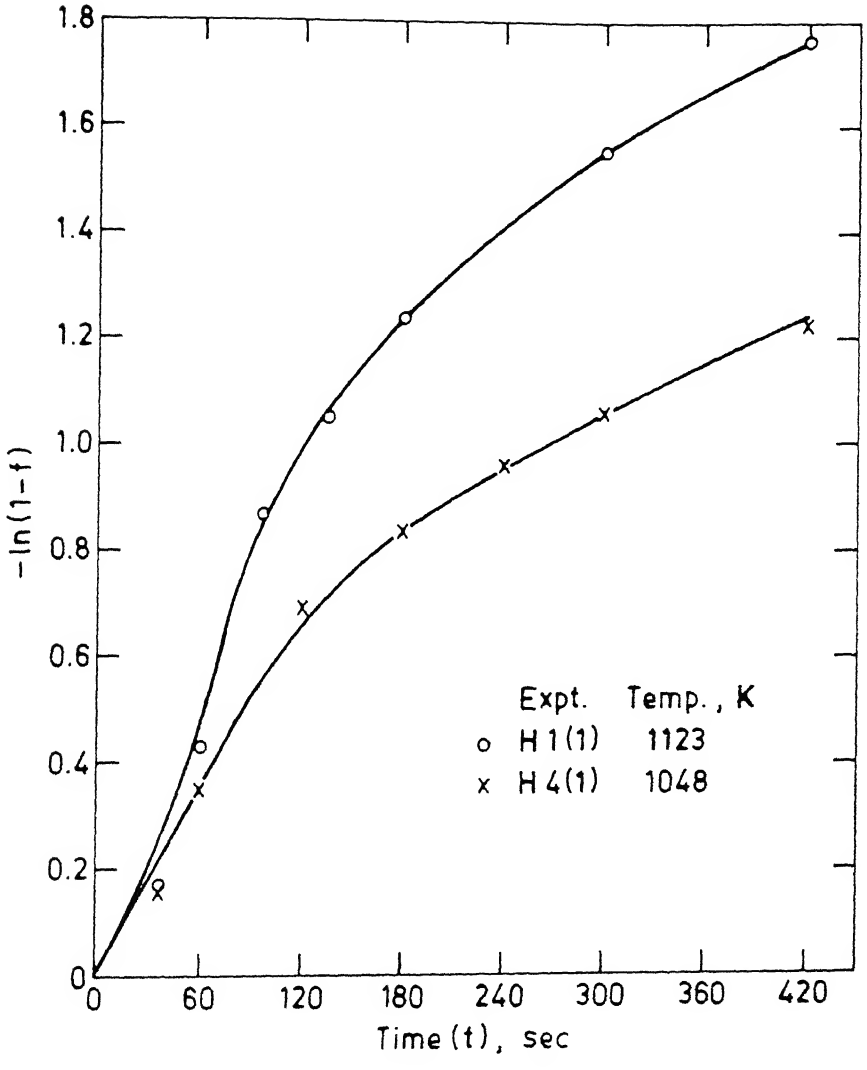

Fig. 6.8. -ln(1-f) vs. t plots for hydrogen reduction of blue dust.

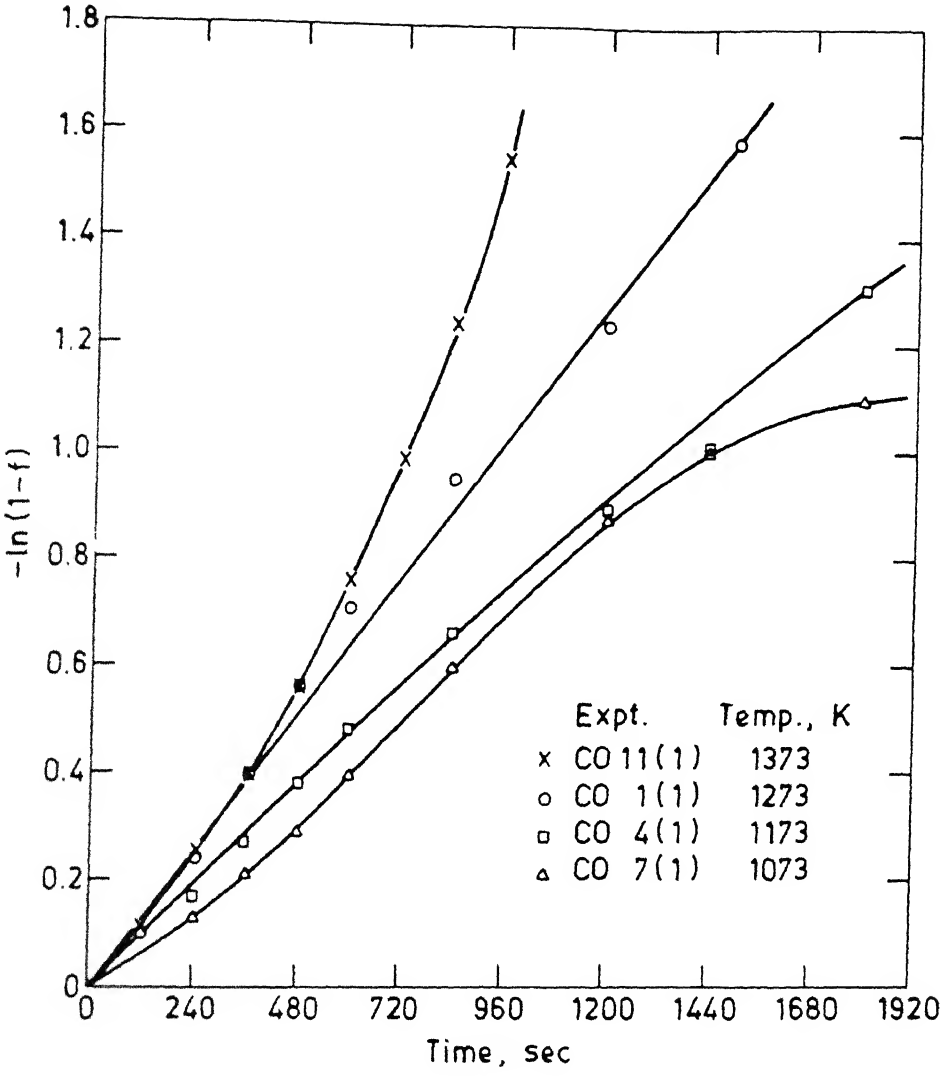

Fig. 6.9. $-\ln(1-f)$ vs time plots for CO reduction.

A plot of log $(\frac{df}{dt})$ vs. log (1 - f) should yield a straight line with the slope giving value of n,and intercept that of log k. As Figure.6.10 shows, here also data could not be fitted as straight lines. Thus it is also not a workable approach of data analysis.

Mckewan's model is not applicable to this investigation due to geometry of the sample (unsintered flat porous bed), since it can be tried only for spherical dense sintered pellet.

If counter diffusion of H_2 and H_2O or CO and CO_2 through the voids of the bed is rate controlling, the Fe/oxide interface shall move inwards with progress of reduction. One can apply the parabolic rate equation which was originally proposed for oxidation of metals[100]. Eq.(6.5) has already presented the rate equation. Figure 6.11 illustrates the attempt to fit f vs. t data with Eq.(6.5). Straight lines could not be obtained demonstrating that it also did not describe the behaviour.

Next approach was to take the initial rate, i.e. $(df/dt)_{t\longrightarrow 0}$ as measure of rate. As discussed in Sec.6.2.2, it can be done by two methods.

i) f vs. t data can be fitted with a polynomial. This has already been done with a 3rd order polynomial as discussed earlier. Mathematically, $(df/dt)_{t\longrightarrow 0}$ is equal to a_1 of Eq.(6.9). However, as discussed in Sec.6.2.2, this method is unreliable due to some sources of initial errors, and hence it has not been tried.

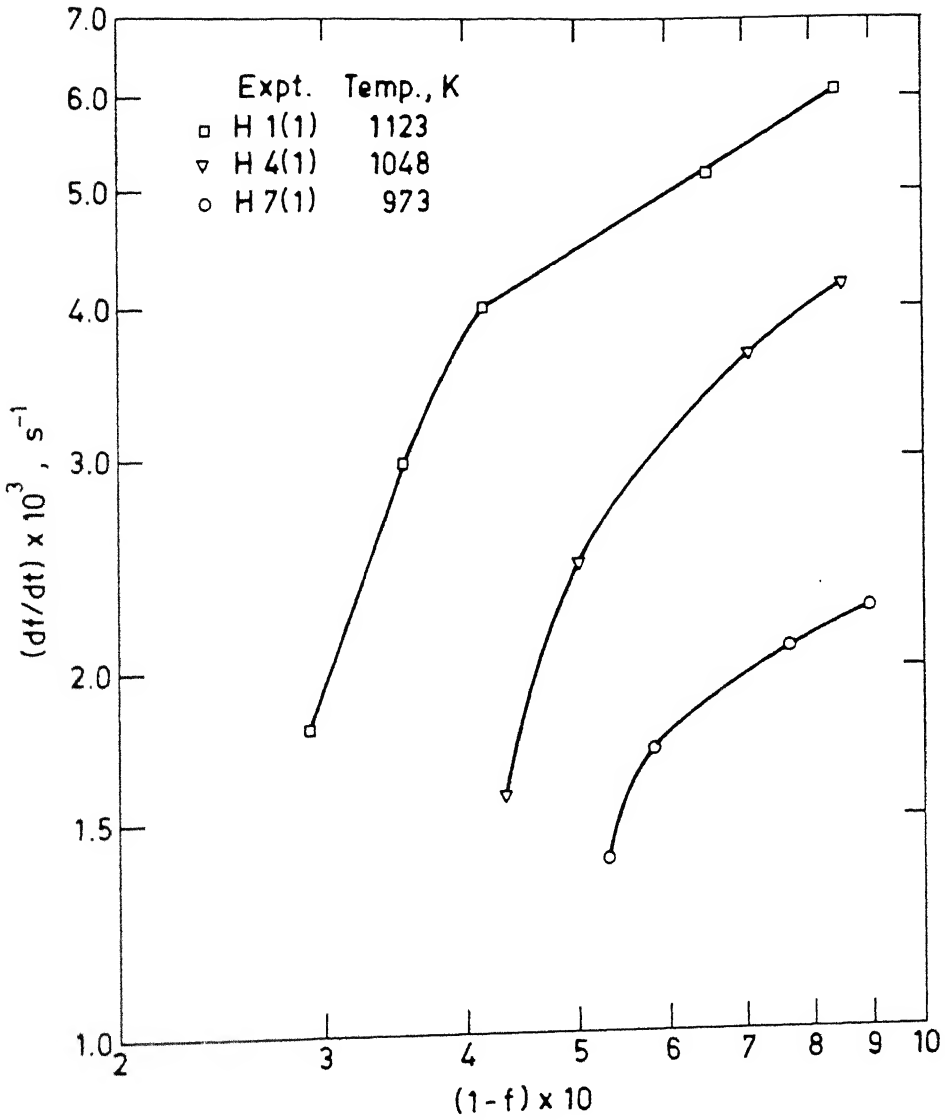

Fig. 6.10. log (df/dt) vs log (1-f) curves for hydrogen reduction of blue dust.

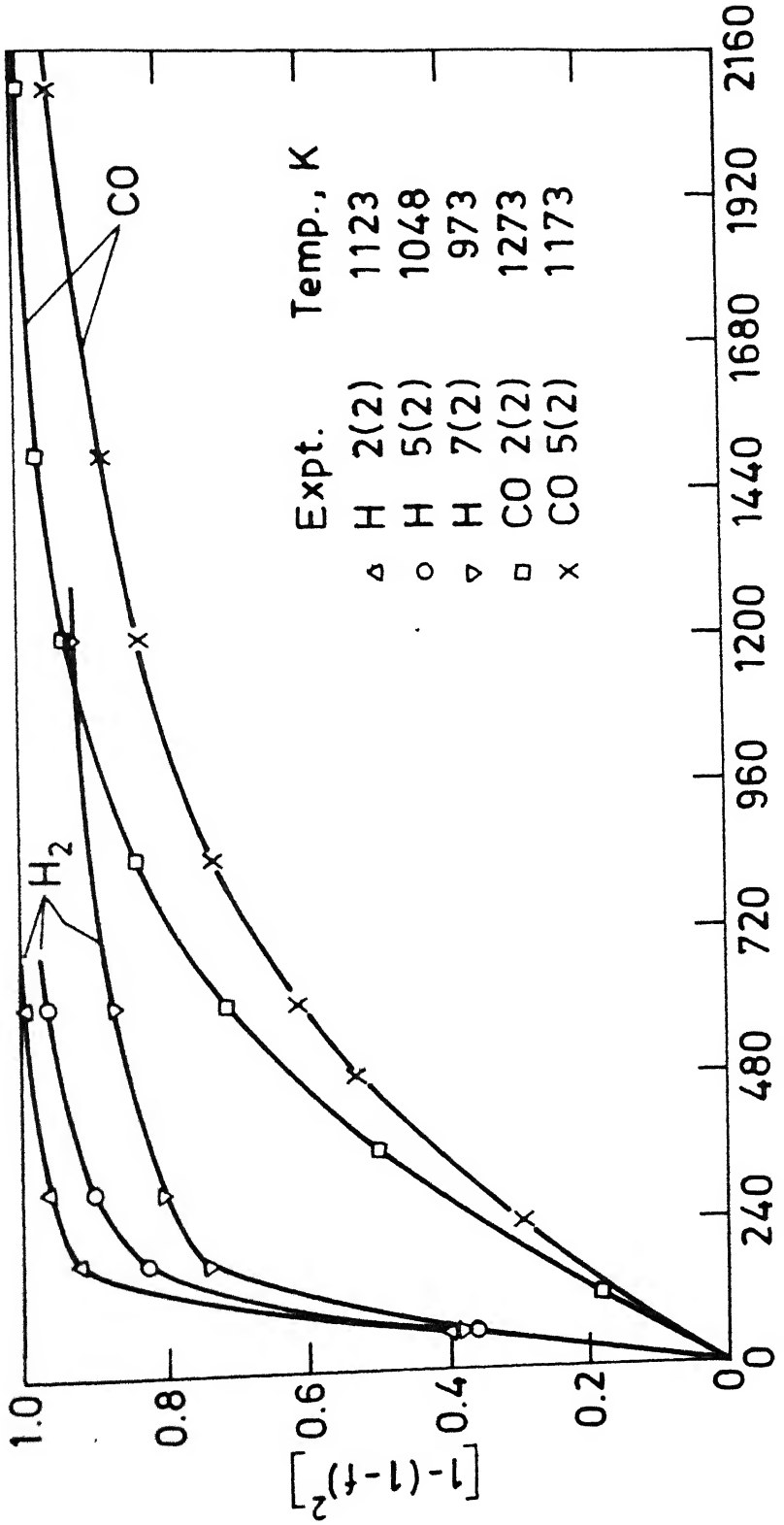

Fig. 6.11. Comparison of reduction data with parabolic rate law.

ii) The second method is based on the observation that f vs. t curves could be approximated by two interconnected straight lines (Figure 6.12). This may be noted in Figures 6.1, 6.2 and 6.4 also. Least square data fitting of the initial straight line yielded value of its slope i.e. $(df/dt)_{initial}$. This is being taken as a measure of rate constant (k) now onwards since this method allowed satisfactory analysis of data. As stated in Sec.6.2.2, it has another major advantage. Rate based on this method gives a measure of initial rate which is free from effects of change of bed conditions (voidage etc.) as a result of reduction.

6.4.2 Determination of rate constant (k_c)

Figures 6.13 and 6.14 present k vs. l data for H_2 and CO reduction respectively. For H_2 reduction it was found that rate (k) decreased with increase of bed depth of sample at different temperatures. By extrapolating the lines to l = 0, values of $(k)_{l\rightarrow 0}$ were obtained. $(k)_{l\rightarrow 0}$ is henceforth being designated as k_c.

The 2nd stage reduction of blue dust was carried out in CO-Ar mixture (50:50). Since rate is proportional to partial pressure of CO, the rate of reduction would be twice in pure CO at 1 bar pressure. In further processing of data, therefore, the experimental rate was multiplied by a factor of 2. For reduction by CO, trends were not systematic (Fig.6.14). Therefore k at l = 0.4 mm was taken as a measure of rate constant (k_c). However, at

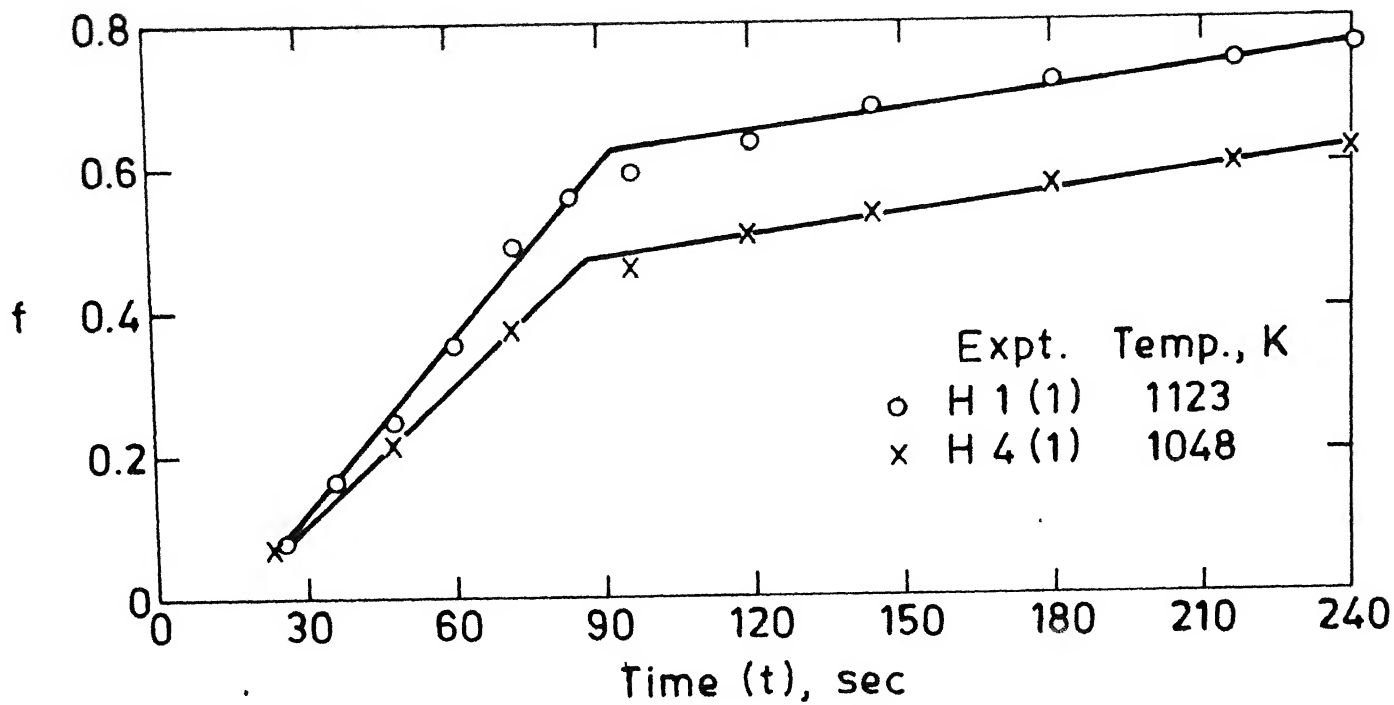

Fig. 6.12. f vs t curves approximated as two intersecting straight lines.

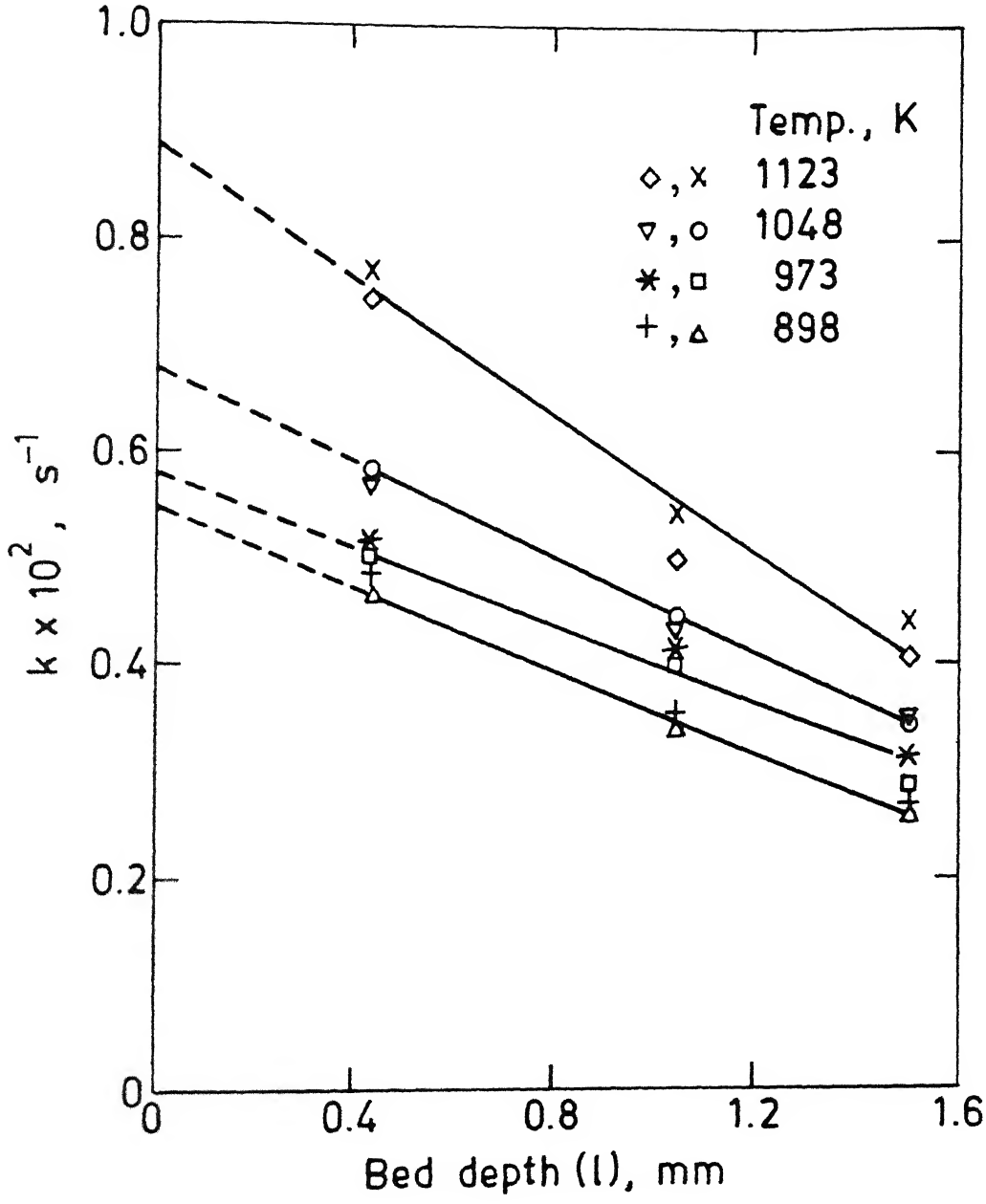

Fig. 6.13. k vs l for hydrogen reduction of blue dust.

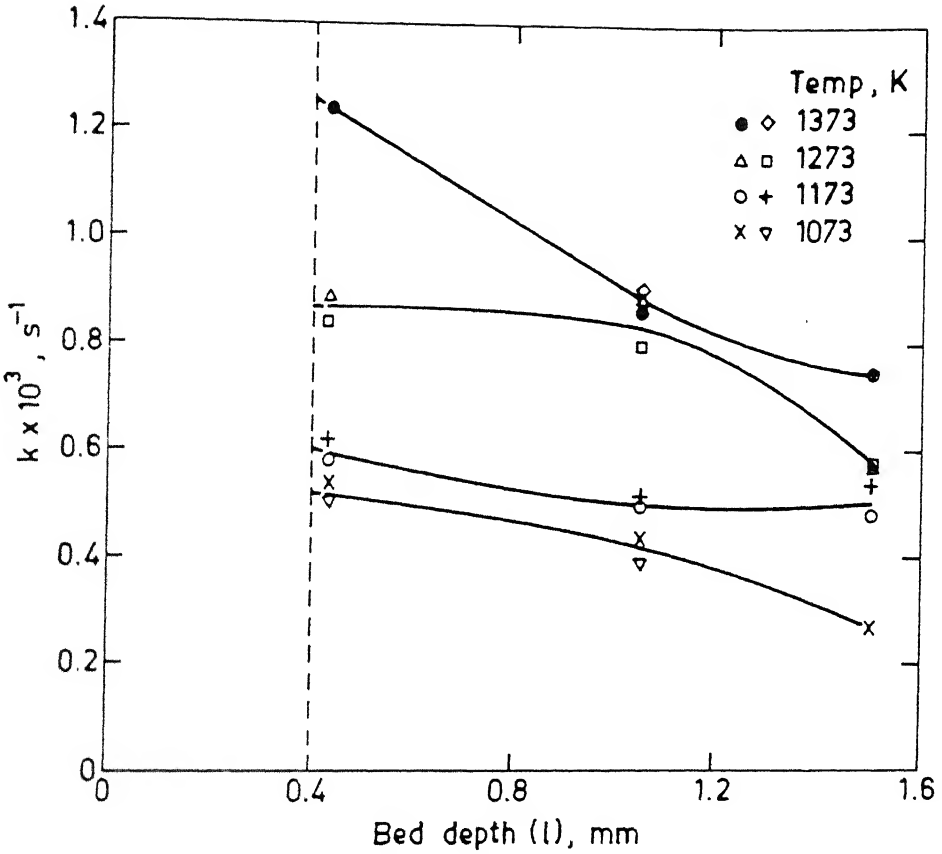

Fig. 6.14. k vs. l for carbon monoxide reduction of blue dust.

higher temperatures, increase of bed depth decreased rate. Therefore the conclusion is that some control of rate by mass transfer resistance in bed of blue dust was present at all temperatures for reduction by H_2 and at higher temperatures for reduction by CO. This is consistent with the findings of Ansari and Bowen[101] who employed a similar geometry as well as unconsolidated bed of fine particles in their reduction studies.

Table 6.2 presents the values of rate constants (k_c) for H_2 and CO-reduction of blue dust. As reported in literatures[57,71] the reduction by CO had been found to be slower (5 to 10 times) as compared to that by H_2. That was also found in this investigation as well (Table 6.2).

6.4.3 Interpretation of k_c

As stated in the previous sub-section (6.4.2) and shown in Fig. 6.12, f vs t curve may be approximated as two intersecting straight lines and the initial straight line was chosen for evaluation of k_c. The values of k_c thus obtained may be taken as the intrinsic rate constant for reduction or they may be partly controlled by mass transfer resistance in the external gas boundary layer.

Table 6.2

Specific Rate Constants (k) and Chemical Rate Constants (k_c) for Reduction by H_2 and CO

Reducing Gas	Temp. (K)	$k \times 10^3$ (s^{-1})			$k_c \times 10^3$ (s^{-1})
		l = 0.44	l = 1.05	l = 1.5	
Pure	898	4.70	3.45	2.62	5.67
Hydrogen		4.91	3.53	2.63	
(P_{H_2}=1 bar)	973	5.03	4.06	2.88	5.96
		5.13	4.10	3.12	
	1048	5.84	4.47	3.46	6.66
		5.69	4.40	3.57	
	1123	7.70	5.46	4.45	8.80
		7.45	5.00	4.09	
Pure Carbon	1073	1.08	0.88	0.53	1.04
monoxide		1.02	0.78	-	
(P_{CO}=1 bar)	1173	1.16	1.00	0.96	1.20
		1.24	1.04	1.08	
	1273	1.78	1.76	1.14	1.72
		1.67	1.59	1.16	
	1373	2.48	1.73	1.31	2.52
		-	1.78	-	

Ansari and Bowen[101] who carried out their reduction study in H_2 with similar arrangement, also observed that f vs t curve could be broadly subdivided into two regions. Interestingly rate per unit mass (i.e. df/dt / gm of Fe_2O_3 in sample) was similar to the present investigation. For example at 1123 K,

$$\text{rate} = 7.33 \times 10^{-3}\ s^{-1}.g^{-1} \qquad \text{(Ansari and Bowen)}$$

and $$\text{rate} = 5.83 \times 10^{-3}\ s^{-1}.g^{-1} \qquad \text{(present investigation)}$$

A search of standard sources failed to provide any dimensionless correlation for mass transfer in gas boundary layer for geometry employed in present investigation. The correlation employed by Ansari and Bowen[101] does not seem to be correct. Therefore, calculation of gas boundary mass transfer coefficient could not be carried out. However, it would follow from the discussions to be presented below that the values of k_c in the present investigation did not suffer from gas boundary mass transfer limitation, and hence it may be taken as intrinsic chemical rate constant for reduction.

Efforts were also made to find out activation energy for reduction. Figure 6.15 (a and b) shows plots of ln k_c vs 1/T for H_2 and CO reduction (II-stage) respectively. It may be noted that points are not falling on straight lines. Even then linear least square fitting of points were made as shown by dotted lines. These yielded values of activation energy (E) as 16 KJ/mol for H_2 and 37 KJ/mol for CO reduction (II-stage). 16 KJ/mol is too low value for chemical control. It is more appropriate for gaseous

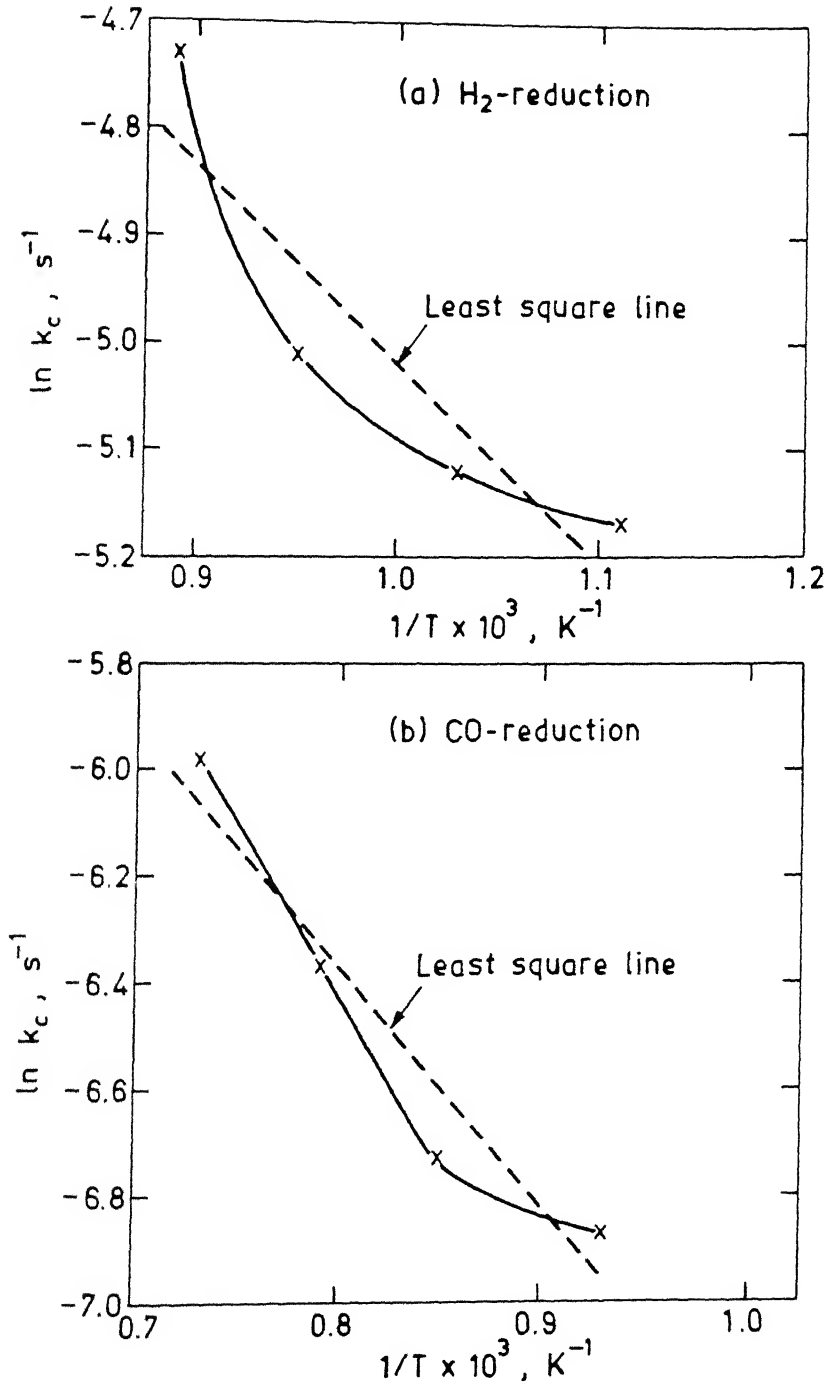

Fig. 6.15. ln k_c vs. 1/T plots for gaseous reduction of blue dust.

mass transfer control. However, from this, conclusion can not be drawn that H_2 reduction was controlled by mass transfer in gas boundary layer in view of the following arguments.

Calculation of binary diffusion coefficients in gases based on kinetic theory of gases[102] show that

$$\frac{D_{CO - CO_2}}{D_{H_2 - H_2O}} \simeq \frac{1}{1.5}$$

If that is so, then CO reduction would tend to exhibit more mass transfer control since rates of reduction by CO is about 4 to 5 times lower only as compared to those for H_2 reduction at corresponding temperatures. However, the value of activation energy for CO reduction is much higher than that for H_2 reduction. This behaviour is contrary to greater mass transfer control for CO reduction.

Hence it is concluded that the non-linearity in ln k_c vs 1/T curves as well as low values of activation energy specially for H_2 reduction are due to morphological changes of the bed such as sintering, densification. The activation energy is really some sort of a temperature coefficient and does not have any significance. It may be mentioned here again that some other investigators who worked with unsintered bed of oxide also had found such anomalous variation of rates with temperature[70,72,79-82].

devolatilization studies were performed with composites containing an inert material (alumina powder) instead of blue dust. Conditions were maintained similar to the fundamental study. Section 7.3 presents results and discussions on these.

Since it was not possible to monitor weight loss as function of time during course of reduction of composite pellet under non-isothermal condition, it was decided to monitor temperature and gas composition as function of time. As stated earlier argon gas at known and controlled flow rate was continuously passed through the reaction chamber to flush out gases evolving from pellet continuously. There were two sets of experiments. Set 1 : H_2 carrier gas in GC to determine Ar, CO, CH_4 , other hydrocarbons and CO_2; and set 2 : Ar carrier gas in GC to determine H_2.

After completion of non-isothermal run, the swelling, after reduction strength and degree of reduction of pellets were determined by procedures presented in chapters 2 and 4.

Section 7.4 presents results and discussions on non-isothermal reduction studies of composite ore-coal and ore-char pellets.

Finally it may be reiterated here that all non-isothermal investigations were carried out, as mentioned in chapter 3, at two speeds of linear downward motion of reaction chamber, designated as high speed (0.124 $mm.s^{-1}$) and low speed (0.062 $mm.s^{-1}$). The former required 48 minutes for the sample to reach the middle of the furnace giving an approximate heating rate of 0.35 $K.s^{-1}$. The latter required 96 minutes for sample to reach

middle of furnace giving a heating rate of approximate 0.175 $K.s^{-1}$.

7.1 Simultaneous Measurement of Ambient and Sample Core Temperature

In this programme of study two thermocouples (Pt-Pt/10pct Rh) were used to measure temperature. The tip of thermocouple 1 was located 4 to 5 mm above the sample (temperature T_1) as usual and that of thermocouple 2 was inserted into the centre of the composite pellet (temperature T_2) for this set of experiments only. Detailed procedure has been presented in Section 3.2.1.3. The difference of their temperatures (ΔT) was calculated as :

$$\Delta T = T_1 - T_2 \qquad \ldots(7.1)$$

The thermocouples were calibrated against Pt-Pt/10pct Rh reference thermocouple. The voltage-time recorder calibrations were checked by a precision potentiometer.

Figures 7.1 to 7.3 show ΔT vs T_1 plots for ore-coal and ore-char composite pellets at both heating rates (low and high). The behaviour pattern of these curves may be summarized as follows.

(i) At temperatures approximately below 600 K, ore-coal composite pellets exhibit a peak which tends to take ΔT from negative value to positive value. This peak is significant at high heating rate.

(ii) At temperature approximately between 600 to 900 K, a trough is exihibited in all samples.

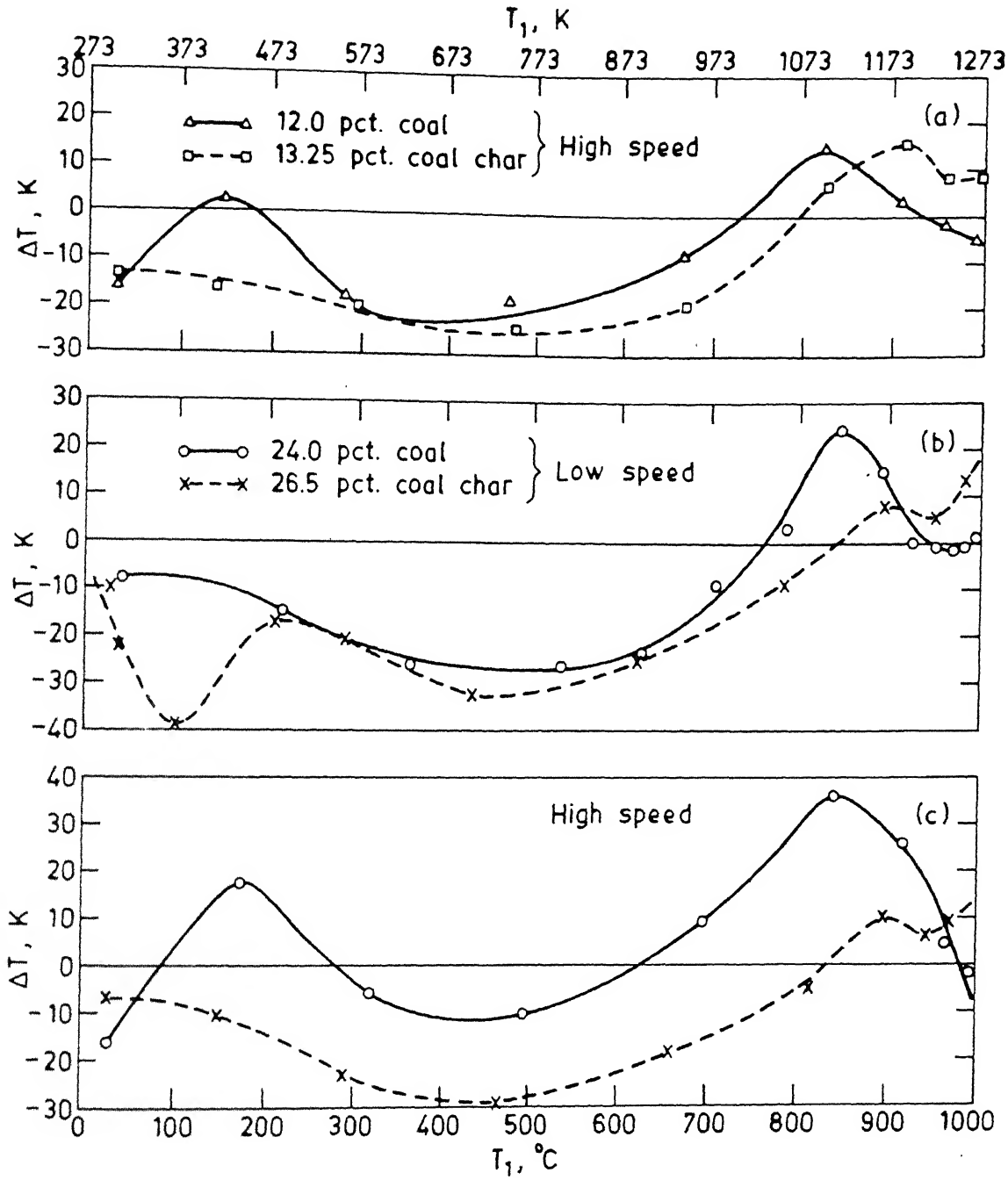

Fig 7.1. Variation of ΔT with temperature in non-isothermal studies of composite pellets (Hutar coal/char).

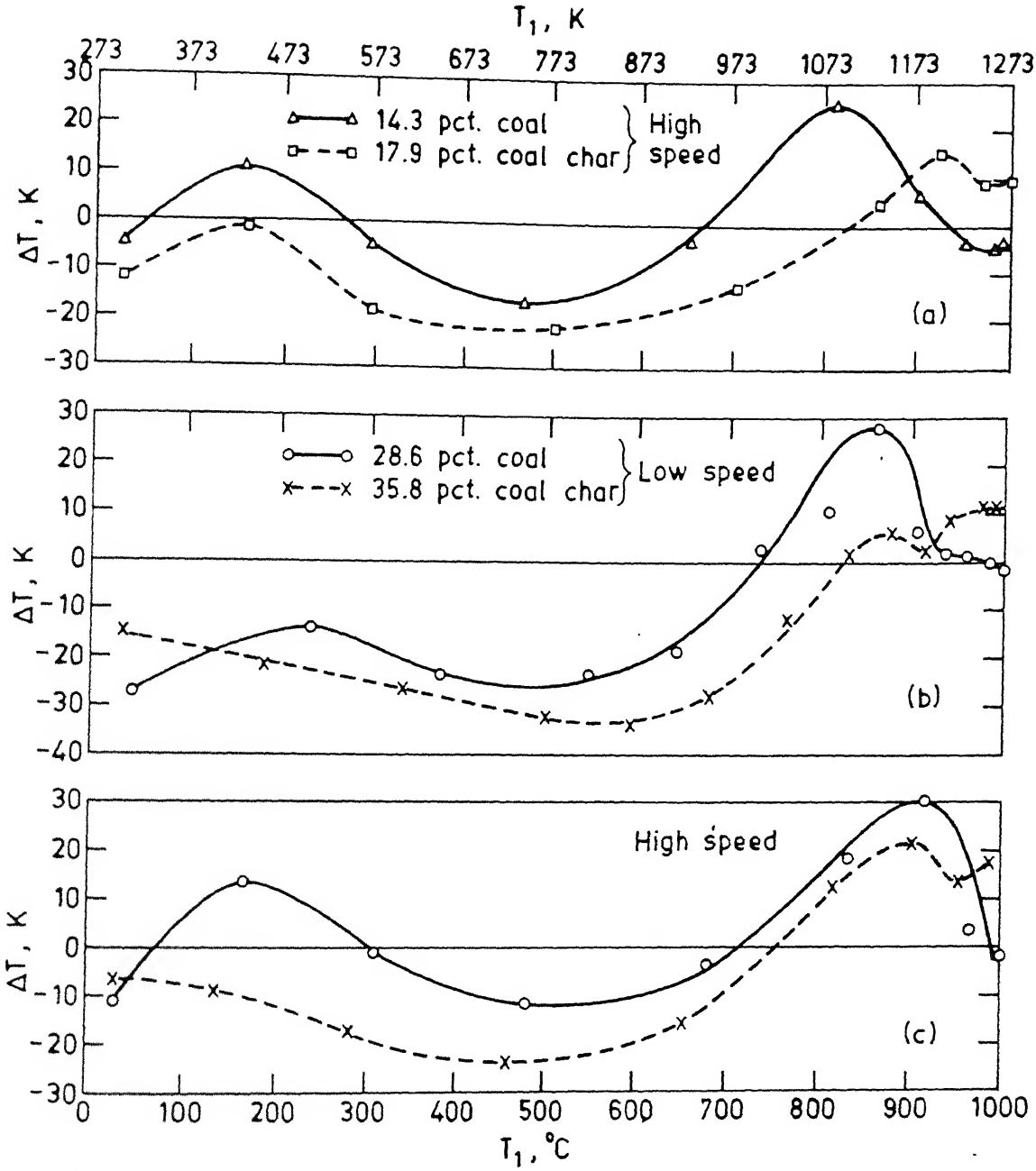

Fig. 7.2. Variation of ΔT with temperature in non-isothermal studies of composite pellets (Bachra coal/char).

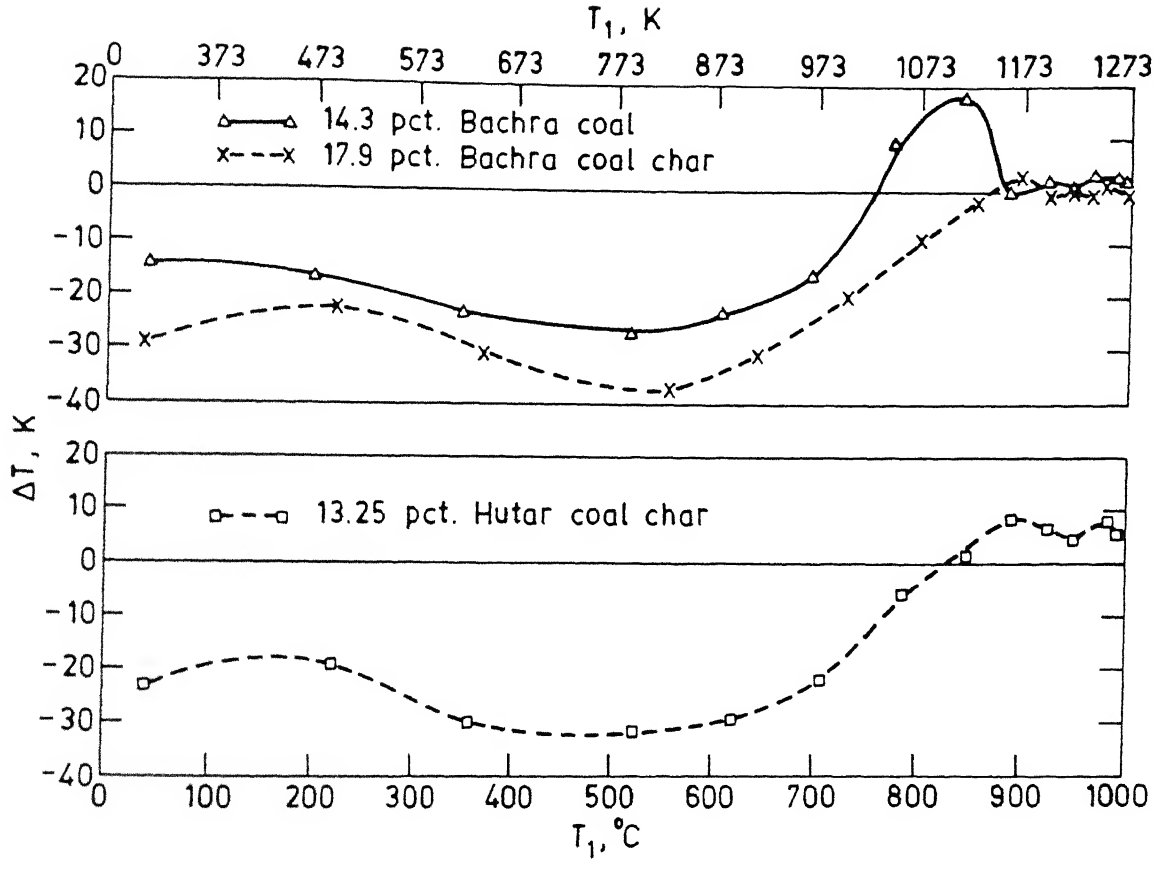

Fig. 7.3. Variation of ΔT with temperature in non-isothermal studies of composite pellets at low speed.

(iii) Above 900 K, a peak appears again in all samples taking ΔT from negative to positive values. For ore-char pellets a minor peak appears after the major peak.

The reactions and phenomena occurring in composites such as pyrolysis of coal, gasification reaction, carbothermic reduction of ore, hydrogen reduction of ore are all endothermic processes. Therefore, T_1 (i.e. ambient temperature) should be higher than T_2 (i.e. temperature inside the pellet). So ΔT should have been positive. However Figs. 7.1 to 7.3 show that ΔT is by and large negative. This is explained by the fact that in non-isothermal experiments the pellet travelled from top of furnace to middle through a temperature gradient. Thermocouple 1 was located 4 to 5 mm above pellet, i.e. about 10 mm above thermocouple 2 and hence at a lower temperature.

Figure 3.2 shows temperature profile of the furnace. It may be divided into three regions .

(i) **Region I (below 600 K) :** here temperature data may be fitted with the equation

$$T = 370 + 8.36\ L \qquad \ldots(7.2)$$

where T is temperature in K and L is distance from top in mm.

(ii) **Region II (600 K to 1150 K) :** here temperature varies linearly according to the following equation

$$T = 600 + 3.014 \times (L - 27.5) \qquad \ldots(7.3)$$

(iii) **Region III (above 1150K) :** here the slope is smaller and variable, the slope tends to zero above 1300 K in the constant temperature zone of the furnace.

Therefore, in an imaginary situation when the pellet is not present, let $T_2 = T_2'$. Then,

$$T_2' = T_1 + 8.36 \times 10 = T_1 + 83.6, \text{ if } T_1 < 600 \text{ K}$$
$$= T_1 + 3.014 \times 10 = T_1 + 30.14, \text{ if } 600 \text{ K} < T_1 < 1150 \text{ K} \quad \ldots(7.4)$$

This is the reason for T_2 to be larger than T_1, i.e. ΔT is negative in general. Of course heat transfer limitation into the pellet would tend to make the difference less. The peaks which tend to shift ΔT towards positive values are attributed to various endothermic reactions.

Below 600 K ore-coal composite pellets exhibit a peak due to evolution of moisture (i.e. drying) and primary devolatilization. All these processes, drying, primary devolatilization are endothermic in nature[49,51]. That is why this type of peak is missing in ore-char composite pellets. This is also not significant at low heating rate since more heat transfer into the pellet tends to nullify this effect more. Bryk and Lu[10] introduced composite samples of iron ore concentrate and coal, and carried out measurement of temperature difference between the centre of the sample and furnace. They observed significant lowering of centre temperature (by as much as 20 K). From 4 to 15 minutes after introduction of the sample to furnace the temperature became equal. This lowering of the temperature was attributed to various endothermic reactions.

At temperature between 600 to 800 K, a trough is exhibited in all samples, due to lower devolatilization rate[51]. The data of the present investigation with composite pellets also reveal

low rate of evolution of CO_2 and H_2 in this temperature range (Figs.7.8 to 7.10). The evolution of CO_2 would not be that endothermic. It may be somewhat exothermic as well. So overall difference of temperature (ΔT) is negative primarily due to locational difference of two thermocouples as mentioned earlier.

Above 900 K, a peak appears in all samples. These may be attributed to high temperature pyrolysis of coal[49,51], gasification of carbon, carbothermic reduction, gaseous reduction of ore etc. All these reactions are endothermic in nature. That is why ΔT is positive in this region for all samples. It may be added further that the dry composite pellets were found to contain appreciable quantities of H_2O and CO_2 as combined and strongly adsorbed. Some of these were released at high temperature and reacted with carbon. This will be fully discussed later in Sec. 7.3 and 7.4.

Inside the sample (i.e. the pellet), temperature would not be uniform. Due to endothermic reactions and heat transfer limitations the pellet centre temperature (T_2) would be less than its surface temperature (T_s). Average pellet temperature (T_p) may be taken as $(T_s + T_2) / 2$. Now T_s may be taken equal to ambient temperature at midpoint location of pellet (i.e. $T_s = T_2'$). Therefore,

$$T_p = \frac{T_2' + T_2}{2} \qquad \ldots(7.5)$$

Now T_2' is related to T_1 by Eq. (7.4) below 1150 K. Above 1150 K, T_1 and T_2' are related as follows.

T_1 (K)	1150	1175	1200	1225	1250	1275	1300
T_2' (K)	1175	1200	1220	1240	1265	1285	1300

Therefore, average pellet temperature (T_p) can be estimated from the readings of the two thermocouples by the above procedure. These data can be used subsequently for non-isothermal reduction studies for estimating T_p when only thermocouple 1 was used. However, this correction was attempted only for quantitative analysis. For qualitative understanding of patterns, corrections were not resorted to.

7.2 Gas Chromatography-Calibration and Data Processing Procedure

Figure 7.4 shows the calibration of gas chromatograph (GC) in hydrogen carrier gas. The calibration was done with pure gases and gas mixtures of known compositions by syringe injection (2 cc). It was found that peak area for auto injected pure gas was not matching with the syringe injected peak area. Since auto injection mode would be employed in experiments, corrections were made to the calibration curves for their use with auto injection mode.

There are many methods available in the literatures[103,104] for measurement of peak area. Out of that, h x w method is a convenient and accurate manual method (standard deviation only 2.5pct)[103]. Height of the peak is measured (h), a point at half the height is marked and then peak width at half height (w) is measured.

Since a known rate of argon gas flow was continuously maintained through the reaction chamber during non-isothermal reduction study, the exit gas mixture contained a high pct of

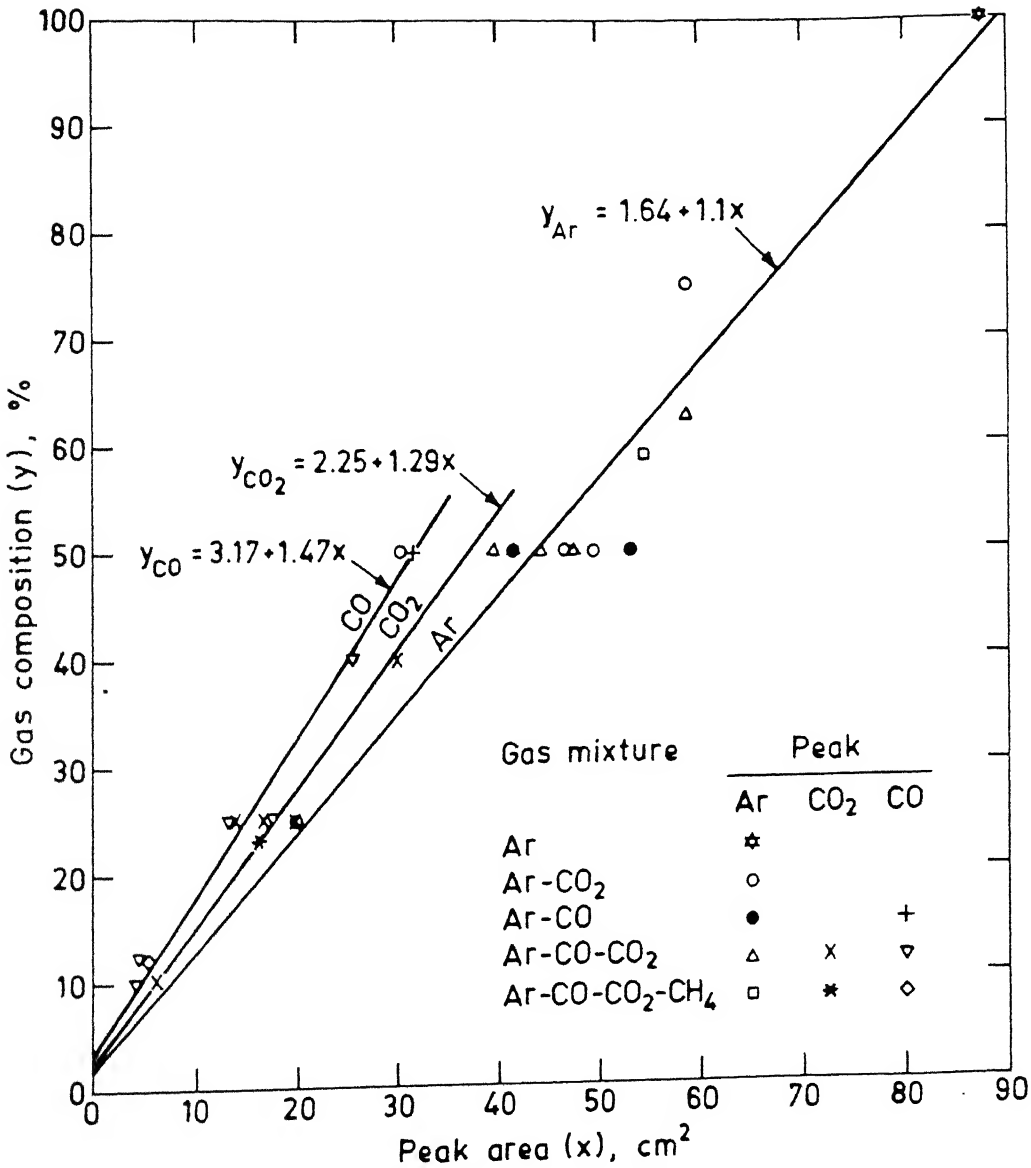

Fig. 7.4. Calibration of gas chromatograph in hydrogen carrier gas.

argon. Again it may be mentioned here that even under the same setting and with precautions such as purification of carrier gas etc., some variation of peak area was observed every time the GC was switched on. In order to minimize the error arising from this, a procedure for rationalization was adopted. This is noted below.

$$\text{Corrected Ar peak area} = \frac{\text{(Actual Ar peak area in expt.)}}{\text{(Actual pure Ar peak area for that expt.)}} \times \text{(Pure Ar peak area in syringe calibration)}$$

$$= \frac{\text{(Actual Ar peak area in expt.)}}{\text{(Actual pure Ar peak area for that expt.)}} \times 87.44\ cm^2 \quad \ldots(7.6)$$

For CO, CH_4 and CO_2 (other hydrocarbons could not be detected),

$$\text{Corrected peak area} = \frac{\text{(Actual peak area in expt.)}}{\text{(Actual pure Ar peak area for that expt.)}} \times \text{(Pure Ar peak area in syringe calibration)}$$

$$= \frac{\text{(Actual peak area in expt.)}}{\text{(Actual pure Ar peak area for that expt.)}} \times 87.44\ cm^2 \quad \ldots(7.7)$$

From these corrected peak areas, the volume pct of each gaseous species was determined from calibration curves (Fig.7.4).

For H_2 determination in product gas, separate experiments were performed and gas analysed in GC in Ar carrier gas.

Attempts were also made to find out H_2O content of product gas mixture. For this a heating tape was wound round the exit tube of reaction chamber to prevent condensation of moisture. But it did not succeed and the effort was abandoned. Hence the exit gas mixture was dried to eliminate moisture by passing through anhydrous $CaCl_2$ before its introduction into the GC.

For H_2,

$$\text{Corrected peak area} = \frac{\text{Actual peak area in expt.}}{\text{Correction factor}} \quad \ldots(7.8)$$

$$\text{Where correction factor} = \frac{\text{Auto injected peak area for pure } H_2}{\text{Syringe injected peak area for pure } H_2}$$

$$= 0.927$$

With the above procedure the total percentage of Ar + CO + CH_4 + CO_2 + H_2 should be 100. However, in all data sets it differed some what and ranged mostly between 95 to 110. Therefore, the volume percentages were normalized further to make the total 100 as follows.

Normalized volume pct of a gaseous species

$$= \frac{\text{Vol.pct as determined by GC}}{\text{Sum of vol.pct of all gases}} \times 100 \quad \ldots(7.9)$$

In non-isothermal studies, as mentioned already, a low flow rate of pure argon (Iolar 2) was continuously passed through the reaction chamber. Therefore, the total gas flow rate (Q) including evolved gases, can be calculated as follows.

$$Q = \frac{Q_{Ar}}{X_{Ar}} \qquad \ldots(7.10)$$

where Q_{Ar} = Volumetric flow rate of Ar, $cm^3.s^{-1}$ (STP)

X_{Ar} = Volume fraction Ar in exit gas mixture.

Volumetric flow rate of any species (Q_i) can be calculated as :

$$Q_i = Q.X_i \qquad \ldots(7.11)$$

where X_i = Volume fraction of species i (CO, CH_4, CO_2 and H_2)

Molar rate of evolution of i (in $mol.s^{-1}$)

$$= (Q.X_i) \times \frac{1}{22400} \qquad \ldots(7.12)$$

Rate of oxygen loss ($\dot{W}_o$, $g.s^{-1}$) associated with evolution of CO and CO_2 is given as :

$$\dot{W}_o = \frac{16Q}{22400} (X_{CO} + 2\,X_{CO_2}) \qquad \ldots(7.13)$$

Now by graphical integration of $\dot{W}_o$ as function of time, total oxygen loss ($\Delta W_o'$) due to evolution of CO and CO_2 can be found out.

$$\Delta W_o' = \int_0^t \dot{W}_o \, dt \qquad \ldots(7.14)$$

7.3 Non-Isothermal Devolatilization of Coal

As mentioned earlier that, for devolatilization study, special pellets were prepared by using inert material (pure alumina powder) instead of blue dust. Low pct of coal and same binder as for composite pellet were employed in the mixture. The purpose of preparation of samples this way was to simulate the composite pellet for devolatilization studies in all other ways except for replacement of Fe_2O_3 by Al_2O_3.

Experimental condition for devolatilization of coals :

1. Coal type : 2 (Hutar, Bachra, low pct)
2. Speed of reaction chamber : 2 (0.124 and 0.062 $mm.s^{-1}$)
3. Max. temperature : 1 (1273 K)
4. Carrier gas in GC : 2 (H_2, Ar)

Figure 7.5 as well as Figs. 7.8 and 7.9 show gas chromatographic data for devolatilization of Hutar and Bachra coal. GC samples were taken several times during one experiment. The pct compositions of various gaseous species as well as rate of oxygen loss due to evolution of CO and CO_2 ($\dot{W}_o$) have been presented. These have been plotted as function of temperature and not time for better fundamental understanding of phenomena.

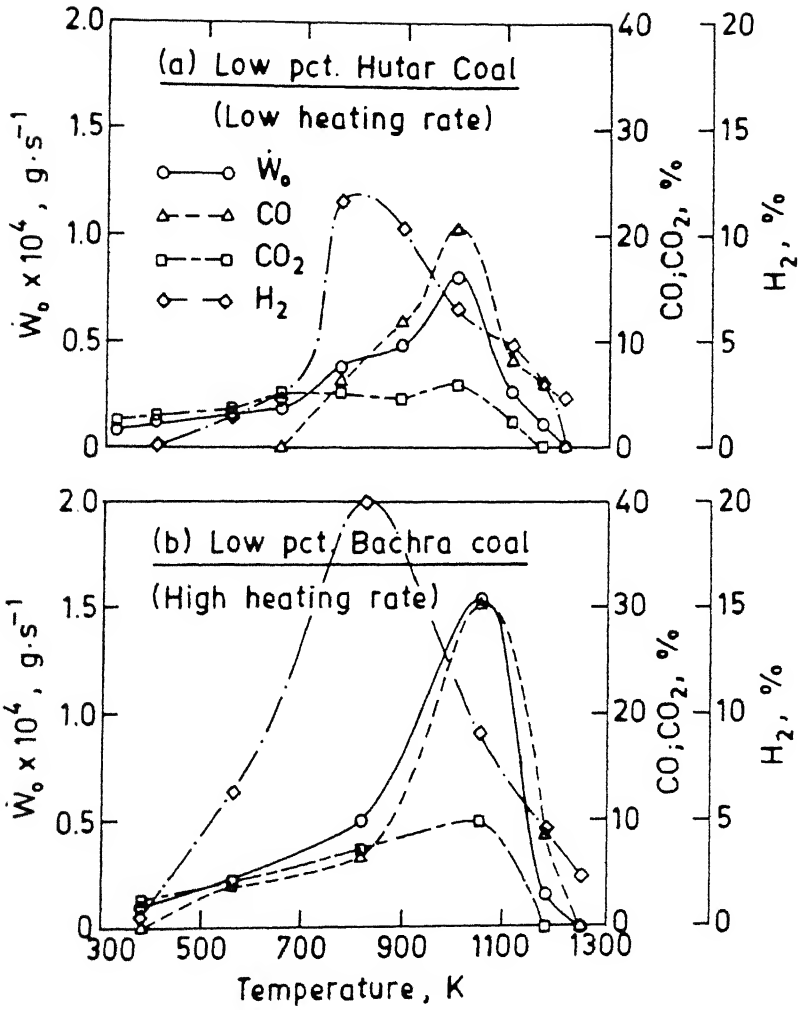

Fig. 7.5. Variation of exit gas composition and $\dot{W}_o$ with temperature in non-isothermal devolatilization studies.

Table 7.1 presents some calculated values from GC data for experiments on the devolatilization of coal. Based on the ultimate analyses of coals (Table 2.4), the oxygen (with organic matters) contents of Hutar and Bachra coal are 23.5 and 15.9 wt.pct respectively. Since this oxygen gets removed with volatiles and gases during the devolatilization, these provide the values of the theoretical removable oxygen in coal (Column 3, Table 7.1(a)).

Total oxygen loss associated with evolution of CO and CO_2 ($\Delta W_o'$) was calculated by graphical integration of $\dot{W}_o$ using Eq. (7.13) as stated earlier. These values are shown in Table 7.1(a) (Column 4). An interesting observation is that $\Delta W_o'$ is much larger than theoretical oxygen content of coal. Likely causes are the binder and pellet making procedure. The binder contains 6 pct of CaO and also combined moisture due to $Ca(OH)_2$ and hydrothermal bonding besides strongly adsorbed moistures. Since during pellet making procedure pellets are exposed to atmosphere, absorption of CO_2 to form $CaCO_3$ to some extent is also likely. In addition the coal and alumina etc. may contain and can pick-up some H_2O as combined moisture or as strognly adsorbed H_2O.

The moisture which is evolved at high temperature, is expected to react with carbon or hydrocarbon generating CO and H_2 to some extent, thus boosting up CO concentration in exit gas leading to larger value of $\Delta W_o'$. If that is so then the total quantity of H_2 evolved should be much higher compared to what is

Table 7.1(a)

Oxygen Balance Calculation for Devolatilization Experiments

Coal code* (speed)**	Wt.of coal present in sample (g)	Theo.removable oxygen present in coal (g)	Total oxygen evolved from sample as CO and CO_2 (g) $(\Delta W'_o)_2$	Oxygen coming from sources other than coal, (g)	
				actual (4-3)	per gm pellet
1	2	3	4	5	6
HCL (HS)	0.098	0.023	0.109	0.086	0.084
BCL (HS)	0.114	0.018	0.098	0.080	0.078
HCL (LS)	0.095	0.022	0.105	0.083	0.081
BCL (LS)	0.118	0.019	0.096	0.077	0.073
				Avg.	0.079

* HCL - Hutar coal, low pct, BCL - Bachra coal, low pct (Table 7.3 for complete information)

** HS - High speed, LS - Low speed

Table 7.1(b)

Hydrogen Balance Calculation for Devolatilization Experiments

Coal code (speed)	Quantity of H_2 liberation expected from coal, $(g)\times10^3$	Total H_2 evolved during devol. $(g)\times10^3$	Additional H_2 liberated, $(g)\times10^3$	Additional oxygen generated from moisture, (g)	
				actual	per gm pellet
1	2	3	4	5	6
HCL (HS)	1.11	0.617	-	-	-
BCL (HS)	1.52	5.31	3.79	0.030	0.030
HCL (LS)	1.08	5.33	4.25	0.034	0.034
BCL (LS)	1.57	5.07	3.50	0.028	0.027

expected from pyrolysis of coal. Therefore the quantity of H_2 evolved was calculated by graphical integration of rate of evolution of H_2 (Q_{H_2}) as function of time. Q_{H_2} for all experiments were calculated by the procedure already mentioned in section 7.2. Quantities of liberated H_2 in devolatilization experiments are noted in Table 7.1(b) (Column 3). It may be noted that 3 experiments yielded almost the same value whereas one experiment gave very low value which is considered unreliable.

Ultimate analyses of coals (Table 2.4) showed the quantity of H_2 associated with organic matters as 3.4 and 4.0 wt. pct for Hutar and Bachra coals respectively. With reference to Table 1.3, it is estimated that 1/3 of this quantity is approximately liberated as H_2. Rest would be associated with hydrocarbons. On the basis of this the quantity of H_2 expected from the reliable devolatilization experiments are noted in Table 7.1(b) (Column 2). It shows that the actual quantities of H_2 liberated are significantly larger than those theoretically expected from coal.

This trend confirms the statement made earlier that some H_2O from sources like binder are likely to react with carbon to liberate H_2 and CO. It may be observed (Fig.7.5) that H_2 peaks are appearing at around 750 to 850 K. Literatures mention that in coal pyrolysis, H_2 peak should be at around 1050 to 1100 K[49,51,54]. This also may be explained as due to reaction of carbon with moisture to some extent.

Table 7.1(b) also shows the quantities of additional oxygen generated from this moisture (Column 5), which is 8 times the mass of additional hydrogen. As the Tables 7.1(a) and 7.1(b) show

that even it does not take into account the total oxygen liberated as CO and CO_2 during devolatilization experiments ($\Delta W_o'$). This may be attributed to liberation of CO_2 from sample by decomposition of carbonate. Some CO_2 would also react with H_2 or carbon to produce CO.

After non-isothermal heating weight losses of pellets had been recorded. Material balance calculations confirmed substantial additional weight loss (11 to 12pct for devolatilization experiments) besides loss of volatile matter. This is in agreement with the conclusions arrived at on the basis of gas chromatographic data.

The methane content in exit gas was maximum 2 pct. Other hydrocarbons could not be detected by gas chromatograph. Most of the hydrocarbons, it seems, were higher ones and got condensed in the exit tube of reaction chamber. Such condensations were observed during experiments. In industrial coke ovens the beds are large. Hence some higher hydrocarbons crack leading to CH_4 etc. Here this is not likely to happen.

7.4 Non-Isothermal Reduction of Composite Pellets

7.4.1 Results and their reproducibility

Table 7.2 lists the variables for non-isothermal reduction studies of composite pellets. As shown in the Table, total number of experiments was 48 including duplicate experiments carried out for testing of reproducibility of results.

Table 7.3 shows experimental conditions for this programme of investigation. As stated in chapter 2, the binder combination and pellet making procedure were standardised for these fundamental studies. For information, binder combination is again mentioned in Table 7.3. All these pellets were prepared through the autoclave route and detailed procedure is available in Section 2.4.

The experimental procedure for non-isothermal runs is given in Section 3.2.1.2. It may be noted from Table 7.2 that the maximum temperature was kept fixed at 1273 K.

Table 7.2

Variables for Non-Isothermal Reduction of Composite Pellets

Sl.No.	Variable	Number	Remarks
1.	Iron ore	1	Blue dust
2.	Coal	2	Hutar, Bachra
3.	Char	2	Hutar, Bachra
4.	Fe_{tol}/C_{fix} ratio	2	5.5 and 11.0 for coal 3.1 and 6.2 for char
5.	Maximum temp.	1	1273 K
6.	Speed of travel of reaction chamber	2	0.062 mm s^{-1}, 0.124 mm s^{-1}
7.	Carrier gas in GC	2	H_2 for Ar, CO, CH_4, CO_2 Ar for H_2
8.	Reproducibility test	2	for H_2 carrier gas

Total number of experiments = 48

Table 7.3

Experimental Conditions for Non-Isothermal Reduction of Composite Pellets

Sample no.	Expt. no.	Rate of heating (**)	Type of coal/ char	Pct of coal/ char (*)	Fe_{tol}/C_{fix}
1	2	3	4	5	6
B 121	FG 1,2	H	Hutar	12.0	11.0
	FG 5,6	L	coal, low		
	FGM 1,2	H,L	(HCL)		
B 122	FG 3,4	H	Bachra	14.3	11.0
	FG 7,8	L	coal, low		
	FGM 3,4	H,L	(BCL)		
B 125	FG 9,10	H	Hutar	13.25	6.2
	FG 11,12	L	coal char, low		
	FGM 5,6	H,L	(HCCL)		
B 126	FG 13,14	H	Bachra	17.9	6.2
	FG 15,16	L	coal char, low		
	FGM 7,8	H,L	(BCCL)		
B 124	FG 17,18	H	Hutar	24.0	5.5
	FG 19,20	L	coal, high		
	FGM 13,14	H,L	(HCH)		
B 123	FG 21,22	H	Bachra	28.6	5.5
	FG 23,24	L	coal, high		
	FGM 16,15	H,L	(BCH)		
B 128	FG 25,26	H	Hutar	26.5	3.1
	FG 27,28	L	coal char, high		
	FGM 11,12	H,L	(HCCH)		
B 127	FG 29,30	H	Bachra	35.8	3.1
	FG 31,32	L	coal char, high		
	FGM 9,10	H,L	(BCCH)		

** Code: H = High, L = Low; * All pct wt. w.r.t. wt.of blue dust; Binder combination: 4pct S Mix V + 9pct S Mix VII for all samples except sample no.B 124 where 6pct S Mix V + 10pct S Mix VII used

Appendix C presents the data on gas chromatographic analyses of exit gas in terms of volume pct of Ar, CO, CH_4, CO_2 and H_2, for all non-isothermal reduction experiments. These data were collected at intervals of time during the experiments by injection of gas sample into GC by auto-injector. Since moisture could not be analysed by GC, the exit gas was dried by anhydrous $CaCl_2$ before introduction into the GC. Section 7.2 has already discussed about the procedure of GC calibration and data processing procedure.

Figure 7.6 compares exit gas analyses amongst the duplicate sets. Each point in the plot has horizontal coordinate equal to data point at some time after start of experiment, and the vertical coordinate equal to the data point at the same time from the duplicate set. Reproducibilities are very good, statistically speaking, at both heating rates. Therefore, it is concluded that gas composition values were fairly reliable.

Table 7.4 presents results of non-isothermal reduction experiments for composite pellets. The procedure for measurement of degree of reduction has already been discussed in Chapter 4. The values reported in Table 7.4 represent averages of the two sets of experiments under the same condition. Reproducibility of results amongst the two sets of experiments can be visualised from Figure 7.7 (a,b).

Figure 7.7(a) shows that degree of reduction (α) for the duplicate sets exhibited good reproducibility. So far as compressive strength (after reduction) is concerned reproducibility is again fairly good. Strength depends on many

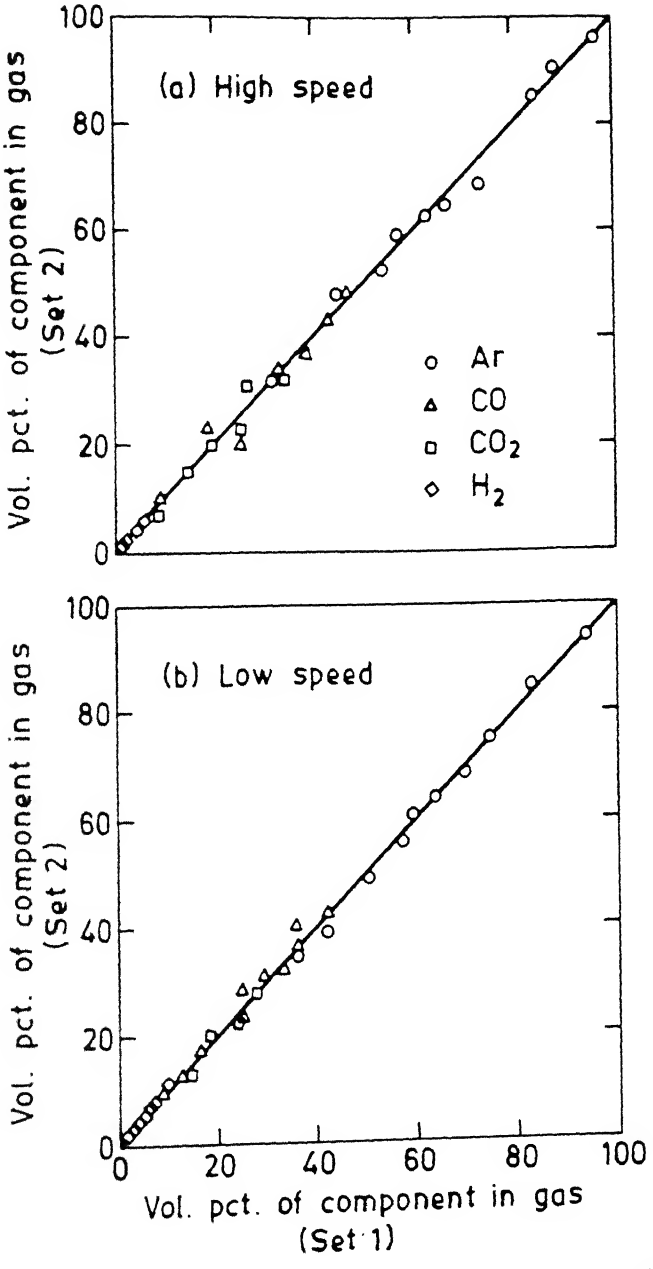

Fig. 7.6. Reproducibility of exit gas compositions amongst duplicate sets of experiments.

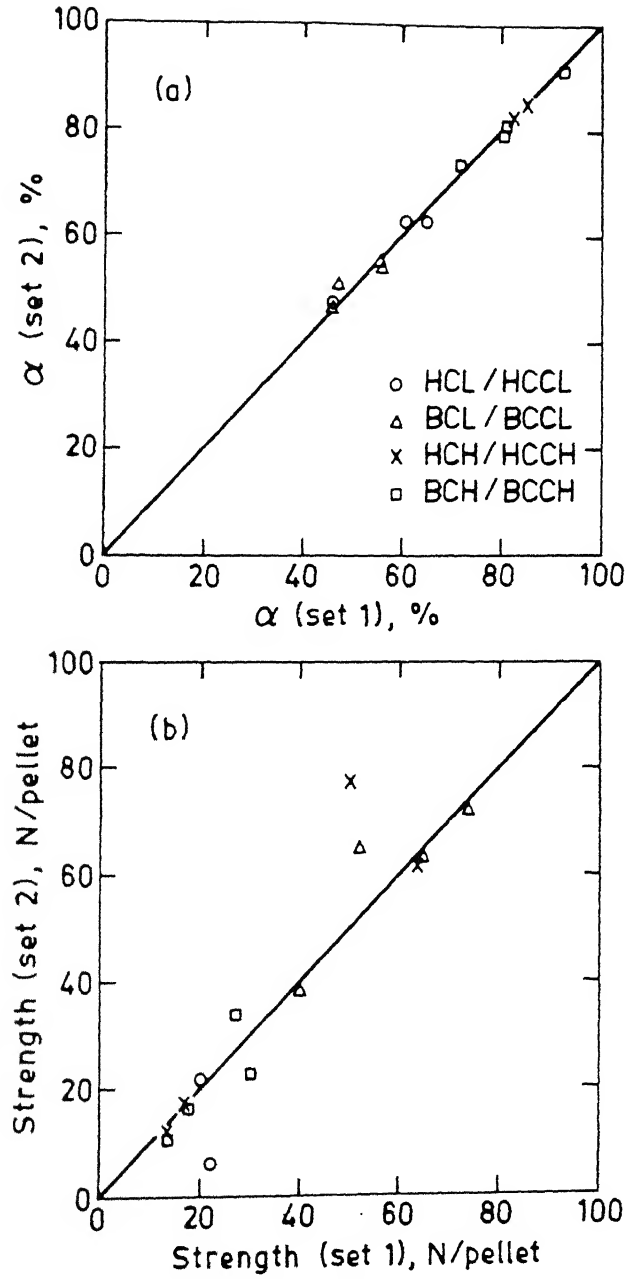

Fig. 7.7. Reproducibility of (a) degree of reduction and (b) strength after reduction amongst duplicate sets of experiments.

variables and significantly on the history. Considering this it may be concluded that the reproducibility of results was quite satisfactory.

Table 7.4

Results for Non-Isothermal Reduction of Composite Pellets

Expt. no.	Type of coal/char	Degree of reduction α (pct)	Compressive strength		Vol.change (pct)	Extra wt. loss (pct)
			Before red. (N/pellet)	After red. (N/pellet)		
FG 2	HCL	46.0	65	27	19.7	9.1
FG 5,6	HCL	46.5	65	14	12.9	9.3
FG 3,4	BCL	46.5	282	73	9.7	9.3
FG 7,8	BCL	49.0	282	58	9.1	9.2
FG 9,10	HCCL	61.8	523	19	12.9	11.9
FG 11,12	HCCL	64.0	523	21	102.1	13.7
FG 13,14	BCCL	55.3	745	64	24.8	9.4
FG 15,16	BCCL	65.1	745	39	41.3	10.6
FG 17,18	HCH	82.8	56	63	-15.8	16.3
FG 19,20	HCH	82.6	56	63	-16.2	16.4
FG 21,22	BCH	80.4	86	27	6.3	15.2
FG 23,24	BCH	80.9	86	30	-0.3	15.1
FG 25,26	HCCH	85.0	525	13	97.3	14.6
FG 27,28	HCCH	99.7	525	17	107.8	20.9
FG 29,30	BCCH	72.6	468	17	60.4	13.2
FG 31,32	BCCH	92.1	468	12	96.5	15.3

1. Above data are average values of two sets of experiments.

2. Code for coal/char is given in Table 7.3.

7.4.2 Discussions on exit gas composition

As noted in Section 7.4.1, compositions of exit gas during non-isothermal experiments at various time intervals have been reported in Appendix C. Figures 7.8 to 7.10 show volume pct of various gaseous species in argon stream plotted as function of temperature for some experiments. The reason for selecting temperature as variable is because temperature of the sample keeps increasing with time during the experiments, and for fundamental understanding of phenomena, temperature is to be preferred rather than time. For comparison purposes, data for experiments on devolatilization of coal have also been included in Figures 7.8 and 7.9.

As Appendix C shows, the concentration of CH_4 in the product gas was very low. That is why, it is not included in the figures. The pattern is similar to experiments on devolatilization of coals and has already been discussed in Section 7.3.

CO evolution generally started above 700 K except in two cases. CO peaks were observed between 1050 to 1250 K, pct of CO going as high as 40. This agrees with non-isothermal studies of coal and iron oxide mixture by Cypres et al[54]. In the devolatilization experiments,CO peaks appeared at 1000 to 1100 K. Reduction of iron oxide by C generates both CO and CO_2. Also the P_{CO}/P_{CO_2} ratio remains higher than the equilibrium ratio for reduction of Fe_xO to Fe. It has been established[4] that the rate of gasification reaction controls reduction by carbon and becomes significant only above 1100 K. This is corroborated from observation on measurement of temperature difference between

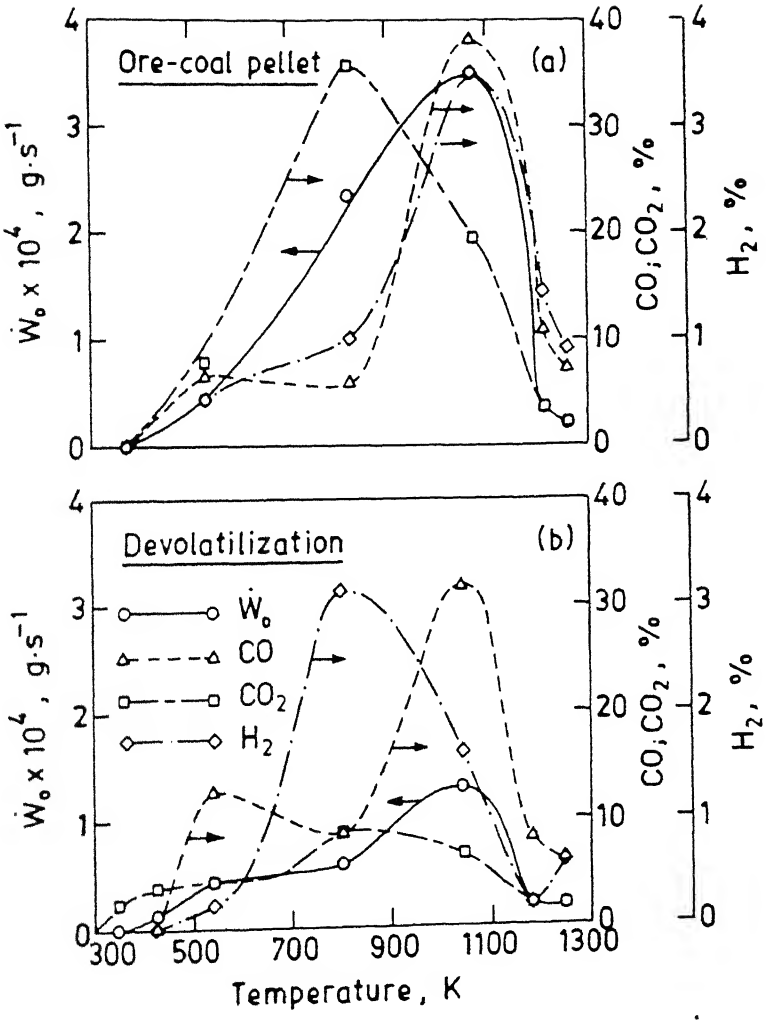

Fig. 7.8. Variation of exit gas composition and $\dot{W}_o$ with temperature in non-isothermal studies at high heating rate for low pct. Hutar coal.

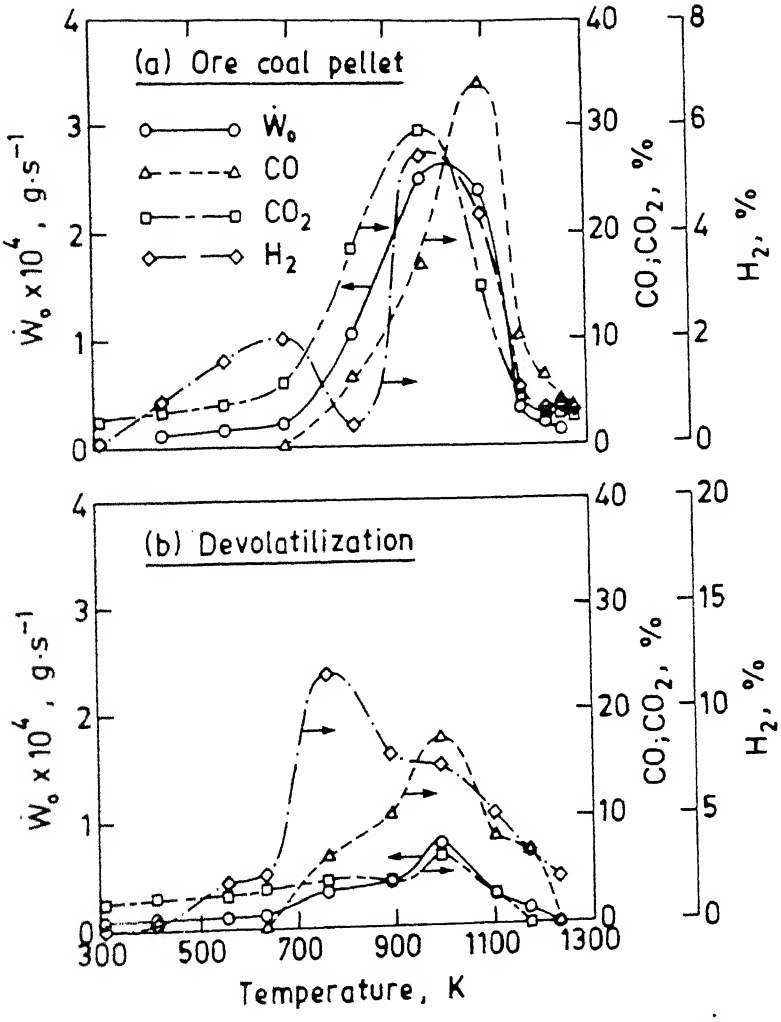

Fig. 7.9. Variation of exit gas composition and $\dot{W}_o$ with temperature in non-isothermal studies at low heating rate for low pct. Bachra coal.

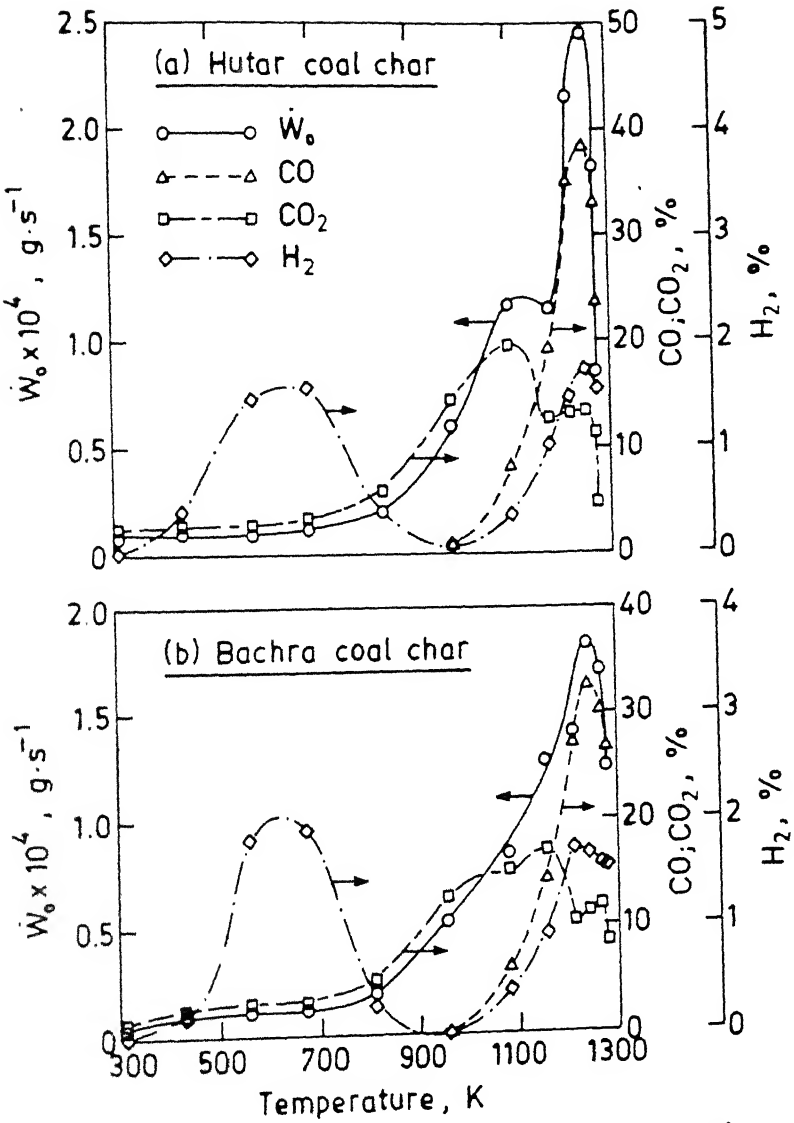

7.10. Variation of exit gas composition and $\dot{W}_o$ with temperature in non-isothermal studies at low heating rate for high pct. char.

pellet centre and outside (Sec.7.4.2). Moreover freshly reduced iron has strong catalytic effect on gasification reaction[1,8,9]. Therefore the reduction of Fe_xO by carbon is the likely reason for enhanced CO content for composite pellets. These reactions also can qualitatively explain shift of CO peak to higher temperature in composite pellet as compared to those in devolatilization experiments.

In general CO_2 peaks appeared at 100 to 200 K less temperature as compared to CO peak. Again it is also be noted that CO_2 content in the gas for ore-coal and ore-char composites were much larger than in devolatilization of coals. This behaviour pattern may be attributed to reduction of iron oxides by carbon generating both CO and CO_2 gas. In this reduction system P_{CO_2}/P_{CO} ratio is higher at a lower temperature[1,8,9]. Moreover carbonate decomposition also starts in this temperature range.

This observation is not matching with that of Cypres et al[54], who obtained CO_2 peaks at the same temperature as CO peaks for iron oxide and coal mixture. Since experimental conditions of Cypres et al[54] were somewhat different, no further discussion is being attempted.

So far as H_2 evolution is concerned the peaks appeared at 1000 to 1100 K for ore-coalcomposite pellets . This is higher than the temperature range (800-850 K) of the same for devolatilization experiments. The likely explanation is that reduction of iron oxides by H_2 gas starts at reasonably high rate above 900 K or so. Therefore, in composite pellets bulk of the

hydrogen gets consumed in this temperature range, and peak was much lower in magnitude as well as got shifted to higher temperature. It is not clear why some H_2 evolved from ore-char composites at as low a temperature as 550 to 750 K. May be it is due to desorption of chemisorbed H_2O on highly porous char.

7.4.3 Estimation of extent of reduction of ore by carbon and hydrogen

In composite pellets the oxygen loss from sample as CO, CO_2 and H_2O is not alone from iron oxides in ore, but also from organic matter in coal. Moreover, it has been concluded from the devolatilization experiments (Sec. 7.3) that a large quantity of oxygen is coming from H_2O and CO_2, combined or strongly adsorbed by the sample. This has been attributed to binder as well as the pelletmaking procedure.

It has already been stated in Sec. 7.3 that weight loss of samples after non-isothermal devolatilization revealed about 11 to 12pct extra loss of weight not accounted for by loss of volatile matter. It is in agreement with the statement above. Similar material balance exercise was carried out on ore-coal/char composite pellets. The oxygen loss from iron ore could be calculated from degree of reduction. This together with loss of volatile matter of coal constituted the theoretically expected weight loss upon non-isothermal reduction. For char, volatile matter was taken as zero.

Experimental weight loss of pellets after non-isothermal runs were much more than the above theoretically expected values.

This may be termed as **extra weight loss**. The last column of Table 7.4 presents this as pct of dry pellet weight before non-isothermal experiment. It ranges between 9.1 to 13.7 pct at low coal/char samples and 14.6 to 20.9 pct for high coal/char samples. This demonstrates that coal and char also absorbed a large quantity of H_2O etc. which did not get eliminated even after oven drying.

In principle, oxygen associated with CO and CO_2 in exit gas during non-isothermal reduction of composite pellets should allow us to estimate extent of ore reduction by carbon. By carbon reduction, both carbothermic reduction (i.e. direct reduction) as well as that by CO (i.e. indirect reduction) are included. As discussed in Secs. 7.2 and 7.3, these were calculated by graphical integration of rate of oxygen loss ($\dot{W}_o$) associated with evolution of CO and CO_2 in exit gas as function of time. These values ($\Delta W_o'$) are noted in Table 7.5 (column 6).

However, a correct estimate requires subtraction of oxygen loss as CO, CO_2 from coal and other sources as discussed just now. These were estimated on the basis of findings in Sec. 7.3 on devolatilization experiments, as follows.

$$\Delta W_o' \text{ (blank)} = \text{pellet weight } [\ (f_{coal} \times f_{o(coal)}) + 0.079\ ] \qquad \ldots(7.15)$$

where, $\Delta W_o'$ (blank) = oxygen associated with CO and CO_2 of exit gas from sources other than iron oxide in ore,

f_{coal} = fraction of coal in pellet,

$f_{o(coal)}$ = fraction of organic oxygen in coal (taken as zero for char).

The factor 0.079 was arrived at from devolatilization experiments [Table 7.1 (a)].

Values of pellet weight (W_p^i), f_{coal}, $\Delta W_o'$ (blank) for different experiments have been presented in Table 7.5. Oxygen loss associated with reduction of iron oxides by C (ΔW_o^C) is obtained as:

$$\Delta W_o^C = \Delta W_o' - \Delta W_o'(\text{blank}) \qquad ...(7.16)$$

Fractional reduction of ore by carbon is given as :

$$f_c = \frac{\Delta W_o^C}{W_o^I} \qquad ...(7.17)$$

where W_o^I is total removable oxygen in ore calculated by Eq. (4.7).

$$\text{Again } f_{H_2} = f - f_c \qquad ...(7.18)$$

where f_{H_2} is fraction of iron oxide reduced by H_2. f is total fractional reduction.

$$f = \frac{\alpha}{100} \qquad ...(7.19)$$

Values of α have been presented in Table 7.4. Values of ΔW_o^C, W_o^I, f, f_c and f_{H_2} are presented in Table 7.5. It may be noted from Table 7.5 that even ore-char pellets are indicating substantial reduction by H_2 sometimes. This is not surprising in view of

conclusions already arrived that extraneous H_2O, while evolving reacts with carbon to give rise to H_2. Figure 7.10 shows that some H_2 evolution also occurred in ore-char pellets.

Table 7.5

Removable Oxygen and Fractional Reductions in Non-Isothermal Studies of Composite Pellets

Expt.no.	Type of coal/ char	W_p^i (g)	f_{coal}	$\Delta W_o'$ (blank) (g)	$\Delta W_o'$ (g)	ΔW_o^c (g)	W_o^i (g)	f	f_c	f_{H_2}
1	2	3	4	5	6	7	8	9	10	11
G 2	HCL	1.798	0.096	0.183	0.314	0.131	0.410	0.460	0.319	0.14
G 5,6	HCL	1.784	0.096	0.181	0.359	0.178	0.407	0.465	0.438	0.02
G 9,10	HCCL	1.958	0.105	0.155	0.295	0.140	0.442	0.618	0.317	0.30
G 11,12	HCCL	1.940	0.105	0.153	0.382	0.229	0.438	0.640	0.522	0.11
G 3,4	BCL	1.843	0.112	0.179	0.331	0.152	0.413	0.465	0.369	0.09
G 7,8	BCL	1.877	0.112	0.181	0.340	0.159	0.420	0.490	0.378	0.11
G 13,14	BCCL	1.869	0.137	0.148	0.257	0.109	0.407	0.553	0.268	0.28
G 15,16	BCCL	1.878	0.137	0.148	0.364	0.216	0.409	0.651	0.527	0.12
G 17,18	HCH	1.495	0.171	0.178	0.439	0.261	0.304	0.828	0.858	-0.03
G 19,20	HCH	1.462	0.171	0.174	0.358	0.184	0.298	0.826	0.616	0.21
G 25,26	HCCH	1.650	0.190	0.130	0.277	0.147	0.337	0.849	0.435	0.41
G 27,28	HCCH	1.670	0.190	0.132	0.484	0.352	0.341	0.997	1.032	-0.03
G 21,22	BCH	1.606	0.202	0.179	0.480	0.301	0.323	0.804	0.932	-0.12
G 23,24	BCH	1.625	0.202	0.180	0.419	0.239	0.327	0.809	0.730	0.07
G 29,30	BCCH	1.565	0.241	0.124	0.205	0.081	0.300	0.726	0.270	0.45
G 31,32	BCCH	1.608	0.241	0.127	0.415	0.288	0.308	0.921	0.935	-0.01

However this way of estimation of f_{H_2} suffers from some uncertainty since, as Table 7.5 shows :

(i) f_{H_2} values for same ore-coal combination at two different speeds are differing significantly and there is no systematic pattern of variation,

(ii) f_{H_2} values are sometimes close to zero and even negative, which are not possible,

(iii) f_{H_2} calculated from H_2 balance in some ore-coal composites are not matching with these values. More details of this are discussed later.

This erratic nature is attributed to uncertainties involved in estimation of $\Delta W_o'$ (blank) on the basis of Eq. (7.15). Even then this exercise has been desirable since it shows the difficulties of separately determining f_c and f_{H_2}. It also can guide future investigators about designing their experiments to aim at more precise and reliable estimates of f_c and f_{H_2}.

There is no doubt that reduction of ore took place significantly by H_2 in ore-coal composities. Table 7.1(b) has presented calculated quantities of H_2 given off by coal during devolatilization. It has also been noted in Sec. 7.4.2 that much less H_2 was evolved from ore-coal composites. Not only that but H_2 peak of coal blanks in temperature range of 750 to 850 K were missing in ore-coal composites. All these can be explained as due to utilization of H_2 for ore reduction in composite.

Quantitative calculations of H_2 reduction of ore were carried out for experiment numbers FGM 2,3,4 [i.e. HCL (LS), BCL

(HS) and BCL (LS)] by subtracting H_2 evolved from composites from hydrogen evolved during respective devolatilization experiments. Table 7.6 presents the estimates of f_{H_2} from hydrogen balance. Since composite pellets with alumina had lower weights than composite pellets with iron ore, so normalization was carried out as follows.

$$\text{Sample wt.ratio} = \frac{\text{weight of pellet with ore}}{\text{weight of pellet with alumina}} \quad \ldots(7.20)$$

H_2 utilized for reduction = Total H_2 evolved during devol. x sample wt. ratio - total H_2 evolved from ore-coal pellet ...(7.21)

Again, equivalent oxygen removed from ore in sample by H_2 reduction (ΔW_o^H) :

$$(\Delta W_o^H) = H_2 \text{ utilized for reduction} \times 8 \quad \ldots(7.22)$$

From this, f_{H_2} values were calculated as :

$$f_{H_2} = \frac{\Delta W_o^H}{W_o^1} \quad \ldots(7.23)$$

As may be noted from Tables 7.4 and7.5, that only the value for BCL (LS) is matching with f_{H_2} estimated by the earlier technique. To conclude, fraction of iron oxide reduced by hydrogen was estimated by two different techniques. At present, sufficient data are not available to decide which method should be recommended. The principal uncertainty lies in estimaion of

blank values, from limited number of devolatilization experiments. To throw more light on this, a separate extensive programme of investigation is required, and the same is included in suggestions for further work.

Table 7.6

Calculation of f_{H_2} from Hydrogen Balance in Non-Isothermal Studies

Coal code* (speed)	H_2 evolved during red. (g) x 10^3	H_2 evolved during devol. (g) x 10^3	Sample wt. ratio	H_2 utilized for red. of iron oxide (g) x 10^3	ΔW_o^H (g)	f_{H_2}
HCL(LS)	1.88	5.33	1.86	8.03	0.064	0.153
BCL(HS)	2.23	5.31	1.84	7.54	0.060	0.145
BCL(LS)	3.00	5.07	1.84	6.33	0.051	0.117

* Details in Table 7.3

7.4.4 Comparison of reduction behaviour of ore-coal and ore-char composites

Literature review (ch.1) revealed that while some investigations have been carried out on ore-char, ore-coke breeze composites, very litter information is available on ore-coal composites. Therefore, one of the objectives of the present investigation was to compare reduction behaviour of ore-coal composites with corresponding ore-char composites. Meaning of corresponding is like this. For composite with low percentage of

Hutar coal (i.e. HCL), the corresponding ore-char composite contained low percentage of Hutar coal char (i.e. HCCL). Also speed of movement of reaction chamber should be the same (HS or LS).

Figure 7.11 compares degree of reduction obtained in ore-coal and in corresponding ore-char composites. Statistically speaking, there is no significant difference between them. Figure 7.12(a) compares compressive strength after reduction for ore-coal and ore-char pellets. Ore-coal pellets have definite superiority over corresponding ore-char pellets. Again as Figure 7.12(b) shows that this may be attributed to very low volume change in ore-coal composites as opposed to large swelling experienced by ore-char composites upon reduction. A possible explanation for this difference is that pyrolysis and also transient plasticity in coal in same temperature range provide additional high temperature strengths to bonds.

7.4.5 X-ray diffraction studies

Table 7.7 presents results of X-ray diffraction studies. From the X-ray results it could be concluded that major phase was wustite, and minor phase was metallic iron for samples at low degrees of reduction (FGM 3 and 6). For high degree of reduction, wustite was not located (FGM 10), or present as minor phase (FGM 13). These observations can be easily explained by assuming that reduction was stage wise, i.e. $Fe_2O_3 \longrightarrow Fe_3O_4 \longrightarrow Fe_xO \longrightarrow Fe$. This observation is in agreement with that reported in literatures for reduction of composite pellets[7,37].

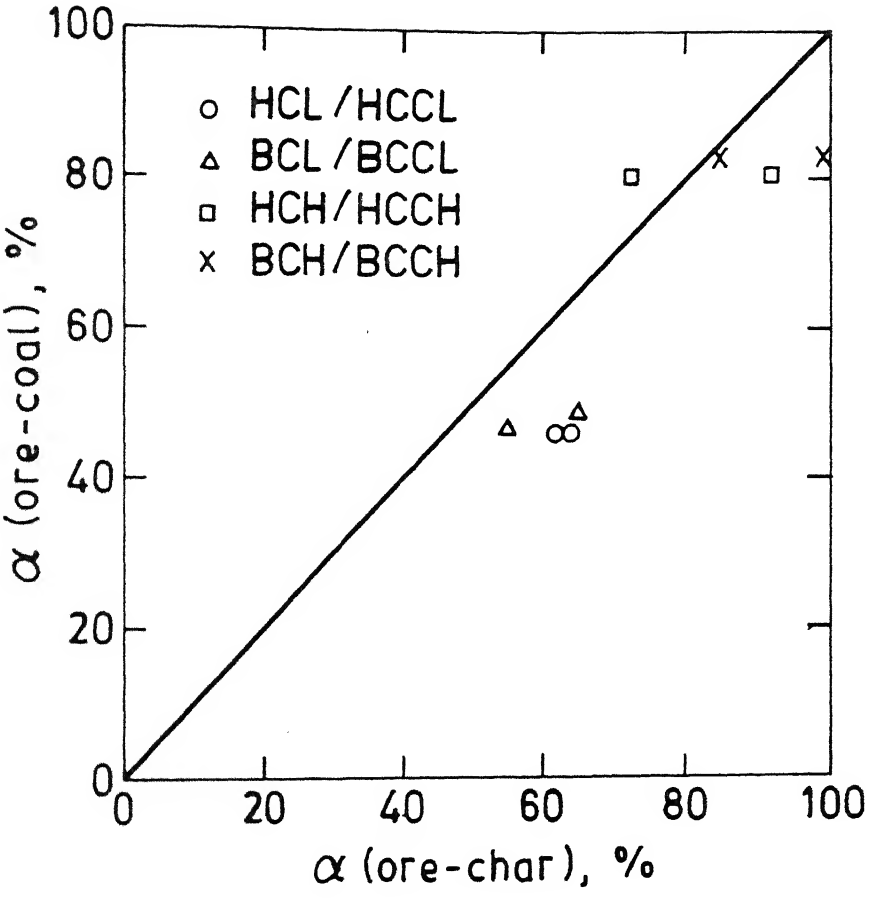

Fig. 7.11. Comparison of degree of reduction of ore-coal and corresponding ore-char composite pellets.

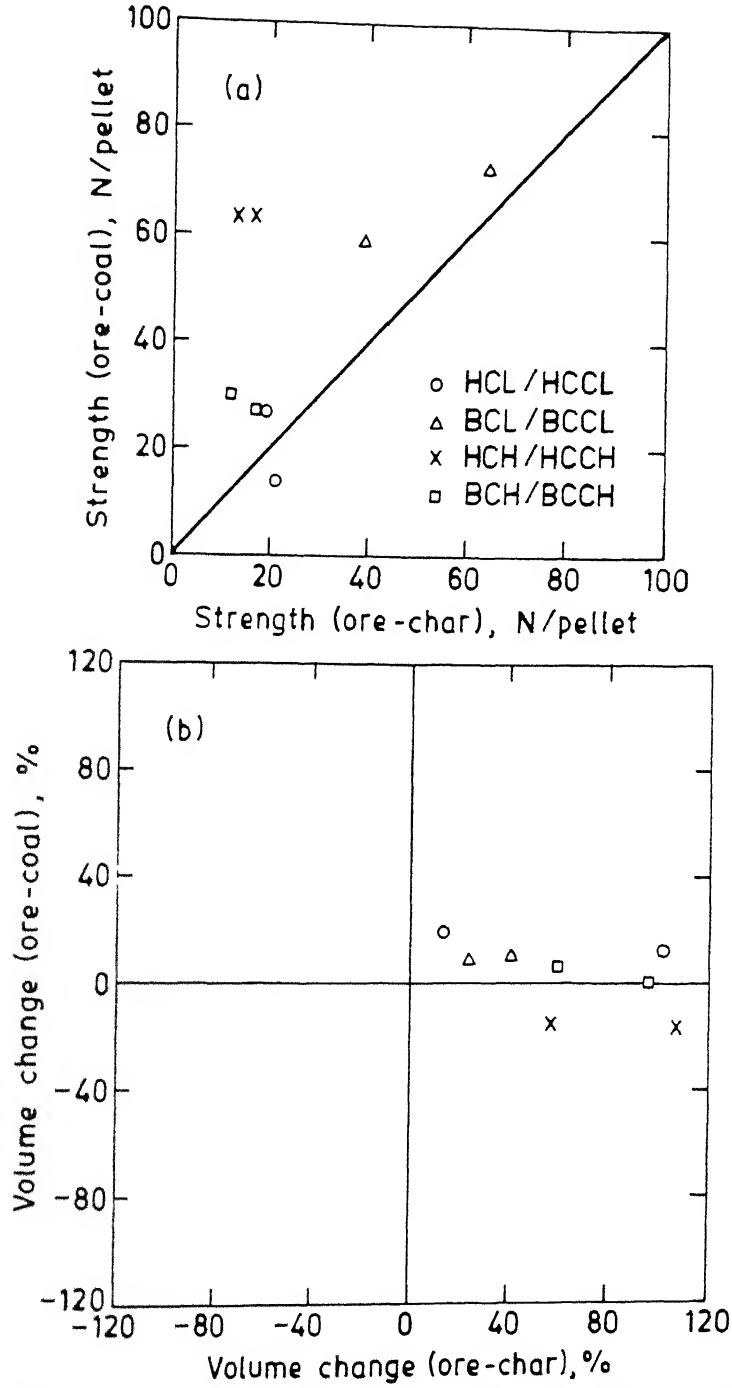

Fig. 7.12. Comparison of (a) strength and (b) volume change upon reduction for ore-coal and ore-char pellets.

7.4.6 Comparison of rate of reduction by CO in non-isothermal and isothermal reduction experiments

From X-ray diffraction results just presented (in Table 7.7), it would be valid to assume that the reduction in non-isothermal experiments towards the end (i.e.above 1100 to 1200 K) were Fe_xO —> Fe.

Table 7.7

Results of X-ray Diffraction Studies

Sl.no.	Expt. no. (speed)	Reductant code*	Degree of reduction (pct)	Phases present	
				Major	Minor
1	FGM 3 (HS)	BCL	46.5	FeO	Fe
2	FGM 6 (LS)	HCCL	64.0	Fe,FeO	-
3	FGM 13(HS)	HCH	82.8	Fe	FeO
4	FGM 10(LS)	BCCH	92.1	Fe	-

* Table 7.3 for details of code

$$Fe_xO + CO = x\ Fe + CO_2 \qquad \ldots(7.24)$$

Assuming, Fe, Fe_xO are pure solid,

$$K_e = \left(\frac{P_{CO_2}}{P_{CO}} \right)_{equilibrium} \qquad \ldots(7.25)$$

where K_e is equlibrium constant for reaction (7.24), P_{CO_2} , P_{CO} are partial pressures of CO_2 and CO.

Again, $$\dot{W}_o = \frac{df}{dt} \times W_o^1 \qquad \ldots(7.26)$$

where df/dt is rate of reduction. If reduction is by CO only, then,

$$\frac{df}{dt} = k_c \left(P_{CO} - \frac{P_{CO_2}}{K_e} \right) \qquad \ldots(7.27)$$

where k_c is chemical rate constant.

Combining Eqs. (7.26) and (7.27), and noting that $\dot{W}_o = \dot{W}_o^c$ for CO reduction,

$$\dot{W}_o^c = W_o^1 \cdot k_c \left(P_{CO} - \frac{P_{CO_2}}{K_e} \right) \qquad \ldots(7.28)$$

Since total pressure was close to 1 bar, P_{CO}, P_{CO_2} could be obtained easily from gas composition. From Eq. (7.28) $\dot{W}_o^c$ can be calculated by taking value of k_c from Table 6.2, and K_e from Fe-C-O equilibrium[55]. Again, $\dot{W}_o^c$ (expt.) can be estimated from gas chromatographic data for composite as well as for devolatilization (i.e. blank) experiments. As mentioned in Sec. 7.4.3, blank or inert pellet has low weight than composite. Hence, the value of $\dot{W}_o$ (blank) should be boosted up for compatibility with composite pellet data.

$$\dot{W}_o^c \text{ (expt.)} = \dot{W}_o \text{ (composite)} - \dot{W}_o \text{ (blank)} \times \text{sample wt. ratio} \qquad \ldots(7.29)$$

Table 7.8 presents $\dot{W}_o^c$ (expt), estimated with the help of Eq. (7.29) with $\dot{W}_o^c$, calculated by Eq. (7.28) at 1173 K. The

agreement is satisfactory.

The above exercise links non-isothermal reduction kinetics with kinetics of isothermal reduction of Fe_xO to Fe by CO. It would have been interesting to carry out similar exercise for hydrogen reduction as well. However, it was not possible since success could not be achieved in analysis of H_2O in exit gas as discussed earlier. Without value of p_{H_2O}, calculations by equation similar to Eq. (7.28) can not be performed.

Table 7.8

Comparison of Experimental and Calculated Rate of Reduction of Iron Oxide by CO for Non-Isothermal Studies

Expt. no.	W_o^1 (g)	p_{CO} (bar)	p_{CO_2} (bar)	$\dot{W}_o$ (comp.) ($g.s^{-1}$) $\times 10^4$	$\dot{W}_o$ (blank) ($g.s^{-1}$) $\times 10^4$	Sample wt. ratio	$\dot{W}_o^c$ (expt.) ($g.s^{-1}$) $\times 10^4$	$\dot{W}_o^c$ (calc.) ($g.s^{-1}$) $\times 10^4$
1	2	3	4	5	6	7	8	9
FG 2	0.410	0.168	0.065	0.950	0.440	1.77	0.171	0.117
FG 5,6	0.407	0.088	0.035	0.298	0.113	1.74	0.101	0.048
FG 3,4	0.413	0.177	0.060	0.950	0.400	1.79	0.234	0.218
FG 7,8	0.420	0.103	0.040	0.375	0.141	1.78	0.124	0.076

At $T = 1173$ K, $k_c = 1.2 \times 10^{-3}$ (s^{-1}), $K_e = 0.451$

7.4.7 Scanning electron microscopic studies

It has been known even several decades back that iron ores/oxides exhibit varieties of product morphologies on reduction depending upon the initial material and how it is reduced[55]. Temperature of reduction, nature and composition of reductant are important variables. Investigators used optical microscope in early days. Scanning Electron Microscope (SEM) has been a more popular tool in the last one to two decades.

In view of the fact that product morphology significantly influences strength after reduction, reduction degradation in furnaces as well as overall reducibility etc., there has been a renewed interest in this area during the last decade. A very brief review of a few investigations has been included in this section just to highlight some important findings.

Seaton et al[105] measured swelling of pellets containing hematite or magnetite along with coal char after reduction in the temperature range of 1173 K to 1473 K. Microstructural features were observed in SEM. Catastrophic swelling of pellets and consequent loss of strength at temperature ranges of 1173 to 1283K were attributed to observed whisker growth. Strength increase and shinkage at higher temperatures were attributed to sintering of iron.

St. John et al[84,85] have carried out fundamental investigations on product morphologies for reduction of wustite in H_2/H_2O and CO/CO_2 gas mixtures. They identified three types of product morphology, viz. type A (porous iron), type B (porous wustite covered with dense iron), and type C (dense wustite

covered with dense iron). They have also proposed a model and attempted to explain the product morphologies in terms of the relative rates of the chemical reaction with the gas and the mass transfer processes both in and on the solid. Type C morphology has been predicted when chemical reaction rates are slower than mass transfer. The reverse is true for type B.

Dube et al[106] reduced magnetite superconcentrate compacts first to wustite by using excess iron and then to iron by reducing gas in the temperautre range 1173 to 1423 K and observed microstructures by SEM. During reduction of Fe_xO to Fe, nuclei of tetrahedral shape were observed. Formation of dense layers by sintering of nuclei took place at even relatively low temperature. Sinnuous porosity observed at higher temperatures were related to sustained growth of iron nuclei normal to surface. Whisker formation was noted.

Moujahid et al[89] reduced dense wustite in a wide range of temperature in various gas mixtures. Most of the experiments were carried out in hot stage microscope. In addition, optical microscope and SEM were also used. Two types of nuclei were identified :

(1) dense nuclei, ranging from regular whiskers to simple protrusions, around which flat bases developed to form a protective film, and

(2) porous nuclei with lenticular shapes, which remained level with the sample surface as they grew (both radially and into wustite) to form a porous layer.

Morphology maps have been proposed by Moujahid et al[89] based on their investigations.

The above brief scan of few papers reveal that development of product morphology is a complex process. There are features which are still not understood properly. However scientific explanations based on controlled laboratory investigations are emerging on relatively simpler situations.

Table 7.9 provides the expt.no. etc. of the iron ore-coal/char composite pellets which were subjected to observation by SEM (Jeol) after non-isothermal reduction. Both top surfaces as well as fracture surfaces of pellets were examined.

Table 7.9

Details of SEM Samples

Sl. no.	Expt. no.	Reductant code*	Degree of reduction (pct)	Vol.change upon red. (pct)	Photograph no.
1	FGM 2(LS)	HCL	46.5	12.9	1,2,3
2	FGM 7(HS)	BCCL	55.3	24.8	4
3	FGM 11(HS)	HCCH	85.0	97.3	5,6
4	FGM 15(LS)	BCH	80.9	- 0.9	7,8

* Table 7.3 provides meaning of code

Figure 7.13 presents 8 SEM photographs. It is to be kept in mind that the maximum temperature was the same for all experiments (1273 K). Differences amongst the samples were in

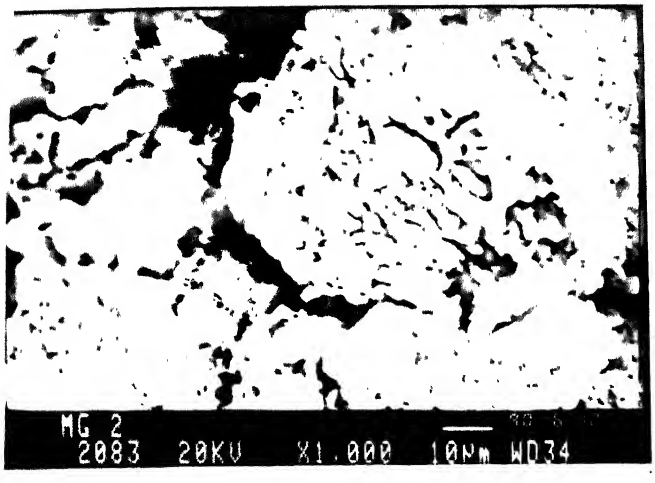

Photograph No. 1

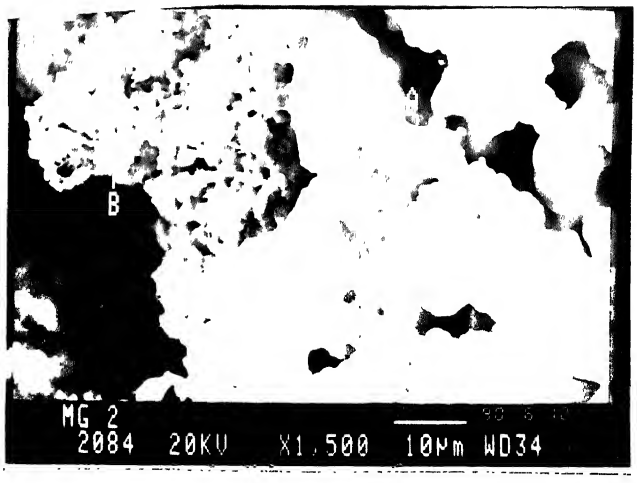

Photograph No. 2

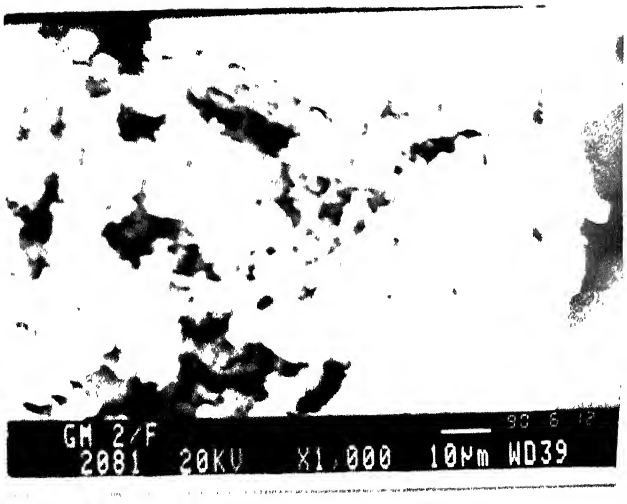

Photograph No. 3

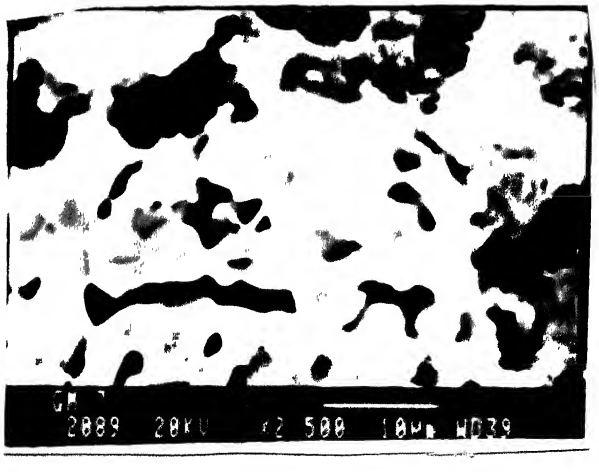

Photograph No. 4

Fig.7.13 Scanning electron micrographs for reduced composite pellets.

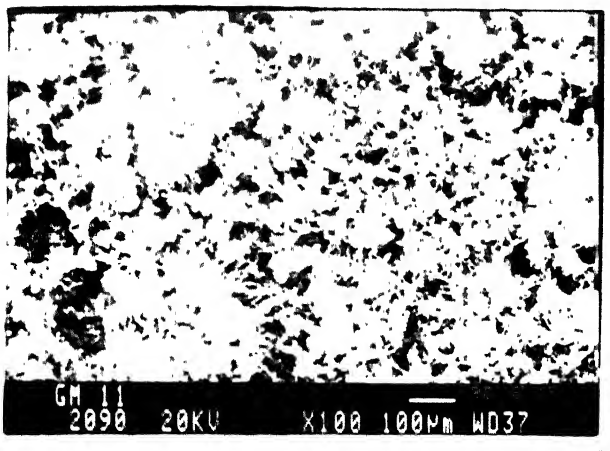

Photograph No. 5

Photograph No. 6

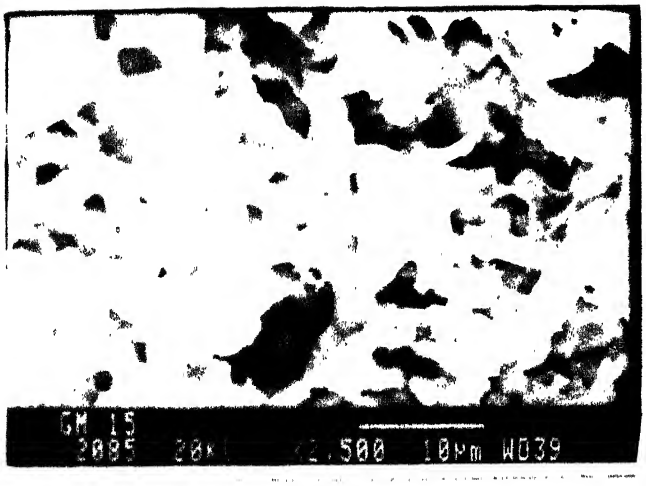

Photograph No. 7

Photograph No. 8

Fig.7.13 (Contd.)

type and fraction of reductant and rate of heating (governed by speed of travel of reaction chamber through the furnace. As Table 7.9 shows that there were considerable differences in degree of reduction and swelling/shrinkage amongst these 4 samples. This was intended to cover the range broadly.

The observations have been summarised in Table 7.10. Some literature references have been cited where investigators noted similar features.

Table 7.10

Summary of SEM Observations

Morphological features	Photograph no. in Fig.7.13	Literature ref. for similar observation	Remarks
Micro and macro-cracks	1,4	84,85,89,105,106	-
Nucleation of iron on wustite	2,4	85,89,106	nuclei: tetrahedral (large), as white tiny spots as well as ridge shaped
Whisker growth	4,6,7,8	84,85,89,105,106	dominant feature at high degrees of reduction (above 80pct)
Porous structure of pellet	5	85,89,105	attributed to large swelling (FGM 11)
Unreduced wustite	3	-	fractured surface
Joining of whiskers	6,7,8	105,106	feature observed at high degree of reduction (above 80pct)
Large scale sintering of iron forming dense cover on surface	2,4,8	84,106	observed at all degrees of reduction

CHAPTER 8

SUMMARY AND CONCLUSIONS

8.1 Summary of Studies

India has large reserves of blue dust (i.e. iron ore fines) as well as non-coking coal. If composite pellets made from blue dust and coal/char/coke fines are subjected to reduction or reduction-smelting in furnaces for extraction of iron values, they would offer several advantages. These pellets are to be cold-bonded to develop sufficient green strength.

The overall programme consisted of three parts :

(1) evaluation of performance of various binders

(2) fundamental studies on reduction of composite pellets

(3) kinetics of reduction of blue dust by H_2 and CO

Significant findings from literature were :

(1) there have been very few fundamental studies on reduction of composite pellets,

(2) most of the investigators employed char/coke breeze as reductant and not coal fines,

and (3) after introduction of composite pellet into a furnace, it takes 10 to 15 minutes to bring it to furnace temperature and by that time some reduction and other reactions occur.

Therefore, from a fundamental point of view, it was decided to carry out non-isothermal reduction studies at controlled heating rates, and some auxiliary experiments for better understanding of reduction behaviour of composite pellets.

Raw materials were :

(1) Blue dust : Bailadila mine, M.P.
(Dark gray colour, 95.4pct Fe_2O_3)

(2) Non-coking coal : a) Hutar mine, Bihar
(32.5pct fixed C, 32.5pct volatile matter)

b) Bachra mine, Bihar
(42.0pct fixed C, 24.0pct volatile matter)

(3) Size ranges : a) Blue dust -100 mesh

b) Coal -100 mesh

(4) Various binders : organic, inorganic and organic + inorganic.

Pellets were cylindrical in shape, 10 mm dia x 12 mm long. With inorganic binders, some green pellets were steam-cured in autoclave at pressure of 13 to 27 bar, temperature 460 to 500 K for 2.5 to 9.5 hours in efforts to develop additional dry compressive strength of pellets trhough hydrothermal reactions. Subsequently a standardized binder and pellet making procedure using autoclave route was adopted for fundamental studies.

The programme of evaluation of performance of various binders consisted of making composite pellets in various ways, measurement of their dry strength. After subjecting them to reduction in non-isothermal set-up, strength as well as volume change of pellets upon reduction and degree of reduction were measured.

In non-isothermal set-up the silica reaction chamber containing the pellet was introducted at uniform speed into the furnace by a stepper motor assembly. Maximum temperature attained by pellet was 1273 K. Average heating rates were 0.35 $K.s^{-1}$ and 0.175 $K.s^{-1}$. A slow flow of pure argon was maintained through reaction chamber. For fundamental studies on composite pellets, variation of not only temperature but also composition of exit gas were measured as function of time. A gas chromatograph was employed for this purpose. Using the above technique, devolatilization of coal samples was also investigated.

A major problem with study of ore-coal / char composite pellets is that the extent of the reduction can not be found out directly from the weight loss of the sample, since the latter is caused not only by loss of oxygen from ore but also loss of carbon, volatile matter etc. Review of literature revealed that there was no satisfactory method. Therefore, after considerations and trials a new procedure, consisting of subjecting the partially reduced pellet to flowing hydrogen at 1023 K for completing reduction and determination of degree of reduction from weight loss, was adopted. For this a thermogravimetry set-up with Cahn 1000 recording balance was employed.

Non-isothermal reduction of composite pellets were carried out for various combinations of ore-coal/char and at two heating rates. Duplicate sets of experiments demonstrated good reproducibility of results. Exit gas (after drying) in these as well as coal devolatilization studies consisted of CO, CO_2, H_2 along with minor quantity of CH_4. Volumetric rates of evolution of gases were calculated from gas composition and argon flow rate. This allowed calculation of oxygen loss associated with CO and CO_2 evolution as well as hydrogen liberated from the samples.

A major auxiliary programme of study was investigations on kinetics of reduction of blue dust by flowing H_2 and CO gas isothermally in the thermogravimetry set-up. Thin (0.4 to 1.5 mm) unconsolidated beds of blue dust particles constituted sample. Temperatures were 898 K to 1123 K for H_2 reduction, and 1073 K to 1373 K for CO reduction. Reduction by CO was carried out in stagewise fashion and only the last stage (Fe_xO —> Fe) was used for data processing. It was found that rates were not increasing with temperature monotonically but were exhibiting maxima/minima type behaviour as function of temperature. Such anomalies have been reported in literature for small particles and unconsolidated beds.

Data analysis for reduction by hydrogen or carbon monoxide required considerations and trials of various approaches and equations. Finally it was decided to take the least square fitted slopes of initial approximate straight line in fractional reduction (f) vs time (t) curves as measure of initial rate (k). Plotting of k as function of bed depth, and taking its value at

zero or close to zero bed depth eliminated mass transfer resistance in bed and allowed determination of chemical rate constant (k_c).

8.2 Salient Findings and Conclusions

8.2.1 Evaluation of binder and pellet making procedure

8.2.1.1 Dry compressive strength

(1) Maximum strength of pellets for organic binders was about 300 N per pellet with either 4pct TSR or 3pct TSR and 1pct dextrin.

(2) Maximum strength of pellets with inorganic binders (without autoclaving) was about 200 N per pellet with 8pct cement, 2pct lime, and 5 days of ageing.

(3) 4pct Mix.V ($CaO + SiO_2$) and 9pct Mix.VII ($Ca(OH)_2 + SiO_2$) combination, after autoclave treatment, gave dry strength of about 225 N per pellet in ore-coal composite. This was chosen for subsequent fundamental studies also.

(4) Finer sizes of ore and coal / char yielded much higher strength.

(5) Ore-char composites developed few times higher strength in comparison to ore-coal composite pellets.

(6) Composites with Bachra coal had more strength (about double) than those with Hutar coal.

8.2.1.2 **Reduction behaviour**

(1) Strength after reduction was maximum 95 N per pellet. It was correlated with volume change upon reduction; larger swelling meant less strength. There was no relationship with dry strength of unreduced pellet.

(2) Degree of reduction (α) could be satisfactorily measured by subsequent reduction of partially reduced composites by hydrogen in thermogravimetry set-up. α ranged from 33.5 to 86.0pct. The degree of reduction for ore-Hutar coal char pellets was higher as compared to ore-Hutar coal pellets.

8.2.2 **Fundamental studies of non-isothermal reduction and coal devolatilization**

(1) Total quantities of oxygen evolved as CO and CO_2 as well as hydrogen evolved from ore-coal / char pellets as well as in coal devolatilization experiments were significantly larger than what are expected from oxygen loss in ore and loss of volatile matter in coal. It was attributed to H_2O and CO_2, chemically combined as well as strongly adsorbed by binder and other materials during pellet making.

(2) The above finding is confirmed by data on weight loss of dry pellets upon reduction.

(3) Fractional reductions separately due to carbon (f_c) and hydrogen (f_{H_2}) were estimated from experimental data. Within scatter they reveal significant hydrogen reduction both for ore-coal and ore-char composites.

(4) Degrees of reduction were much larger for higher percentages of coal/char in comparison to lower percentages. α ranged from 46.0 to 99.7pct.

(5) Ore-coal and corresponding ore-char composites showed comparable degrees of reduction.

(6) Ore-coal composites had higher strength after reduction in comparison to corresonding ore-char composites.

(7) X-ray diffraction studies of partially reduced pellets showed that they consisted of wustite and metallic iron, thus confirming stagewise reduction.

(8) Quantitative calculations of rate of reduction of ore by CO at 1173 K in non-isothermal experiments agreed satisfactorily with those calculated from isothermal reduction studies of blue dust.

(9) Simultaneous temperature measurements at centre of pellet and 4 to 5 mm above the pellet showed a difference of 20 K and sometime upto 30 K. These also revealed peaks and troughs due to endothermic reactions etc.

(10) Scanning electron micrographs of partially reduced pellets revealed typical features such as growth

of whiskers, sintering of iron layer, ridges in wustites. Whiskers were dominant at α larger than 80pct.

8.2.3 Kinetics of reduction of blue dust by H_2 and CO

(1) Rates of reduction, expressed by df/dt at fixed values of f, exhibited maxima/minima type variation with temperature, where f is fractional reduction.

(2) Least square fitted slopes of initial straight lines in f vs t curves were found to provide the most satisfactory measure of rate constants (k).

(3) Chemical rate constant (k_c) at various temperatures were determined from variation of k with thickness of blue dust layer.

(4) k_c for hydrogen reduction was 5 to 10 times larger than k_c for reduction by CO at same temperature.

(5) ln k_c vs 1/T plots were not linear.

(6) The anomalous behaviour noted in points (1) and (5) above may be attributed to morphological changes of the bed during reduction, such as sintering and consequent densification.

8.3 Suggestions for Further Work

It is understood that commercial development of composite pellet technology would call for pellet making at larger scale, trials of the same in furnaces, performance and economic evaluation. Other specific suggestions having bearing with the present study are as follows.

(1) Ore-char pellets had better dry strength but lower strength after reduction as compared to ore-coal pellets. Hence, mixture of char and coal may be tried.

(2) Pellets may be made in bulk by disc pelletisers and properties evaluated. For this purpose few combinations in the present study which yielded high strengths may be tried.

(3) Specific investigations aimed at better understanding of the mechanism of reduction and gasification by chemically held H_2O and CO_2 by binders etc. would be very desirable for further scientific advancement in composite pellet technology.

(4) Economic evaluation of cost of cold bonding would help in selection of binder combinations and pellet making procedure from data of present study as well as future trials.

REFERENCES

1 K. Otsuka and D. Kunii: J. Chem. Eng. Japan, 1969, 2, p.46

2 P.C. Ghosh and S.N. Tiwari: J. Iron and Steel Inst., 1970, 208, p.255

3 Y.K. Rao: Metall.Trans., 1971, 2, p.1439

4 R.S. Ghosh, N.G. De, J. Singh and A. Lahiri: Iron and Steel Inter., 1975, p.459

5 D.A. Reeve, N.J. Ramey and J.H. Walsh: **Metal-Slag-Gas Reactions and Processes**, Eds. Z.A. Foroulis and W.W. Smeltzer, p.950, The electrochemical Soc., New Jersey, 1975

6 N.S. Srinivasan and A.K. Lahiri: Metall.Trans., 1977, 8B, p.175

7 R.J. Fruehan: ibid, 1977, 8B, p.279

8 M.C. Abraham and A. Ghosh: Ironmaking and Steelmaking, 1979, 6, p.14

9 A.K. Gokhale, A.K. Sengupta and A. Ghosh: Steel India, 1979, 2, p.36

10 C. Bryk and W.K. Lu: Ironmaking and Steelmaking, 1986, 13, p.70

11 S. Mookherjee, H.S. Ray and A. Mukherjee: ibid, 1986, 13, p.229

12 F. Ajersch: Can.Metall. Q., 1987, 26, p.137

13 G.C. Srivastava and T. Sharma: Proc.Sym. on **Kinetics of Metall.Processes**, p.31, Kharagpur, 1987

14 D. Bandyopadhyay: Ph.D.Thesis, Met.Eng.Deptt., IIT, Kanpur, 1989

15 S. Samarapungavan: Trans.Ind.Inst.Met., 1982, 35, p.vii

16 Editorial: Ind.Foun. J., 1989, **35** (9,10), p.7

17 Tool and Alloy Steel, 1990, **24**, p.220

18 S.K. Dutta and V.L. Gadgeel: ibid, 1988, **22**, p.347

19 S.K. Dutta and P.J. Roychowdhury: Inst.Eng. (Ind.) J-MM, 1986, **66**, p.91

20 P.R. Mehta, Essar Gujarat Ltd., Private Communication

21 K.K. Mehrotra, S. Ritwik and S.R. Basu: Proc.Sym. on **Direct Reduction Processes in Iron and Steelmaking**, p.107, Rourkela, 1982

22 S.K. Dutta, P.J. Roychowdhury and V.L. Gadgeel: Inst.Eng. (Ind.) J-MM (Spl.), 1988, **68**, p.52

23 Annual Report 1986-87, R&D Centre for Iron and Steel, SAIL, Ranchi

24 J.F. Gransden et al: Can.Min and Metall.Bull., 1978, **71**, p.153

25 F.T. Kaiser, L.L. French and H.G. Rachner: Giesserei, 1980, **67**, p.200

26 P.V. Duran et al: Proc.Conf. 38th Annual Congress ABM, Vol 1 p.203, Sao Paulo, Brezil, 1983 (in Portuguese) (Met.A: 8312 42-1587)

27 M.A. Goksel, T.A. Schott and F.T. Kaiser: Proc. 4th Int. Sym.on **Agglomeration**, p.401, Toronto, Canada, 1985

28 F.J. Weiss, M.A. Goksel and F.T. Kaiser: Iron and Steel Eng., 1986, **63**, p.34

29 H. Xi-Lun: Iron Steel (China), 1979, **14**, p.45 (Met.A: 8002 42-0157)

30 N. Shivaramakrishna et al: Trans. Ind. Inst. Met., 1990, **43**, p.95

31 D.K. Dutta et al: Proc.Int.Sym. on **Beneficiation and Agglomeration**, p.405, Bhubaneswar, 1986

32 N.K. Kakkar and A.K. Satsangi: ibid, p.118

33 V.E. Lotosh et al: Metallurg, 1987, **12**, p.8 (in Russian) (Met.A: 8804 42-0707)

34 M.A. Goksel: **Agglomeration 77**, Vol.2, Ed. K.V.S. Sartry, p.877, AIME, New York, 1977

35 H.D. George and E.B. Boardman: Iron and Steel Eng., 1973, **50**, p.60

36 V.A. Kiselev et al: Izv. Akad Nank SSSR, Met., 1982, 6, p.33 (in Russian) (Met.A: 8307 42-0866)

37 C.E. Seaton, J.S. Foster and J. Velaseo: Trans.Iron and Steel Inst. Jpn., 1983, **23**, p.490

38 G.C. Srivastava and T. Sharma: Trans.Ind.Inst.Met.,1988, **41**, p.567

39 C.E. Seaton et al: Proc.Conf. 48th Ironmaking, p.73, Chicago, USA, 1989, (Met.A: 9004 42-0330)

40 P. Basu, S.B. Sarkar and H.S. Ray: Trans.Ind.Inst.Met., 1989, **42**, p.165

41 R. Takahashi et al: Proc.of 6th Inter.Iron & Steel Congress, 1990, Nagoye, Vol.1, p.108

42 A. Ganguly and A.A. Patalah: Trans.Ind.Inst.Met., 1990, **43**, p.288

43 J. Srb and Z. Ruziekova: **Pelletization of Fines**, Elsevier Science Publishers, Amsterdam, 1988

44 K. Meyer: **Pelletizing of Iron Ores**, Springer-Verlag, Berlin, Heidelberg, 1980

45 Ov.Hatarasen and L. Dian: Metallurgia, 1973, **25**, p.7, (in Romanian) (Met.A: 7502 42-0077)

46 R. Takahashi et al: Miner.Dressing Metall., 1985, **41**, p.109, (in Japanese) (Met.A: 8609 42-1103)

47 A.A. Golubeva et al: **Iron Ore Processing and B.F. Ironmaking,** Eds. S.K. Gupta, V.I. Litvinenko and E.F. Vegmann, p.197, Oxford & IBH Publishing Co.Pvt. Ltd., New Delhi, 1990

48 A.V. Sidorskii et al: IZV. VUZ. Chernaya Metall., 1987, **9**, p.126, (in Russian) (Met.A: 8802 42-0326)

49 C.Y. Wen and S. Dutta: **Coal Conversion Technology,** Eds. C.Y. Wen and E. Stanley Lee, p.57, Addison-Wesley Publishing Co.,Inc., Massachusath, 1979

50 L.D. Smoot and P.J. Smith: **Coal Combustion and Gasification**, p.37, Planum Press, New York, 1985

51 S. Sarkar: **Frontiers in Applied Chemistry**, Ed. A.K. Biswas, p.119, Narosa Publishing House, New Delhi, 1989

52 R. Cypres and C. Soudan-Moinet: Fuel, 1980, **59**, p.48

53 J.L. Johnson: **Kinetics of coal Gasification**, p.19, John Wiley & Sons., New York, 1979

54 R. Cypres and C. Soudan-Moinet: Fuel, 1981, **60**, p.33

55 L.V. Bogdandy and H.J. Engell: **The Reduction of Iron Ores,** Springer-Verlag, Barlin, 1971

56 M.C. Abraham and A. Ghosh: Engi. World, 1973, p.19

57 A. Ghosh: Proc.Workshop on **Role of Reductants in Sponge Ironmaking**, p.25, Ranchi, 1983

58 A. Ghosh and S.K. Ajmani: Proc.Sym. on **Kinetics of Metallurgical Processes**, p.1, Kharagpur, 1987

59 H.S. Ray and P.A. Sewell: Proc.Int.Conf. on **Advances in Chemical Metallurgy,** Vol.II, p.43/I/1, Bombay, 1979

60 S. Mookherjee, H.S. Ray and A. Mukherjee: Thermochim. Acta, 1985, **95**, p.247

61 H.S. Ray: Proc.Int.Conf. on **Advances in Chemical Metallurgy**, Vol.II, p.43/II/1, Bombay, 1979

62 S. Prakash and H.S. Ray: Thermochim. Acta, 1987, **111**, p.143

63 A.I. Vogel: **A Text Book of Quantitative Inorganic Analysis Including Elementary Instrumental Analysis**, 3rd Ed.,Longman Group Ltd., London, 1973

64 **Encyclopedia of Chemical Technology**, 3rd Ed., Vol.5, p.163, 1979

65 **Handbook of Chemistry and Physies**, Eds. C.D. Hodgman, R.C. Weast and S.M. Selby, 43rd Ed., p.1706, The Chemical Rubber Publishing Co., USA, 1961

66 **Lange's Handbook of Chemistry**, Ed. J.A. Dean, 13nd Ed., p.10-4,10-5, McGraw-Hill Book Co., New York, 1987

67 O.G. Dam Gonzales and J.H.E. Jeffes: Ironmaking and Steelmaking, 1987, **14**, p.217

68 O. Kubaschewski and C.B. Alcock: **Metallurgical Thermochemistry,** 5th Ed., p.378, Pergamon Press, Oxford,1989

69 A.K. Biswas: **Principles of Blast Furnace Ironmaking**, p.233, SBA Publications, Calcutta, 1984

70 J.O. Edstrom: J. Iron Steel Inst., 1953, **175**, p.289

71 A. Ghosh: Proc.Int. Conf. on **Advances in Chemical Metallurgy**, Vol.I, p.21/1, Bombay, 1979

72 E.T. Turkdogan: **Physical Chemistry of High Temperature Technology**, p.303, Academic Press, New York, 1980

73 **Direct Reduced Iron (Tech. & Ecomomics of Production and Use)**, Ed. R.L. Stephenson, The Iron & Steel Society of AIME, 1980

74 P. Tiwari: Process Research Lab., IIT, Kanpur, private communication

75 R.N. Singh and A. Ghosh: Ind.J.Tech.,1968, 6, p.334

76 S.N. Basu and A. Ghosh: J.Iron Steel Inst., 1970, **208**, p.765

77 A. Ali, S.N. Basu and A. Ghosh: Trans. IIM, 1973, **26**, p.54

78 P.K. Strangway, H.O. Lien and H.U. Ross: Can. Metall. Q., 1969, **8**, p.235

79 P.K. Strangway and H.U. Ross: Trans. Metall. Soc. AIME, 1968, **242**, p.1981

80 E.T. Turkdogan and J.V. Vinters: Metall. Trans., 1971, 2, p.3175

81 A.A. El-Geassy and V. Rajakumar: Trans. ISIJ., 1985, **25**, p.1202

82 A.A. El-Geassy and M.I. Nasr: Trans. ISIJ., 1988, **28**, p.650

83 M.M. Al-Kahtany and Y.K. Rao: Ironmaking and Steelmaking, 1980, 7, p.49

84 D.H. St.John, S.P. Matthew and P.C. Hayes: Metall. Trans.B, 1984, **15B**, p.701

85 D.H. St.John et al, ibid, p.709

86 M. Et-Tabirou, B. Dupre and C. Gleitzer: Steel Research, 1986, **57**, p.306

87 C. Bodsworth and S.K. Taheri: Ironmaking and Steelmaking, 1987, **14**, p.278

88 M. Et-Tabirou, B. Dupre and C. Gleitzer: Metall. Trans.B, 1988, **19B**, p.311

89 S. El-Moujahid and A. Rist: Metall. Trans.B, 1988, **19B**, p.787

90 M. Moinpour and Y.K. Rao: Trans. ISIJ, 1988, **28**, p.714

91 S.P. Matthew and P.C. Hayes: Metall. Trans.B, 1990, **21B**, p.141

92 E.T. Turkdogan, R.G. Olsson and J.V. Vinters: Metall. Trans., 1971, **2**, p.3189

93 Y. Hara et al: Trans. ISIJ, 1972, **12**, p.223

94 E.T. Turkdogan and J.v. Vinters: Metall. Trans., 1972, **3**, p.1561

95 S.P. Trushenski et al: Metall. Trans., 1974, **5**, p.1149

96 N.B. Gray and J. Henderson: Trans. Metall. Soc. AIME, 1966, **236**, p.1213

97 Y. Hara: Trans. ISIJ, 1972, **12**, p.358

98 J. Szekely and J.W. Evans: **B.F. Tech. (Sc.& Practics)**, Ed. J. Szekely, p.35, Marcel`Dekker, Inc., New York, 1972

99 A.G. Guy: **Elements of Physical Metallurgy**, 2nd Ed., p.435, Oxford and IBM Publishing Co., Calcutta, 1967

100 N. Birks and G.H. Meier: **Introduction to High Temperature Oxidation of Metals**, p.41, Eeward Arnold, London, 1983

101 Q.A.K. Ansari and J.H. Bowen: Trans.Inst.Min.Metall. (Sec.C), 1985, **94**, p. C89

102 A. Ghosh and H.S. Ray: **Principles of Extractive Metallurgy**, ch.7, Ind.Inst.Met., Calcutta, 1984

103 R.N. Nigam: **Analytical Gas Chromatography**, p.45, Sarabhai M Chemicals, Baroda

104 M.K. Shingari: **Hand Book on Chromatography for Chemists and Engineers**, 1st Ed., p.16, Research and Development Centre, CIC, Baroda, 1988

105 C.E. Seaton, J.S. Foster and J. Velasco: Trans.Iron and Steel Inst.Japn., 1983, **23**, p.497

106 R.K. Dube and B. Deo: Steel Research, 1987, p.395

Appendix A

Data on Reduction of Blue Dust by Hydrogen

****

Exp No = H 1 Temp (K)=1123.0

Set No = 1 Sample Wt (mg)=100.90

Bed Depth (mm)= 0.43 Wt of Removable Oxygen (mg)= 29.04

A0=-0.3337E-01 A1=0.7455E-02 A2=-0.2050E-04 A3=0.1764E-07

Std Dev.=0.4725E-01

****

Time(s)	Wt Loss(mg)	Fr Redn.(f)	f(Best Fit)	df/dt(1/s)
36.00	4.704	0.161992	0.209290	0.6048E-02
60.00	10.160	0.349881	0.343984	0.5186E-02
96.00	16.992	0.585155	0.509065	0.4008E-02
132.00	18.848	0.649070	0.634183	0.2966E-02
180.00	20.640	0.710782	0.747377	0.1791E-02
300.00	22.912	0.789023	0.834737	-0.8088E-04
420.00	24.080	0.829245	0.788915	-0.4289E-03
600.00	25.056	0.862856	0.870452	0.1906E-02

f=0.30 t= 51.75 df/dt=0.5476E-02

f=0.50 t= 93.76 df/dt=0.4077E-02

f=0.70 t= 156.93 df/dt=0.2325E-02

****

Exp No = H 1 Temp (K)=1123.0

Set No = 2 Sample Wt (mg)=100.40

Bed Depth (mm)= 0.43 Wt of Removable Oxygen (mg)= 28.89

A0=-0.2478E-01 A1=0.7325E-02 A2=-0.2030E-04 A3=0.1751E-07

Std Dev.=0.4443E-01

****

Time(s)	Wt Loss(mg)	Fr Redn.(f)	f(Best Fit)	df/dt(1/s)
36.00	4.896	0.169444	0.213432	0.5932E-02
60.00	10.280	0.355776	0.345435	0.5079E-02
102.00	17.216	0.595821	0.529786	0.3731E-02
132.00	18.680	0.646488	0.628743	0.2882E-02
180.00	20.280	0.701862	0.738223	0.1720E-02
300.00	22.320	0.772464	0.818790	-0.1252E-03
420.00	23.368	0.808733	0.768711	-0.4573E-03
600.00	24.224	0.838358	0.845828	0.1882E-02

f=0.30 t= 51.31 df/dt=0.5380E-02

f=0.50 t= 94.26 df/dt=0.3965E-02

f=0.70 t= 160.30 df/dt=0.2168E-02

****

Exp No = H 2 Temp (K)=1123.0
Set No = 1 Sample Wt (mg)=193.00
Bed Depth (mm)= 1.02 Wt of Removable Oxygen (mg)= 55.54

A0=-0.1312E+00 A1=0.7980E-02 A2=-0.2065E-04 A3=0.1712E-07
Std Dev.=0.3728E-01

Time(s)	Wt Loss(mg)	Fr Redn.(f)	f(Best Fit)	df/dt(1/s)
36.00	7.104	0.127898	0.130156	0.6560E-02
60.00	13.624	0.245282	0.277010	0.5687E-02
120.00	34.584	0.622638	0.558722	0.3765E-02
180.00	41.240	0.742470	0.736147	0.2211E-02
240.00	44.328	0.798065	0.831466	0.1028E-02
306.00	46.520	0.837529	0.867957	0.1527E-03
420.00	48.888	0.880162	0.846597	-0.3050E-03
600.00	50.840	0.915305	0.921294	0.1689E-02

f=0.30 t= 64.09 df/dt=0.5545E-02

f=0.50 t= 105.25 df/dt=0.4203E-02

f=0.70 t= 164.86 df/dt=0.2568E-02

Exp No = H 2 Temp (K)=1123.0
Set No = 2 Sample Wt (mg)=198.70
Bed Depth (mm)= 1.05 Wt of Removable Oxygen (mg)= 57.18

A0=-0.1319E+00 A1=0.7590E-02 A2=-0.1927E-04 A3=0.1582E-07
Std Dev.=0.3230E-01

Time(s)	Wt Loss(mg)	Fr Redn.(f)	f(Best Fit)	df/dt(1/s)
36.00	6.800	0.118913	0.117154	0.6264E-02
60.00	12.920	0.225934	0.257593	0.5448E-02
120.00	33.240	0.581274	0.528778	0.3648E-02
180.00	40.750	0.712603	0.702210	0.2190E-02
240.00	44.040	0.770135	0.798395	0.1073E-02
300.00	46.320	0.810006	0.837843	0.2986E-03
420.00	48.990	0.856697	0.828554	-0.2255E-03
600.00	51.280	0.896742	0.901776	0.1552E-02

f=0.30 t= 67.97 df/dt=0.5189E-02

f=0.50 t= 112.33 df/dt=0.3859E-02

f=0.70 t= 179.00 df/dt=0.2211E-02

Exp No = H 3 Temp (K)=1123.0
Set No = 1 Sample Wt (mg)=298.00
Bed Depth (mm)= 1.50 Wt of Removable Oxygen (mg)= 85.76

A0=-0.1595E+00 A1=0.7323E-02 A2=-0.1661E-04 A3=0.1250E-07
Std Dev.=0.1983E-01

Time(s)	Wt Loss(mg)	Fr Redn.(f)	f(Best Fit)	df/dt(1/s)
36.00	8.780	0.102375	0.083143	0.6175E-02
60.00	17.400	0.202885	0.222736	0.5464E-02
120.00	41.200	0.480395	0.501600	0.3876E-02
180.00	61.970	0.722575	0.693260	0.2558E-02
240.00	70.280	0.819470	0.813917	0.1509E-02
300.00	74.100	0.864012	0.879774	0.7310E-03
420.00	78.430	0.914500	0.911898	-0.1554E-04
600.00	81.840	0.954261	0.954144	0.8900E-03

f=0.30 t= 74.70 df/dt=0.5050E-02

f=0.50 t= 119.59 df/dt=0.3886E-02

f=0.70 t= 182.66 df/dt=0.2505E-02

Exp No = H 3 Temp (K)=1123.0
Set No = 2 Sample Wt (mg)=297.00
Bed Depth (mm)= 1.49 Wt of Removable Oxygen (mg)= 85.47

A0=-0.1534E+00 A1=0.6742E-02 A2=-0.1527E-04 A3=0.1157E-07
Std Dev.=0.1956E-01

Time(s)	Wt Loss(mg)	Fr Redn.(f)	f(Best Fit)	df/dt(1/s)
36.00	7.600	0.088915	0.070079	0.5688E-02
60.00	15.144	0.177175	0.198675	0.5035E-02
120.00	37.600	0.439895	0.455810	0.3578E-02
186.00	57.888	0.677251	0.646902	0.2263E-02
240.00	63.776	0.746137	0.745243	0.1413E-02
300.00	67.584	0.790688	0.807524	0.7050E-03
420.00	72.360	0.846564	0.842173	0.3908E-04
600.00	76.416	0.894016	0.894234	0.9142E-03

f=0.30 t= 81.29 df/dt=0.4489E-02

f=0.50 t= 132.86 df/dt=0.3298E-02

f=0.70 t= 212.00 df/dt=0.1828E-02

Exp No = H 4
Set No = 1
Bed Depth (mm)= 0.43
Temp (K)=1048.0
Sample Wt (mg)= 99.80
Wt of Removable Oxygen (mg)= 28.72

A0= 0.1363E-01 A1=0.5063E-02 A2=-0.1276E-04 A3=0.1067E-07
Std Dev.=0.2882E-01

Time(s)	Wt Loss(mg)	Fr Redn.(f)	f(Best Fit)	df/dt(1/s)
36.00	4.240	0.147623	0.179860	0.4186E-02
60.00	8.424	0.293296	0.273784	0.3647E-02
120.00	14.320	0.498575	0.455908	0.2462E-02
180.00	16.296	0.567372	0.573828	0.1507E-02
240.00	17.720	0.616951	0.641375	0.7828E-03
300.00	18.736	0.652325	0.672375	0.2890E-03
420.00	20.280	0.706082	0.680056	-0.7303E-05
600.00	21.776	0.758168	0.763205	0.1277E-02

f=0.30 t= 67.35 df/dt=0.3490E-02

f=0.50 t= 139.22 df/dt=0.2131E-02

f=0.70 t= 526.60 df/dt=0.5028E-03

Exp No = H 4
Set No = 2
Bed Depth (mm)= 0.41
Temp (K)=1048.0
Sample Wt (mg)= 95.50
Wt of Removable Oxygen (mg)= 27.48

A0= 0.1635E-01 A1=0.4844E-02 A2=-0.1224E-04 A3=0.1027E-07
Std Dev.=0.2848E-01

Time(s)	Wt Loss(mg)	Fr Redn.(f)	f(Best Fit)	df/dt(1/s)
36.00	3.840	0.139716	0.175347	0.4003E-02
60.00	8.024	0.291948	0.265137	0.3486E-02
120.00	13.072	0.475616	0.439087	0.2349E-02
180.00	15.000	0.545765	0.551512	0.1435E-02
240.00	16.280	0.592337	0.615723	0.7423E-03
300.00	17.224	0.626683	0.645031	0.2716E-03
420.00	18.600	0.676748	0.652184	-0.4426E-05
600.00	20.040	0.729142	0.733933	0.1246E-02

f=0.30 t= 70.32 df/dt=0.3275E-02

f=0.50 t= 148.85 df/dt=0.1882E-02

f=0.70 t= 567.85 df/dt=0.8758E-03

****

Exp No = H 5 Temp (K)=1048.0

Set No = 1 Sample Wt (mg)=198.80

Bed Depth (mm)= 1.06 Wt of Removable Oxygen (mg)= 57.21

A0=-0.8872E-01 A1=0.6027E-02 A2=-0.1491E-04 A3=0.1223E-07

Std Dev.=0.2462E-01

****

Time(s)	Wt Loss(mg)	Fr Redn.(f)	f(Best Fit)	df/dt(1/s)
36.00	5.984	0.104591	0.109517	0.5002E-02
60.00	11.744	0.205266	0.221900	0.4371E-02
120.00	27.584	0.482124	0.441040	0.2978E-02
180.00	33.840	0.591468	0.584545	0.1849E-02
240.00	36.896	0.644882	0.668260	0.9850E-03
300.00	39.240	0.685852	0.708032	0.3847E-03
420.00	42.480	0.742482	0.719133	-0.2363E-04
600.00	45.664	0.798133	0.802371	0.1345E-02

f=0.30 t= 78.89 df/dt=0.3904E-02

f=0.50 t= 141.37 df/dt=0.2546E-02

f=0.70 t= 282.43 df/dt=0.5332E-03

****

Exp No = H 5 Temp (K)=1048.0

Set No = 2 Sample Wt (mg)=201.10

Bed Depth (mm)= 1.06 Wt of Removable Oxygen (mg)= 57.88

A0=-0.9928E-01 A1=0.6122E-02 A2=-0.1515E-04 A3=0.1242E-07

Std Dev.=0.2420E-01

****

Time(s)	Wt Loss(mg)	Fr Redn.(f)	f(Best Fit)	df/dt(1/s)
36.00	5.680	0.098142	0.102075	0.5080E-02
60.00	11.608	0.200569	0.216210	0.4439E-02
126.00	28.704	0.495961	0.456466	0.2896E-02
180.00	34.248	0.591753	0.584323	0.1876E-02
240.00	37.344	0.645248	0.669144	0.9965E-03
300.00	39.744	0.686716	0.709270	0.3857E-03
420.00	43.008	0.743113	0.719826	-0.3096E-04
600.00	46.224	0.798680	0.802869	0.1356E-02

f=0.30 t= 80.02 df/dt=0.3936E-02

f=0.50 t= 141.93 df/dt=0.2572E-02

f=0.70 t= 280.24 df/dt=0.5573E-03

****

****

Exp No = H 6 Temp (K)=1048.0

Set No = 1 Sample Wt (mg)=295.60

Bed Depth (mm)= 1.48 Wt of Removable Oxygen (mg)= 85.07

A0=-0.1158E+00 A1=0.5527E-02 A2=-0.1191E-04 A3=0.8861E-08

Std Dev.=0.1328E-01

****

Time(s)	Wt Loss(mg)	Fr Redn.(f)	f(Best Fit)	df/dt(1/s)
36.00	6.688	0.078616	0.068174	0.4704E-02
60.00	14.048	0.165131	0.174873	0.4193E-02
120.00	31.936	0.375400	0.391226	0.3051E-02
180.00	48.136	0.565826	0.544773	0.2100E-02
240.00	55.328	0.650366	0.647000	0.1340E-02
300.00	59.336	0.697479	0.709390	0.7717E-03
420.00	64.936	0.763306	0.760598	0.2094E-03
600.00	70.240	0.825653	0.825743	0.8015E-03

f=0.30 t= 92.34 df/dt=0.3553E-02

f=0.50 t= 160.06 df/dt=0.2394E-02

f=0.70 t= 288.52 df/dt=0.8656E-03

****

Exp No = H 6 Temp (K)=1048.0

Set No = 2 Sample Wt (mg)=300.30

Bed Depth (mm)= 1.50 Wt of Removable Oxygen (mg)= 86.42

A0=-0.1098E+00 A1=0.5635E-02 A2=-0.1249E-04 A3=0.9494E-08

Std Dev.=0.1412E-01

****

Time(s)	Wt Loss(mg)	Fr Redn.(f)	f(Best Fit)	df/dt(1/s)
36.00	7.512	0.086920	0.077354	0.4773E-02
60.00	14.984	0.173376	0.185435	0.4239E-02
120.00	33.936	0.392666	0.403022	0.3048E-02
180.00	50.080	0.579464	0.555289	0.2062E-02
240.00	56.384	0.652406	0.654540	0.1281E-02
300.00	60.344	0.698227	0.713079	0.7047E-03
420.00	66.000	0.763671	0.757235	0.1679E-03
600.00	71.296	0.824950	0.825724	0.9007E-03

f=0.30 t= 89.13 df/dt=0.3635E-02

f=0.50 t= 155.41 df/dt=0.2441E-02

f=0.70 t= 283.10 df/dt=0.8462E-03

****

Exp No = H 7 Temp (K)= 973.0
Set No = 1 Sample Wt (mg)= 99.30
Bed Depth (mm)= 0.43 Wt of Removable Oxygen (mg)= 28.58

A0= 0.9335E-01 A1=0.2480E-02 A2=-0.3446E-05 A3=0.1517E-08
Std Dev.=0.5333E-01

Time(s)	Wt Loss(mg)	Fr Redn.(f)	f(Best Fit)	df/dt(1/s)
36.00	3.030	0.106026	0.178240	0.2238E-02
60.00	6.860	0.240045	0.230081	0.2083E-02
120.00	12.000	0.419904	0.343969	0.1719E-02
180.00	13.470	0.471342	0.436981	0.1387E-02
300.00	15.270	0.534327	0.568239	0.8223E-03
600.00	17.870	0.625306	0.668662	-0.1633E-04
900.00	19.460	0.680944	0.640354	-0.3587E-04
1200.00	20.510	0.717685	0.729051	0.7637E-03

f=0.30 t= 95.45 df/dt=0.1864E-02

f=0.50 t= 230.03 df/dt=0.1136E-02

f=0.70 t=1157.31 df/dt=0.5999E-03

Exp No = H 7 Temp (K)= 973.0
Set No = 2 Sample Wt (mg)=102.00
Bed Depth (mm)= 0.44 Wt of Removable Oxygen (mg)= 29.36

A0= 0.7324E-01 A1=0.2759E-02 A2=-0.3913E-05 A3=0.1736E-08
Std Dev.=0.6018E-01

Time(s)	Wt Loss(mg)	Fr Redn.(f)	f(Best Fit)	df/dt(1/s)
36.00	2.770	0.094362	0.167564	0.2484E-02
60.00	6.520	0.222108	0.225053	0.2308E-02
120.00	12.980	0.442173	0.350947	0.1895E-02
180.00	14.500	0.493953	0.453169	0.1519E-02
300.00	16.320	0.555952	0.595600	0.8799E-03
600.00	18.940	0.645205	0.694933	-0.6143E-04
900.00	20.520	0.699028	0.652490	-0.6527E-04
1200.00	21.620	0.736501	0.749525	0.8684E-03

f=0.30 t= 94.27 df/dt=0.2067E-02

f=0.50 t= 212.91 df/dt=0.1329E-02

f=0.70 t=1130.72 df/dt=0.5695E-03

Exp No = H 8 Temp (K)= 973.0
Set No = 1 Sample Wt (mg)=195.20
Bed Depth (mm)= 1.03 Wt of Removable Oxygen (mg)= 56.18

A0=-0.1154E+00 A1=0.6082E-02 A2=-0.1531E-04 A3=0.1258E-07
Std Dev.=0.2026E-01

Time(s)	Wt Loss(mg)	Fr Redn.(f)	f(Best Fit)	df/dt(1/s)
36.00	4.860	0.086512	0.084306	0.5028E-02
60.00	10.060	0.179075	0.197117	0.4380E-02
120.00	24.520	0.436474	0.415659	0.2950E-02
180.00	32.400	0.576744	0.556551	0.1792E-02
240.00	34.750	0.618575	0.636102	0.9053E-03
300.00	36.320	0.646522	0.670620	0.2906E-03
420.00	38.740	0.689600	0.669795	-0.1232E-03
600.00	41.300	0.735170	0.738524	0.1295E-02

f=0.30 t= 85.36 df/dt=0.3742E-02

f=0.50 t= 152.25 df/dt=0.2294E-02

f=0.70 t= 562.96 df/dt=0.8030E-03

Exp No = H 8 Temp (K)= 973.0
Set No = 2 Sample Wt (mg)=198.20
Bed Depth (mm)= 1.04 Wt of Removable Oxygen (mg)= 57.04

A0=-0.1216E+00 A1=0.6142E-02 A2=-0.1549E-04 A3=0.1274E-07
Std Dev.=0.2054E-01

Time(s)	Wt Loss(mg)	Fr Redn.(f)	f(Best Fit)	df/dt(1/s)
36.00	4.670	0.081871	0.080085	0.5076E-02
60.00	10.010	0.175488	0.193963	0.4421E-02
120.00	24.980	0.437932	0.414451	0.2975E-02
180.00	32.780	0.574676	0.556425	0.1804E-02
240.00	35.280	0.618504	0.636398	0.9079E-03
300.00	36.910	0.647080	0.670881	0.2874E-03
420.00	39.330	0.689506	0.669425	-0.1282E-03
600.00	41.950	0.735438	0.738868	0.1313E-02

f=0.30 t= 85.95 df/dt=0.3762E-02

f=0.50 t= 152.48 df/dt=0.2307E-02

f=0.70 t= 563.19 df/dt=0.8164E-03

Exp No = H10 Temp (K)= 898.0
Set No = 1 Sample Wt (mg)=102.30
Bed Depth (mm)= 0.44 Wt of Removable Oxygen (mg)= 29.44

A0=-0.4145E-01 A1=0.4306E-02 A2=-0.8064E-05 A3=0.4702E-08
Std Dev.=0.5429E-01

Time(s)	Wt Loss(mg)	Fr Redn.(f)	f(Best Fit)	df/dt(1/s)
36.00	2.080	0.070649	0.103324	0.3744E-02
60.00	4.680	0.158960	0.188881	0.3389E-02
120.00	13.820	0.469407	0.367250	0.2574E-02
180.00	15.500	0.526470	0.499745	0.1860E-02
240.00	16.630	0.564851	0.592459	0.1248E-02
300.00	17.500	0.594402	0.651487	0.7369E-03
600.00	19.950	0.677618	0.654578	-0.2932E-03
900.00	21.340	0.724830	0.729464	0.1216E-02

f=0.30 t= 95.40 df/dt=0.2896E-02

f=0.50 t= 180.14 df/dt=0.1858E-02

f=0.70 t= 873.07 df/dt=0.9764E-03

Exp No = H10 Temp (K)= 898.0
Set No = 2 Sample Wt (mg)=100.00
Bed Depth (mm)= 0.43 Wt of Removable Oxygen (mg)= 28.78

A0=-0.2951E-01 A1=0.4413E-02 A2=-0.8332E-05 A3=0.4870E-08
Std Dev.=0.5623E-01

Time(s)	Wt Loss(mg)	Fr Redn.(f)	f(Best Fit)	df/dt(1/s)
36.00	2.300	0.079918	0.118785	0.3832E-02
60.00	5.230	0.181727	0.206326	0.3466E-02
120.00	14.200	0.493408	0.388485	0.2624E-02
180.00	15.870	0.551435	0.523277	0.1887E-02
240.00	16.920	0.587920	0.617011	0.1255E-02
300.00	17.730	0.616065	0.675999	0.7287E-03
600.00	20.000	0.694940	0.670635	-0.3261E-03
900.00	21.250	0.738374	0.743268	0.1249E-02

f=0.30 t= 88.78 df/dt=0.3049E-02

f=0.50 t= 168.10 df/dt=0.2025E-02

f=0.70 t= 342.01 df/dt=0.4226E-03

Exp No = H11 Temp (K)= 898.0
Set No = 1 Sample Wt (mg)=199.10
Bed Depth (mm)= 1.06 Wt of Removable Oxygen (mg)= 57.30

A0=-0.1352E+00 A1=0.5999E-02 A2=-0.1373E-04 A3=0.1038E-07
Std Dev.=0.2027E-01

Time(s)	Wt Loss(mg)	Fr Redn.(f)	f(Best Fit)	df/dt(1/s)
36.00	4.800	0.083770	0.063453	0.5051E-02
60.00	9.200	0.160559	0.177553	0.4464E-02
120.00	21.600	0.376964	0.404923	0.3153E-02
180.00	33.550	0.585516	0.560372	0.2066E-02
240.00	38.430	0.670682	0.657360	0.1204E-02
300.00	39.900	0.696337	0.709343	0.5661E-03
420.00	41.850	0.730368	0.732126	-0.3686E-04
600.00	43.900	0.766145	0.765211	0.7409E-03

f=0.30 t= 89.72 df/dt=0.3786E-02

f=0.50 t= 153.61 df/dt=0.2517E-02

f=0.70 t= 285.24 df/dt=0.7022E-03

Exp No = H11 Temp (K)= 898.0
Set No = 2 Sample Wt (mg)=196.90
Bed Depth (mm)= 1.04 Wt of Removable Oxygen (mg)= 56.67

A0=-0.1362E+00 A1=0.6014E-02 A2=-0.1411E-04 A3=0.1092E-07
Std Dev.=0.2027E-01

Time(s)	Wt Loss(mg)	Fr Redn.(f)	f(Best Fit)	df/dt(1/s)
36.00	4.620	0.081529	0.062556	0.5040E-02
60.00	8.900	0.157059	0.176220	0.4438E-02
120.00	21.460	0.378705	0.401132	0.3098E-02
180.00	33.050	0.583235	0.552722	0.1994E-02
240.00	36.870	0.650646	0.645142	0.1126E-02
300.00	38.320	0.676235	0.692542	0.4935E-03
420.00	40.330	0.711705	0.708891	-0.6375E-04
600.00	42.480	0.749646	0.749555	0.8693E-03

f=0.30 t= 90.34 df/dt=0.3731E-02

f=0.50 t= 156.01 df/dt=0.2407E-02

f=0.70 t= 317.72 df/dt=0.3518E-03

Exp No = H12 Temp (K)= 898.0
Set No = 1 Sample Wt (mg)=305.70
Bed Depth (mm)= 1.53 Wt of Removable Oxygen (mg)= 87.98

A0=-0.8573E-01 A1=0.3742E-02 A2=-0.4582E-05 A3=0.1254E-08
Std Dev.=0.1928E-01

Time(s)	Wt Loss(mg)	Fr Redn.(f)	f(Best Fit)	df/dt(1/s)
36.00	5.000	0.056832	0.043114	0.3417E-02
60.00	10.500	0.119347	0.122589	0.3206E-02
120.00	24.500	0.278476	0.299549	0.2697E-02
180.00	38.300	0.435332	0.446770	0.2215E-02
240.00	50.950	0.579117	0.565878	0.1760E-02
300.00	60.350	0.685961	0.658496	0.1332E-02
420.00	65.820	0.748135	0.770764	0.5573E-03
600.00	69.070	0.785076	0.781117	-0.4016E-03

f=0.30 t= 120.17 df/dt=0.2696E-02

f=0.50 t= 205.14 df/dt=0.2021E-02

f=0.70 t= 334.15 df/dt=0.1100E-02

Exp No = H12 Temp (K)= 898.0
Set No = 2 Sample Wt (mg)=295.00
Bed Depth (mm)= 1.48 Wt of Removable Oxygen (mg)= 84.90

A0=-0.6680E-01 A1=0.3286E-02 A2=-0.2793E-05 A3=-.3651E-09
Std Dev.=0.1431E-01

Time(s)	Wt Loss(mg)	Fr Redn.(f)	f(Best Fit)	df/dt(1/s)
36.00	4.780	0.056302	0.047869	0.3084E-02
60.00	10.180	0.119907	0.120247	0.2947E-02
120.00	23.100	0.272087	0.286719	0.2600E-02
180.00	35.900	0.422854	0.432138	0.2246E-02
240.00	47.800	0.563020	0.556030	0.1883E-02
300.00	57.800	0.680806	0.657923	0.1512E-02
420.00	65.980	0.777155	0.793817	0.7474E-03
612.00	69.400	0.817438	0.814825	-0.5420E-03

f=0.30 t= 125.14 df/dt=0.2570E-02

f=0.50 t= 211.55 df/dt=0.2056E-02

f=0.70 t= 329.64 df/dt=0.1326E-02

Appendix B

Data on Reduction of Blue Dust by Carbon Monoxide

Exp No = CO 1 — Temp (K)=1273.0
Set No = 1 — Sample Wt (mg)= 93.43
Bed Depth (mm)= 0.40 — Wt of Removable Oxygen (mg)= 26.89
Wt of Oxygen Consume During Stage I (mg)= 4.42
A0=-0.6831E-01 A1= 0.1427E-02 A2=-0.9513E-06 A3= 0.2549E-09
Std.Dev.=0.7080E-02

Time(s)	Wt Loss(mg)	Fr Redn (f)	f(Best Fit)	df/dt(1/s)
120.00	2.192	0.097541	0.089726	0.1210E-02
240.00	4.800	0.213593	0.223012	0.1015E-02
360.00	7.344	0.326797	0.334187	0.8417E-03
480.00	9.664	0.430034	0.425894	0.6904E-03
600.00	11.384	0.506572	0.500775	0.5612E-03
840.00	13.784	0.613368	0.610630	0.3689E-03
1200.00	15.944	0.709485	0.715286	0.2456E-03
1500.00	17.864	0.794922	0.792803	0.2942E-03

f=0.30 t= 320.64 df/dt=0.8961E-03

f=0.50 t= 598.62 df/dt=0.5626E-03

f=0.70 t= 1138.51 df/dt=0.2526E-03

Exp No = CO 1 — Temp (K)=1273.0
Set No = 2 — Sample Wt (mg)= 96.48
Bed Depth (mm)= 0.41 — Wt of Removable Oxygen (mg)= 27.77
Wt of Oxygen Consume During Stage I (mg)= 4.96
A0=-0.4212E-01 A1= 0.1219E-02 A2=-0.6630E-06 A3= 0.1338E-09
Std.Dev.=0.5830E-02

Time(s)	Wt Loss(mg)	Fr Redn (f)	f(Best Fit)	df/dt(1/s)
120.00	2.296	0.100673	0.094789	0.1065E-02
240.00	4.744	0.208012	0.213986	0.9234E-03
360.00	7.056	0.309387	0.316863	0.7932E-03
480.00	9.280	0.406903	0.404806	0.6745E-03
600.00	11.088	0.486179	0.479204	0.5674E-03
840.00	13.552	0.594219	0.592914	0.3879E-03
1200.00	15.784	0.692086	0.696575	0.2053E-03
1500.00	17.040	0.747158	0.745480	0.1327E-03

f=0.30 t= 339.03 df/dt=0.8151E-03

f=0.50 t= 637.70 df/dt=0.5361E-03

f=0.70 t= 1216.93 df/dt=0.1993E-03

****

Exp No = CO 2 Temp (K)=1273.0

Set No = 1 Sample Wt (mg)=194.78

Bed Depth (mm)= 1.03 Wt of Removable Oxygen (mg)= 56.06

Wt of Oxygen Consume During Stage I (mg)= 10.58

A0=-0.2421E-01 A1= 0.1060E-02 A2=-0.2791E-06 A3=-0.1926E-10

Std.Dev.=0.2946E-02

****

Time(s)	Wt Loss(mg)	Fr Redn (f)	f(Best Fit)	df/dt(1/s)
120.00	4.616	0.101512	0.098924	0.9920E-03
240.00	9.616	0.211468	0.213817	0.9226E-03
360.00	14.456	0.317906	0.320272	0.8514E-03
480.00	18.976	0.417306	0.418090	0.7786E-03
600.00	23.136	0.508790	0.507070	0.7041E-03
840.00	30.080	0.661497	0.657721	0.5502E-03
1200.00	36.768	0.808575	0.812425	0.3068E-03
1500.00	39.736	0.873845	0.872580	0.9251E-04

f=0.30 t= 336.39 df/dt=0.8655E-03

f=0.50 t= 590.00 df/dt=0.7104E-03

f=0.70 t= 920.75 df/dt=0.4969E-03

****

Exp No = CO 2 Temp (K)=1273.0

Set No = 2 Sample Wt (mg)=195.67

Bed Depth (mm)= 1.04 Wt of Removable Oxygen (mg)= 56.31

Wt of Oxygen Consume During Stage I (mg)= 10.36

A0=-0.1453E-01 A1= 0.9696E-03 A2=-0.2950E-06 A3= 0.1569E-10

Std.Dev.=0.2528E-02

****

Time(s)	Wt Loss(mg)	Fr Redn (f)	f(Best Fit)	df/dt(1/s)
120.00	4.400	0.095751	0.097596	0.8994E-03
240.00	9.440	0.205428	0.201388	0.8307E-03
360.00	13.624	0.296479	0.297008	0.7632E-03
480.00	17.600	0.383002	0.384620	0.6972E-03
600.00	21.240	0.462214	0.464385	0.6325E-03
840.00	27.760	0.604099	0.601026	0.5071E-03
1200.00	34.464	0.749988	0.751205	0.3292E-03
1500.00	38.104	0.829200	0.828933	0.1903E-03

f=0.30 t= 363.93 df/dt=0.7611E-03

f=0.50 t= 657.71 df/dt=0.6018E-03

f=0.70 t= 1059.01 df/dt=0.3975E-03

****

****

Exp No = CO 3 Temp (K)=1273.0

Set No = 1 Sample Wt (mg)=294.33

Bed Depth (mm)= 1.47 Wt of Removable Oxygen (mg)= 84.71

Wt of Oxygen Consume During Stage I (mg)= 13.00

A0=-0.2751E-02 A1= 0.6042E-03 A2=-0.3893E-08 A3=-0.3671E-10

Std.Dev.=0.1495E-02

****

Time(s)	Wt Loss(mg)	Fr Redn (f)	f(Best Fit)	df/dt(1/s)
120.00	4.904	0.068390	0.069629	0.6016E-03
240.00	10.224	0.142581	0.141517	0.5960E-03
360.00	15.384	0.214541	0.212531	0.5871E-03
480.00	20.144	0.280923	0.282291	0.5751E-03
600.00	25.112	0.350205	0.350417	0.5598E-03
900.00	36.560	0.509856	0.511082	0.5079E-03
1260.00	48.800	0.680552	0.678881	0.4195E-03
1500.00	55.224	0.770139	0.770838	0.3447E-03

f=0.30 t= 510.89 df/dt=0.5714E-03

f=0.50 t= 878.28 df/dt=0.5124E-03

f=0.70 t= 1311.25 df/dt=0.4046E-03

****

Exp No = CO 3 Temp (K)=1273.0

Set No = 2 Sample Wt (mg)=299.60

Bed Depth (mm)= 1.50 Wt of Removable Oxygen (mg)= 86.22

Wt of Oxygen Consume During Stage I (mg)= 11.04

A0=-0.1103E-01 A1= 0.6054E-03 A2= 0.2598E-07 A3=-0.6442E-10

Std.Dev.=0.1470E-02

****

Time(s)	Wt Loss(mg)	Fr Redn (f)	f(Best Fit)	df/dt(1/s)
120.00	4.680	0.062248	0.061885	0.6089E-03
300.00	12.880	0.171315	0.171195	0.6036E-03
480.00	20.760	0.276125	0.278431	0.5858E-03
600.00	26.240	0.349014	0.347656	0.5670E-03
900.00	38.304	0.509475	0.507920	0.4956E-03
1140.00	46.360	0.616627	0.617456	0.4135E-03
1380.00	52.880	0.703348	0.704602	0.3090E-03
1500.00	55.568	0.739101	0.738110	0.2485E-03

f=0.30 t= 516.98 df/dt=0.5806E-03

f=0.50 t= 884.09 df/dt=0.5003E-03

f=0.70 t= 1365.28 df/dt=0.3161E-03

****

****

Exp No = CO 4 Temp (K)=1173.0

Set No = 1 Sample Wt (mg)=102.63

Bed Depth (mm)= 0.44 Wt of Removable Oxygen (mg)= 29.54

Wt of Oxygen Consume During Stage I (mg)= 5.08

A0=-0.4565E-01 A1= 0.9490E-03 A2=-0.4673E-06 A3= 0.9964E-10

Std.Dev.=0.2507E-02

****

Time(s)	Wt Loss(mg)	Fr Redn (f)	f(Best Fit)	df/dt(1/s)
240.00	3.880	0.158650	0.156567	0.7419E-03
360.00	5.760	0.235522	0.240072	0.6513E-03
480.00	7.680	0.314029	0.313218	0.5693E-03
600.00	9.280	0.379452	0.377041	0.4959E-03
840.00	11.760	0.480857	0.480844	0.3749E-03
1200.00	14.440	0.590440	0.592442	0.2580E-03
1440.00	15.920	0.650956	0.649489	0.2231E-03
1800.00	17.840	0.729463	0.729695	0.2354E-03

f=0.30 t= 457.08 df/dt=0.5843E-03

f=0.50 t= 892.66 df/dt=0.3530E-03

f=0.70 t= 1669.67 df/dt=0.2220E-03

****

Exp No = CO 4 Temp (K)=1173.0

Set No = 2 Sample Wt (mg)= 93.86

Bed Depth (mm)= 0.40 Wt of Removable Oxygen (mg)= 27.01

Wt of Oxygen Consume During Stage I (mg)= 4.03

A0=-0.7763E-01 A1= 0.1171E-02 A2=-0.6830E-06 A3= 0.1562E-09

Std.Dev.=0.7734E-02

****

Time(s)	Wt Loss(mg)	Fr Redn (f)	f(Best Fit)	df/dt(1/s)
240.00	3.800	0.165358	0.166330	0.8706E-03
300.00	4.800	0.208874	0.216543	0.8038E-03
420.00	7.304	0.317836	0.305456	0.6803E-03
600.00	9.560	0.416007	0.413078	0.5205E-03
840.00	11.680	0.508260	0.517012	0.3546E-03
1200.00	14.056	0.611652	0.614458	0.2070E-03
1440.00	15.312	0.666307	0.659346	0.1761E-03
1800.00	16.704	0.726881	0.728952	0.2309E-03

f=0.30 t= 412.03 df/dt=0.6881E-03

f=0.50 t= 793.81 df/dt=0.3823E-03

f=0.70 t= 1663.35 df/dt=0.1958E-03

****

****

Exp No = CO 5 Temp (K)=1173.0

Set No = 1 Sample Wt (mg)=196.98

Bed Depth (mm)= 1.05 Wt of Removable Oxygen (mg)= 56.69

Wt of Oxygen Consume During Stage I (mg)= 10.84

A0=-0.5223E-01 A1= 0.9500E-03 A2=-0.4844E-06 A3= 0.1059E-09

Std.Dev.=0.1446E-02

****

Time(s)	Wt Loss(mg)	Fr Redn (f)	f(Best Fit)	df/dt(1/s)
240.00	6.880	0.150055	0.149325	0.7357E-03
360.00	10.560	0.230318	0.231920	0.6424E-03
480.00	13.912	0.303426	0.303858	0.5581E-03
600.00	16.880	0.368159	0.366238	0.4831E-03
840.00	21.400	0.466742	0.466713	0.3603E-03
1200.00	26.200	0.571432	0.573183	0.2449E-03
1500.00	29.424	0.641748	0.640225	0.2116E-03
1800.00	32.344	0.705435	0.705852	0.2355E-03

f=0.30 t= 473.12 df/dt=0.5627E-03

f=0.50 t= 937.89 df/dt=0.3208E-03

f=0.70 t= 1774.92 df/dt=0.2313E-03

****

Exp No = CO 5 Temp (K)=1173.0

Set No = 2 Sample Wt (mg)=196.48

Bed Depth (mm)= 1.05 Wt of Removable Oxygen (mg)= 56.55

Wt of Oxygen Consume During Stage I (mg)= 11.22

A0=-0.5389E-01 A1= 0.9777E-03 A2=-0.4920E-06 A3= 0.1033E-09

Std.Dev.=0.1950E-02

****

Time(s)	Wt Loss(mg)	Fr Redn (f)	f(Best Fit)	df/dt(1/s)
240.00	7.056	0.155659	0.153837	0.7594E-03
360.00	10.728	0.236665	0.239127	0.6636E-03
480.00	14.152	0.312200	0.313460	0.5768E-03
600.00	17.176	0.378911	0.377907	0.4988E-03
840.00	21.928	0.483743	0.481430	0.3698E-03
1200.00	26.616	0.587163	0.589349	0.2431E-03
1500.00	29.696	0.655109	0.654269	0.1990E-03
1800.00	32.376	0.714231	0.714303	0.2106E-03

f=0.30 t= 456.98 df/dt=0.5927E-03

f=0.50 t= 891.86 df/dt=0.3466E-03

f=0.70 t= 1730.74 df/dt=0.2029E-03

****

Exp No = CO 6 Temp (K)=1173.0
Set No = 1 Sample Wt (mg)=294.98
Bed Depth (mm)= 1.48 Wt of Removable Oxygen (mg)= 84.89
Wt of Oxygen Consume During Stage I (mg)= 14.78
A0=-0.1856E-01 A1= 0.4651E-03 A2= 0.5622E-07 A3=-0.5226E-10
Std.Dev.=0.1100E-01

Time(s)	Wt Loss(mg)	Fr Redn (f)	f(Best Fit)	df/dt(1/s)
240.00	7.272	0.103723	0.095592	0.4831E-03
480.00	14.096	0.201057	0.211885	0.4830E-03
660.00	20.192	0.288006	0.297902	0.4711E-03
900.00	29.040	0.414209	0.407512	0.4393E-03
1140.00	36.552	0.521355	0.507344	0.3896E-03
1500.00	44.000	0.627589	0.629276	0.2811E-03
1800.00	47.912	0.683387	0.696075	0.1596E-03
2100.00	51.072	0.728459	0.722198	0.9875E-05

f=0.30 t= 664.46 df/dt=0.4706E-03

f=0.50 t= 1121.26 df/dt=0.3941E-03

f=0.70 t= 1825.52 df/dt=0.1479E-03

Exp No = CO 6 Temp (K)=1173.0
Set No = 2 Sample Wt (mg)=278.30
Bed Depth (mm)= 1.40 Wt of Removable Oxygen (mg)= 80.09
Wt of Oxygen Consume During Stage I (mg)= 14.56
A0=-0.3922E-02 A1= 0.4627E-03 A2= 0.1201E-06 A3=-0.7714E-10
Std.Dev.=0.1349E-01

Time(s)	Wt Loss(mg)	Fr Redn (f)	f(Best Fit)	df/dt(1/s)
240.00	8.040	0.122686	0.112969	0.5070E-03
480.00	14.720	0.224619	0.237292	0.5246E-03
600.00	18.920	0.288709	0.300241	0.5234E-03
720.00	23.680	0.361344	0.362649	0.5156E-03
900.00	30.600	0.466939	0.453497	0.4913E-03
1140.00	38.080	0.581080	0.565269	0.4357E-03
1500.00	44.800	0.683623	0.699875	0.3022E-03
2100.00	51.480	0.785556	0.782762	-0.5364E-04

f=0.30 t= 599.54 df/dt=0.5235E-03

f=0.50 t= 996.46 df/dt=0.4722E-03

f=0.70 t= 1500.41 df/dt=0.3020E-03

Exp No = CO 7 Temp (K)=1073.0
Set No = 1 Sample Wt (mg)= 96.95
Bed Depth (mm)= 0.42 Wt of Removable Oxygen (mg)= 27.90
Wt of Oxygen Consume During Stage I (mg)= 4.99
A0=-0.3190E-01 A1= 0.6341E-03 A2=-0.2719E-07 A3=-0.6040E-10
Std.Dev.=0.4536E-02

Time(s)	Wt Loss(mg)	Fr Redn (f)	f(Best Fit)	df/dt(1/s)
240.00	2.800	0.122219	0.117871	0.6106E-03
360.00	4.288	0.187170	0.190017	0.5910E-03
480.00	5.800	0.253168	0.259502	0.5662E-03
600.00	7.480	0.326500	0.325698	0.5362E-03
840.00	10.344	0.451512	0.445724	0.4605E-03
1200.00	13.440	0.586652	0.585449	0.3079E-03
1440.00	14.664	0.640079	0.644419	0.1800E-03
1800.00	15.360	0.670459	0.669079	-0.5087E-04

f=0.30 t= 552.63 df/dt=0.5487E-03

f=0.50 t= 964.11 df/dt=0.4132E-03

f=0.70 t=-3918.57 df/dt=-.1935E-02

Exp No = CO 7 Temp (K)=1073.0
Set No = 2 Sample Wt (mg)=100.86
Bed Depth (mm)= 0.43 Wt of Removable Oxygen (mg)= 29.03
Wt of Oxygen Consume During Stage I (mg)= 5.86
A0=-0.4202E-01 A1= 0.6098E-03 A2=-0.4665E-07 A3=-0.4026E-10
Std.Dev.=0.6922E-02

Time(s)	Wt Loss(mg)	Fr Redn (f)	f(Best Fit)	df/dt(1/s)
240.00	2.520	0.108757	0.101092	0.5805E-03
360.00	3.760	0.162272	0.169587	0.5606E-03
480.00	5.296	0.228562	0.235487	0.5372E-03
600.00	6.944	0.299686	0.298373	0.5103E-03
900.00	10.400	0.448838	0.439667	0.4280E-03
1200.00	12.800	0.552416	0.552995	0.3239E-03
1500.00	14.504	0.625956	0.631837	0.1981E-03
1800.00	15.576	0.672221	0.669669	0.5051E-04

f=0.30 t= 603.19 df/dt=0.5096E-03

f=0.50 t= 1049.38 df/dt=0.3789E-03

f=0.70 t=-4960.77 df/dt=-.1900E-02

****

Exp No = CO 8 Temp (K)=1073.0

Set No = 1 Sample Wt (mg)=197.53

Bed Depth (mm)= 1.04 Wt of Removable Oxygen (mg)= 56.85

Wt of Oxygen Consume During Stage I (mg)= 11.20

A0=-0.1010E+00 A1= 0.8736E-03 A2=-0.3731E-06 A3= 0.5570E-10

Std.Dev.=0.1102E-01

****

Time(s)	Wt Loss(mg)	Fr Redn (f)	f(Best Fit)	df/dt(1/s)
240.00	4.584	0.100421	0.087952	0.7042E-03
360.00	7.320	0.160357	0.167752	0.6266E-03
480.00	10.112	0.221521	0.238539	0.5539E-03
720.00	16.280	0.356642	0.355382	0.4230E-03
840.00	19.040	0.417104	0.402593	0.3647E-03
1200.00	23.040	0.504731	0.506313	0.2188E-03
1800.00	26.656	0.583946	0.587455	0.7177E-04
2340.00	28.080	0.615141	0.613879	0.4234E-04

f=0.30 t= 598.17 df/dt=0.4870E-03

f=0.50 t= 1171.77 df/dt=0.2286E-03

f=0.70 t= 3205.42 df/dt=0.1984E-03

****

Exp No = CO 9 Temp (K)=1073.0

Set No = 1 Sample Wt (mg)=301.80

Bed Depth (mm)= 1.52 Wt of Removable Oxygen (mg)= 86.86

Wt of Oxygen Consume During Stage I (mg)= 17.02

A0=-0.1200E-01 A1= 0.2496E-03 A2= 0.4842E-07 A3=-0.1802E-10

Std.Dev.=0.3492E-01

****

Time(s)	Wt Loss(mg)	Fr Redn (f)	f(Best Fit)	df/dt(1/s)
240.00	5.264	0.075372	0.050439	0.2697E-03
480.00	8.016	0.114776	0.116962	0.2836E-03
720.00	10.600	0.151775	0.186074	0.2913E-03
960.00	15.560	0.222794	0.256278	0.2927E-03
1260.00	24.680	0.353377	0.343293	0.2858E-03
1620.00	34.960	0.500570	0.442769	0.2646E-03
2700.00	44.008	0.630123	0.660085	0.1169E-03
3720.00	46.496	0.665747	0.658634	-0.1385E-03

f=0.30 t= 1109.84 df/dt=0.2905E-03

f=0.50 t= 1844.57 df/dt=0.2442E-03

f=0.70 t=-3768.88 df/dt=-.8834E-03

****

****

Exp No = C010 Temp (K)=1373.0

Set No = 1 Sample Wt (mg)= 99.27

Bed Depth (mm)= 0.43 Wt of Removable Oxygen (mg)= 28.57

Wt of Oxygen Consume During Stage I (mg)= 2.38

A0= 0.1706E-01 A1= 0.1529E-02 A2=-0.2489E-06 A3=-0.4728E-09

Std.Dev.=0.1866E-02

****

Time(s)	Wt Loss(mg)	Fr Redn (f)	f(Best Fit)	df/dt(1/s)
120.00	5.100	0.194736	0.196109	0.1449E-02
180.00	7.420	0.283321	0.281414	0.1393E-02
240.00	9.560	0.365034	0.363089	0.1328E-02
300.00	11.480	0.438346	0.440522	0.1252E-02
360.00	13.392	0.511353	0.513099	0.1166E-02
480.00	16.832	0.642704	0.641236	0.9630E-03
540.00	18.240	0.696466	0.695569	0.8464E-03
600.00	19.424	0.741675	0.742597	0.7195E-03

f=0.30 t= 193.41 df/dt=0.1379E-02

f=0.50 t= 348.84 df/dt=0.1183E-02

f=0.70 t= 545.27 df/dt=0.8356E-03

****

Exp No = C011 Temp (K)=1373.0

Set No = 1 Sample Wt (mg)=195.51

Bed Depth (mm)= 1.04 Wt of Removable Oxygen (mg)= 56.27

Wt of Oxygen Consume During Stage I (mg)= 6.60

A0=-0.1709E-01 A1= 0.1035E-02 A2=-0.1875E-06 A3=-0.1765E-10

Std.Dev.=0.2739E-02

****

Time(s)	Wt Loss(mg)	Fr Redn (f)	f(Best Fit)	df/dt(1/s)
120.00	5.080	0.102282	0.104381	0.9892E-03
240.00	11.160	0.224698	0.220265	0.9419E-03
360.00	16.400	0.330201	0.330384	0.8931E-03
480.00	21.440	0.431678	0.434556	0.8428E-03
600.00	26.360	0.530738	0.532596	0.7910E-03
720.00	31.120	0.626577	0.624323	0.7376E-03
840.00	35.320	0.711141	0.709553	0.6827E-03
960.00	39.080	0.786845	0.788102	0.6262E-03

f=0.30 t= 326.24 df/dt=0.9070E-03

f=0.50 t= 559.25 df/dt=0.8087E-03

f=0.70 t= 826.07 df/dt=0.6891E-03

****

****

Exp No = C011 Temp (K)=1373.0

Set No = 2 Sample Wt (mg)=197.21

Bed Depth (mm)= 1.04 Wt of Removable Oxygen (mg)= 56.76

Wt of Oxygen Consume During Stage I (mg)= 4.61

A0= 0.9903E-02 A1= 0.9227E-03 A2= 0.8686E-07 A3=-0.1675E-09

Std.Dev.=0.2236E-02

****

Time(s)	Wt Loss(mg)	Fr Redn (f)	f(Best Fit)	df/dt(1/s)
180.00	9.200	0.176421	0.177818	0.9376E-03
300.00	15.320	0.293780	0.289994	0.9295E-03
360.00	17.960	0.344405	0.345501	0.9201E-03
480.00	23.640	0.453326	0.454267	0.8903E-03
600.00	29.000	0.556110	0.558589	0.8460E-03
720.00	34.360	0.658895	0.656730	0.7873E-03
840.00	38.984	0.747565	0.746955	0.7141E-03
960.00	43.120	0.826878	0.827526	0.6264E-03

f=0.30 t= 310.77 df/dt=0.9281E-03

f=0.50 t= 531.86 df/dt=0.8729E-03

f=0.70 t= 776.10 df/dt=0.7548E-03

****

Exp No = C012 Temp (K)=1373.0

Set No = 1 Sample Wt (mg)=293.55

Bed Depth (mm)= 1.47 Wt of Removable Oxygen (mg)= 84.48

Wt of Oxygen Consume During Stage I (mg)= 9.73

A0=-0.8600E-02 A1= 0.9668E-03 A2=-0.4552E-06 A3= 0.1721E-09

Std.Dev.=0.3811E-02

****

Time(s)	Wt Loss(mg)	Fr Redn (f)	f(Best Fit)	df/dt(1/s)
120.00	7.360	0.098456	0.101154	0.8649E-03
240.00	15.104	0.202049	0.199583	0.7780E-03
360.00	21.880	0.292693	0.288469	0.7059E-03
600.00	32.880	0.439842	0.444750	0.6063E-03
720.00	38.360	0.513149	0.515713	0.5789E-03
960.00	49.040	0.656018	0.652203	0.5685E-03
1080.00	54.080	0.723439	0.721298	0.5856E-03
1200.00	59.120	0.790860	0.793338	0.6176E-03

f=0.30 t= 376.44 df/dt=0.6972E-03

f=0.50 t= 692.97 df/dt=0.5837E-03

f=0.70 t= 1043.41 df/dt=0.5788E-03

****

Appendix C

Data on Gas Chromatographic Analyses of Exit Gas for Non-Isothermal Reduction of Composite Pellets

1 : Expt.no. 2 : Speed 3 : Coal/char code

4 : Ar flow rate ($cm^3.s^{-1}$ at STP)

Expt.no. etc.	Time (Min.)	Temp. (K)	Gas composition, vol.pct					$\dot{W}_o \times 10^4$ ($g.s^{-1}$)
			Ar	CO	CH_4	CO_2	H_2	
1	2	3	4	5	6	7	8	9
1:FG 2	8	371	100	0	0	0	0	0
FGM 1	14	527	85.57	6.72	0	7.29	0.42	0.425
2:HS	22	820	56.44	5.85	1.02	35.68	1.00	2.335
3:HCL	29	1064	38.13	38.73	0	19.62	3.52	3.491
4:0.239	38	1209	84.28	10.81	0	3.46	1.45	0.359
	46	1255	89.25	7.41	0	2.43	0.91	0.235
1:FG 5,6	10	315	100	0	0	0	0	0
FGM 2	18	440	95.99	0	0	3.77	0.25	0.129
2:LS	26	572	88.91	5.71	0	4.72	0.66	0.28
3:HCL	34	694	85.54	5.66	1.06	7.43	0.34	0.394
4:0.23	42	837	69.54	6.13	0.53	20.97	2.84	1.136
	50.5	1001	48.11	20.26	0	27.88	3.77	2.596
	58	1103	45.94	36.09	0	16.27	1.7	2.454
	66	1171	87.05	8.76	0	3.51	0.69	0.298
	74	1214	90.91	6.11	0	2.43	0.55	0.198
	82	1243	91.68	5.55	0	2.22	0.58	0.179
	90	1265	89.92	7.25	0	2.19	0.66	0.212

1	2	3	4	5	6	7	8	9
1:FG 9,10	6	306	100	0	0	0	0	0
FGM 5	14	536	96.58	0	0	2.21	2.31	0.076
2:HS	22	827	96.58	0	0	2.73	0.7	0.094
3:HCCL	30	1100	50.41	13.71	0	35.42	0.45	2.791
4:0.233	38	1215	48.13	33.91	0	16.14	1.82	2.289
	46	1261	46.38	37.74	0	14.38	1.52	2.386
1:FG 11,12	11	315	100	0	0	0	0	0
FGM 6	18	456	98.84	0	0	1.17	0	0.039
2:LS	26	575	98.5	0	0	0.0	1.51	0
3:HCCL	34	697	93.94	0	0	0.0	6.06	0
4:0.229	42	835	96.65	0	0	2.86	0.49	0.097
	50	980	78.29	6.59	0	14.95	0.17	0.761
	58	1097	56.69	12.37	0	30.4	0.56	2.107
	66	1171	61.08	23.85	0	14.25	0.83	1.4
	74	1218	50.0	34.22	0	13.96	1.83	2.028
	82	1247	60.84	27.04	0	10.31	1.82	1.279
	90	1266	82.92	9.82	0	5.54	1.72	0.411
	96	1279	88.3	7.32	0	3.02	1.36	0.247

1	2	3	4	5	6	7	8	9
1:FG 3,4	6	304	100	0	0	0	0	0
FGM 3	14	538	85.3	6.08	0	5.36	3.28	0.324
2:HS	22	815	58.32	6.22	0.97	33.2	1.3	2.046
3:BCL	30	1083	31.93	43.7	0	19.94	4.44	4.3
4:0.23	38	1203	85.02	10.01	0	3.89	1.09	0.344
	46	1256	90.97	5.99	0	2.26	0.79	0.19
1:FG 7,8	10	311	97.64	0	0	2.37	0	0.084
FGM 4	18	437	95.76	0	0	3.39	0.85	0.123
2:LS	26	559	94.34	0	0.1	3.95	1.62	0.145
3:BCL	34	687	90.39	0	1.66	6.02	1.94	0.231
4:0.243	42	825	73.66	6.62	0.5	18.83	0.4	1.043
	50	965	49.86	17.11	0.19	29.5	5.44	2.51
	58	1086	46.25	34.15	0	15.19	4.41	2.422
	66	1166	84.65	10.34	0	3.98	1.05	0.375
	74	1215	90.17	6.5	0	2.67	0.66	0.228
	82	1245	93.73	3.19	0	2.43	0.68	0.149
	90	1266	96.98	0	0	2.42	0.61	0.087
	96	1271	100	0	0	0	0	0

1	2	3	4	5	6	7	8	9
1:FG 13,14	6	305	100	0	0	0	0	0
FGM 7	14	543	94.56	0	0	2.95	2.5	0.104
2:HS	22	856	93.96	0	0	4.78	1.27	0.17
3:BCCL	30	1123	60.31	6.3	0	33.39	0.0	2.02
4:0.234	38	1226	53.28	21.39	0	24.37	0.97	2.2
	46	1268	51.83	33.19	0	13.09	1.91	1.91
1:FG 15,16	10	310	98.85	0	0	1.16	0	0.039
FGM 8	18	456	96.48	0	0	2.65	0.88	0.091
2:LS	26.25	586	95.35	0	0	2.64	2.01	0.09
3:BCCL	34.5	724	95.84	0	0	2.83	1.34	0.098
4:0.233	42	862	94.37	0	0	5.23	0.4	0.184
	50	1001	84.08	0	0	15.92	0.0	0.63
	58	1106	70.46	9.64	0	19.48	0.42	1.148
	66	1176	64.02	11.04	0	24.25	0.69	1.548
	74	1216	64.06	24.59	0	9.49	1.87	1.132
	82	1242	59.57	27.97	0	10.67	1.81	1.378
	90	1260	62.67	23.97	0	11.9	1.46	1.269
	96	1268	73.0	18.26	0	7.44	1.31	0.756

1	2	3	4	5	6	7	8	9
1:FG 17,18	6.25	304	98.71	0	0	1.3	0	0.043
FGM 13	14	561	89.65	0	0	8.84	1.51	0.32
2:HS	22	847	66.35	6.61	2.03	26.53	1.5	1.527
3:HCH	30	1113	23.19	47.58	0	23.01	6.22	6.544
4:0.227	38	1220	74.83	15.8	0	7.93	1.45	0.686
	46	1259	96.42	0	0	2.6	0.98	0.087
1:FG 19,20	10	314	97.26	0	0	2.74	0	0.09
FGM 14	18	452	94.84	0	0	4.97	0.21	0.168
2:LS	26	575	92.42	0	0.13	6.51	0.94	0.225
3:HCH	34	702	81.29	6.6	1.75	8.66	1.71	0.471
4:0.224	42	841	68.94	10.38	1.05	17.0	2.63	1.03
	50	979	44.65	31.55	0.23	15.92	7.65	2.272
	58	1095	40.83	38.31	0	16.38	4.49	2.785
	66	1172	83.41	10.4	0	4.59	1.6	0.376
	74	1218	90.17	6.65	0	2.54	0.65	0.208
	82	1248	97.04	0	0	2.37	0.6	0.078
	90	1269	99.4	0	0	0	0.6	0
	96	1276	99.35	0	0	0	0.65	0

1	2	3	4	5	6	7	8	9
1:FG 25,26	6	304	100	0	0	0	0	0
FGM 11	14.5	546	94.35	0	0	3.17	2.48	0.118
2:HS	22	813	92.56	0	0	6.52	0.93	0.244
3:HCCH	30	1089	63.05	7.45	0	29.14	0.37	1.802
4:0.242	38	1200	48.28	36.01	0	13.98	1.74	2.29
	46	1247	40.36	42.89	0	14.95	1.81	3.118
1:FG 27,28	10	309	97.6	0	0	2.4	0	0.086
FGM 12	18	437	96.75	0	0	2.86	0.4	0.103
2:LS	26	574	95.94	0	0	2.62	1.45	0.096
3:HCCH	34	690	95.17	0	0	3.25	1.59	0.12
4:0.245	42	834	94.06	0	0	5.54	0.4	0.206
	50	976	85.35	0	0	14.65	0.1	0.601
	58	1096	71.45	8.19	0	19.97	0.39	1.179
	66	1173	66.95	19.3	0	12.72	1.04	1.169
	74	1217	50.12	35.01	0	13.4	1.47	2.158
	82.25	1248	46.4	38.46	0	13.41	1.73	2.462
	90	1264	53.68	33.12	0	11.5	1.72	1.83
	96	1271	69.48	24.17	0	4.75	1.59	0.848

1	2	3	4	5	6	7	8	9
1:FG 21,22	6	304	98.68	0	0	1.33	0	0.045
FGM 16	14	552	91.99	0	0.11	6.59	1.32	0.237
2:HS	22	834	65.72	6.17	2.67	24.62	0.84	1.397
3:BCH	30	1106	23.69	49.26	0.09	20.68	6.29	6.339
4:0.232	38	1218	66.46	22.84	0	9.06	1.65	1.021
	46	1262	88.34	8.06	0	2.88	0.73	0.259
1:FG 23,24	10	317	97.59	0	0	2.41	0	0.083
FGM 15	18	467	95.65	0	0	4.15	0.2	0.145
2:LS	26	592	93.76	0	0.25	4.79	1.3	0.171
3:BCH	34	718	88.55	0	2.67	7.09	1.69	0.268
4:0.234	42	858	74.86	6.08	1.32	16.81	0.94	0.886
	50	1006	48.74	20.87	0.33	23.47	6.58	2.325
	58	1113	35.5	42.54	0	17.4	4.57	3.641
	66	1183	72.39	18.37	0	7.64	1.61	0.777
	74	1227	84.48	9.66	0	5.16	0.71	0.395
	82	1252	96.62	0	0	2.7	0.69	0.093
	90	1265	96.66	0	0	2.66	0.69	0.092
	96	1272	96.93	0	0	2.38	0.69	0.082

1	2	3	4	5	6	7	8	9
1:FG 29,30	6	303	100	0	0	0	0	0
FGM 9	14	526	93.99	0	0	2.98	3.05	0.113
2:HS	22	810	93.1	0	0	6.09	0.82	0.233
3:BCCH	30	1090	71.11	7.12	0	21.38	0.4	1.248
4:0.249	38	1207	57.91	29.07	0	11.12	1.91	1.576
	46	1260	45.48	38.88	0	13.63	2.0	2.587
1:FG 31,32	10	308	98.85	0	0	1.15	0	0.041
FGM 10	18	429	96.97	0	0	2.79	0.25	0.102
2:LS	26.5	557	95.51	0	0	2.63	1.87	0.097
3:BCCH	34	675	95.13	0	0	3.01	1.88	0.112
4:0.248	42	811	94.5	0	0	5.22	0.3	0.195
	50	953	86.88	0	0	13.12	0.0	0.534
	58	1080	77.75	6.45	0	15.41	0.4	0.847
	66	1158	67.32	14.5	0	17.26	0.94	1.287
	74	1209	60.21	27.44	0	10.61	1.75	1.429
	82	1241	53.96	32.77	0	11.58	1.7	1.832
	90	1263	55.99	30.39	0	12.03	1.61	1.719
	98	1272	62.72	27.04	0	8.65	1.61	1.25

Appendix D

Program for Data Processing of H_2 Reduction of Blue Dust

```
C*************************************************************************
C       REDUCTION OF BLUE DUST BY HYDROGEN
C       CALCULATION BY POLYNOMIAL CURVE FITTING
C*************************************************************************
C       T= TEMPERATURE (K)
C       L= EXP NO
C       M= SET NO
C       N= NO OF DATA ON EACH SET
C       WO=SAMPLE WT (mg), WO=SAMPLE WT (g)
C       BD=BED HEIGHT (mm)
C       X= TIME (s)
C       W= WT LOSS (mg)
C       FE=Fr OF Fe IN BLUE DUST
C       WOX=TOTAL WT OF REMOVABLE OXYGEN PRESENT IN BLUE DUST (mg)
C       Y= Fr OF REDUCTION (f)
C       MM=For Diff Temp
C       LL=For Diff Bed Heights
C       J=For Reproducibility Of Exp
C*************************************************************************
        IMPLICIT REAL *8(A-H,O-Z)
        REAL *8 X(20,2),XX(20,2),YB(20,2),AY(20),AYY(20),AYB(20)
        REAL *8 AX(10),FF(3),DF(3),DEF(10,2),XI(3,2),AXI(3),SIGMA(3)
        REAL *8 A0(3),A1(3),A2(3),A3(3),Y(20,2),WW(20,2),AW(20),W(20,2)
        REAL *8 A(4,4),B(4,4),C(4,1),D(4,1),BB(4,4),E(4,4),XT(20,2)
        REAL *8 SUMX(20),SUMY(20),SUMSX(20),SUMCX(20),SUMFOX(20)
        REAL *8 SUMFX(20),SUMSIX(20),SUMXY(20),SUMSXY(20)
        REAL *8 SUMCXY(20),DFL(10,5),YA(20,2)
C-----------------------------------------------------------------
        OPEN (UNIT=21, FILE='B:RED.IN')
        OPEN (UNIT=22, FILE='B:REDH.OUT')
C-----------------------------------------------------------------
        MM=0
5       MM=MM+1
        LL=0
10      READ (21,*) T
        IF (T .EQ. 9999.0) GO TO 99
        T=T+273.00
15      LL=LL+1
        J=0
20      READ (21,*) L,M
25      J=J+1
        READ (21,*) N,WO,BD
        DO 30 I=1,N
        READ (21,*) X(I,J),W(I,J)
30      CONTINUE
        FE=0.9574
        WO=WO*1000.0
        WOX=FE*WO*0.3006
        DO 40 I=1,N
        Y(I,J)=W(I,J)/WOX
40      CONTINUE
        SUMX(J)=0.0
        SUMY(J)=0.0
        SUMSX(J)=0.0
        SUMCX(J)=0.0
```

```
      SUMFOX(J)=0.0
      SUMFX(J)=0.0
      SUMSIX(J)=0.0
      SUMXY(J)=0.0
      SUMSXY(J)=0.0
      SUMCXY(J)=0.0
      DO 50 I=1,N
      SUMX(J)=SUMX(J)+X(I,J)
      SUMY(J)=SUMY(J)+Y(I,J)
      SUMSX(J)=SUMSX(J)+X(I,J)**2
      SUMCX(J)=SUMCX(J)+X(I,J)**3
      SUMFOX(J)=SUMFOX(J)+X(I,J)**4
      SUMFX(J)=SUMFX(J)+X(I,J)**5
      SUMSIX(J)=SUMSIX(J)+X(I,J)**6
      SUMXY(J)=SUMXY(J)+X(I,J)*Y(I,J)
      SUMSXY(J)=SUMSXY(J)+X(I,J)**2*Y(I,J)
      SUMCXY(J)=SUMCXY(J)+X(I,J)**3*Y(I,J)
50    CONTINUE
      A(1,1)=REAL(N)/SUMY(J)
      A(1,2)=SUMX(J)/SUMY(J)
      A(1,3)=SUMSX(J)/SUMY(J)
      A(1,4)=SUMCX(J)/SUMY(J)
      A(2,1)=SUMX(J)/SUMXY(J)
      A(2,2)=SUMSX(J)/SUMXY(J)
      A(2,3)=SUMCX(J)/SUMXY(J)
      A(2,4)=SUMFOX(J)/SUMXY(J)
      A(3,1)=SUMSX(J)/SUMSXY(J)
      A(3,2)=SUMCX(J)/SUMSXY(J)
      A(3,3)=SUMFOX(J)/SUMSXY(J)
      A(3,4)=SUMFX(J)/SUMSXY(J)
      A(4,1)=SUMCX(J)/SUMCXY(J)
      A(4,2)=SUMFOX(J)/SUMCXY(J)
      A(4,3)=SUMFX(J)/SUMCXY(J)
      A(4,4)=SUMSIX(J)/SUMCXY(J)
      CALL GJORD(4,A)
      C(1,1)=1.0
      C(2,1)=1.0
      C(3,1)=1.0
      C(4,1)=1.0
      CALL MATMUL (A,4,  C,4,  4,4,1,  D,4)
      A0(J)=D(1,1)
      A1(J)=D(2,1)
      A2(J)=D(3,1)
      A3(J)=D(4,1)
      DO 60 I=1,N
      YB(I,J)=A0(J)+A1(J)*X(I,J)+A2(J)*X(I,J)**2+A3(J)*X(I,J)**3
60    CONTINUE
C****** Calculation of standard deviation (SIGMA)*******************
65    SUMZ=0.0
      DO 70 I=1,N
      SUMZ=SUMZ+(Y(I,J)-YB(I,J))**2
70    CONTINUE
      SIGMA(J)=SQRT(SUMZ/(FLOAT(N-2)))
C*****************************************************************
      WRITE(22,80) L,T,J,W0,BD,WOX
```

```
0       FORMAT(/66('*')/2X,'Exp No = H',I2,36X,'Temp (K)=',F6.1
     1  /2X,'Set No =',I2,32X,'Sample Wt (mg)=',F6.2/2X,
     2  'Bed Depth (mm)=',F5.2,9X,'Wt of Removable Oxygen (mg)=',F6.2)
        WRITE (22,90) A0(J),A1(J),A2(J),A3(J),SIGMA(J)
0       FORMAT (/2X,'A0=',E11.4,3X,'A1=',E10.4,3X,'A2=',E11.4,
     1  3X,'A3=',E10.4/2X,'Std Dev.=',E10.4/66('*'))
        WRITE(22,100)
00      FORMAT(2X,'Time(s)',3X,'Wt Loss(mg)',3X,'Fr Redn.(f)',3X,
     1  'f(Best Fit)',4X,'df/dt(1/s)')
        DO 120  I=1,N
        DEF(I,J)=A1(J)+2.*A2(J)*X(I,J)+3.*A3(J)*X(I,J)**2.0
        WRITE (22,110) X(I,J),W(I,J),Y(I,J),YB(I,J),DEF(I,J)
10      FORMAT(1X,F7.2,6X,F6.3,7X,F8.6,6X,F8.6,5X,E11.4)
20      CONTINUE
-------------------------------------------------------------------------
        FF(1)=0.30
        FF(2)=0.50
        FF(3)=0.70
        DO 130 K=1,3
        CALL NEWRAP (K,FF,XI,J,A0,A1,A2,A3,DEF)
30      CONTINUE
        IF (J .LT. M) GO TO 25
        IF (LL .LT. 3) GO TO 15
        IF (MM .LT. 4) GO TO 5
?       STOP
        END
*************************************************************************
      Calculation of dF/dt for F=0.3, 0.5 & 0.7 using NEWTON-RAPHSON METH
*************************************************************************
        SUBROUTINE NEWRAP (K,F,XI,J,A0,A1,A2,A3,DEF)
        IMPLICIT REAL *8(A-H,O-Z)
        DIMENSION F(3),A0(J),A1(J),A2(J),A3(J),XI(3,J)
        DIMENSION DEF(3,J),X(100),FF(100),DF(100)
        X(1)=10.00
        NIT=100
        ER=0.001
        I=0
0       I=I+1
        FF(I)=F(K)-(A0(J)+A1(J)*X(I)+A2(J)*X(I)**2+
     1  A3(J)*X(I)**3)
        DF(I)=-(A1(J)+2.0*A2(J)*X(I)+3.0*A3(J)*(X(I)**2))
        XIP=X(I)-FF(I)/DF(I)
        ERROR=DABS((XIP-X(I))/XIP)
        WRITE(5,*) XIP,ERROR
        IF (ERROR .LE. ER) GO TO 20
        X(I+1)=XIP
        IF (I .EQ. NIT) GO TO 30
        GO TO 10
0       X(I)=XIP
        DEF(K,J)=(A1(J)+2.0*A2(J)*X(I)+3.0*A3(J)*X(I)**2)
        XI(K,J)=X(I)
        GO TO 40
-------------------------------------------------------------------
0       WRITE(5,31)
1       FORMAT('INSUFFICIENT NO. OF ITERATION')
```

```
      WRITE(5,32)
32    FORMAT('DO YOU WANT FURTHER ITERATION ? IF YES TYPE 1')
      READ(5,*) MORE
      IF (MORE .NE. 1) GO TO 50
      WRITE(5,33)
33    FORMAT('INCREASE THE NO. OF ITERATION BY :')
      READ(5,*) INCR
      NIT=NIT+INCR
      GO TO 10
40    WRITE(22,200) F(K),XI(K,J),DEF(K,J)
200   FORMAT(/5X,'f=',F4.2,10X,'t=',F7.2,10X,'df/dt=',E10.4)
50    RETURN
      END
C*************************************************************************
C     SUBROUTINE FOR MATRIX INVERSION BY GAUSS JORDON METHOD
C*************************************************************************
      SUBROUTINE GJORD (N4,A)
      REAL*8 A(N4,N4)
      DO 50 K=1,N4
         DO 10 J=1,N4
            IF (J.EQ.K) GO TO 10
            A(K,J)=A(K,J)/A(K,K)
10       CONTINUE
         A(K,K)=1/A(K,K)
         DO 30 I=1,N4
            IF (I.EQ.K) GO TO 30
            DO 20 J=1,N4
               IF (J.EQ.K) GO TO 20
               A(I,J)=A(I,J)-A(K,J)*A(I,K)
20          CONTINUE
30       CONTINUE
         DO 40 I=1,N4
            IF (I.EQ.K) GO TO 40
            A(I,K)=-A(I,K)*A(K,K)
40       CONTINUE
50    CONTINUE
      RETURN
      END
C*************************************************************************
C      SUBROUTINE  FOR   MATRIX  MULTIPLICATION
C      matD (L X N) = matC(L X M) X matB(M X N)
C*************************************************************************
      SUBROUTINE MATMUL (B,IB,C,IC,L,M,N,D,ID)
      REAL*8 B(IB,M),C(IC,N),D(ID,N)
      DO I=1,L
         DO J=1,N
            D(I,J)=0.0
            DO K=1,M
               D(I,J)=D(I,J)+B(I,K)*C(K,J)
            ENDDO
         ENDDO
      ENDDO
      RETURN
      END
C*************************************************************************
```